Towards Clinical Application of Urinary Extracellular Vesicles

Urine extracellulaire vesikels: op weg naar klinische toepassing

Charles J. Blijdorp

Doctoral thesis, Erasmus University Rotterdam, The Netherlands

The studies described in this thesis were financially supported by the Dutch Kidney Foundation, and performed at the Division of Nephrology and Transplantation, Department of Internal Medicine, Erasmus Medical Center, Rotterdam, the Netherlands.

Printing of this thesis was kindly supported by:
Eurocept Homecare
Ipsen Farmaceutica
Kaivogen
Sysmex
Bio-services
Chipsoft

Cover model: Anna M. B. Blijdorp
Coverphoto, design and lay-out: Bram Vreugdenhil, studio Roodenburch
Printing: Optima Grafische Communicatie, Rotterdam

ISBN: 978-94-6361-685-0

Towards Clinical Application of Urinary Extracellular Vesicles

Urine extracellulaire vesikels:
op weg naar klinische toepassing

Proefschrift

ter verkrijging van de graad van doctor aan de
Erasmus Universiteit Rotterdam
op gezag van de rector magnificus
Prof. dr. A.L. Bredenoord

en volgens besluit van het college voor promoties

De openbare verdediging zal plaatsvinden op
woensdag 11 mei 2022 om 15.30 uur door

Charles Johannes Blijdorp
Geboren te Leiderdorp

Erasmus University Rotterdam

Promotiecommissie

Promotoren:	Prof. dr. E.J. Hoorn Prof. dr. R. Zietse
Overige leden:	Prof. dr. A.H.J. Danser Prof. dr. C.C. Baan Prof. dr. D.J.M. Peters
Copromotor:	Dr. M. Salih

CONTENTS

ABBREVIATIONS

ADPKD	Autosomal dominant polycystic kidney disease
ALIX	Apoptosis-linked gene 2-interacting protein X
AQP2	Aquaporin-2
CD63	Cluster of differentiation-63
CD81	Cluster of differentiation-81
CD9	Cluster of differentiation-9
CHMP4A	Charged multivesicular body protein 4a
CKD	Chronic kidney disease
DIPAK	Developing Interventions to halt Progression of ADPKD
eGFR	Estimated glomerular filtration rate
EM	Electron microscopy
EV	Extracellular vesicle
FCM	Flow cytometry
GFR	Glomerular filtration rate
HFD	Hydrostatic filtration dialysis
hr-FCM	High resolution flow cytometry
htTKV	Height adjusted total kidney volume
htTLV	Height adjusted total liver volume
ISEV	International society of extracellular vesicles
MISEV2018	Minimal information for studies of extracellular vesicles-2018
MMP7	Matrix metallopeptidase-7
MS	Mass spectrometry
NaPi-IIa	Sodium-dependent phosphate transport protein-2A
NCC	Sodium-chloride cotransporter
NHE3	Sodium-hydrogen exchanger-3
NKCC2	Sodium potassium chloride cotransporter-2
NTA	Nanoparticle tracking analysis
PKD	Polycystic kidney disease
PLD	Polycystic liver disease
PROPKD	Predicting renal outcomes in polycystic kidney disease
RDP	Rapid disease progression
RTM	Raman tweezers microspectroscopy

SDG	Sucrose density gradient
SDP	Slow disease progression
SDS	Sodium dodecyl sulfate
SEC	Size exclusion chromatography
TEM	Transmission electron microscopy
THP	Tamm-Horsfall protein
TKV	Total kidney volume
TR-FIA	Time-resolved fluorescence immunoassay
TRPS	Tunable resistive pulse Sensing
TSG101	Tumor susceptibility gene-101
UC	Ultracentrifigation
uEV	Urinary extracellular vesicle
UF	Ultrafiltration
WB	Western Blot
WT1	Wilms' tumor protein 1

CHAPTER 1

Introduction and aims of the thesis

Hippocrates was one of the first well-known *uroscopists*, using the appearance and smell of urine to determine urinary tract infections and proteinuria, and more broadly for prognosis and prediction of illness [1]. Physicians have since made grateful use of urine for diagnostic purposes, labelling it a 'Window to the Body' (Figure 1.1, De Piskijker by Jan Steen) [2]. For example, urine was used to identify patients with diabetes by its sweet taste [3]. Nowadays, urine remains indispensable in daily clinical practice, and is still extensively studied for new biomarkers. A promising new development in this field is the discovery of urinary extracellular vesicles.

FIGURE 1.1 *De Piskijker,* **Jan Steen - ca. 1663-1665, collectie Museum de Lakenhal**

Urinary Extracellular Vesicles

Extracellular vesicles (EVs) are membrane vesicles released by all cells, and may be classified into exosomes, microvesicles and apoptotic bodies (Figure 1.2) [4]. Because these subpopulations are hard to distinguish, they are often categorized as small (<200 nm, enriched for exosomes) or large EVs (>200 nm, mainly microvesicles or apoptotic bodies) [5]. Urinary EVs (uEVs) likely have biological functions in the urinary tract, such as RNA and protein transfer between tubular segments and defense against pathogens [6, 7]. However, they have particularly gained interest as potential biomarkers for various kidney and urological diseases. This is because protein and RNA in uEVs reflect molecular processes in epithelial cells lining the kidney tubules and the urological tract [8]. Additional advantages of uEVs are that they can be enriched, and separated from high abundant proteins that preclude analyses; and that they may be traced to their originating part of the urological tract by segment-specific markers [9]. Biomarkers have been identified for a variety of kidney diseases, including both glomerular diseases [10, 11] and tubular diseases [12]. In addition, uEVs have enabled the non-invasive study of physiological processes in humans [13, 14]. This may be used to validate findings of animal studies in the human setting, and in some cases prevent the need for animal studies in the first place.

To date, a kidney biopsy is often necessary for the diagnosis of kidney disease, especially glomerular disease. This is an invasive procedure with a risk of bleeding and therefore reserved for diagnosing kidney diseases which have therapeutic implications. uEVs, however, may in time prove to be a fast and non-invasive alternative. For example, mRNA or proteins in uEVs can signal kidney transplant rejection [15, 16] and IgA nephropathy [17, 18], both of which currently require a kidney biopsy for diagnosis. In addition, uEVs may facilitate personalized medicine, for example by non-invasively assessing drug target effects [19], and function as early markers of kidney disease [20].

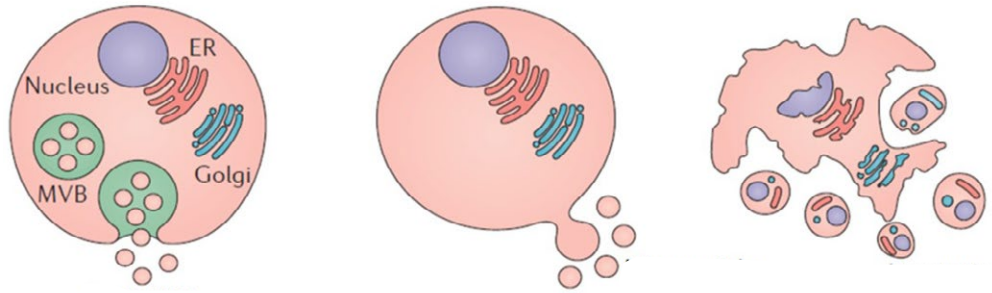

FIGURE 1.2 **Exosomes, Microvesicles, Apoptotic bodies**

Exosomes (left panel) are excreted by the fusion of multivesicular bodies (MVBs) with the plasma membrane. Microvesicles (middle panel) and apoptotic bodies (right panel) are formed by outward budding of the plasma membrane. From Karpmann, *et al.*, Nat Rev Nephrol, 2017.

Isolation and Normalization

Until recently, uEVs were almost exclusively studied after applying enrichment methods, including ultracentrifugation, ultrafiltration, hydrostatic dialysis and sucrose gradient [9]. These methods, however, are time-consuming and induce variation and loss of uEVs [21]. Recently, novel methods have been developed to directly characterize uEVs [22-27]. Several of these methods are high throughput, enabling development towards clinical application of uEVs. In **chapter 2** we review the current state of the art in uEV research, identify knowledge gaps, and formulate a position statement with recommendations to improve rigor, reproducibility and interoperability in uEV research.

Feasible application of uEVs in the clinic requires that uEVs can be reliably characterized in random spot urine samples. Therefore, another key topic in uEV research is normalization, which is necessary for the interpretation of changes in biomarker abundances [28]. In a recent survey among 78 researchers within the International Society of Extracellular Vesicles (ISEV) community, normalization was identified as the most pressing knowledge gap [29]. In **chapter 3** we argue that, while marked pathophysiological changes in the kidney can be detected in uEVs, subtle differences are difficult to detect because of variation in uEV excretion. There are three reasons for this:

1. uEV enrichment techniques are rather inefficient with uEV loss up to 70%. In addition, differences in techniques cause isolation of different subsets of uEVs [21].

2. Urinary concentration varies from 50 to 1200 mOsm/kg [30]. Accordingly, the concentration of uEVs can be highly variable [24].

3. There is considerable variation in nephron number among individuals [31, 32]. Because the majority of uEVs is kidney-derived, variation in nephron number is expected to impact the uEV number.

Urinary creatinine is frequently used to normalize uEV concentration [24, 33-35], because its excretion rate is constant in steady state. However, this normalization method has not been validated. Therefore, in **chapter 4**, three high-throughput methods were used to quantify uEVs directly in cell-free urine, with the goal to validate normalization of uEV concentration to urinary creatinine. In addition, we aimed to determine whether uEVs can be reliably quantified and characterized by methods that do not require uEV isolation. To study the effect of nephron number on uEV excretion, we performed correlation analyses of kidney function and kidney volume to uEV excretion rate, and analyzed the effect of nephron loss on uEV excretion (**chapter 5**).

Autosomal Dominant Polycystic Kidney Disease

As mentioned, uEVs can be applied as biomarkers for various kidney diseases. We studied uEVs in the setting of autosomal dominant polycystic kidney disease (ADPKD). ADPKD is the most common inherited kidney disease, most often caused by a mutation in the polycystin genes (*PKD1* or *PKD2*). The development of fluid filled cysts in both kidneys leads to disruption of kidney parenchyma and deteriorating kidney function, with 70% of patients requiring kidney replacement therapy [36, 37]. In the **appendix** we describe a multicenter trial, the DIPAK intervention trial, comparing the effect of somatostatin analog Lanreotide with standard of care on kidney outcomes in 305 patients with ADPKD. The only approved therapeutic option for ADPKD is the vasopressin V2 receptor antagonist Tolvaptan [38, 39]. An important side effect is polyuria and polydipsia, which raises concerns about patient tolerability of this expensive drug and emphasizes the need to identify patients at risk for rapid disease progression. The currently well-established prognostic markers are total kidney volume (TKV) and kidney function (glomerular filtration rate, GFR) relative to age (Mayo prediction score [40]), as well as early onset of hypertension or hematuria, sex, and *PKD* mutation, which are combined in the PROPKD prediction score [41]. Although these tools predict disease progression at a population level, individually they remain of little value. The field may therefore benefit from (molecular) markers of disease progression.

uEVs in ADPKD

General urinary kidney damage markers have some prognostic value in ADPKD but remain of limited value [42, 43]. uEVs may contain more relevant biomarkers for ADPKD. This is because they mirror specific processes in ADPKD, including those related to polycystins [44]. ADPKD is considered a “ciliopathy”, a disease that causes dysfunction of cellular cilia, hair-like structures that have a role in intercellular signaling. Both polycystin 1 and 2 are located at the base of these cilia, and are important for signaling; polycystin 1 regulates a variety of pathways and interacts with polycystin 2, which is considered a calcium channel [45]. uEVs are excreted by and interact with primary cilia and may form an important part of the intercellular communication processes in ciliopathies [46-48]. In **chapter 6**, we performed a proteomic analysis of uEVs isolated from patients with ADPKD included in the DIPAK intervention trial (**appendix**), in order to identify early molecular markers that distinguish rapid progression from slow progression.

Acid-Base Balance in ADPKD

Metabolic acidosis causes a more rapid progression of chronic kidney disease (CKD), which may be attenuated by alkali therapy [49]. Both diet and endogenous metabolism produce a daily

acid load which is excreted by the kidney, mostly in the form of ammonium. With deteriorating kidney function, per-nephron ammoniagenesis increases, but this may also cause inflammation and ultimately fibrosis [50]. In ADPKD, ammonium excretion is already disturbed in patients with normal kidney function, which is attributed to structural changes of the kidneys [51]. In Han:SPRD rats, an animal model for PKD, acid loading increased cyst formation and inflammation [52], while alkali decreased cyst size and improved GFR [53]. The role of acid-base balance in patients with ADPKD has never been studied prospectively. Therefore, in **chapter 7**, we study the association between serum bicarbonate and kidney outcomes in patients with ADPKD within the DIPAK intervention trial (**appendix**).

AIMS OF THE THESIS

1. To explore the current state of the art and identify knowledge gaps in uEV research, and to make recommendations for improved rigor, reproducibility and interoperability in uEV research (**chapter 2**)

2. To discuss whether changes in protein abundance in the kidney always occur in the same direction in uEVs (**chapter 3**)

3. To validate the use of urinary creatinine as normalization marker for uEV concentration (**chapter 4**)

4. To quantify and characterize uEVs by methods that do not require isolation (**chapter 4**)

5. To analyze the relationship between nephron mass and uEV excretion (**chapter 5**)

6. To identify uEV markers for rapid disease progression in patients with ADPKD (**chapter 6**)

7. To analyze the relationship between serum bicarbonate and kidney outcomes in ADPKD (**chapter 7**)

PART 1

URINARY EXTRACELLULAR VESICLES: STEPS TOWARDS CLINICAL APPLICATION

“Urine can provide us day by day, month by month, and year by year with a serial story of the major events within the kidney”

– Dr. Thomas Addis. Glomerular Nephritis, Diagnosis and Treatment (1948)

CHAPTER 2

Urinary Extracellular Vesicles: A Position Paper by the Urine Task Force of the International Society for Extracellular Vesicles

Uta Erdbrügger*, Charles J. Blijdorp*, Irene V. Bijnsdorp, Francesc E. Borràs, Dylan Burger, Benedetta Bussolati, James Brian Byrd, Aled Clayton, James W. Dear, Juan M. Falcón-Pérez, Cristina Grange, Andrew F. Hill, Harry Holthöfer, Ewout J. Hoorn, Guido Jenster, Connie R. Jimenez, Kerstin Junker, John Klein, Mark A. Knepper, Erik H. Koritzinsky, James M. Luther, Metka Lenassi, Janne Leivo, Inge Mertens, Luca Musante, Eline Oeyen, Maija Puhka, Martin E. van Royen, Catherine Sánchez, Carolina Soekmadji, Visith Thongboonkerd, Volkert van Steijn, Gerald Verhaegh, Jason P. Webber, Kenneth Witwer, Peter S.T. Yuen, Lei Zheng, Alicia Llorente*, and Elena S. Martens-Uzunova*

*These authors share first and last authorship

Journal of Extracellular Vesicles 2021

2.1 Abstract

Urine is commonly used for clinical diagnosis and biomedical research. The discovery of extracellular vesicles (EV) in urine opened a new fast-growing scientific field. In the last decade urinary extracellular vesicles (uEVs) were shown to mirror molecular processes as well as physiological and pathological conditions in kidney, urothelial and prostate tissue. Therefore, several methods to isolate and characterize uEVs have been developed. However, methodological aspects of EV separation and analysis, including normalization of results, need further optimization and standardization to foster scientific advances in uEV research and a subsequent successful translation into clinical practice. This *position paper* is written by the Urine Task Force of the Rigor and Standardization Subcommittee of ISEV consisting of nephrologists, urologists, cardiologists and biologists with active experience in uEV research. Our aim is to present the *state of the art* and identify challenges and gaps in current uEV-based analyses for clinical applications. Finally, recommendations for improved rigor, reproducibility and interoperability in uEV research are provided in order to facilitate advances in the field.

2.2 Introduction

Urinalysis has been part of standard clinical practice since antiquity [54]. Today, urine is the second most commonly used biofluid for clinical diagnostics after blood. Urine is produced by the kidneys to eliminate waste products (*e.g.*, urea, metabolites) from the body and to maintain the homeostasis of water, ions, and pH in blood. Humans normally generate approximately 1-2 liters of urine per day, which is released via the urinary tract (ureters, urinary bladder, and urethra). In addition to soluble components like organic and inorganic molecules, urine typically contains some epithelial and blood cells, bacteria, viruses and importantly also extracellular vesicles (EVs) [8, 55]. One key advantage of working with urine compared to other biofluids is that it can be easily and frequently collected in large quantities in a noninvasive manner [56, 57]. However, urinary concentration and contents are highly variable and of dynamic nature due to differences in fluid intake, time of collection, diet and exercise, age, gender, medications and health status. These well recognized factors can complicate data interpretation and the use of urine in diagnostics, particularly when reference normality ranges are to be set [58-61]. These variables may be equally relevant for uEV analyses, and hence lessons from other fields employing urine analysis are likely to be important and applicable for uEV research.

The presence of EVs in urine was first documented by electron microscopy images in 1986 when Wiggins *et al.* investigated the procoagulant activity of pelletable material (100,000 x g ultracentrifugation) in normal urine [62]. Representative examples for images of EVs including electron microscopy are shown in Figure 2.1. Several years later, membrane vesicles of tubular (100,000 x g pellet) [63] and podocyte (200,000 x g pellet) [64] origin were described in urine from patients with glomerulonephritis. However, uEVs caught wider attention in 2004 when Pisitkun *et al.* provided a thorough characterization of uEVs pelleted by ultracentrifugation of urine at 200,000 x g [8]. In this pioneering mass spectrometry analysis, the authors identified 295 proteins including typical proteins originating from nephron epithelial cells and urothelial cells, as well as proteins involved in the formation of multivesicular bodies. This initial overview of the proteome of uEVs and the evident alteration of the molecular composition of uEVs in pathological conditions opened a new frontier of biomarker discovery, sparking an exponential growth in uEV research and providing new possibilities for the use of urine in noninvasive clinical diagnostics. Urinary EV isolates enabled the detection of molecules that were not previously identified in urine because of their low concentration in the bulk fluid or because of their location inside EVs. Importantly, many of these low concentration proteins are connected to specific cells and/or organs [65, 66].

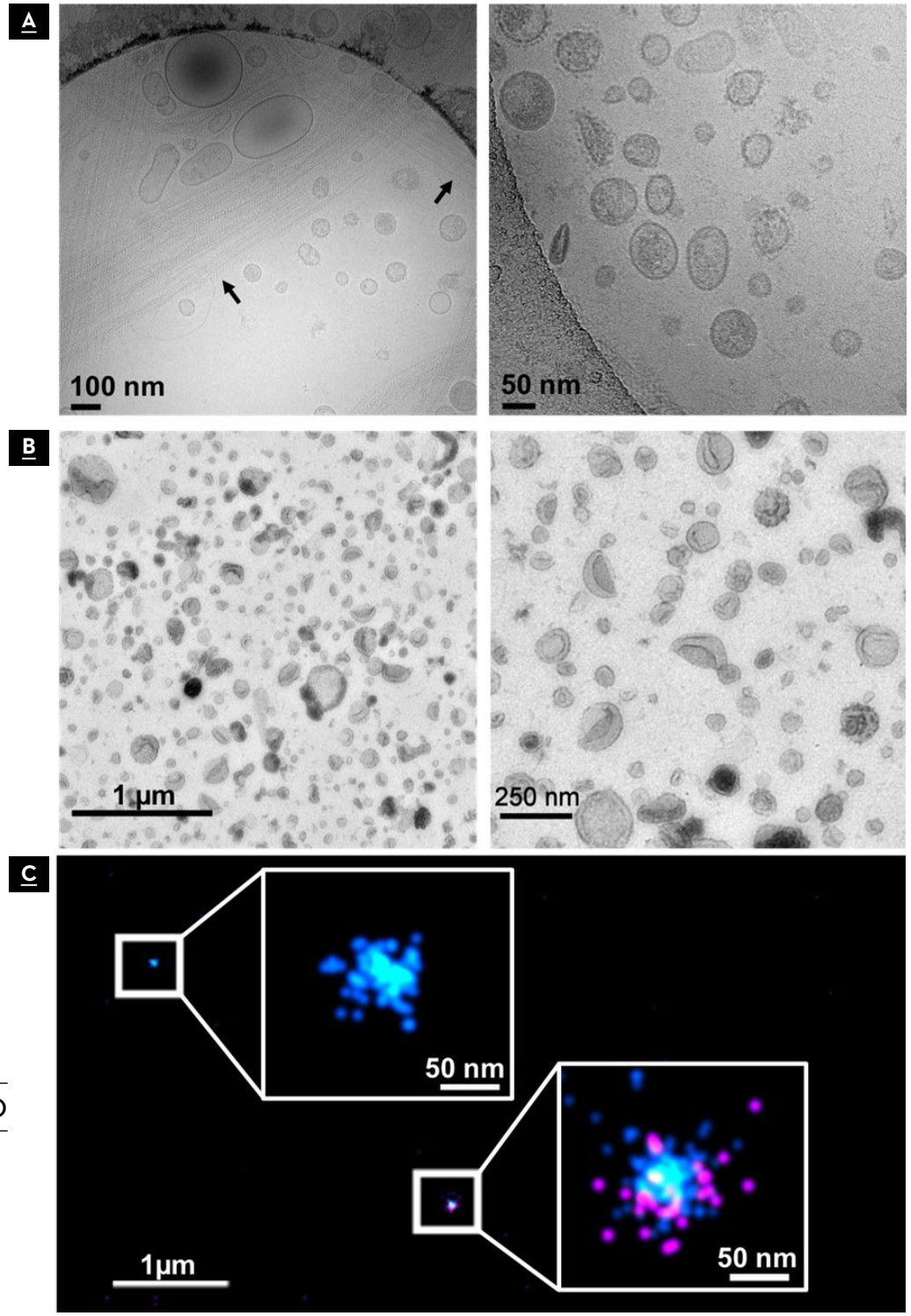

FIGURE 2.1 **uEV microscopy**

A Urinary EVs (uEVs) were isolated by centrifugation (20,000 x g pellet) and processed for cryoelectron microscopy (as described in [25]). The left image shows a wide variety of EVs in size, density and shape. In addition, polymers of uromodulin are shown which seem to entrap uEVs (see arrows). The right image shows a higher magnification of uEVs demonstrating spike like structures emerging from the phosphobilipid layer which likely represents the glycocalyx of some uEVs.

B uEVs were isolated with ultracentrifugation (100,000 x g pellet) and processed for Transmission electron microscopy (TEM) using a negative staining protocol (as described in [139]). To the left we see a lower magnification image displaying a large number and variety of uEVs in size, shape and density. The right image shows a higher magnification demonstrating the uEV heterogeneity with differential staining densities and some spike like surface features that can be visualized despite the cup shape morphology which is due the processing of TEM.

C Super-resolution images were obtained using a Nanoimager S Mark II microscope from ONI (Oxford Nanoimaging) equipped with 405 nm/150mW, 473 nm/1W, 560 nm/1W, 640 nm/1W lasers and dual emission channels split at 640nm. The figure shows uEVs stained for CD81 (cyan) and Klotho (magenta) using primary antibodies conjugated with Alexa Fluor 555 and 647 respectively. Representative images with zoomed in insets show the expression and nanoscale distribution of the peptide and tetraspanin on the surface of two representative EVs bound to the coverslip surface. Two-channel dSTORM data was acquired sequentially at 30 Hz in total internal reflection fluorescence (TIRF) mode. Single molecule data was filtered using NimOS (Version 1.7.1.10213, ONI) based on point spread function shape, photon count and localization precision to minimize background noise and remove low precision localizations.

Urinary EVs have generally been considered to originate from cells of the urogenital tract and the residing bacteria and may be mixed with similarly-sized viruses (Figure 2.2). Therefore, uEVs constitute a source of potential molecular biomarkers for diseases of the kidneys, bladder and urogenital tract (prostate, uterus/vagina), and likely play a functional role in the physiology and pathology of these organs [4, 67, 68]. Importantly, however, proteins arising from other distant anatomical sites in the body have also been identified in uEVs. For example, uEVs have been proposed as a source of biomarkers for diseases such as Parkinson's disease and lung cancer [69, 70]. Nevertheless, analysis of uEVs may open a window into the EV-repertoire of the circulation and provide a systemic readout of disease states from a non-invasive sample.

Both standard analytical methods and high-throughput omics technologies have been applied in (urinary) EV biomarker research, leading to the discovery of numerous potential EV-based biomarkers for a range of diseases. Early studies focused mainly on cancers related to the urogenital system and led to the identification of protein, mRNA, miRNA, lipid and metabolite biomarkers for prostate, bladder, and renal cancers [71-87]. In particular, two prostate-associated

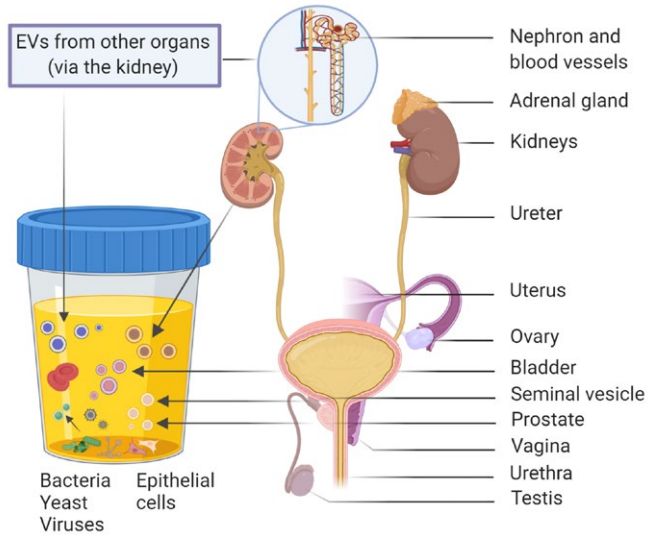

FIGURE 2.2 **Origins of urinary EVs**

RNAs, PCA3 and TMPRSS2:ERG, were identified in urinary extracellular vesicles by Nilsson et al. in 2019 [80]. These results were the foundation for a prostate cancer diagnostic test that has been extensively validated in two prospective multi-center US studies [88, 89]. Altogether, these promising results inspired the search for uEV-based biomarkers for other urogenital tract pathologies such as polycystic kidney disease, cystinuria, diabetic nephropathy, acute kidney injury/ renal ischemia-reperfusion injury, glomerulonephritis, renal interstitial fibrosis/ chronic kidney disease, lupus nephritis, nephronophthisis-related ciliopathies, tubulopathies and primary and secondary hypertension [11, 90-108]. Many of the newly identified candidate biomarkers have not yet been validated in large independent cohorts or in additional laboratories, but nevertheless these examples highlight the enormous potential for uEV analyses as readouts for pathophysiological alterations within the urogenital and other systems.

The diverse origins and dynamic molecular composition of uEVs present an enormous analytical challenge. It is therefore unlikely that a single standardized approach for urine collection, uEV isolation and measurement will effectively cover all disease scenarios and questions. Nevertheless, arriving at a consensus on best methodological practices is of particular importance in preclinical and clinical uEV studies addressing biomarker discovery and validation, where new understanding would ultimately be applied to inform clinical decisions. Herein, we give a brief overview of the state of the art in uEV research and identify the critical knowledge gaps. We also provide recommendations regarding biospecimen handling, processing and reporting requirements to improve experimental reproducibility and interoperability. This is of utmost importance for the development of high quality, multi-site studies and realization of the true potential of uEVs in varied clinical settings.

2.3 Biology of urinary EVs

2.3.1 Origins of uEVs

Urine contains a mixture of EVs that originate from several parts of the urogenital tract, including the kidneys, bladder, prostate (males), and utero-vaginal tract (females) (Table 2.1 and Figure 2.2) [8, 65, 109]. The biogenesis of this heterogeneous EV population including exosomes, microvesicles, apoptotic bodies, is illustrated in Figure 2.3 and discussed in detail in other review papers [110, 111]. The relative contributions of each part of the urogenital tract to the total population of uEVs has not yet been determined, but it has been shown that specific subpopulations of uEVs in urine can be enriched by particular interventions, *e.g.* the collection of urine after digital rectal examination (DRE) increases the amount of prostatic fluid in urine and subsequently the quantity of EVs originating from prostatic luminal epithelium cells [112, 113]. Hence, it is possible to manipulate the uEV composition in this and perhaps other ways, in order to facilitate the detection of specific uEV-associated molecules.

Apart from being produced by different cell types in the urogenital tract, uEVs can also originate from residing immune cells, bacteria and yeast, while enveloped viruses, themselves a type of EV, may also be present [7, 90, 114, 115]. In addition, some reports suggest that a subset of uEVs enters the urine from the circulation and contain many immunity-related proteins [6, 116]. It is unclear how these EVs reach the urine [116, 117]. In order to pass the glomerular filtration barrier (GFB) and basement membrane of the kidney the EVs would have to be smaller than the membrane-pores (6 nm in the healthy state), or the integrity of the membrane-pores would need to be perturbed (something seen in various pathological states), allowing passage of larger structures like EVs from the circulation into the urinary space [118, 119]. Larger pores of the slit diaphragm of up to 70nm in size are found in minimal change disease, an example of a proteinuric disease state with podocyte damage. Small EVs are likely able to move through this barrier in this disease state. In addition, the endothelial barrier of the GFB might also be penetrated as it has fenestrae of up to 100nm in size which can also allow EVs to move through the GFB [120]. Alternatively, it is possible that uEVs preparations include non-vesicular circulating proteins. It is likely that these are endocytosed from the blood by renal tubular cells as it has been demonstrated for modified circulating albumin molecules in diabetes [121]. The proteins are then released into the urinary space within EVs. This is supported also by proteomic data, in the case of albumin it is shown that uEVs contain this protein [25]. Similar mechanisms have been described as early as 1989 suggesting that EVs might be transported by transcytosis through podocytes and secreted into the luminal side as 'waste' [122].

TABLE 2.1 **List of uEV markers characterizing different structures of the urinary tract. The markers were described in uEVs isolated from human urine and identified by Western blot and/or flow cytometric analyses**

ORGAN	STRUCTURE/CELL OF ORIGIN	EV MARKER	REF
Kidney	Glomerulus (Podocytes)	Podocin	[319]
		Podocalyxin	[319]
		Wilms' tumor 1 (WT 1)	[320]
		Complement receptor 1 (CR1)	[321]
		Canonical transient receptor potential 6 (TRPC6)	[319]
		Nephrin	[319]
	Glomerulus / proximal tubule	Angiotensin-converting enzyme (ACE)	[8]
	Proximal tubule	Megalin	[8]
		Aminopeptidase N (APN)	[8]
		Cubilin	[319]
		Sodium/glucose cotransporter 2 (SGLT 2)	[74]
		Carbonic anhydrase (CA IV)	[8]
		Na^+/H^+ exchanger isoform 3 (NHE3)	[131]
	Renal progenitor cells	CD133 (Prominin 1)	[137]
	Tubular epithelial cells	CD24	[278]
	Proximal tubule / Henle's loop	Aquaporin 1 (AQP1)	[8]
	Henle's loop	Uromodulin (UMOD, Tamm-Horsfall Protein, THP)	[8]
		Na-K-2Cl cotransporter (NKCC2)	[8]
	Proximal tubule / distal tubule	Klotho	[322]
	Distal tubule	Prominin 2	[323]
		Thiazide-sensitive Na-Cl cotransporter (NCC)	[8]
	Distal tubule / collecting duct	Aquaporin 2 (AQP2)	[8]
		Claudin 1	[323]
	Collecting duct	Mucin-1	[8]
Bladder	Transitional epithelial cells	Uroplakin-1	[8]
		Uroplakin-2	[8]
		Mucin-1 (MUC-1)	[8]
Prostate	Epithelial cells	Prostatic acid phosphatase (PPAP)	[74]
		Prostate transglutaminase (TGM4)	[75]
		Prostate-specific membrane antigen (PSMA)	[81]

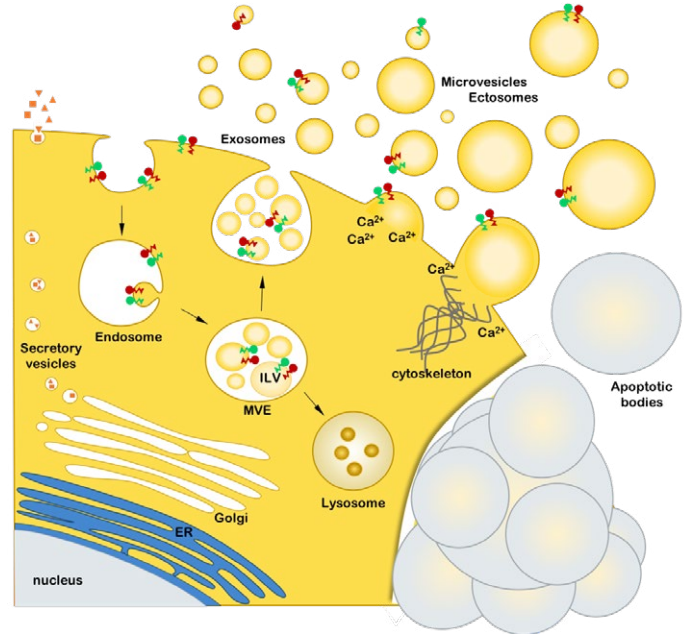

FIGURE 2.3 **Biogenesis pathways of urinary extracellular vesicles (uEVs).**

EVs are a highly heterogeneous group of membrane-bound particles released by both healthy and malignant cells. Biosynthesis of exosomes, a specific population of **small uEVs**, occurs via formation and maturation of **multivesicular endosomes (MVEs)**. Exosomes are formed as **Intraluminal vesicles (ILVs)** in the lumen of MVEs by inward budding of the endosomal membrane. Upon fusion with the cell membrane, exosomes are released into the intercellular space. **Microvesicles and ectosomes** represent both smaller and larger EVs and are formed by outward budding and scission of the plasma membrane. The process is associated with the accumulation of Ca2+-dependent enzymes that change the polarity of membrane phospholipids. This causes physical bending of the cellular membrane and rearrangements in the underlying cytoskeleton, leading to the formation of microvesicles. Once released by the cell, small uEVs formed at the PM and MVB-derived exosomes exhibit overlapping size and composition, which makes it difficult to establish their biosynthetic origin. **Apoptotic bodies** are formed during apoptosis (programed cell death) when cells undergo characteristic outward blebbing caused by breaks in the cytoskeleton. During this process the cellular membrane bulges outward and portions of the cytoplasm and its contents separate forming apoptotic bodies. **Secretory vesicles (SV)** are produced by the ER and Golgi apparatus. Most of them have specialized cargo such as hormones and neurotransmitters. SVs fuse with the cell membrane at specialized supramolecular structures (porosomes) to release their cargo in the extracellular space.

An additional enigmatic particle type, known as nanobacteria or calcifying nanoparticles [123] is discussed controversially. These entities are composed of crystalline minerals, nucleic acids, and other organic material and appear to be replication competent, albeit through ill-defined processes. Nanobacteria have been associated with various diseases like nephrolithiasis, poly-

cystic kidney diseases, chronic prostatitis, and pelvic pain syndrome [124-126]. It remains unclear to what extent these structures contribute to the uEV pool. Further, EVs from both Gram-positive and Gram-negative microorganisms, along with viruses inhabiting the urinary system, are also readily detectable in urine and can be indicative of metabolic or pathological microbial activity [127-129].

2.3.2 Molecular composition of uEVs

Urinary EVs contain proteins, nucleic acids, lipids and metabolites. In recent years, the Vesiclepedia repository (V4.1; microvesicles.org, accessed 17 July 2020) [130] has expanded exponentially and, at time of this writing, contains data from 1254 EV studies, including 38,146 RNA entries, 349,988 protein entries and 639 lipid/metabolite entries. From this list, 89 studies (7%) used urine as the EV sample source.

The protein composition of EVs pelleted at 100,000 - 200,000 x g from urine of healthy individuals has been extensively investigated. In these conditions, approximately 0.6 - 3% of the protein in urine is associated with this EV fraction [131, 132]. The first mass spectrometry study of uEVs in 2004 (200,000 x g pellet) detected 295 proteins [8, 65]. By 2009 the number of identified proteins reached 1132 [8, 65], likely due to improvements in mass spectrometric techniques. The use of newer generation mass spectrometry instrumentation has expanded the uEV proteome to over 3,000 proteins, enabling deeper analysis of EV biology and identification of additional biomarker candidates [73, 98, 133, 134]. Proteins identified in uEVs include membrane trafficking components, cytoskeletal proteins, motor proteins, membrane transporters and glycosylphosphatidylinositol-linked proteins [131]. In agreement with the idea of uEVs having diverse cellular origins, characteristic proteins of the different organs of the urogenital system, *i.e.* the kidneys (glomeruli, proximal tubule and distal tubule), the bladder and the prostate, have been detected in uEVs [8, 65, 135] (Table 2.1 and Figure 2.2). For comprehensive discussions of the proteomic analysis of uEVs we refer the reader to review papers on this topic [67, 116]. The analysis of uEV surface markers by flow cytometry and Western blotting has confirmed the presence of uEVs derived from the cells lining all nephron segments (Table 2.1) [136]. The presence of podocin, podocalyxin or nephrin indicate uEVs from glomerular podocytes, whereas the presence of megalin, cubilin, aminopeptidase or aquaporin-1 (AQP1) indicate uEVs from proximal tubular cells. Uromodulin (UMOD, also known as Tamm-Horsfall protein (THP), CD9, and type 2 Na-K-2Cl cotransporter (NKCC2) mark uEVs from the cells of Henle's loop and aquaporin-2 (AQP2) marks uEVs from collecting ducts. CD133 identifies uEVs from proliferating/progenitor tubular cells [137]. Finally, bladder derived uEVs contain uroplakin [8].
Lipids and different metabolites are also components of uEVs, but only a few studies have focused on these molecules [77, 82, 85]. A recent lipidomic study identified over 100 lipid species by mass spectrometry in uEVs (100,000 x g pellet). These EVs showed a remarkably high content of cholesterol (63%), with phosphatidyl serine 18:0/18:1 being the next most abundant lipid species [77]. In addition, uEVs have a higher cholesterol content compared to plasma derived EVs [138]. Another recent study using targeted ultra-performance liquid chromatography-tandem mass spectrometry identified metabolites from five main categories of metabolites in uEVs (organic acids and their derivatives, nucleotides, sugars and derivatives, carnitines, vitamin B/ related metabolites and amines). The most abundant metabolites detected were ornithine, creatinine, D-ribose 5-phosphate, L-cystathionine, alanine and serine [139].
The membrane of uEVs is highly decorated with a variety of glycans linked directly to the proteins and lipids of the EV membrane. The abundance of different glycosylations adds to the biomolecular complexity of uEVs and it has been shown that these integral structural and functional components play a role in EV uptake [140]. Analysis of uEV carbohydrate content by mass spectrometry and lectin arrays demonstrated that uEVs are highly enriched in complex type N-glycans, with terminal modification consisting of mannose and fucose residues [111, 141]. For a detailed review of EV glycosylation see Williams *et al.* [142].

The presence of RNA in EVs was discovered in 2006 and the first reports of mRNAs and miRNAs in uEVs followed soon after [80, 143-148]. So far, most studies of small noncoding RNAs in uEVs have focused on miRNAs, but other noncoding RNAs such as small nuclear RNAs, small nucleolar RNAs, tRNAs and lncRNAs or fragments thereof have also been found in pelleted uEVs [149-153] and in SEC-enriched uEVs [154]. Non-coding RNAs were found to be the predominant nucleic acid cargo in the deep sequencing study of uEVs by Miranda *et al.* [155]. However, more than 13,000 protein coding genes were detected as well, along with abundantly present rRNA transcripts. A total RNA sequencing approach by Everaert *et al.* and a poly-A based RNA sequencing approach targeting mRNAs by Barreiro *et al*, confirmed this vast representation, as they reproducibly detected transcripts from over 10,000 genes in uEVs, which was found to be the highest number of all evaluated biofluids [156, 157]. Interestingly, uEVs were also shown to be a good source of novel RNA species, such as circular RNAs. In conclusion, many studies have shown the association of RNA and uEVs. However, since RNA can also be found in other molecular structures than EVs, it is recommended to show that the EV-RNAs resist mild degradation by proteinases and nucleases [5, 158, 159]. It is not yet clear whether DNA is present in the lumen of uEVs, but DNA may be found on their exterior [132, 147]. Concerning DNA in the uEV lumen, a study showed that no large differences were observed when comparing the read distribution of the uEV inner nucleic acid cargo with and without DNase I digestion following deep sequencing [155].

These and many other studies have given us an overview of the molecular composition of uEVs. Nevertheless, it is generally recognized that the different EV isolation methods do not entirely remove all non-vesicular material and that the methods separate distinct EV populations to a different extent [5]. Hence when reviewing such data, care and caution are needed, as some of the identified molecules may not represent genuine EV-related components and/or the specific EV population that is being investigated.

2.3.3 Physiological functions of uEVs

Increasing evidence indicates that EVs released into the urine can be internalized by other cells and can modulate their function, suggesting the presence of intra-nephron communication along the urinary lumen [160]. By electron microscopy studies, EVs were shown to be internalized by proximal tubular epithelial cells through cilia *in vitro* [46]. Moreover, other *in vitro* studies showed that collecting duct-derived EVs could be internalized by tubular cells, transferring AQP2 [161]. Treatment of cultured tubular epithelial cells with podocyte-derived EVs induced a profibrotic phenotype, potentially identifying a novel form of glomerular-tubular communication [162]. Studies have also identified a role for uEVs in innate immunity [7].

In addition, the accumulation of a diverse mixture of uEVs in the bladder followed by their expulsion from the body through urination strongly suggests a principal role for uEVs as a route of elimination. It remains undetermined if excretion through urine is the primary mode for eliminating EVs in general including circulating ones or whether this is mostly related to EVs of the genitourinary system. The study of the physiological functions of uEVs is still in its infancy.

2.4 Current state of the art of urinary EV research

2.4.1 Collection, processing, and storage of urine for uEV research

Urine collection, processing and storage are important topics that should be carefully considered in uEV studies because they are major sources of data variability and can limit reproducibility [71, 131, 163]. Currently, only general guidelines like the Biospecimen Reporting for Improved Study Quality (BRISQ), including urinalysis and standards (ISO 20387:2018) are established for best practices in urine biobanking [164, 165]. Studies addressing collection, processing and storage of urine specifically for uEV research are very limited. The data can be profoundly influenced by the up-front pre-analytical variables, where biospecimen handling is subject to different methods, *e.g.* in collection times, preservatives or centrifugation (Table 2.2). These differences can lead to selective and variable inclusion of EV subpopulations and non-EV contaminants such as cells or their fragments, uromodulin networks and protein aggregates. Therefore, it is of utmost importance that the modality of urine handling is consistent within any study. In addition, for interoperability, it is essential that the reporting of such methods is also harmonized across research teams. The EV field would highly benefit from proficiency testing trials that could ideally be conducted in collaboration with biobanks (*e.g.* www.ibbl.lu/ibbl-bioservices/biospecimen-proficiency-testing/). Within ongoing and future urine biobanking studies, we consider that special focus should be put on method validation/consistency and particularly on identifying the most and the least variable preanalytical parameters that affect EV research (Table 2.2)

Individual research studies have typically employed different urine collection and storage approaches. This is often a result of study-specific protocols and/or logistic restrictions. Large professional biobanks are designed to allow measurement of a wide variety of urine analysis parameters, meaning that the sample collection and storage protocols used might be sub-optimal for uEVs. Therefore, it is unlikely that a universal pre-analytical procedure will be adopted for all uEV studies. Instead, it is more likely that different best practice protocols will be established depending on the molecular component of interest, the choice of analytical platform(s) and the investigated health condition or disorder. As long as standard operating procedures for collection and storage of uEVs are not established by the community, it is safest to report all available pre-analytical information related to the studies in the EV-TRACK knowledgebase, in accordance with the Minimal Information for Studies of Extracellular Vesicles 2018 (MISEV2018) and other ISEV rigor initiatives as well as other suited guidelines developed particularly for preanalytical variables of fluid samples [5, 166-171]. This will enable a better understanding of the impact of these variables and ideally enable more meaningful comparisons between different studies. In the future, the evaluation of pre-analytical conditions could be used to establish case-specific "Best Practice" protocols. Below we provide the current state of the art of uEV research which also includes common practices. This will be followed by consensus recommendations and an indication of knowledge gaps in the field of uEV research.

2.4.1.1 Patient information

Demographic and clinical parameters including gender, age, ethnic background, weight, height, fluid intake, diet, time of urine collection, laboratory measurements and medication *etc.* should be recorded to identify potential sources of variability, confounders and introduction of unintended bias through the selection of inappropriate members in these cohorts [172]. When possible, particular attention should be paid to clinical information about kidney function (*e.g.* glomerular filtration rate, albuminuria) as a pathological condition of the kidney has a major effect on the urine and uEV composition [173]. Kidney pathology may also affect uEV excretion, potentially biasing normalization at a later stage (see below). A good example of a study in which careful clinical characterization was done and kidney disease was ruled out as a confounder is a recent examination of uEV cargo as markers for neurological disorders [174]. It is also important to record a patient's use of diuretics or other drugs which may drastically affect urine composition and pH. pH has been reported to affect uEV physiology and isolation [58, 175]. In addition, urinary pH is highly influenced by diet, i.e. vegetarian diet causes a high alkaline load [176, 177]. Therefore, reporting general dietary information may improve interpretation of results. Guidelines for appropriate biospecimen reporting for initiation of studies have been developed by several organizations, and some offer online tools to assist with this [178]. Nonetheless, detailed information about the patient population under investigation is an aspect that is notoriously under-reported in the literature, a recognized general failing of biomarker studies [164].

TABLE 2.2

Reporting on urine collection, processing and storage. Reporting priority level is primarily meant to indicate the importance of recording a specific parameter in a biobank database. Not all of these parameters are relevant for publication reports. The evidence level is an expert consensus opinion of the current level of confidence that the parameter is a variable to consider during sample biobanking and data analysis and interpretation.

PARAMETERS	REPORTING PRIORITY LEVEL	EVIDENCE LEVEL	WHAT TO REPORT	RECOMMENDATION
Research subject information (demographical and clinical data)				
Species	Obligatory	High: There are clear species-specific differences that impact all of their characteristics	Species, subspecies	Record: Species and subspecies information
Gender/ Biological Sex	Obligatory	High: There are clear gender/sex differences between urine biomarkers (e.g. creatinine, prostate EVs)	Male, Female, Genderqueer	Make sure to gender-balance cohorts to be compared
Age	High/Obligatory	Medium: Based on mesenchymal stem cells and blood EVs (reviewed in [324])	Age in years	Make sure to age-match cohorts to be compared
Clinical Data, e.g. diseases, kidney function parameters, medication, comorbidities	High/Obligatory	High: Clinical parameters are essential for disease/condition/ organ-related EV research	Clinical parameters in standard units	• Utilize urine dipstick • Measure urine creatinine • Measure disease-specific markers (e.g. urinary PSA for prostate and albumin for kidney research) • Record all relevant clinical parameters
Supporting information, e.g. BMI, ethnicity, diet, fluid intake, geographical information.	Medium	Medium-High: Certain supportive information is important to record as it might influence urine EVs	Supporting parameters in standard units	Determine relevant supporting information and record them: Based on the study goal, supporting information can be crucial
Urine collection				
Pretreatment	Obligatory	High: The most common pretreatment methods prior to urine collection (DRE, prostate massage, catheterization) can have an effect on the EV content of the sample[113]	DRE and/or prostate massage (yes/no, Number of strokes) Catheterization (yes/no)	Any manipulation which could affect the composition of the urine should be reported in detail
Ethical approvals	Obligatory	N/A	Approving authority, Informed consent forms, collection details (origin, type and number of samples)	All collected samples should be linked to designated ethical approval, applied for uEV research
Collection method	Obligatory	Medium: The information of the transition of urine through the urethra is important particularly for disease-related uEV studies	• Clean-catch • Sterile urine bag • Assisted (urethral catheterization, suprapubic aspiration, • pediatric specimen • Animal collection cage	Details of the collection method e.g. use of syringe, possible transfer of the sample to container
Time and type	Obligatory	Medium: uEV concentration can vary depending on the urine transition time from the bladder	• Collection type (morning/random/spot) • Timed collection, e.g. 24 hour	Type of collection e.g. random/spot urine, first or second morning urine. Record: Time between the last uncollected and collected void
Volume and void	Obligatory	Medium: The collection of first void urine transitioning from the urethra may affect the uEV quantity/composition	• Void (first/mid/full) • Volume in ml	Collection of midstream urine is recommended to avoid microbial contamination
Collection device and container type	Medium	High-Medium: Certain containers and devices may have an effect on the uEV content; e.g. the material may bind EVs or contain microbial contaminants if not sterile	• Brand • Sterile yes/no • Material • Open/closed	The container should be clean, leak-proof, urine pH-range resistant and not shed plastic particles. Record: Material, manufacturer, lot number
Storage prior to processing				
Storage Time	Obligatory	High: Longer storage time may lead to microbial growth, cell debris and particularly to degradation of more labile biomolecules (e.g. RNA)	Hours	Samples should be stored max. 8 hours before processing
Storage Temperature	Obligatory	High: Freshly collected urine samples should be cooled promptly to avoid microbial growth or biomolecule degradation	Degrees Celsius	Max 40C is recommended
Light Protection	Medium	Low: Some urinary analytes may be light sensitive (e.g. bilirubin, porphyrins); impact on uEVs unknown	Light protection (yes/no)	Use of amber-colored/dark collection tubes

TABLE 2.2

PARAMETERS	REPORTING PRIORITY LEVEL	EVIDENCE LEVEL	WHAT TO REPORT	RECOMMENDATION
Urine quality control				
Use of Dipstick	High	High: Presence of *e.g.* cells, microbes and high protein levels affects purity and composition of uEV population	• Yes/no • Brand • Deviating parameter(s)	Recommended for preliminary urine assessment (pH, protein level) and exclusion of deviating samples (blood, microbes)
Preprocessing				
Collection Container preparation	Medium	Medium: Preservative might be affected by time and storage in collection container	• Preservative already present in collection container (yes/no) • Preservative in container freshly prepared (yes/no)	• Keep the protease inhibitor cocktail on ice or at the manufacturer's recommended temperature at all times • If protease inhibitors are used at collection time, it is recommended that sample containers are prepared by adding protease inhibitor cocktail and keep frozen at -20oC for max. 6 months until use • Alternatively, prepare fresh and use immediately
Urine sample preprocessing	High	High: Freshly collected urine samples should be cooled promptly to avoid microbial growth or biomolecule degradation	• Time • Temperature	• Process urine within 4-6 hours from sample collection • Consider addition of protease inhibitors or preservatives when fast processing (>6 hours at 4oC) is not possible (see below)
Urine Centrifugation	Obligatory	Medium: 800 g to sediment cells and debris without damaging urine cells	• G-force • Volume/tubes • Temperature • Time	• Homogenize urine sample before centrifugation • G-force range 500 to 800 g • Centrifugation at 4oC
Recovered Supernatant (method/volume)	High	Medium: Largely operator-dependent	• Pipetting, decanting, pouring • Recovered volume	• Loose pellets (low speed centrifugation, *e.g.* <1,000 x g): Pipetting without disturbing the pellet is recommended to avoid pellet carry over • Tight pellets: uniform procedure for all samples
Other urine fractions	Low	Medium-High: To monitor the purification process of EVs	• Pellet • Whole Urine	• Less-used source of EVs • Collection for use as controls or exploration of EVs in these fractions is recommended
Collected aliquots of Supernatant	Obligatory	Medium: As samples may be used for several techniques/ isolation protocols, aliquots of different volume may be required to avoid repeated freeze/thawing and to optimize workflows and storage capacity	• Number of aliquots • Date • Volume (if different volumes are collected)	• Immediate freezing at -70°C or colder is recommended after aliquoting • Suggested volumes of aliquots: Large (up to 30 mL) Medium (5 - 10 mL) Small (1 - 2 mL)
Storage				
Storage container	High	Medium: Should resist pH range of urine and not shed any particles, low EV (protein or lipid) binding properties generally beneficial	• Brand • Volume	Use of the maximum volume of the container is recommended to accommodate the expansion of the sample due to freezing
Temperature	Obligatory	Medium-High: EV yield may be lower from samples stored at -20°C	• Degrees Celsius	-70°C or colder is recommended
Method of freezing	High	Low: Quick freezing is generally recommended to preserve biological specimens, but tests and impact on uEVs of about speed of freezing speed or cryoprotective agents in urine are lacking	• Snap freezing in liquid nitrogen • Freezing at a freezer • other if applicable, e.g. gradual freezing or use of cryoprotective agents	Freezing quickly at -70°C or colder or in liquid nitrogen is recommended
Defrosting				
Temperature	Obligatory	Low: The effect of thawing temperature on uEVs has not been extensively studied, but might affect heat labile biomolecules or to sediment formation	Degrees Celsius	Record: The temperature(s) at which the sample has been thawed

TABLE 2.2

PARAMETERS	REPORTING PRIORITY LEVEL	EVIDENCE LEVEL	WHAT TO REPORT	RECOMMENDATION
Method	Obligatory	N/A	Heating pad, water bath, incubator, room temperature, refrigerator	• If applicable, the model and type of the device used for the thawing • Defrosting should be done equally for all compared samples
Time	High	Medium: For longer thawing times preservatives may be needed	Minutes, hours	• Record: The time it takes to completely thaw the sample • Prolonged warming not recommended to avoid microbial growth
Additives at time of collection:				
• Protease inhibitors • RNase Inhibitors • Chemical preservatives, e.g. azide	Obligatory	Medium: Preservatives inhibit microbial growth and protease inhibitors preserve certain urine proteins (many proteins are not prone to proteolysis)	• Type • Name • Brand • Final concentration • Stage/time at which additive was used (to whole or pre-cleared urine)	• Relevant only for longer collection times (inhibiting microbial growth) or for specific down-stream EV applications (e.g. surface antigen characterization). • Preferably use preservatives targeting specific enzymes (e.g. RNase), as general (RNA) protecting agents likely affect EVs • Add selected preservatives immediately at the time of urine collection
Sample transportation				
Temperature	Obligatory	Medium-High: EV quality and quantity diminish with long-term RT and by multiple freeze-thawing. Preservatives can prevent protein/RNA breakdown and bacterial outgrowth	• Degrees Celsius at transport and degrees Celsius at arrival • Cooling system, when applicable (e.g. ice)	Aliquot urine and freeze at -80°C to be transported frozen at -80°C. For non-aliquoted fresh urine (e.g. home-testing), immediate transport at RT or 4°C can be considered, particularly when preservatives are added
Time and Method	High	Medium-High: EV quality and quantity diminish with long-term at RT. Container leakage could introduce contamination	• Transport duration in hours • Container damage/leakage	Record: Transport duration and container damage
Existing biobanks				
Existing urine sample collections	N/A	High: Existing urine biobanks with protocols not optimal for EV preservation are often used for research	N/A	• Collect all above-mentioned parameters and determine appropriateness of the sample collection for your research purpose • Perform tests to determine urine quality, number and characteristics of EVs as described in sections 3.3-3.4

2.4.1.2 Instructions and donors

Urine collection is typically performed by the donors themselves. Thus, before the collection, clear and concise instructions on the sample collection process including appropriate hygiene should be given, ideally in both spoken and written forms. As the collection methods may be quite complex or laborious and instructions as well as donors differ greatly, highly standardized collections are difficult to achieve [179].

2.4.1.3 Time and void

Urine can be collected during a single voiding episode ("spot urine collection") or can be collected across several voiding episodes during a fixed time period ("timed urine collection"). Spot urine collections can be done at a random time ("random" spot urine) or standardized to the first or second morning urine. Timed urine collections can be over the course of hours or a day (called "24-hour urine"). The volume of urine collection can be "full void" or "midstream urine" (*e.g.* without collecting the earliest portion of the voided urine). Relatively little is known about the impact of different collection types on uEV measurements.

The first morning urine is generally more concentrated than a random spot urine [180], possibly resulting in a higher uEV concentration in the first morning urine. Zhou *et al.* found only minor differences between first and second morning urine with respect to total protein in uEVs or exosome-associated proteins [131]. Another study of uEVs from first and second morning voids in three control males showed that only 4 % of the identified proteins by mass spectrometry were significantly altered in abundance between the two conditions [74]. Nevertheless, specific uEV biomarkers may fall within this fraction, and it is therefore recommended to determine the stability of identified biomarkers in relation to pre-analytical variables. In addition, physiological processes in the kidney and some kidney bio-markers follow a circadian rhythm [181]. It is currently unknown whether the release of uEVs or the composition of their cargo demonstrate a circadian rhythm in humans, although one study has examined these questions in rodents [182]. Periodicity would be discovered only by analyzing timed urine collections, ideally gathered in fractions over 24 hours [181].

In the case of a timed collection, documenting and reporting the time between the last uncollected and first collected void would help with assessing urine transition time in the bladder and may be of additional value for normalization. For example, uEV protein content could be related to a time period of 4 or 6 hours, which might be easier to collect than 24-hour urines. In many prostate cancer studies, urine samples are collected after a DRE by the urologist. Collection at this time point can greatly increase the amount of prostatic fluid in the urine and consequently enriches the sample for prostate-derived EVs [112, 113, 183].

The collected urine void impacts the availability or enrichment of specific EVs and other urine components. First void after DRE has been shown to increase the chance of finding prostate cancer associated EVs [88, 183]. However, first void also contains more cells and bacteria than the mid-stream void, leading to 36% of urine samples to exceed health related upper reference limit vs 10% of mid voids [184]. It is unclear which urine collection is the "cleanest" without significant contamination by cells or bacteria. Reduction of microbe content requires attention to the entire uEV workflow [185]. Another point to be addressed is the need to establish an optimal workflow that addresses the presence of bacterial outer membrane vesicles (OMVs) in urine (derived from either normal or pathogenic urinary tract microbiota) [127, 128, 186]. Another mechanism that may influence EV secretion rate includes urinary flow; *i.e.* kidney tubule cells have cilia that may be activated by flow and have an important role in EV secretion [48]. However, the *in vivo* implications have not been studied.

Little is known about the inter-day variation of uEVs. For example, Wang and others investigated the variability of the uEV proteome in morning urine from two healthy volunteers over a two-month period [174, 187]. They showed that approximately 50% or hundreds of uEV proteins were stable at the inter-day and intra-individual level. As expected, most variation was found within the low abundance proteins. Some of the stable proteins could be classified as housekeeping, including numerous heat shock proteins, actin and annexin A4. On the RNA level, Murakami *et al.* [188] have found that the expression of some uEV mRNAs from different parts of the kidney were stable on the intra-individual level over a two-week period. On the other hand, larger inter-individual differences were found. While the authors could confirm the stability of five mRNAs among the subjects, further studies are needed for discovery and validation of truly stable control uEV RNAs.

2.4.1.4 Collection containers and devices

Urine collection containers are typically made of plastics, such as high-density polyethylene or polypropylene, can be sterile or unsterile, open or closed, anatomically compatible or have tube transfer systems. Some even have a urine temperature thermometer affixed to the outside of the cup. There are no studies known to have tested the impact of different containers on uEV collection. However, it is important to ascertain that containers should not bind uEVs or shed (plastic micro-) particles. Models with a lid are preferable to prevent the introduction of external EVs. Sterile tubes may be especially important for studying microbial uEVs. Specialized collection devices might be needed (*e.g.* urine bag for infants) or part of a protocol for standardized collection of different voids (*e.g.* first 20 mL void using a Colli-Pee device, Novosanis, Belgium).

2.4.1.5 Preservation: storage before freezing

Unprocessed urine should be kept at 0-4 oC and processed within to 8 hours to avoid bacterial growth, cell lysis, molecular degradation of RNA and protein, and formation of sediments [189-191]. However, it may not be universally recommended to keep urine cold. Armstrong *et al.* found that miRNA and other small RNA contents of uEVs declined during 4-24 hours of storage

after collection, and the decline was greater when samples were kept at 2-40C rather than at room temperature (RT) [192]. The authors discussed that the decline could be due to cold induced precipitation and that it could be rescued by warming the urine sample for 5 min at 370C. Indeed, heating increased RNA yields from frozen samples that had formed precipitates. However, this could also be related to the formation of uromodulin polymers that form when urine is kept cold, *e.g.* below 4 oC [193]. These polymers can trap EVs to some extent, which are subsequently removed from the sample after low-speed centrifugation [193].
With longer timed collections, such as 24h collections, fast processing cannot be achieved, and studies of the possible effect of repeated warming (37oC) and cooling (either to RT or +4oC) of the urine specimen during collection are lacking. However, generally, if long urine collection times are required, the addition of preservatives such as azide should be considered to avoid microbial overgrowth, at least when the preservative is compatible with further uEV processing steps [194, 195]. Effects of RNase inhibitor addition have not been investigated systematically, even though RNAses are present in urine.

Several studies have investigated whether protease inhibitors should be added to urine to avoid uEV protein degradation [81, 131]. Although this may preserve some specific uEV proteins such as NKCC2, analysis of CD9 and TSG101 showed that not all EV proteins are prone to proteolysis in urine [81, 131]. It is important to address this issue more conclusively because urine samples in biobanks are not typically collected with protease inhibitors because the use of protease inhibitors would increase costs considerably, especially in large sample studies. Similarly, when analyzing phosphorylated proteins, the use of phosphatase inhibitors should be considered although it has not been thoroughly studied.

2.4.1.6 Urine quality control

Commercially available dipsticks can be used as a form of rapid quality control by measuring urine pH and various contents (*e.g.* leukocytes, erythrocytes, protein, glucose, nitrate, ketones, blood, bilirubin, urobilinogen) [74, 196, 197]. Information obtained by these rapid, simple procedures identify patient status and allow exclusion of deviating samples, such as those heavily contaminated by microbial infection or blood. However, dipstick use for inclusion/exclusion in uEV studies has been rather arbitrary to date: there is no consensus in defining which dipstick test is most suitable, or on where to set inclusion/exclusion criteria.

2.4.1.7 Clearing before freezing

Frozen, precleared urine is used in many uEV studies. Preclearing usually involves centrifugation to remove cells, large cell debris and often also the bulk of uromodulin, and it is done so that these materials do not contaminate uEV preparations with artifactual, similarly sized particles during freeze-thaw cycles. Interestingly, however, one study found that uEV miRNA/small RNA correlated highly when comparing urine aliquots that had been centrifuged alternatively before freezing or after a freeze-thaw [192].

Several urine processing protocols are currently available from uEV researchers and biobanks *e.g.* the European Association of Urology Standard Operating Procedures in UroWeb (uroweb.org/research/how-we-work/) and the MMI Guidelines for Standardized Biobanking (crdi.ie/resources/biobanking-guidelines/) from the Clinical Research Development Ireland. According to these sources as well as other uEV literature, centrifugation parameters used for preclearing vary widely. For example, the centrifugation speed used ranges from roughly 1-20,000 x g, centrifugation time varies between 0-30 min, and both one- and two-spin approaches are used. Centrifugation volumes, use of a brake and supernatant removal methods also vary between studies, although these parameters are rarely specified in publications. Low speed centrifugation (<1,000 x g) is generally used to remove whole cells and large cell debris, but data has shown that lower speeds may not suffice for this task. A single 400 x g step for 5 minutes results in inadequate removal of cells while efficient cell pelleting was achieved by centrifugation of 10 ml volumes at 1358 x g for 10 minutes in round bottom tubes [198].

Uromodulin, also known as Tamm-Horsfall protein, is the most abundant protein excreted into urine [199]. Most uromodulin can be sedimented with a 2,000 x g spin for 30 minutes without a gross loss of uEVs, whereas speeds ≥ 10,000 x g result in pelleting of uromodulin and EVs [25, 200-202]. Some studies have combined first a lower speed spin, *e.g.* 300 x g, with a second higher speed spin, *e.g.* 2,000 x g [203], to deplete the larger and smaller contaminants consecutively. While this method might be more effective than a single spin, it also adds to the handling time and steps, which can be limiting for large sample numbers.Loss of EVs due to binding to polymeric uromodulin can be reduced or eliminated through use of reducing agents that depolymerize uromodulin by breaking disulfide bridges between individual uromodulin monomers [202].
The choice of preclearing parameters usually depends on the study goal. Ammerlaan *et al.* optimized urine processing (centrifugation speed, time, temperature and brake) for reproducibility in proteomic and metabolomics studies with the criteria that the urine supernatant should still contain the EV component [204]. As depletion of larger EVs (microparticles) was preferred in the original study, the best protocol with low microparticle counts in the recovered supernatant was a 20 min, 12,000 x g centrifugation at 4oC with a hard brake. An optimal pre-clearing/pre-freezing protocol might thus be EV subtype-specific, but in practice, compromises may be necessary when using biobanked samples, because these resources are designed to provide urine samples for a variety of uses.

2.4.1.8 Collection volume and freezing aliquots

The volume of urine required for uEV analysis depends on the yield of the method used to isolate EVs and the sensitivity of the analytical method, but 10-30 ml of urine is sufficient for many purposes, for example RNA sequencing or proteomics [25]. It is advisable to collect and store processed urine in aliquots (as a backup or for use in different analyses). Most urine collection containers collect sufficient volume to allow division into multiple aliquots of suitable size (*e.g.* 1 to 30 ml) which speeds up the freeze and thaw processes and avoids unnecessary pooling of

aliquots or multiple freeze/thaw cycles. Whenever possible, it is recommended to preserve the cellular pellet or the low-speed centrifugation pellet, which may also contain uEVs [25], as well as aliquots of whole urine for monitoring of the purification process, for comparative analyses or as controls.

2.4.1.9 Freezing temperature and storage time

Freezing and storage at -70°C or lower temperature is preferred. Zhou *et al.* showed that storage at -20°C caused more than 50 % loss of EVs compared with storage at -80°C where EV loss was 14 % [131]. Partially supporting these findings, Oosthuyzen *et al.* measured particle count by nanoparticle tracking analysis (NTA) in urine samples stored at room temperature, at +4°C, or frozen for 2h to 1 week [22]. Particle counts were lower in the samples stored at -20°C compared with -80°C or other temperatures. Protease inhibitors in this study also had a positive effect increasing the recovery of particles from less than 40% to over 80% from the original counts. A later study reported that concentration and particle size remain similar after freezing at different temperatures, *i.e.* -20°C, -80°C or -196°C without gross changes in uEVs morphology as observed by TEM. Particle concentration analysis by NTA showed approximately 2-fold increase and similar decrease as measured by resistive pulse sensing (RPS), in comparison with fresh samples. [205]. Particle mode size increased by 17% during 1 year of storage at -80°C. Overall, uEVs were found to be more stable during 1-year storage at -80°C as compared with EVs from other body fluids. Thus, most evidence for uEVs storage temperature is in line with the recommendations for EVs from other body fluids and storage at -70°C or colder is recommended [206]. Regarding antigenicity after freezing and long-term storage, it is of importance to note that the uEVs proteome includes thousands of proteins, therefore it cannot be excluded that some proteins can be more prone than others to lose antigenicity after long term storage. For example, in The Finnish Diabetic Nephropathy Study (www.finndiane.fi), a well-established cohort of urine samples with different levels of albuminuria, many isolated uEVs were associated with antigens including proteases, protease inhibitors and ubiquitin [207]. These proteins might lead to loss of antigenicity in different cohorts after thawing, but the process of freezing and thawing by itself could affect the antigenicity. Only dedicated studies of uEVs can established the best condition for freezing temperature and storage time for the protein(s) under investigation. Frozen uEVs might interact with cryoprecipitates, mainly calcium oxalate dehydrate and amorphous calcium or polymerized proteins, leading to uEVs entrapment and apparent loss unless released by measures such as vortexing, dilution, lowering of ionic strength or depolymerization of proteins [191, 200]. Early studies reported that vortexing after thawing can considerably increase uEV recovery from urine frozen either at -20°C (87% recovery) or -80°C (to 100% recovery), even after 7 months of storage [131]. However, it is not known if vortexing damages vesicles or if it leads to loss of luminal content and other studies did not observe significant effect of post-thaw vortexing [22]. Additional work is needed to investigate in a comprehensive manner to which extend the size, number and molecular composition of uEVs is affected by freezing temperature and storage time.

2.4.2 uEV separation

Several EV separation methods that show specific advantages and disadvantages have been developed [208, 209]. Moreover, the selected isolation method may affect the characteristics and analysis of both isolated EVs and contaminants [67, 197, 203, 210, 211]. A main focus has been on purity and yield of uEVs and usually one improves at the expense of the other. In addition to yield and purity, emphasis should also be given to practical considerations such as speed, scalability and throughput, as any high-impact clinical research, and biomarker research in particular, requires validation of the results in hundreds to thousands of samples. Further, all isolation techniques yield only a subset of uEVs, which does not necessarily contain all uEVs of interest. However, in some cases, specific enrichment of a subset may be advantageous and improve the detection of some markers.

Traditionally, uEVs have been separated by ultracentrifugation. However, "ultracentrifugation" is not one technique, and there are a host of protocol variants and specifics across studies contributing to variable results within this category of separation modality (EV-TRACK, [166]). Sequential centrifugation is more commonly used and involves low speed centrifugation to remove cells and debris, followed by the subsequent consecutive collection of large and small EVs at increasing centrifugation speed (in general 10,000 - 20,000 x g for 20-30 minutes for large EVs, and 100,000 - 200,000 x g for 1-2 hours for smaller EVs) [212]. However, it has been reported that ultracentrifugation (UC) can have poor efficiency, with up to 40% of small uEVs retained in the supernatant after UC at 200,000 x g [21].

A major challenge to effective EV separation is the highly abundant urinary protein uromodulin, which forms long polymers that can entrap small EVs [8, 25]. Trapped EVs will then co-pellet with uromodulin at low centrifugation speeds and may reduce the recovery of small uEVs isolated by sequential centrifugation (Figure 2.1A). Several approaches have been shown to release entrapped vesicles such as addition of the reducing agent dithiothreitol (DTT) Tris (2-carboxyethyl) phosphine hydrochloride (TCEP-HCl), the detergent 3-[(3-Cholamidopropyl) dimethylammonio]-1-propanesulfonate (CHAPS) or alkaline buffers)[25, 200, 202, 213]. Some groups have reported that DTT only slightly improves the yield [152]. A recent study demonstrated that removal of uromodulin using TCEP-HCl does not affect particle counting with NTA/Tunable Resistive Pulse Sensing (NTA/TRPS), or results of flow cytometry or, qPCR, but did influence Western blotting and mass spectrometry results [25]. Of note, detection of antigens depends on the analytical technique in use. SDS-PAGE followed by western blot is usually performed in reducing conditions without affecting the detection of the antigen of interest. However, there are exceptions depending on the type of antibody used and the nature of the antigen studied. For example, detection of tetraspanin in WB seems to be favored when the sample is solubilized without any reducing antigen [214]. Nevertheless, this evidence originates from very few examples and it would not be correct to extend this conclusion to the whole uEVs proteome

which accounts for more than a thousand proteins. In addition, the use of reducing agents does not seems to affect the integrity of uEVs as reported by electron microscopy pictures of several studies which included either the use of DTT and / or TCEP [25, 202]. A heterogeneous population of EVs was found in the pellet with size and morphology not dissimilar from the fraction before treatment including multi-lamellar or composite structure with smaller EVs enclosed in larger ones. These findings reaffirm the importance of depleting uromodulin for certain downstream uEV analyses.

Disease-related changes in urine content, such as proteinuria, can also complicate EV isolation. In particular, albumin (and other proteins) that leak into the urine in glomerular disease can bind to the surface of EVs or co-elute as a protein complex [67, 215]. This can impair certain ultrafiltration-based approaches and interfere with protein-based characterization, e.g. mass spectrometry or Western blot following ultracentrifugation [216]. Coupling ultracentrifugation with size exclusion chromatography, the use of sucrose or other density gradients, or the isolation via filtration dialysis have been shown to reduce albumin and other proteins in EV isolates [201, 215]. Another consideration is that proteinuria can alter urine viscosity which is a critical determinant of EV recovery in centrifugation-based approaches [217, 218]. However, the impact of changes in urine viscosity in proteinuria on EV recovery is not known. The presence of red blood cells in urine samples (hematuria) can also alter the purity of EV isolates. A trypsin treatment performed before uEV isolation was recently described to prevent hematuria-related proteomic alterations [219].

Many of the new methodologies developed for EV separation have been applied to uEVs, including filtration, precipitation, hydrostatic dialysis, ultrafiltration combined with size exclusion chromatography, acoustic trapping and immunocapture [67, 166, 201, 220-227]. The efficacy and yield, and potential contaminants of these EV isolation techniques still need to be evaluated. Multiple studies have shown that the choice of isolation method can have a significant effect on measured EV molecular content [153, 228]. Co-isolation of abundant proteins in urine with uEVs hampers the detection of less abundant proteins in uEVs. One strategy to account for high-abundance uromodulin contamination in mass-spectrometry proteomics analysis of uEVs is the use of an exclusion list of uromodulin peptides [229]. However, it should be noted that highly abundant proteins will still influence the identification and quantification of low abundant peptides, even with computational filtering after spectrum acquisition.

Finally, it is important to investigate to which extend the different EV isolation methods remove potential molecules/structures that may contaminate the uEV pellet. Main contaminants of uEV pellets can be bacteria, blood cells and lymphocytes, uromodulin and albumin. In normal conditions the main contaminant of the uEV fraction is considered to be uromodulin. Urine test strips can be used to detect abnormal levels of bacteria and protein (albumin), and the presence of blood cells and lymphocytes in the urine samples. A gel electrophoresis can also show the protein pattern of each urine sample before and after uEV enrichment. This information can be considered during sample inclusion as well as when analyzing the uEV fraction. Electron microscopy can be used to detect the presence of abnormal vesicle morphology or other structures in the uEV sample, such as uromodulin (precipitates). Western blot can be used to detect specific co-isolating proteins that may be present in the EV sample such as uromodulin or albumin. Proteomics analysis is also useful as it allows to compare the abundance of these and other co-isolating proteins in relation to uEV proteins.

In conclusion, we note limited consistency and coherence between uEV separation methods. These limitations also apply to methods for characterization and analysis of EVs (addressed in the next section).

2.4.3 uEV characterization

2.4.3.1 Post-separation characterization and analysis of enriched uEVs

Authors reporting uEV characterization should be guided by MISEV reporting requirements [5]. There are additional specific considerations for uEVs since urine is a particularly dynamic body fluid that contains EVs derived from a variety of cells. Parameters that vary in urine include concentration, osmolality, electrolytes, pH level, excreted/secreted proteins as well as cellular, bacterial, and viral quantity and content. There is no single technique that can characterize uEV heterogeneity by describing EV morphology, size, count and content. Each post-isolation characterization is affected by the EV separation method used (see section 3.3.2 for further discussion of this topic). In many cases (*i.e.* animal work, archived random time spot urine) the amount of urine available may limit the number of complementary analyses that can be conducted [25].

The **morphology of uEVs** has been described by transmission electron microscopy (TEM), cryogenic electron microscopy (cryo-EM), atomic force microscopy (AFM) and super resolution fluorescence microscopy (Figure 2.1). In particular, TEM and cryo-EM show a heterogeneous group of EVs of different sizes and shapes, and cryo-EM also allows the visualization of intraluminal structures [25] (Figure 2.1A). In addition to providing information about uEV size distribution, EM can also be used to assess sample purity, as gross protein aggregates, major vault proteins and other structural contaminants can be visualized and distinguished from EVs. See for example the presence of uromodulin in uEV samples in Figure 2.1. Cryo-EM preserves EV morphology and shows the lipid bilayers at high resolution, making it well suited for structural characterization of the EVs. However, performing systematic quantification of these parameters by cryo-EM is time consuming and thus low throughput. Additionally, cryo-EM requires costly equipment and specialized technical staff, which limits its accessibility and makes broader adoption of this approach to quality control unlikely. TEM (Figure 2.1B) also requires specialized facilities, but is generally more accessible. TEM negative staining protocols are straight-

forward, allowing visualization and sizing of EVs, and rough estimation of their purity in a large number of samples relatively quickly. TEM can also show EVs heterogeneity by differential staining densities to highlight morphological characteristics and surface features. Recently, super-resolution microscopy has been used to directly visualize fluorescently labeled molecules within vesicles with 20nm resolution, revealing the biomarker distribution and expression levels on single vesicles [230]. Many investigators have found SDS-PAGE gel electrophoresis of the uEV sample to be useful as a general profiling tool to explore the protein pattern and detect potential protein degradation or protein contaminants, such as uromodulin [25, 131, 201]. Of note, uromodulin is rarely fully eliminated from uEV preparations, regardless of the separation method used, because there is a GPI-anchored, membrane-associated form of uromodulin which may be a normal constituent of tubular cell-derived EVs [25, 231].

uEV size distribution and counts can be measured with commercially available particle analyzers including NTA, based on Brownian motion and tunable resistive pulse sensing (TRPS), based on the Coulter principle [22, 25.]. Both methods are discussed below, however there is only limited data comparing these methods.

Several technologies are utilized to study **EV content** (*e.g.* proteins, RNA, lipids, glycans). Western blot or ELISA techniques are based on bulk analysis of uEV content, whereas flow cytometry offers high-throughput single-EV surface protein analysis but requires advanced instrumental setup and experience to obtain sufficient resolution [232]. In addition, specialized cytometers with higher scatter sensitivity to measure small particles are not widely available (high-resolution flow cytometry). As an alternative, bead-based cytofluorimetric analysis can provide semi-quantitative analyses of EV surface markers [233, 234]. Recently, a bead-based commercial kit detected up to 37 surface markers of EVs captured by CD63, CD9 and CD81-coated beads [235]. For uEVs, CD24 and CD133 might be of interest as markers of kidney function whereas other markers may identify kidney infiltrating cells [10]. Numerous omics analyses have also been performed to define the molecular content of uEVs and identify novel biomarkers for several diseases. Such studies include (small) RNA-Seq and other transcriptomics analyses as well as mass spectrometry-based proteomics [78, 90, 98, 116, 152, 153, 156, 236-239]. Metabolomic and lipidomic studies of uEVs are also under development, but remain rather complicated, with workflows requiring specialized instrumentation and expertise [82, 240].

Recently, a systematic comparison of 10 different isolation methods for small RNA EV-cargo across 5 biofluids revealed marked differences in the complexity and reproducibility of the resulting small RNA-Seq and mRNA-fragment profiles with the type of the RNA (*i.e.* miRNA, tRNA or mRNA fragments) being a major factor in the choice of isolation method. An interactive web-based application (miRDaR) with incorporated comparative statistics was also developed to help investigators select the optimal RNA isolation method for their studies [153]. Results for uEVs demonstrated that when miRNAs are the RNA type under investigation, none of the tested methods has both high reproducibility and high sample complexity, suggesting that choice of (small) RNA extraction method should be driven by the overall small RNA-Seq data quality metrics to be applied. Interestingly, uEV small RNAs were almost entirely comprised of tRNA fragments (tRFs), and tRF profiles grouped in 2 clusters based on separation method, suggesting the presence of two major uEV subclasses that carry these small RNAs. For mRNA fragments present in the sequencing libraries, a clear separation of samples based on both sex and type of isolation method was observed, suggesting that gender should be taken into consideration early in study design [153].

Capture of uEVs, followed by direct RNA isolation with an optional uEV purification step in-between and followed by next generation sequencing is common for uEV-RNA analysis [203, 236]. Such approaches can be utilized to minimize sample handling and maximize EV recovery, both of which are attractive for clinical utilization. Acoustic trapping of uEVs followed by RNA isolation and next generation sequencing is another recent example [224, 241]. Importantly, a recent study comparing a variety of EV separation methods clearly demonstrates that some widely used methods are not suitable for small and long RNA sequencing, particularly those that combine uEV isolation/separation and RNA isolation [242]. Thus, it is highly recommended that appropriate pilot studies are performed to assess key performance characteristics of the planned RNA sequencing methods, especially when newly available commercial isolation kits are used. This is particularly vital in studies where small and long RNA sequencing are equally important targets.

A pipeline application for proteomic analysis, including a heat-shock protein-based EV capture (Vn96-peptide ligand) and a subsequent protein fractionation step followed by mass spectrometry was recently described and applied for biomarker discovery in nephronophthisis-related ciliopathies [98, 133, 243, 244]. A variety of ELISA immunoassay methods exploit unique biophysical features of EVs to facilitate large-scale and high- throughput screening of uEVs for clinical applications (Reviewed in [245]). Microfluidic devices such as nanoscale lateral displacement arrays on a chip (Nano-DLD arrays), double filtration microfluidic system on a microchip, microfluidic nanowires followed by *in situ* RNA extraction, centrifugal lab-on-a-disc nanofilters, and nanoparticle-based time resolved fluorescence immunoassay (NP-TRFIA) are prototypes showing the feasibility of isolating and analyzing uEVs directly from cell-free urine [113, 246-250]. Important developments allow multiplexing and enable the detection of combinations of markers on the EV surface [251]. In line with this, a single particle interferometric reflectance imaging sensor platform (SP-IRIS) is now commercially available [252]. A capture chip based on a tetraspanin (CD63, CD9 and CD81) can obtain particle size distribution, images of vesicles and detect up to four different protein markers per EV. These are just few examples applied to the analysis of urine and more information can be found in [253-255]. Such technologies are advancing at pace, but none of these have become a consensus standard approach within the community. Uncertainty remains regarding which technology would be the most the optimal system for developing a uEV assay that is truly fit for purpose in clinical diagnostic laboratories.

2.4.3.2 Direct quantification and characterization of uEVs in cell-free urine

Reliability of EV separation techniques often correlates with investment of time and money. As stated earlier, all isolation techniques yield a subset of uEVs, which does not necessarily contain all uEVs of interest. Therefore, ideally analysis and assessment of uEVs should be performed on cell-depleted urine (urine supernatant). Overall, urine analytes are relatively dilute and few platforms are sensitive enough to perform analysis without any pre-enrichment processing, but quantification and characterization techniques developed for the analysis of cell-depleted urine are making important progress, and might someday facilitate clinical application of uEVs. One of the best-defined techniques for direct quantification and characterization of uEVs is NTA, which can measure particle size distribution and concentration in biofluids [22]. However, NTA (Patrick Hole, J Nanopart Res 2013) is prone to user and equipment/software bias, which can further complicate the comparison of multiple datasets. NTA measures all particles present in urine, including protein aggregates, *e.g.* uromodulin or human serum albumin (HSA) aggregates in patients with proteinuria or albuminuria. This can distort the quantification and characterization of uEVs [256, 257]. Conversely, NTA has a lower size detection limit for particles in urine of less than 70 nm in diameter in scatter mode [22]. Thus, NTA may not detect smaller uEVs, which are thought to be the majority [8], resulting in an under representation of uEVs. Appropriate resuspension and dilution are necessary since NTA measures clumped particles as a single particle.

Other techniques used to detect and characterize uEVs in cell-free urine include specialized flow cytometry and TRPS [23]. EV flow cytometry uses specific antibodies and/or ligands to either enrich uEVs or exploit the signal of a fluorescent tag linked to the antibody. An example is the use of anti-tetraspanin coated magnetic beads when analyzing EVs with conventional flow cytometry, which offers combined isolation and analysis of uEVs [232, 258]. Further developments of flow cytometric based analysis of EVs include use of imaging flow cytometry [25] and nano-flow cytometry [26] for direct uEV analysis in cell-free urine. Whilst relatively new techniques, both of these offer the potential for analysis of individual EVs. Another newly developed assay for the quantification of EVs and detection of multiple biomarkers on the EV surface, without the bias induced by marker dependent EV capture, is EVQuant [27]. In EVQuant, in-gel immobilization of fluorescently labeled EVs allows high throughput detection of individual EVs and the detection of EV subpopulations and their size distribution [259]. Another recent technique that could assess the global composition of uEVs at the single particle level or in a limited group of EVs is Raman Tweezers microspectroscopy (RTM) which could help to determine the percentage of different EV subpopulations and contaminants present in the preparation [260].
In general, all EV analysis approaches and assays currently developed are hampered by the small size and large heterogeneity of EVs in bio-fluids. Improvements in sensitivity and specificity are needed to truly access the whole range of EVs and EV subpopulations in both research and clinical applications.

2.4.4 Normalization

In order to effectively maintain water and salt homeostasis, urine production can be highly variable. Consequently, the concentration of EVs in urine may vary more than in blood and other body fluids. In addition, uEV processing protocols invariably induce additional variation that may need to be corrected for [218, 261]. Thus, a major challenge of uEV research is the lack of robust methods to normalize uEV content to adjust for confounding factors such as excretion rate and uEV-processing-related variation [262]. Normalization approaches for urine biomarkers can be broadly classified as calculating an absolute or relative excretion rate. **Relative excretion rate** defines the abundance of the uEV marker in relation to another marker, such as uEV number, a protein or RNA marker, or total EV protein, RNA or lipid amount (Table 2.3). This is most commonly applied in urologic and in proteomics studies but also used in kidney-related studies [8, 22, 65, 83, 133, 134, 263-265]. **Absolute excretion rate** defines the rate (per unit of time) in which a uEV marker is excreted. This can be measured using a timed collection, or may be approximated by normalization to urine osmolality or creatinine in a spot urine [266, 267]. This is mostly used in kidney-related research, and is of particular importance in physiological studies [245] Blijdorp, Tutakhel, JASN 2021).

2.4.4.1 Relative excretion rate

A commonly used normalization strategy for proteomic analyses is to start with a reproducible method to enrich for uEVs and conduct the experiment with the same **amount of total protein** (for example 20 μg) per sample. After acquisition, protein data can be processed using quantile normalization, which assumes that the majority of proteins present in the sample are stable. Protein variation in uEVs has been recently determined by Oeyen, *et al.* [221]. Such global normalization approaches (*e.g.* Linear scaling to Counts Per Million) are also applicable to transcriptomics studies and were recently demonstrated for small RNA-Seq data generated from EVs in different biofluids, including uEVs [153]. Nevertheless, the effect of different normalization approaches, in particular for long transcripts, remains to be systematically evaluated. Importantly, in urine, uromodulin and albumin are known to be overrepresented in protein content after uEV enrichment protocols [202, 213, 268].

Expression of uEV-biomarkers as a ratio to **uEV number** or to a **uEV-biomarker** (*e.g.* a housekeeping control transcript or a protein, present in uEVs) that is considered to be stable in the studied condition has been also proposed [78, 269]. However, such ratios can be affected by the quality of the chosen control(s) in terms of expression stability. In addition, common EV-markers such as CD9 or CD63 may be differentially expressed throughout the urogenital system, and therefore not be generally applicable on urine samples (Blijdorp Tutakhel JASN 2021).External factors such as an undetected infection or damage/injury/inflammation in any part of the urogenital system affect the total excretion of uEVs and the composition of the uEV pool [112, 113].

TABLE 2.3

Normalization methods

NORMALIZATION METHOD	APPLICATION	STRENGTHS	LIMITATIONS
Constitutively expressed uEV biomarker	Relative excretion rate	• Adjusts for isolation variability or incomplete THP depletion • Simple normalization rationale • Possible surrogate measure for EV number (requires further validation)	• Currently limited to proteins • Biomarker not always valid for the analyte of interest • Affected by changes in (external) excretion of biomarker from any part of the system (*e.g.* urothelial release when studying kidney disease) • Some EV biomarkers may not be as universal as originally believed
Relation to total uEV quantity	Relative excretion rate	• Adjusts for isolation variability or incomplete THP depletion • Simple normalization rationale • Adjusts for changes in general EV release	• Problematic if change in total excretion of uEVs is part of underlying pathology (*e.g.* after nephrectomy) • Highly dependent on the method of uEV characterization • Affected by change in (external/crossover) EV secretion from any part of the system (*e.g.* urothelial release when studying kidney disease)
Specific biomarker ratio: ratio of two or more (disease) related biomarkers, ideally with a (known) similar source	Relative excretion rate	• Adjusts for isolation variability or incomplete THP depletion • Can leverage mechanism of action of biomarkers, especially when they go in opposite directions • Less sensitive to external/crossover secretion of uEVs	• Depends on the existence of a biomarker ratio that steadily predicts an outcome • Often high variability • Each ratio should be independently validated
MassSpec Proteomics; Z- or quantile normalization	Relative excretion rate	• Adjusts for isolation variability • Uses all protein information available to normalize content – less sensitive to external/crossover factors provided they are small	• Albumin and/or THP can dominate the uEV proteome and can vary more than other uEV proteins • Affected by change in (external) EV secretion from any part of the system (*e.g.* urothelial release when studying kidney disease)
RNAseq; Z- or quantile normalization	Relative excretion rate	• Adjusts for isolation variability • Uses all RNA information available to normalize content – less sensitive to external/crossover factors provided they are small	• May be biased when comparing two different patient groups • Affected by change in (external) EV secretion from any part of the system (*e.g.* urothelial release when studying kidney disease)
Timed collection (ideally 24 hours)	Absolute excretion rate	• Compare intra- and inter-individual differences without further normalizations • Eliminates variability due to circadian rhythm	• Inconvenient • Often incomplete collections • Long processing time increases chances of sample degradation • Does not adjust for possible variability in uEV processing protocols • Consider longer cycical variation periods (*e.g.* changes over several days or even weeks)
Urine creatinine/osmolality	Measure of absolute excretion rate in random spot urine	• Commonly used clinically • Easy and inexpensive to assay • May correct for circadian rhythm in GFR	• Differences or changes in muscle mass / creatinine excretion require correction • Does not adjust for possible variability in uEV processing protocols, or circadian rhythm in uEV release. • Requires further validation in uEVs
GFR / nephron number	Excretion relative to kidney size	• Commonly used clinically (GFR) • May help to compare patients with different stages of kidney disease	Non-invasive methods to estimate nephron number are unreliable Requires validation in uEVs
urinary PSA	Excretion relative to prostate size	• Commonly used clinically (PSA) • Easy to assay	Requires further validation in uEVs

2.4.4.2. Absolute excretion rate

Timed collection, and in particular 24-hour collection (*i.e.* during an exact 24-hour time-course discarding first morning void and including first morning void of following day) is considered the gold standard to determine excretion rate of general urinary biomarkers such as albumin, because it is less sensitive to fluctuations due to circadian rhythm [270]. However, 24-hour urine collections are time consuming and impractical for the patient and can lead to collection errors [271]. Moreover, prolonged collection of uEVs may accelerate their degradation [22], although this remains under debate [81]. The measurement of an absolute excretion rate of a urine biomarker using a timed collection can be approximated in a spot urine measurement by a **ratio to urinary creatinine** [28], which has been shown to be highly effective for both intra-individual comparison (96% of uEV variation explained by creatinine concentration) and inter-individual comparison (47-82%) (Blijdorp, Tutakhel, JASN 2021). Creatinine is a waste product of muscle catabolism. In the healthy kidney, the excretion rate of creatinine is constant when the glomerular filtration rate, secretion by organic cation transporters, and body muscle mass do not change. Thus, the ratio to creatinine should be validated in acute kidney injury or different stages of chronic kidney disease [272, 273]. In addition, comparing individuals may need correction for creatinine excretion or muscle mass. Urine osmolality has also been applied as an alternative urine normalization factor in targeted metabolomics [274]. **Urine osmolality** assumes there is constant excretion of osmoles in steady state, which was shown not to be the case during water loading (Blijdorp Tutakhel JASN 2021). Ginsberg, *et al.* [275] show that the protein/creatinine ratio of single void urine collected after the first voided morning specimen and before bedtime best correlates with the quantity of protein excreted during 24 hours.

2.4.4.3. Normalization to organ-specific biomarkers

In some cases, organ-related biomarkers can be utilized for normalization. For example, in studies addressing prostate-derived EVs, the **urinary Prostate Specific Antigen** (uPSA) can be used as a measure of the amount of prostatic fluid released in the urine and as a surrogate marker and normalization factor for the number of prostate-derived uEVs [113, 276, 277]. CD24, a kidney-specific uEV marker, could possibly be used as a reference for kidney-derived EVs [278]. While normalization to GFR or nephron mass has not been used in the literature, it may improve results of studies concerning the kidney.

2.5 Recommendations and considerations

2.5.1 Urine collection and biobanking for uEV research

Biobanking of urine is crucial for future biomarker studies. Academic institutions, hospitals and professional biobanks worldwide often share biobanking protocols. However, collection, processing and storage methods as well as the extent of gathered sample/donor information differ greatly between sites. As specific biobank guidelines covering all uEV research have not been established and EV-dedicated biobanks/collections are rare, it is recommended to follow the general recommendations related to the collection, storage, preprocessing and transportation of the urine samples by the authorities in the urine analysis field, including the Clinical Laboratories and Standard Institute (CLSI) [165]. It is important to be aware of the preanalytical variables and follow as much as possible, the recommendations for their reporting summarized in (Table 2.2).

Based on the expertise existing among the actual members of the ISEV Urine Task Force some recommendations for uEV research can be given. However, it should be clarified that this is a rapidly evolving field and that the recommendations are part of an ongoing work. Moreover, at this stage these recommendations do not represent the view of all the uEV researchers.

- When starting research with **existing biobank** samples collections, gather all available sample and donor related data for reporting and analysis purposes.
  - » Dipstick data can be gathered after thawing to indicate the presence of interfering or abnormal components.

- When **starting a new urine collection or a biobank**, consider and record the parameters in the whole logistics chain from donor recruitment to data management and urine collection, transport, preprocessing, aliquoting and storage. It is safest to consider the broadest possible future uses of the urine and uEV samples.
  - » Keep collection, processing, and storage procedures the same throughout the study. If this is not possible, perform controls to identify the possible effect of the varied step.
  - » Aim for fast processing (hours), keep samples cold (+4°C, ice or equivalent) and consider additives (*e.g.* azide, protease inhibitors, EDTA) to avoid microbial growth and maximize preservation of the EVs.
  - » Gather dipstick data to indicate the presence of interfering or abnormal components.
  - » Centrifuge urine before freezing to remove cells that could be disrupted during freezing. Aliquot samples according to future use and available space. Freeze at -70°C or colder.
  - » Use only hygienic collection devices, containers and plastics that resist urine pH and do not bind uEVs (lipids/proteins) or shed particles.

It is also important to collect and report low evidence level items to improve our understanding of the impact of these factors and reduce current uncertainties. These may include:

- Need for light protection or for some sample protecting agents, such as RNase inhibitors or cryoprotectants.
- Freezing speed. Quick freezing appears to work, but tests for a range of freezing speeds are lacking.
- Defrosting temperature.

2.5.2 Downstream analysis of uEVs

As with most body fluids, urine contains EVs from a plethora of different organs, tissues and cell types from the urinary tract (Figure 2.2). Together with the wide variety of analytical parameters that can be obtained from EVs, this results in several important considerations for the analysis of uEVs (Figure 2.4).

The first consideration is **the type of analytical parameter** that is going to be studied. uEV analysis can be focused on physical parameters (*e.g.* concentration, size distribution, morphology) and/or the biochemical content of uEVs (*e.g.* proteins, nucleic acids, lipids and metabolites). This is reflected by the wealth of state of the art and newly emerging EV assays and analysis technologies available [240, 255, 279-282].

However, there is no single consensus protocol for pre-processing EVs, or analytical technology that suites most or all analytical parameters. Importantly, the MISEV2018 and EV-TRACK guidelines recommend to report on several complementary analytical parameters (*e.g.* concentration, size distribution, morphology, EV markers) to confirm the presence of EVs [5, 166].

The requirement of pre-analysis **separation and purification** of uEVs is essential for many of the (biochemical) analyses to avoid interference of non-EV contaminants in urine, but might be nonessential or maybe even disadvantageous for other analyses as any isolation or purification protocol unavoidably leads to significant loss of EVs and EV material. In addition, isolation procedures are generally biased towards certain EV size and density ranges. It is therefore recommended to avoid EV isolation or purification protocols as much as possible (except for the pre-freezing clearing as described in section 3.1.2.6) and only implement extensive EV isolation and purification when needed due to interference by other components of urine [193, 268, 283]. Direct analysis of uEVs without time-consuming and costly extensive pre-processing would be highly beneficial for clinical implementation. However, when EV isolation is required, different approaches (*e.g.* ultracentrifugation and precipitation) should be evaluated for urine as specific biofluid and the analytical parameter of choice [187, 197, 203, 222, 279, 284]. Regarding estimates of size and concentration, different techniques can be applied. While NTA and TRPS offer particle counting and sizing including non-EV particles, flow cytometry for example can offer single EV detection and might be more precise. To our knowledge studies are needed to understand if counting with these techniques are suitable for normalization.

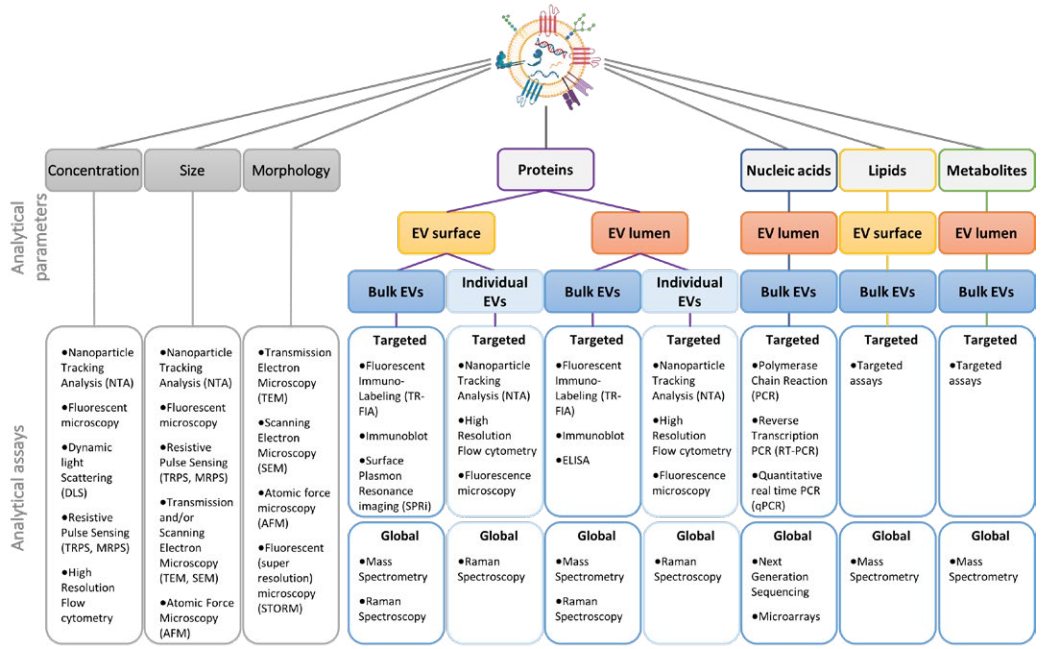

FIGURE 2.4 **Analytical method selection in uEV research**

Analytical methods used for the characterization of EVs explore their physical properties (gray) and/or molecular components (color). Commonly studied molecular components found in EVs are proteins, nucleic acids, lipids and metabolites. Localization of these molecular components largely defines the choice of an analytical approach. Proteins (purple) can be localized in the EV membrane or lumen. EV surface proteins can be assessed specifically by antibodies, both in bulk analysis, *e.g.* by a time-resolved fluoroimmunoassay (TR-FIA), Immunoblot, immuno-bead capture-based flow cytometry, or surface plasmon resonance imaging (SPRi) and with assays that analyze individual EVs such as fluorescent NTA, high-resolution flow cytometry and microscopy. Analysis of luminal proteins can be performed in bulk assays, *e.g.* immunoblot, ELISA and time-resolved TR-FIA after membrane permeabilization. Generally, labelling of luminal cargo can facilitate individual EV analysis through the use of membrane-permeable fluorescent dyes that label proteins or nucleic acids such as ExoGlow™ or Syto™13. Whilst such dyes lack the specificity of more targeted approaches, they enable analysis of EVs by fluorescent microscopy, fluorescent NTA, and high-resolution flow cytometry. Specific analyses of nucleic acids (blue) and metabolites (green), generally considered to be luminal, are usually achieved in bulk EV assays by either omics-based approaches, or by transcript-specific PCR based techniques. Lipids (yellow), are localized within the EV membrane and are commonly analyzed in bulk assays either by mass spectrometry or colorimetric reagents, like the sulfo-phospho-vanillin (SPV) lipid assay.

A third consideration is a result of the wide variety of organs, tissues and cell types that contribute to the uEV pool. Depending on the scientific or medical question being asked, **initial (on-assay) capture of specific uEVs of interest** (*e.g.* uEVs derived from specific organs or diseased tissue) can enhance the specificity and sensitivity of the analysis. Such capture within the analytical assay relies on the availability of suitable capture targets on the EV surface and the efficiency of capture. Moreover, the yield of specific uEVs in these capture approaches could be a concern. Capture based assays often use the (so called) general and abundant EV surface markers CD9, CD63 and CD81 for capture, for example time-resolved fluoroimmunoassay (TR-FIA), surface plasmon resonance imaging (SPRi), ExoView® [113, 252, 285]. However, it has become increasingly apparent that only fractions of EVs carry these 'general' EV markers, and that expression of these markers is largely dependent on the cells of origin [245, 286].
The need for capture of tissue or disease specific EVs can be overcome by analysis of **individual uEVs rather than bulk analysis**. The analysis of individual EVs allows the identification and subsequent characterization of specific uEV subtypes without the need for specific isolation. For example, multiplexing strategies allow the analysis of multiple EV surface markers on individual EVs [27, 287], sometimes after capture of the EVs [235, 252, 288]. This is again dependent on the availability of specific EV (surface) markers that can be used for detection. Moreover, the analysis of individual EVs is currently restricted to measuring physical parameters like concentration, size and morphology, as well as proteins on the EV surface and lumen. Super-resolution imaging for instance may enable visualization of structure, biomarker distribution, and relative abundance of each biomarker on single EVs. Technologies to analyze RNAs, DNA, lipids and metabolites in individual EVs are not yet available.

The level of EV analysis varies from global, discovery based approaches using the 'omics' family of technologies (*e.g.* proteomics, transcriptomics, genomics, lipidomics and metabolomics) [84, 152, 236, 289, 290], to more targeted analysis of specific EV contents using immune detection or PCR-like approaches to measure specific proteins or RNAs of interest [264, 291-293]. The latter is more present in target-specific EV assays and is more suitable for clinical implementation. Analytical technologies and assays for these two levels of uEV analysis differ and require different levels of pre-processing and purification.

The last consideration is the requirement of **scalability**. Many current technologies for the analysis of (individual) EVs require individual samples be measured independently. Large-scale experiments and studies on larger cohorts of uEV samples will require more high/medium throughput technologies. To support the scalability of uEV analysis, several technologies are being developed that enable higher throughput using automation and miniaturization of assays in (microfluidic) devices. Related to scalability is standardization. At this moment, many of the analytical assays for EVs are highly dependent on details in the protocols and settings. It is therefore pivotal to introduce optimal levels of standardization and reporting in the analysis of uEVs to improve reproducibility [5, 166].

2.5.2.1 Analysis of the uEV proteome

Many of the potential challenges of working with uEVs highlighted elsewhere in this manuscript also apply to proteomic analysis of uEVs, especially those relating to vesicle isolation and purity (section 3.2). Abundant proteins in urine such as uromodulin, previously reported to be present in uEVs [8], may in fact be co-isolated or partially related to EVs that have been co-isolated with uEVs [25]. Moreover, problems associated with a high abundance of soluble proteins are exacerbated in various clinical scenarios such as proteinuria, hematuria, and other conditions. Therefore, one must be careful when analyzing complex data sets from broad proteomic studies of uEVs. Whilst additional techniques can be used to remove soluble proteins from the sample, it remains a challenge to distinguish proteins that are genuinely uEV-associated from soluble contaminants. Furthermore, issues with protein contaminants make normalization based on vesicular proteins extremely difficult. An alternative approach is to normalize sample inputs based on vesicle count. The challenges associated with either approach are summarized in section 3.6. There have been several advances in technologies for focused analysis of the uEV proteome. Technologies such as aptamers or proximity extension assays (PEA) have been utilized for analysis of EV proteins [294-296]. Such techniques offer greater sensitivity and limit the background noise which may accompany traditional mass spectrometric approaches, but the breadth of analytes assessed is limited. Additional approaches utilizing immuno-based capture and detection of proteins can also be used for assessment of selected uEV proteins. Low density array (LDA) profiling can be adapted for the study of vesicular proteins [297, 298]. Whilst such arrays are limited in their coverage, they do not require access to specialized equipment. In addition, there are several commercially available platforms for assessment of multiple uEV surface markers in plate- or chip-based formats [214, 299]. However, such immuno-affinity assays are susceptible to soluble protein contaminants that can interfere with uEV capture and detection. A comparison of techniques for uEV protein analysis described above is shown in Table 2.4.

2.5.2.2 Analysis of the uEV transcriptome

RNAs carried by uEVs are biologically active, can reflect the physiological status of cells of origin, and have been intensely studied in the search for biomarkers [145, 300]. Characterization of the RNA species in uEVs depends on the preanalytical and analytical conditions. The RNA yield from uEVs is related to the uEV separation technique used (*e.g.*, 2.6 - 50 pg/ml for uEVs isolated by ultracentrifugation (UC) followed by 0.1 μm filtration) [132], and 17 – 46 pg total RNA per million uEVs obtained by UC alone [301]. An extensive description of analytical conditions for RNA analysis was recently reviewed [156]. Furthermore, microfluidic techniques have been developed to reduce bias introduced by high manipulation of the sample for targeted detection [248]. A comparison of techniques for uEV RNA analysis is shown in Table 2.5.

2.5.2.3 Analysis of the uEV lipidome

Preanalytical and analytical parameters can affect outcomes of EV lipid analyses and should be reported [299, 302, 303]. Protocols for sample preparation, lipid extraction, and separation must be

reproducible. For example, it is not clear yet to which extent uEV lipids can be degraded under different conditions. Moreover, the presence of lipoparticles in EV samples can affect lipid analysis, which should be considered in studies of conditions that can lead to an increased lipid concentration in urine. Recent studies of the EV lipidome have often used mass spectrometry. Because of the high molecular diversity of lipids, overlaps of mass spectrometric ions of lipid species frequently occur. Therefore, using high-resolution MS is recommended for analysis of the uEV lipidome [304]. In addition, proper internal standards, normalization and/or labelling are crucially required for precise quantitative lipidomics of uEVs [302-306].

TABLE 2.4 **Summary of techniques for EV proteome analysis**

TECHNIQUE	REQUIRED SAMPLE INPUT	STRENGTHS	LIMITATIONS	REF
Mass spectrometry	High	Broad spectrum of analytes Non-biased Well established protocols	Susceptible to "noise" from contaminants Data requires trimming/ cleaning	[8, 325, 326]
Aptamers	Medium	High sensitivity High specificity Can measure 1,000 s of analytes Focused	Limited coverage (analytes assessed: 1,000 s)	[294, 295]
Proximity extension assays (PEA)	Medium - low	High sensitivity High specificity Focused High throughput	Severely limited coverage (analytes assessed: 100 s)	[296]
Proteome Profiler Arrays	Medium	Focused No specialist equipment required Relatively low cost	Minimal coverage (analytes assessed: 10 s) Low dynamic range Potential interference to immuo-capture by soluble contaminants	[297, 298]
Immuno-affinity assays (high-resolution flow cytometry, chip/plate-based analyses)	Minimal	Focused Relatively low cost Versatility	Minimal coverage (analytes assessed: 10 s) Potential interference to immuno-capture by soluble contaminants	[214, 285, 299]

2.5.2.4 Analysis of the uEVs metabolome

uEVs carry different types of metabolites such as many organic acids involved in the TCA cycle, bile acids, amino acids, nucleotides and steroid hormones pointing to these vesicles as indicators of the metabolic status of tumor tissue [82, 139, 301]. However, several issues exist with the analysis of EVs by MS-based metabolomics. The technique is very sensitive, and it is likely that some non-EV metabolites will be retained by most EV separation methods. Background metabolites can be assessed easily for cell culture conditions by analyzing unconditioned medium [307, 308], but it is not as easy to judge background metabolites for urine. Therefore, it is recommended to study multiple biological replicates and take into consideration only those metabolites that are consistently detected among technical replicates and samples [82]. Another aspect to consider is that a minimum amount of uEVs will be required to obtain reliable measurements, for example 50 micrograms of total uEV protein. Finally, the varied chemical nature of the metabolites in uEVs means that there is no single method capable to analyze all uEV metabolites at once. A combination of different extraction methods chromatographic parameters and mass spectrometric conditions are likely needed to construct a complete picture of the uEV metabolome.

2.5.3 Normalization of uEV data

Normalization approaches for urine biomarkers can be broadly categorized as absolute or relative excretion rates. The **relative excretion rate**, is generally applicable as a normalization method for uEV samples subjected to any isolation protocol while the **absolute excretion rate** is ideally used with techniques that characterize uEVs directly in cell-depleted urine. Without a universal approach to normalize uEV samples, we list here current normalization methods in use:

- Timed collection (gold standard: 24-hour collection) – absolute excretion rate
- Creatinine/osmolality normalization – estimate of absolute excretion rate using spot urine
- Constitutively expressed uEV marker – relative excretion rate
- Specific marker ratio (e.g. organ specific proteins) – relative excretion rate
- Relation to total uEV count – relative excretion rate
- Z-normalization (RNAseq / MassSpec) - relative excretion rate
- To GFR (or nephron number) – relative excretion rate (organ-related: kidney)
- Relation to PSA (e.g. after DRE) – relative excretion rate (organ-related: prostate)

The strengths and limitations of each normalization method are mentioned in Table 2.3.

Important criteria for developing new normalization tools are:

- Decreases variation within normal or expected range
- Widespread availability and feasibility
- Can be validated internally and across testing sites, ideally with (shared) external standards
- Compatibility with commonly used isolation and/or analysis methods.

TABLE 2.5 **Summary of techniques for EV RNA analysis.** [132, 156, 203, 211, 236, 301, 327-329]

TECHNIQUE	STRENGTHS	LIMITATIONS	COMMENTS	GENERAL RECOMMENDATIONS	PARTICULAR RECOMMENDATIONS
RNA-seq Describes quantity and sequences of RNA using NGS	• Detection of low and high expressed genes • Detection of isoforms/splice variants • Detection of new sequences • High sensitivity • Identifies different RNA species in one analysis (coding and non- coding) • Raw data can be used by different researchers to make new analysis.	• Cost • Training for data analysis • Data management and storage • Small amount of reference databases. • Lack of internal controls • The RNAs described by the analysis depends on the database used.	• RNA can be isolated as total RNA or small RNAs by using different RNA isolation kits, before library construction. • Different libraries can be created previous to NGS to enrich and/or deplete RNA populations (important in samples with low starting material): Whole transcriptome, targeted transcriptome (10 ng), targeted RNAs (500 pg- 5 ng), small RNAs. • Data analysis parameters, raw data, pre- and analytical conditions should be available to compare between different studies	• Preanalytical: • Centrifugation of urine upon receive to remove cells, manage at 4°C to avoid cell rupture and microbial contamination. • Cell free urine as starting material. • Long term storage of cell free urine at -70°C • Reporting pre- analytical conditions according to MISEV2018 guidelines. • Analytical: • Organic extraction increases RNA yield • RNA extraction method must be reported • Share raw data in public databases (EV- TRACK, Exocarta, *etc.*)	• Preanalytical: • uEV isolation method: All methods available to date works well • Analytical: • Library construction must be reported • Data analysis: • Describe data analysis parameters
RNA array Describes quantity of predefined RNA sequences	• Easier data analysis • Less data storage required • Detects expression of a set of predefined transcripts • High amount of reference databases	• Detection of highly expressed genes. • Depends on the affinity of the probes.	• RNA can be isolated as total RNA or small RNAs by using different RNA isolation kits.		• Use multiple probe sets per target
qPCR Describes quantity of predefined RNA sequences	• Low cost for processing and implementation • Low starting material	• Lack of normalization parameters • Depends on the affinity of the probes.	• Targets can be obtained from RNA-seq data		• Preanalytical: • When based in RNA-seq data, process sample under the same conditions • Analytical: • Add synthetic RNA sequences to starting material to normalize • Use same volume of starting material • Characterize the reproducibility of the expression of internal controls

2.5.4 Functional studies of uEVs

2.5.4.1 General recommendations for uEV functional studies

Common issues and general recommendations to be considered for attributing a functional activity to EVs are extensively detailed in MISEV 2018 [5]. Therefore, refer to the MISEV 2018 guidelines for the design of experiments evaluating functional activities of uEVs or uEV subtypes. Here, we briefly summarize the most relevant points of interest:

- Possible artifacts due to EV contaminants should be excluded. This can be achieved by comparative evaluation of the effect of the biofluid of interest before and after EV removal, together with that of the isolated EVs; when possible, the main contaminants must be isolated and their effect tested as well. Moreover, the role of co-isolated non-EV material should be studied using (combined) enzymatic degradation of proteins or RNA/DNA species to allow investigations addressing the "EV-corona" [309]. In particular, low dose trypsin, proteinases, RNAses and DNAses might be useful. Appropriate protocols should be optimized in order to avoid EV disruption or degradation in the same time.
- Isolation of the crude EV population and, when of interest, of the different EV fractions, should be achieved using multiple and accurate methods. To ascribe a functional property to specific fractions, side-by-side analysis of all fractions is recommended.
- Appropriate controls should be included such as unrelated EV sources and disease EV controls such as healthy, untreated or otherwise matched donors,
- Functional activity should be quantitatively related to the amount of EVs or of a specific EV component; this can be achieved by EV normalization strategy supporting comparison of different EVs, fractions and active cargo and possibly by the evaluation of dose response effects.

2.5.4.2 Specific considerations for uEV functional studies

While the fundamental practical considerations detailed above must be applied to all functional analysis studies (regardless of the source of EVs), urine presents certain specific challenges that must be considered when evaluating the functional activity of urine EVs. As detailed earlier, the timing and type of collection method may lead to dramatically different levels of cellular

elements, including EVs in urine samples. Thus, when possible, the same collection method should be used for any comparative analysis. In addition, uromodulin can entrap small EVs in polymer "nets" and reduce recovery. Releasing EVs from uromodulin is therefore necessary to avoid a biased functional analysis which focuses on a small subset of urinary EVs. However, complicating this is the fact that procedures which disrupt the uromodulin network and release EVs (*i.e.* DTT [202]) may also lead to co-elution of uromodulin in the EV pellet. As uromodulin is well known to modulate a diverse array of processes (*i.e.* immune function, sodium handling, complement system [310]) one must consider whether co-eluted uromodulin is responsible for any effects attributed to EVs. Similarly, as bacteria may also co-elute in EV isolation procedures, one must consider the possibility of bacterial contamination in urine samples. This could also lead to biological activity that is incorrectly attributed to EVs. One strategy to address this may be to assess contamination after collection and discard contaminated samples [311], however this is not practical for all applications. Ultimately the task force recognizes that functional analysis of uEVs is very early in its evolution and identification of strategies to address the above challenges should be a research priority.

2.6 Future perspectives

2.6.1 Clinical challenges

Use of uEVs as novel biomarkers for diagnosis, prognosis and guidance for treatment also has its challenges. The uEVs research community faces several gaps that should be overcome to systematically advance the field (Figure 2.5). Validation studies are needed to show superiority of uEV-shuttled biomarkers to direct measurement of the protein/RNA/lipid biomarker of interest in urine, *i.e.* is there a genuine advantage to concentrating uEVs. It is also important to note that a single standardized approach for urine collection, uEV separation and measurement has not yet been adopted and likely will not be. The impact of different pre-analytical variables on the nature and quality of uEV isolates has to be understood in order to design, optimize and escalate protocols towards real-world clinical applications. Use of uEVs from existing biobanks also represents a clinical challenge because the standardization necessary for many assays may be insufficient or different compared with what is needed for uEV assays. An additional challenge in the field relates to normalizing biomarker signals [28] because urine is one of the most dynamic biofluids. In order to move the field of uEV research forward, uEV reference standards are needed for many experimental purposes, including single EV analysis, *e.g.* for flow cytometry and particle analyzers for assessment of size and concentration or normalization to excretion rate and uEV processing-related variation.

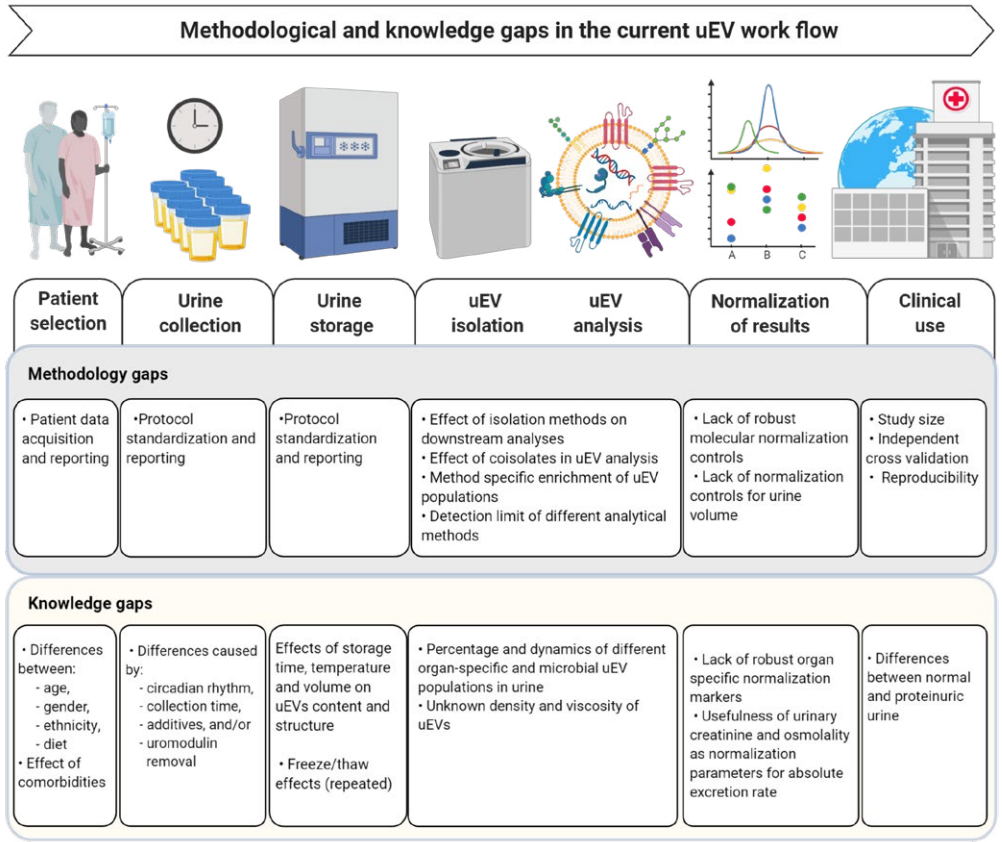

FIGURE 2.5 **Methodological and knowledge gaps in the current uEV work flow**

The urine EV task force of the International Society for Extracellular Vesicles is in the process of recruiting uEV researchers to perform collaborative studies of rigor and reproducibility to address the outlined knowledge gaps.

Among the many issues mentioned herein is the overriding need for more cost effective and tractable assay approaches that can provide fast quantitative information in a standardized fashion. Currently, the technologies available for EV analysis are highly diverse and somewhat idiosyncratic. Many of these platforms have limited accessibility, residing within specialized laboratories or within companies providing analytical services based on their proprietary technologies. Although healthcare systems globally operate differently, development of uEV biomarker measurement technologies that can be broadly deployed to diagnostic centers, *e.g.* within hospitals, will be needed to fully realize the biomarker potential of uEVs [312]. These are not trivial issues and will require continuous collaborative discussions involving industry, regulatory bodies and standards agencies to ensure success.

2.6.2 Clinical potential of uEVs

Currently the diagnosis of many diseases of the kidney and urinary tract are based on insensitive and non-specific biomarkers. For instance, changes in kidney function are still measured using changes in serum creatinine (SCr) – a late and nonspecific marker of kidney dysfunction [313]. Despite years of intense research, there are only a few biomarkers approved for clinical use. Examples include tissue inhibitor of metalloproteinase 2 (TIMP2) and insulin-like growth factor-binding protein (IGFBP7), urinary biomarkers for acute kidney injury (AKI) incorporated in a commercial test (Nephrocheck) [314, 315]. Even this FDA-approved test is falsely positive in 50% of people without AKI [316] pointing to a clear requirement for a new approach to identify and measure fit- for purpose disease markers. Early identification of disease processes in the kidney and urinary tract is clearly needed to improve the specificity of diagnosis, facilitate earlier and better tailored interventions and ultimately for improved outcome for patients.

Urinary EVs hold excellent potential as a multiplex-biomarker source. They are easily accessible non-invasively, **available in large quantities, and amenable to frequent longitudinal sampling**. uEVs in part resemble the molecular content of the parent cells from which they are released [317]. They carry cell specific markers from every segment of the nephron and urogenital tract and therefore are ideal for sampling the health status of these systems. Moreover, reports of EVs arriving into the urinary system from distant sites such as in lung cancer [69, 70] are important, as they highlight the potential for identifying diseases in unrelated organ systems through urinary sampling. These are avenues ripe for future exploration and development, potentially establishing uEVs as the ultimate biomarker source.

It is also increasingly recognized that improvements in the diagnosis, prognosis and treatment of disease processes require a better understanding of distinct underlying cellular and molecular mechanisms. Therefore, researchers in this field are exploring **site-specific or disease-specific damage/injury markers and pathways** with the intent to combine them with functional testing and clinical information. This approach may facilitate an earlier diagnosis in kidney and genitourinary tract diseases and thereby provide a more accurate diagnosis and prognostic assessment, and potentially identify novel routes for intervention. Valuable biomarkers, including uEVs should be linked to mechanistic components of disease processes.

EV-based biomarkers in urine are currently investigated for an array of malignancies and other diseases such as polycystic kidney disease [90, 91], cystinuria [92], diabetes [20, 93, 94], renal ischemia-reperfusion injury [95], glomerulonephritis [11], renal interstitial fibrosis [96, 238], hypertension or lupus nephritis [97] and in calcineurin inhibitor-induced nephrotoxicity [239]. However, many of the identified candidate biomarkers have not yet been validated in large independent cohorts or tested in more than one laboratory. An exception is the uEV biomarker test for prostate cancer based on PCA3 and ERG that reduces the number of unnecessary prostate biopsies performed [88, 89, 318]. Candidate uEV markers require more expansive, multicenter validation, that can provide the large datasets needed to support eventual clinical deployment.

SUMMARY

Characteristics specific to urine and uEVs that influence uEVs analysis

Biology:

- uEVs are (mostly) derived from epithelial cells
- uEVs are (mostly) derived from three major organs: kidney, urothelium, prostate
- Normally, urine does not contain platelets or lipid particles other than EVs
- Urine has variable contamination with microbiota
- Urine composition is highly variable (pH; osmolality, concentration) and influenced by certain medications and diet

Collection:

- Urine collection is minimally invasive
- Urine can be collected in large quantities
- Urine collection is sensitive to collection errors by the patients, i.e. mid-stream vs first void; incomplete timed collections, etc.
- Release of prostate EVs can be stimulated by digital rectal examination (DRE)
- Urine dipstick may be used as an easy quality control of urine
- Urine can contain cells that should (and can easily) be cleared before freezing

Separation / characterization:

- Uromodulin lowers yield of uEV separation techniques
- Kidney disease can cause proteinuria / albuminuria and interfere with molecular uEV analysis

Normalization:

- An absolute uEV excretion rate can be determined from timed urine collection

CHAPTER 3

Urinary Extracellular Vesicles:

The Mothership Connection

Charles J. Blijdorp, Ewout J. Hoorn

American Journal of Physiology – Renal Physiology 2019

Urinary extracellular vesicles (uEVs) are nanosized vesicles excreted into urine by cells from the kidneys and urinary tract [67]. uEVs hold the promise of being utilized as non-invasive read-outs of kidney cellular function in health and disease [67]. For biomarker purposes, it is sufficient that a certain uEV expression pattern discriminates diseased from healthy [67]. However, in understanding the mechanism of uEV formation, a physiologically relevant question is whether uEV protein abundance reflects protein abundance in the parental cell. This requirement may be necessary if uEVs are truly to serve as "liquid biopsy". But do uEVs really provide a mirror image of their parental cells – how strong is the "mothership connection"?

Two previous animal studies analyzed protein abundance in kidney and uEVs in parallel and found that the direction of change is generally the same. Esteva-Font *et al.* showed that the abundance of the sodium-chloride cotransporter (NCC) in both kidney and uEVs is two-fold higher in rats on a low sodium than on a high sodium diet [34]. Higashijima *et al.* showed that furosemide and acetazolamide increased plasma vasopressin and the abundance of the water channel aquaporin-2 (AQP2) in uEVs [13]. In the kidney AQP2 was decreased in cortex, but increased at the apical plasma membrane, the site of its action. In studies with human subjects it is challenging to perform such parallel studies because it requires kidney tissue. Instead, patients with mutations in tubular transport proteins serve as a suitable alternative, because their genotype predicts protein abundance. Indeed, in patients with mutations that activate or inactivate NCC (Gitelman or Gordon syndrome), NCC in uEVs is also higher or lower compared to healthy subjects [245]. Furthermore, protein abundance in human uEVs agrees with what has been observed in the kidneys of animals in similar settings. In acquired diseases of steroid excess, a linear relationship between the plasma potassium concentration and phosphorylated NCC in uEVs was observed [103, 105], and recapitulates the relationship between plasma potassium and phosphorylated NCC in mouse kidney [14].

Sabaratnam *et al.* now challenge the assumption that uEV protein abundance always reflects kidney protein abundance [330]. In patients undergoing nephrectomy, they collected kidney tissue and uEVs to analyze how well protein abundances correlate. The proteins selected for the study each represented a nephron segment, including NaPi-2a for proximal tubule, uromodulin and ROMK for thick ascending limb, NCC for distal convoluted tubule, and ATP6V1G3 and AQP2 for collecting duct. The nephrectomy samples were processed for protein quantification by immunofluorescence and immunoblot, including fractions enriched for membranes and intracellular vesicles. Using this elegant approach, they were unable to reject the null hypothesis, as they did not identify significant correlations between protein abundance in uEVs and any of the kidney fractions [330].

How to reconcile these findings with the previous studies discussed above? We propose two possible explanations. First, variability may be a specific issue in healthy subjects. In other words, a relationship between kidney and uEV protein abundance may only become apparent in disease. Although the patients in the study by Sabaratam *et al.* were not healthy – the majority underwent nephrectomy for cancer – a healthy portion of the kidney was selected for analysis [330]. Under normal circumstances changes in kidney protein abundance occur rapidly and constantly and the protein abundance at a given time is determined by the prevailing regulatory factor. This likely explains the high inter-subject variability in uEV protein abundance that was observed by Sabaratnam *et al.* [330] and in other studies with healthy subjects [19, 103]. The continuous and rapid changes in protein abundance may not be captured by uEVs isolated from spot urine. Disease, however, may overrule normal regulation and cause a more generalized and prolonged change in protein abundance that is reflected in uEVs. This would explain why previous studies were able to detect differences between patients and healthy subjects [19, 103]. The same may be seen when uEV protein abundance is analyzed before and after a specific dietary intervention [34, 245, 331] and with or without medication [13, 19].

A second explanation why kidney and uEV protein abundances did not correlate could be the experimental set-up of the study [330]. Urine was collected prior to surgery so that any changes during surgery may have influenced kidney protein abundance. Changes in fluid balance, blood pressure, and plasma electrolyte concentrations are likely to occur during surgery – such factors can rapidly alter tubular protein abundance, at least in mice [332]. Furthermore, different techniques were used to prepare the kidney and uEV fractions, potentially affecting protein abundance. For example, the kidney fractions were prepared using differential centrifugation, whereas extracellular vesicles were isolated using precipitation with polyethylene glycol. The type of isolation technique will not only determine the number of vesicles (and therefore protein abundance), but also the type of vesicles that are isolated. uEV is the umbrella term for microvesicles, exosomes, and apoptotic bodies and each subpopulation may express tubular proteins differently. Finally, it remains unclear what uEV protein abundance really means. In principle, uEV protein abundance can be determined by the overall uEV excretion rate, the excretion rate of uEVs expressing the protein of interest, or the amount of protein per uEV. Emerging technologies such as nanoparticle tracking analysis are instrumental to address these questions, because they allow quantification and characterization of uEVs [22].

Despite these methodological considerations, the study by Sabaratnam *et al.* offers important insights for the uEV field [330]. Because of the high inter-subject variability in uEV protein abundance, it becomes even more important to select an homogenous group for human uEV studies. Furthermore, future studies that directly compare kidney and uEV protein abundance should try to align the time of collection as much as possible, for example by collecting a spot urine just before a kidney biopsy. The study by Sabaratnam *et al.* therefore serves as an important caveat when using random uEV samples and also illustrates the remaining technical challenges in the uEV field.

CHAPTER 4

Comparing Approaches to Normalize, Quantify, and Characterize Urinary Extracellular Vesicles

Charles J. Blijdorp*, Omar A. Z. Tutakhel*, Thomas A. Hartjes, Thierry P. P. van den Bosch, Martijn H. van Heugten, Juan Pablo Rigalli, Rob Willemsen, Usha M. Musterd-Bhaggoe, Eric R. Barros, Roger Carles-Fontana, Cristian A. Carvajal, Onno J. Arntz, Fons A. J. van de Loo, Guido Jenster, Marian C. Clahsen-van Groningen, Cathy A. Cuevas, David Severs, Robert A. Fenton, Martin E. van Royen, Joost G. J. Hoenderop, René J. M. Bindels* and Ewout J. Hoorn*

* Authors contributed equally
Journal of the American Society of Nephrology 2021

4.1 Abstract

Background: Urinary extracellular vesicles (uEVs) are a promising source for biomarker discovery, but optimal approaches for normalization, quantification, and characterization in spot urines are unclear.

Methods: Urine samples were analyzed in a water loading study, and from healthy subjects and kidney disease patients. Urine particles were quantified in whole urine using nanoparticle tracking analysis (NTA), time-resolved fluorescence immunoassay (TR-FIA), and EVQuant, a novel method quantifying particles via gel-immobilization.

Results: Urine particle and creatinine concentrations were highly correlated in the water loading study (R^2 0.96), and in random spot urines from healthy subjects (R^2 0.47–0.95) and patients (R^2 0.41–0.81). Water loading reduced aquaporin-2 but increased Tamm-Horsfall protein (THP) and particle detection by NTA. This was attributed to hypotonicity increasing uEV-size (more EV's reach NTA's size detection limit) and reducing THP polymerization. Adding THP to urine also significantly increased particle count by NTA. In both fluorescence NTA and EVQuant adding 0.01% sodium dodecyl sulfate maintained uEV-integrity and increased aquaporin-2 detection. Comparison of intracellular- and extracellular-epitope antibodies suggested the presence of reverse topology uEVs. The exosome markers CD9 and CD63 co-localized and immunoprecipitated selectively with distal nephron markers.

Conclusions: uEV concentration is highly correlated with urine creatinine, potentially replacing the need for uEV-quantification to normalize spot urines. Additional findings relevant for future uEV studies in whole urine include the interference of THP with NTA, excretion of larger uEVs in dilute urine, the ability to use detergent to increase intracellular-epitope recognition in uEVs, and CD9 or CD63 capture of nephron segment-specific EVs.

4.2 Introduction

Urinary extracellular vesicles (uEVs) provide a non-invasive read-out of cellular processes in kidney epithelial cells during health and disease [9]. Large-scale proteomics have shown that uEVs contain many proteins implicated in kidney function and pathology [8]. Indeed, uEVs have been studied in acute kidney injury [333, 334], polycystic kidney disease [44, 335], glomerular disease [336], and tubulopathies [101]. Therefore, the application of uEVs offers an attractive non-invasive alternative to current diagnostic tests, in particular for early diagnosis of kidney disease [67]. However, clinical application of uEV analysis in random spot urine requires validated normalization and quantification methods. The uEV concentration depends on the uEV excretion rate (secretion minus possible uptake) and the overall urine concentration. Therefore, a normalization variable is required to substitute for time in analyzing the relative excretion rate of uEV proteins [202].

Several normalization variables have been proposed, including urine creatinine, exosomal markers, and Tamm-Horsfall protein (THP). In clinical practice, urine creatinine is routinely used to normalize analytes in spot urines, for example in the urine protein to creatinine ratio [275]. Although many investigators use urine creatinine to normalize uEVs [33-35, 245], this is not universal [22, 23, 202] and the relationship between uEV number and urine creatinine has not been systematically studied. Exosomal markers include proteins implied in exosomal biogenesis (ALIX, TSG101), and the tetraspanin surface markers CD9 and CD63, which can also be used to capture uEVs. However, it is not known if CD9 and CD63 capture antibodies isolate EVs from all nephron segments [9]. Finally, THP highly correlates with exosomal markers such as ALIX and TSG101 and may be analyzed on Coomassie gel [202].

At present, a myriad of uEV isolation and detection techniques is available. uEV isolation techniques include differential ultracentrifugation, density gradient centrifugation, size-exclusion chromatography, ultrafiltration, precipitation, and affinity isolation [227]. An example of affinity isolation is time-resolved fluorescence immunoassay (TR-FIA) with uEV-capture antibodies (typically CD9 or CD63) [113]. uEV detection can be performed by (imaging) flow cytometry, dynamic light scattering, nanoparticle tracking analysis (NTA), electron microscopy, atomic force microscopy, and resistive pulse sensing [68]. Recently, a novel method called EVQuant was developed which detects EVs by using fluorescence after immobilization in a gel [27].

Of these techniques, we selected three techniques that allow a determination of the uEV excretion rate in whole urine, including NTA, TR-FIA, and EVQuant. A direct comparison between uEV and creatinine excretion rates would address the question whether urine creatinine can be used to normalize for uEV-concentration in spot urines. Therefore, we tested the hypothesis that urine creatinine can be used to normalize for uEV concentration in spot urines. A second

aim of this study was to compare and further characterize the three uEV quantification techniques NTA, CD9-TR-FIA, and EVQuant. Our results show that urine creatinine is a reliable normalization marker and identify unique strengths and limitations of the three uEV techniques relevant for future uEV studies.

4.3 Methods

Urine sample collections

Urine samples were collected from five groups, including (1) before and after a water loading study in healthy male subjects (Table 4.S1), (2) random spot urine samples in healthy male and female subjects (Table 4.S1), (3) spot urines from male and female patients with kidney disease (autosomal dominant polycystic kidney disease, Table 4.S2), (4) second morning urines from healthy subjects for the immunoprecipitation studies (n = 6, 27 ± 2 years, 50% female) and fluorescence NTA studies (n = 3-7, 28 ± 2 years, all males). The protocols for the studies in healthy subjects (NL52107.078.15) and patients (NL43496.042.13) were approved by the medical ethics committee of the Erasmus Medical Center, and all participants provided informed consent. Healthy subjects had no previous medical history and did not use medication. For the water loading study eleven healthy male subjects were water deprivated starting at 10 pm until noon the next day when they received a water load (20 ml/kg body weight in 30 min) and a standardized meal (Figure 4.S1). They were also instructed to void at 7 am (discarded), 10 am and noon (water deprivated samples T1 and T2), and 2, 3, 5, and 7 pm (water loading samples W1-4). Three healthy males also served as time-controls on a separate day and were instructed to drink to thirst and did not receive the water load.

Processing of urine samples

All urine samples were processed within two hours. All urine samples were centrifuged at 2,000 x g and 4 °C for 10 minutes (Hettich Rotanta centrifuge, Beck Coulter), after which they were aliquoted at room temperature and stored with protease inhibitors ('cOmplete' protease inhibitor cocktail tablets, product code 11836145001, Roche, Basel, Switzerland) at -80 °C until further analysis. These samples are referred to as "whole urine". When describing the results of our uEV quantification studies we will use the term "particles", because not all particles are uEVs.[232] All particle counts were performed in whole urine, unless otherwise specified. Urine creatinine, electrolytes, and urea were measured by our center's clinical chemistry laboratory using the ISE and C702 modules of the Cobas 8000 (Roche); urine osmolality was measured with a freezing-point osmometer (Osmo Station OM-6050, Arkray). Antibodies were used to characterize uEVs using different techniques (described below); an overview of the antibodies used in this study is provided in Table 4.S3.

FIGURE 4.S1 **Schematic overview of water loading test**

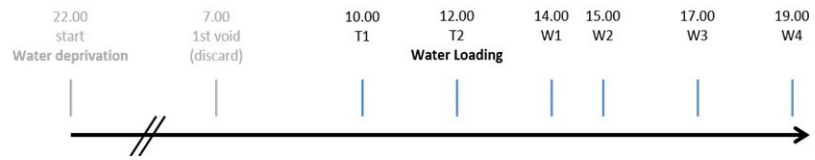

Schematic overview of the time points in the water loading test in healthy subjects. Water deprivation started at 10 p.m. the day before the test. The first urine void at 7.00 a.m. was discarded. T1-2 (urine voids at 10.00 a.m. and noon, respectively) are samples obtained during the water deprivation period, while W1-4 (urine voids at 2.00, 3.00, 5.00, and 7.00 p.m.) are samples obtained after water loading. Participants did not urinate between these time points. Water loading consisted of 20 mL/kg water within 30 minutes at noon, and was combined with a standardized meal.

Nanoparticle tracking analysis

NTA was performed using a NanoSight NS300 (Sysmex, Etten-Leur, the Netherlands) with Nanoparticle Tracking Analysis 3.1 software (NanoSight, Amesbury, UK). Whole urine samples were diluted in phosphate-buffered saline (PBS, pH 7.4, 137 mM NaCl, used throughout the studies) to obtain around 40 – 100 particles per field, then inserted in an O-ring top plate NTA chamber with a syringe. Particles were detected by scattering of a 350 nm laser, with the same settings for each experiment (scatter mode; camera level = 14, i.e., highest level without pixel saturation; detection threshold = 3; i.e, lowest threshold without excessive noise or false results; 5 videos of 30 seconds each), and the Brownian motion was determined frame to frame. Based on these settings, the lower limit of detection was approximately 70 nm. To determine the effect of THP on particle counts by NTA, THP (human native uromodulin derived from multiple donors, Biovendor, Czech Republic) was added in physiological concentrations (40 μg/mL)[337] to PBS or whole urine from 15 healthy subjects (subjects 12-26 in Table 4.S1) and incubated for 1 hour at room temperature. To determine the effect of tonicity on particle count and size, different aliquots from these healthy subjects were also diluted in water, 0.9% NaCl or 2.5% NaCl and measured by NTA. In addition, Fluorescent Flow NTA was performed in a low volume flow cell top-plate NTA chamber with a syringe. Whole urine samples were treated with sodium dodecyl sulfate (SDS, dissolved in water 2% v/v, final concentration 0.01% v/v) for 10 minutes at room temperature. Then, the samples (with SDS) were incubated with the primary antibody for 2 hours at 4 °C, followed by the corresponding secondary antibody conjugated to Alexa488 in the dark at room temperature for 75 minutes. A 488 nm laser beam was used to track antibody-labeled particles (camera level = 15; detection threshold = 6; flow speed = 100). As control, 10 ml whole urine was ultrafiltered (Amicon Ultra-0.5 100 kDa, ACS510012, Merck Millipore, Germany) and centrifuged (20 min at 4,000 x g at 4 °C using a swinging bucket rotor) and the flow-through was measured with NTA.

EVQuant

The characteristics of the EVQuant methodology have recently been reported (doi.org/10.1101/2020.10.21.348375 on BioRxiv). Briefly, the whole urine sample was diluted threefold in PBS and non-specifically labeled by the generic fluorescent membrane dye Rhodamine R18 (0.33 ng/μl, 568 nm). Subsequently, the labelled samples were mixed with a non-denaturing polyacrylamide gel solution. The mixtures were transferred to a 96-wells plate (SensoPlate glass bottom 96 wells plate, Greiner). Immobilized particles were imaged using a spinning disk confocal microscope system (Opera Phenix, Perkin Elmer). Individual EVs were detected and analyzed based on the generic membrane label Rhodamine-R18. Particle concentration was corrected by dye in control solution (PBS). To determine CD9 and CD63 expression, this protocol was preceded by labeling the sample with CD9-alexa647 and CD63-alexa488 in bovine serum albumin (BSA, 0.03% w/v) for two hours. In this analysis, each detected EV (Rhodamine-R18 +) was assessed for CD9 or CD63 expression. The detection threshold (mean plus three times the standard deviation) was determined using a 100 nm liposome sample lacking protein markers. To determine the effect of SDS on the detection of aquaporin-2(AQP2)+ particles, urine samples from 15 healthy subjects (subjects 12-26 in Table 4.S1) were incubated without SDS or with 0.01% v/v SDS for 10 minutes, followed by 1 hour incubation with AQP2, followed by 1 hour incubation with anti-rabbit alexa488.

CD9 TR-FIA

A white neutravidin-plate (Life Technologies) was coated with biotinylated anti-human CD9 overnight at 4 °C. 100 μl of thawed whole urine was vortexed and added to incubate for 1 hour at room temperature. Then, Europium-conjugated anti-CD9 was added and incubated for 1 hour at room temperature. Incubation steps were performed on a plate shaker and were followed by 6 washes with wash buffer (Kaivogen, Finland). Before signal measurement on a Victor 1420 multilabel counter, a Europium enhancer (Kaivogen, Finland) was added to the empty well and incubated for 15 minutes in the dark.

Ultracentrifugation

Prior to immunoprecipitation, immunoblotting and electron microscopy, a '200K' pellet was obtained with ultracentrifugation using 50 ml whole urine as starting volume (Table 4.S4). Briefly, after the first 17,000 x g spin, the pellet was dissolved in 250 ml freshly made 200 mg/ml dithiothreitol (DTT) diluted in ddH2O, heated and added to isolation buffer (10mM triethanolamine, 250 mM sucrose, pH 7.6) and again centrifuged at 17,000 x g. The two supernatants were combined and centrifuged at 200,000 x g for 2 hours. EVQuant was used to determine the yield of ultracentrifugation (Figure 4.S2).[214] NTA was used to determine size before and after ultracentrifugation (Figure 4.S3).

Immunoprecipitation

200K pellets were dissolved in 100 μL PBS and divided into two equal samples of 50 μL, which were incubated overnight at 4 °C with a biotinylated antibody against CD9 or CD63, followed by a 2-hour incubation at room temperature with streptavidin-coated magnetic beads (10 μL M280 beads, Invitrogen, ThermoFisher Scientific, USA). The supernatant of the magnet separation was kept at 4 °C, while the beads were resuspended in 50 μl RIPA buffer (50 mM Tris HCl pH 8.0, Igepal 630 (1% v/v), deoxycholate (0.5% w/v), SDS (0.1% v/v), 150 mM NaCl) by vortexing for 10 minutes at 4 °C. Both the precipitate and the supernatant were heated in Laemmli for 10 minutes at 60 °C. Finally, the beads were separated from the precipitated proteins by the magnet.

Immunoblotting

The 200K pellet was suspended in PBS and divided into aliquots. For immunoblot analysis 6X Laemmli solution (440 mM Tris HCl pH 6.8, SDS 10% v/v, Glycerol 25% v/v, Bromphenolblue 0.1% w/v, β-mercaptoethanol 6% v/v) was added and heated for 10 minutes at 60 °C. SDS-PAGE was carried out on a gradient gel 4-12% Criterion precast gel, 26 well, 15 μl, Bio-Rad, USA) and transferred semi-wet to PVDF membranes (0.2 um PVDF, Bio-Rad, USA) using a Trans-Blot Turbo Transfer system by Bio-Rad at 25V, 1A during 30 minutes. The membranes were blocked (TBS with 0.1% v/v tween20 and 5% w/v BSA or milk) and probed overnight at 4 °C with the appropriate antibodies (Table 4.S3). Subsequently membranes were washed and incubated with a secondary antibody. After washing of the membranes, they were exposed to enhanced chemiluminescence substrate (Clarity Western ECL substrate, Bio-Rad, USA) and analyzed by an Amersham system (GE Life Sciences, USA). Analysis of exosomal markers ALIX, TSG101, CD63, CD81 and CD9 was performed by loading relative to original urine volume (50 ml of urine was ultracentrifuged and the pellet dissolved in 180 μl Laemmli of which 15 μl was loaded). Analysis of AQP2 was performed with loading based on urine volume and urine creatinine. After immunoprecipitation, the precipitated fractions were loaded in equal volumes, along with equal volume of the supernatant fractions.

Transmission Electron Microscopy

Thawed 200K pellets before and after the water load (T1 vs W1) of four subjects were spotted onto Formvar-coated grids (200 mesh; Agar Scientific Ltd.). Adsorbed particles were directly negatively stained using UranyLess EM stain according to manufacturer instructions (Electron Microscopy Sciences; Catalog #22409). Briefly, grids were placed on a drop of UranyLess solution for 1 minute. Subsequently, grids were drained on filter paper and examined under a Philips CM100 electron microscope at 80 kV. Of each sample, ~50 particles were analyzed. EVs were defined as round shaped membrane vesicles rather homogenous in size not exceeding 100–150 nm in diameter.

Immunolocalization

The localization of CD9, CD63, and CD81 was determined in human kidney, bladder and prostate tissue obtained from healthy subjects which were procured according to the Dutch Code

of Conduct legislation concerning the use of residual tissue for research. The Code of Conduct maintains an opt-out consent system and therefore, no written informed consent was required. Staining was done by automated immunohistochemistry using the Ventana Benchmark ULTRA (Ventana Medical Systems, USA). Sequential 4-μm formalin-fixed paraffin-embedded (FFPE) sections were stained using the Ultraview Universal DAB detection Kit (Ventana Medical Systems, USA). In brief, following deparaffinization and heat-induced antigen retrieval with cell conditioning 1 (CC1, Ventana Medical Systems, USA) for 32 minutes at 100 °C, the tissue samples were incubated with either anti-CD9, anti-CD63, or anti-CD81 for 32 minutes at 37 °C. Incubation was followed by a hematoxylin II counter stain for 8 minutes and then a blue coloring reagent for 8 minutes at room temperature according to the manufacturer's instructions (Ventana medical systems, USA). Double staining protocols were performed by automated multiplex immunofluorescence using the Ventana Benchmark Discovery (Ventana Medical Systems, USA). In brief, following deparaffinization and heat-induced antigen retrieval with CC1 for 32 minutes, the tissue samples were incubated first with either CD9, CD63 or CD81 for 32 minutes at 37 °C, followed by detection with FAM (6-carboxyfluorescein) at 37°C for 12 minutes. An antigen denature step was performed using CC2 for 8 minutes at 100 °C. Slides were then incubated with either anti-NHE3 (proximal tubule marker), anti-NKCC2 (thick ascending limb marker), anti-parvalbumin (distal convoluted tubule marker), anti-AQP2 (collecting duct marker) or anti-WT1 (glomerular marker) for 32 minutes at 37 °C followed by detection with Red610 at 37°C for 12 minutes (Ventana Medical Systems, USA). Slides were washed in PBS and covered with DAPI in Vectashield (Vector Labs, United Kingdom).

Statistical analysis

Results were first tested for normal distribution and the statistical analysis was selected accordingly (see Table 4.S5 for overview). Correlations were calculated using Pearson's correlation coefficient. The serially obtained parameters in the water loading test were analyzed using repeated measures analysis of variance (ANOVA). Comparison of particle quantification techniques was performed by Bland-Altman analysis. The electron microscopy data were analyzed using a mixed linear model. A *P*-value < 0.05 was considered significant. Data are presented as mean ± SEM, unless stated otherwise.

4.4 Results

Urine creatinine correlates with particle number

In the concentrated and dilute urine samples from the water loading experiment, urine creatinine concentration highly correlated with particle count per time point (NTA and EVQuant, R2 0.99, *P* < 0.001, Figure 4.1A). This finding was confirmed in the individual (intra-person) correlations with an average R2 of 0.96 ± 0.05 using NTA and 0.96 ± 0.06 using EVQuant (Figure 4.1B). No differences were identified in the individual slopes (NTA *P* = 0.13, EVQuant *P* = 0.12). When analyzing the correlations for each time-point, the (inter-person) correlations were still high (Figure 4.1C). The uEV marker CD9 was also analyzed with EVQuant and urine creatinine concentration also showed a high correlation with CD9+ particles (Figure 4.S4). In random spot urines of another cohort of healthy subjects, we again identified high correlations between particle count and urine creatinine (Figure 4.1D). In random spot urines of patients with polycystic kidney disease, correlations also remained high, although slightly lower than in healthy subjects (Figure 4.1E). Correction of urine creatinine for body surface area did not improve the correlations (data not shown). Of note, the lowest correlations were identified with EVQuant in male healthy subjects and male patients.

Water loading reduces AQP2 but increases THP recovery

Water loading increased urine flow rate and decreased urine osmolality, and urine creatinine concentration, (Figures 4.2A-C, Figure 4.S5). Water loading significantly decreased urine particle concentration as measured by NTA and EVQuant (Figure 4.2D). In the 200K pellet, water loading reduced the abundance per unit volume of the exosome markers ALIX, TSG101, CD63, CD81 and CD9, and of AQP2. In contrast, water loading increased the amount of THP recovered in the 200 k pellet (Figure 4.2E). The excretion rate of creatinine remained constant, whereas osmole excretion rate significantly increased upon water loading (Figure 4.2F). This rise was mostly explained by an increase in urea, sodium and potassium (Table 4.S6). When loading the immunoblots normalized to urine creatinine, AQP2 abundance per creatinine decreased after water loading, confirming the biological response to the water load (Figure 4.2G).

FIGURE 4.1 **Correlations between urine creatinine and particle concentrations**

(next page)

A Correlation between average urine creatinine and particle concentrations per time-point of the water loading experiment as measured by NTA and EVQuant in whole urine (*n* = 11/time-point).

B Inter-individual correlations between urine creatinine and particle concentrations as measured by NTA and EVQuant. The reported R2 is the average of individual R2 ± SD. Each symbol represents a healthy subject (6 samples per subject, *n* = 66).

C Intra-individual correlations per time-point of the water loading experiment. Each symbol represents a time-point (samples per time-point, *n* = 66).

D Correlations between urine creatinine and particle concentrations in random spot urines from healthy male and female subjects (*n* = 15).

E Correlations between urine creatinine and particle concentrations in random spot urines from male and female patients with polycystic kidney disease (*n* = 26).

FIGURE 4.1 Correlations between urine creatinine and particle concentrations

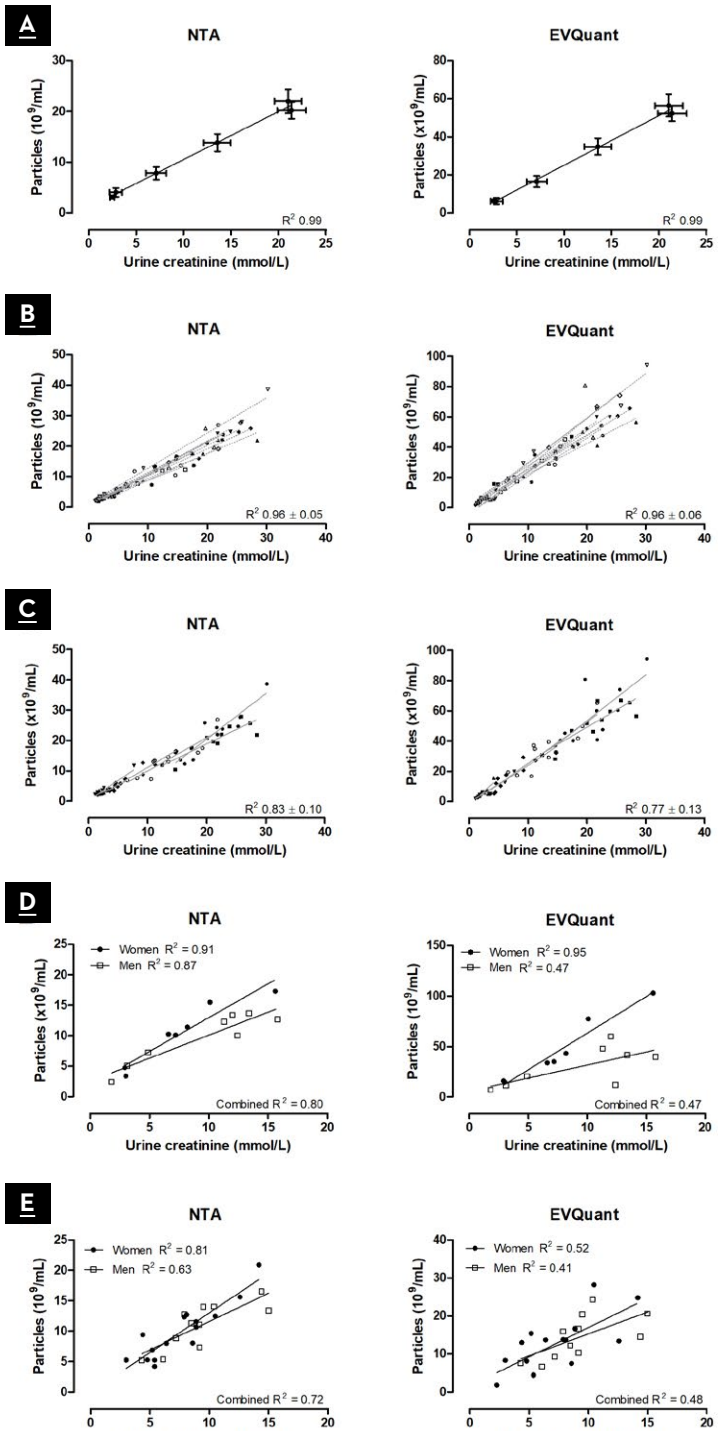

FIGURE 4.2 Effects of water deprivation and water loading on urine osmolality, urine creatinine, and urinary extracellular vesicle proteins

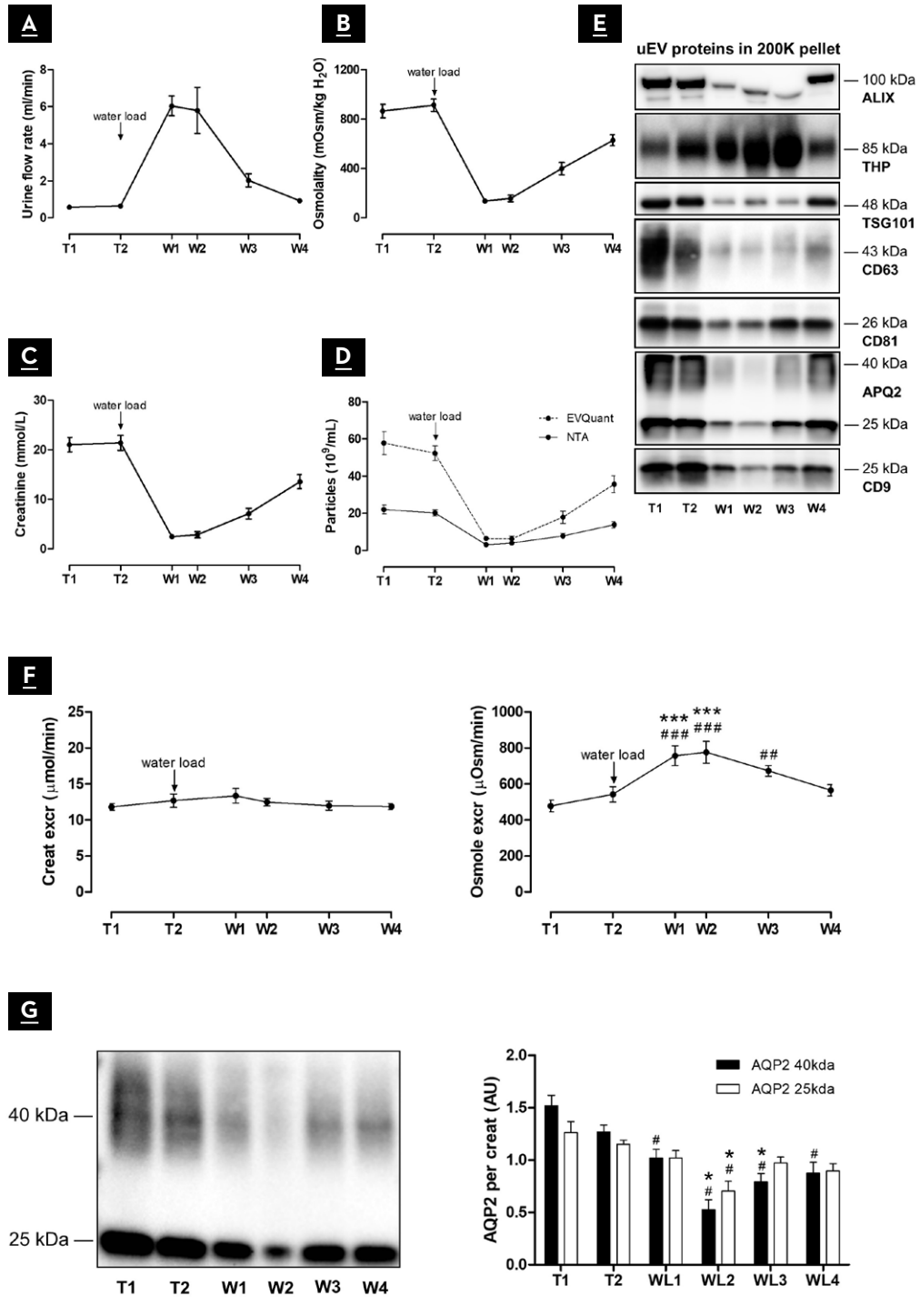

FIGURE 4.2 **Effects of water deprivation and water loading on urine osmolality, urine creatinine, and urinary extracellular vesicle proteins**

(previous page)

Urine flow rate **A**, urine osmolality **B** urine creatinine **C** and urine particle concentration, **D** during water deprivation (T1-2) and water loading (W1-4) in 11 healthy subjects.

E Representative immunoblots of uEV markers ALIX, TSG101, CD63, CD81, and CD9, and of THP and AQP2 loaded relative to original urine volume (50 ml of urine subjected to ultracentrifugation, pellet suspended in 180 μl, 15 μl loaded in each lane). Densitometry for all immunoblots (n = 11) showed ANOVA P < 0.001 with P < 0.001 for post-hoc testing of W1 vs. T2.

F Urinary excretion rates of creatinine and osmoles (urine volume was recorded for n = 8; formula: concentration x volume, expressed per minute). ### and *** P < 0.001 vs. T1 and T2, respectively; ## P < 0.01 vs. T1.

G Representative immunoblot of AQP2 loaded by urine creatinine level and densitometry of the two AQP2 bands per creatinine in the 11 participants, with the average normalized to one. Repeated measures ANOVA was performed on the average of the two bands (25 and 40 kDa, # P < 0.05 vs. T1, * P < 0.05 vs. T2 in post-hoc tests).

THP interferes with NTA, water loading increases uEV size

A 50% increase of urine particle excretion rate after water loading was detected by NTA (P < 0.001, Figure 4.3A), which was accompanied by a 11 nm increase in median size (P < 0.001, Figure 4.3B, Figure 4.S6). In contrast, the excretion rate of particles as measured by EVQuant or CD9-TR-FIA was not increased by water loading (Figures 4.3C-D). We hypothesized that NTA detected THP as particles. To test this possibility, we added physiological amounts of THP to urine[337] and showed that THP increased particle count (Figure 4.4A) and was visible as non-spherical particles (Videos 4.S1 and 4.S2). However, this did not yet explain the increase in particle size. Therefore, we analyzed whether the *ex vivo* addition of hypotonic or hypertonic solutions affected particle count and particle size (Figure 4.4B). Increasing tonicity

VIDEO 4.S1-4.S2 **Representative NTA videos before and after the addition of THP**

See uploaded videos **on jasn.asnjournals.org/content/32/5/1210/tab-figures-data**

When visually inspecting the NTA recordings for samples before and after THP addition, the increased small particle numbers appear to also include non-spherical objects. While NTA is not a platform intended to assess the shape or structural properties of particles, visual inspection is compatible with THP-vesicle or THP-protein aggregate formation, as could be expected due to THP multimer formation.

FIGURE 4.3 **Particle excretion rate and size during water deprivation (T1-2) and after water loading (W1-4)**

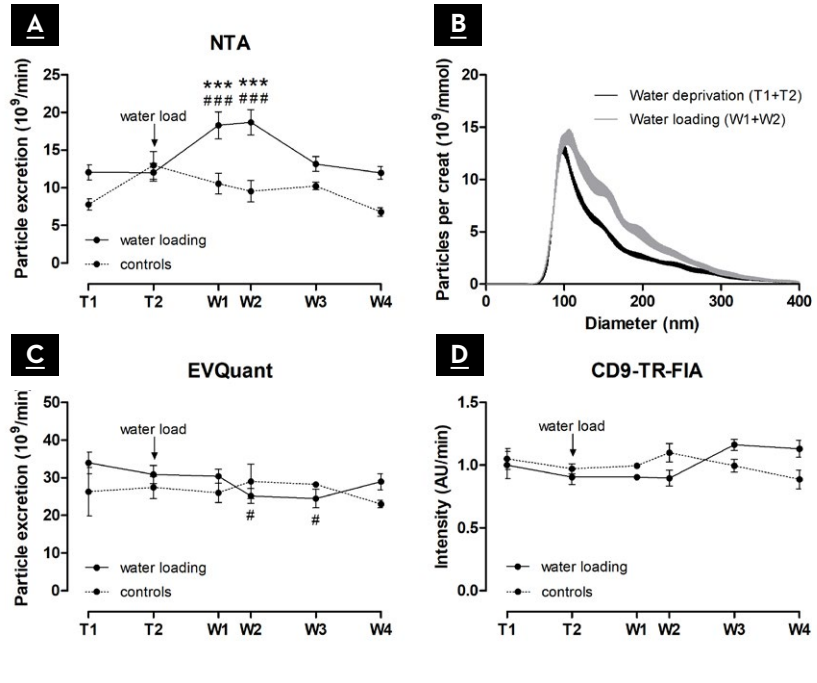

A uEV excretion rate by NTA in subjects undergoing the water loading protocol (urine volume was recorded for n = 8) and controls (n = 3). ### and *** P < 0.001 vs. T1 and T2 in post-hoc tests, **B** NTA-based size distribution of particles/mmol creatinine at every time point of the water loading in whole urine (per 1 nm size bin ± SEM, n = 8, see also Figure S5). **C-D** Particle excretion rate as measured by EVQuant and CD9-TR-FIA in subjects undergoing the water loading protocol (n = 8) and controls (n = 3). # P < 0.05 *vs.* T1 in post-hoc test.

reduced particle count (Figure 4.4C), but both hypotonic and hypertonic solutions significantly increased particle size compared to isotonic solution (Figure 4.4D). To address this further, TEM was performed to compare the size of EVs in urine samples collected during water deprivation and water loading (Figure 4.4E) and after excluding an effect of ultracentrifugation on particle size (Figure 4.S3). Median uEV size by TEM during water deprivation was 47 nm (range 32 – 63 nm), which increased to 71 nm (39 – 103 nm) after water loading (P < 0.001, Figure 4.4F). The TEM data were mathematically modeled using a 6th degree polynomial equation to analyze whether the increase in uEV size after water loading could explain the enhanced detection by NTA (Figure 4.4G). With the detection limit set between 35 – 65 nm, 57% of uEVs in water deprivation samples and 27% of uEVs in water loading samples were missed. Therefore, water loading may have increased particle detection by NTA with as much as 70%.

FIGURE 4.4 **Effect of Tamm-Horsfall Protein (THP) and urinary concentration on particle count and size**

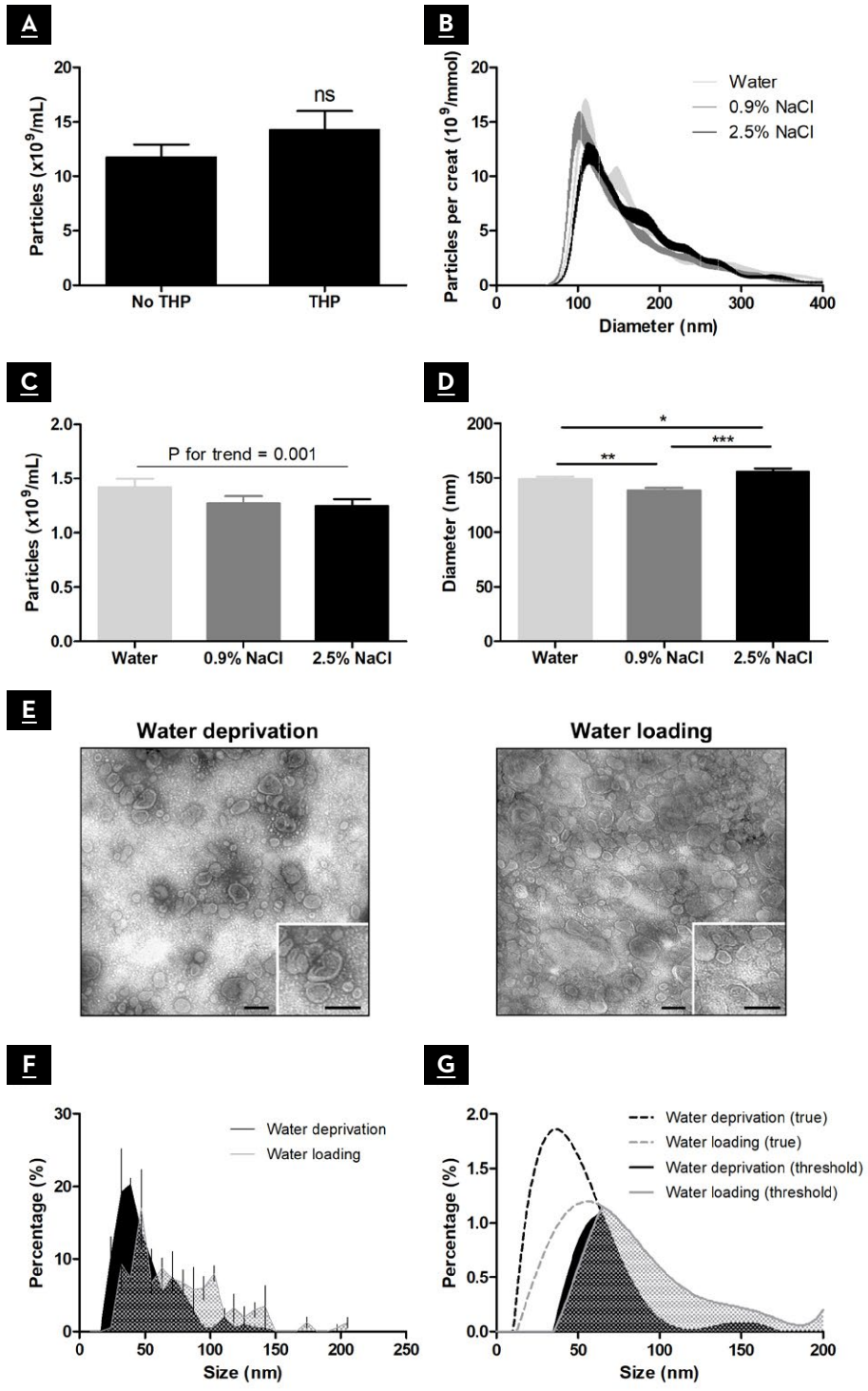

FIGURE 4.4 **Effect of Tamm-Horsfall Protein (THP) and urinary concentration on particle count and size**

A The addition of THP (40 μg/mL) significantly increased particle count by NTA (*n* = 12/treatment).

B NTA size distribution graph with different solutions added to whole urine (*n* = 15/treatment).

C Particle count was significantly lower when solutions with increasing tonicity were added to whole urine (*n* = 15/treatment).

D Particle size was significantly higher when adding hypotonic or hypertonic solution to whole urine (*n* = 15/treatment; * $P < 0.05$, ** $P < 0.01$, *** $P < 0.001$).

E Representative image of negative staining transmission electron microscopy (TEM) of 200K pellets from urine sample during water deprivation (T1, left panel) and directly after water loading (W1, right panel). The black bar represents 100 nm.

F TEM size distribution of double membrane vesicles of water deprivation and water loading samples (*n* = 4, per 8 nm size bin ± SEM). Analysis was performed by mixed linear model.

G Polynomial model based on TEM size distribution, with an arbitrary linear threshold between 35 and 65 nm representing the possible threshold of NTA. Areas under the curves were used to determine the percentage of uEVs that are missed with this threshold (per 1 nm size bin).

FIGURE 4.5 **Comparison of three whole urine uEV quantification techniques**

(next page)

Nanoparticle tracking analysis (NTA), EVQuant, and CD9 time-resolved fluorescence immunoassay (TR-FIA) were compared using the urine samples from the water loading study (*n* = 66). Correlation **A** and Bland-Altman plot **B** of particle concentrations measured by EVQuant versus NTA. Limits of agreements are not shown because of the severe skewing ($P < 0.001$) at low concentrations. **C** Ratio of particles as measured by NTA *vs.* EVQuant in relation to urinary creatinine and **D** osmolality, with representation of the deflection points, to determine at which urine creatinine concentration or urine osmolality skewing starts (dashed lines), **E** correlation and **F** Bland-Altman plot of urinary particle concentrations measured by NTA *vs.* TR-FIA . Correlation **G** and Bland-Altman plot **H** of EVQuant *vs.* CD9-TR-FIA. In the Bland-Altman plots limits of agreements are shown by the dotted lines.

FIGURE 4.5 **Comparison of three whole urine uEV quantification techniques**

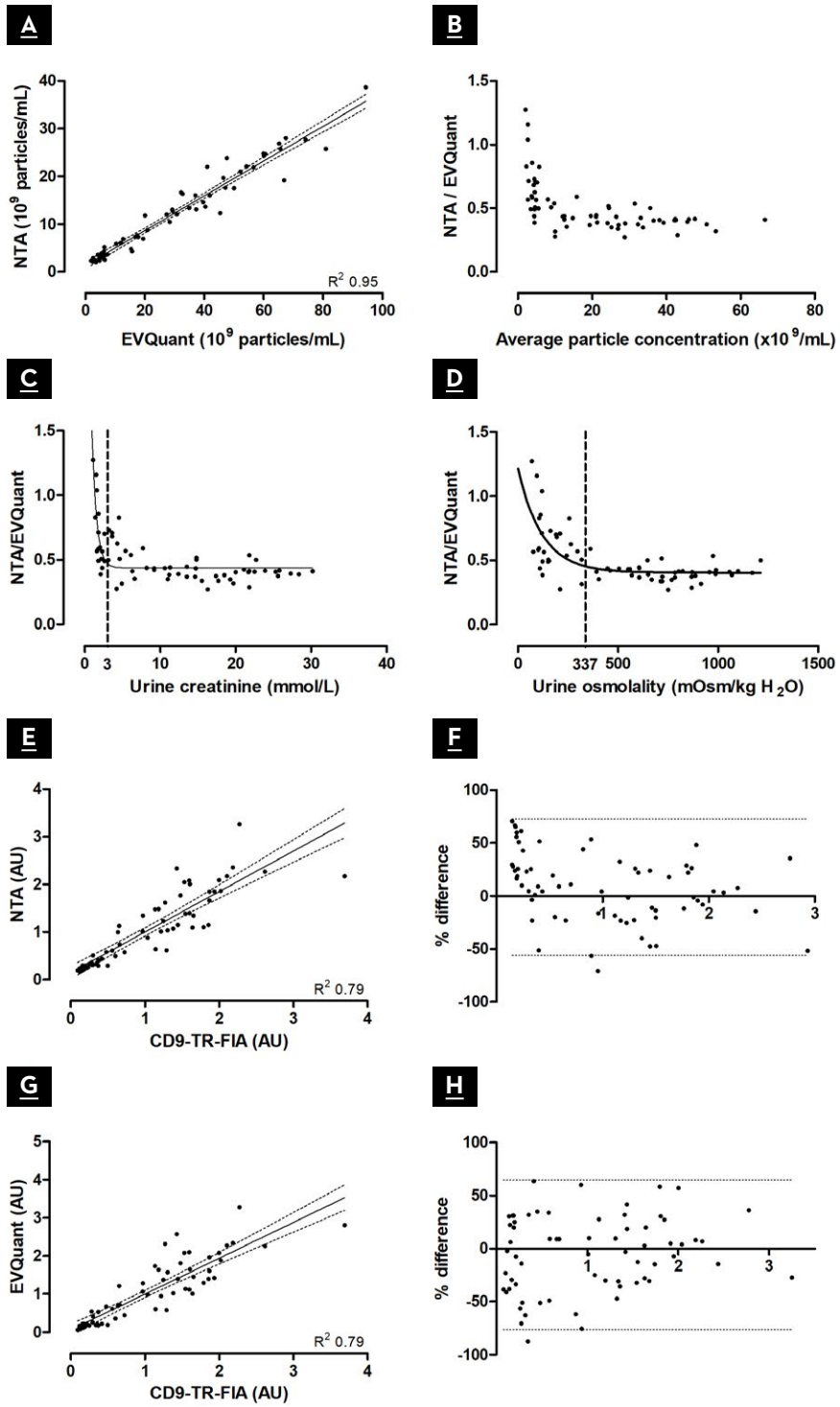

FIGURE 4.6 **Immunohistochemistry and immunolocalization of CD9 and CD63 in healthy human kidney, bladder, and prostate tissue**

A Immunohistochemistry of CD9 and CD63 (both brown).

B Immunofluorescence of normal human kidney, prostate and bladder tissue, to determine co-localization of CD9 and CD63. The following markers were used for nephron segments, including villin for proximal tubule, NKCC2 for the thick ascending limb, parvalbumin for the distal convoluted tubule, and AQP2 for the collecting duct. Blue: nuclear staining with DAPI.

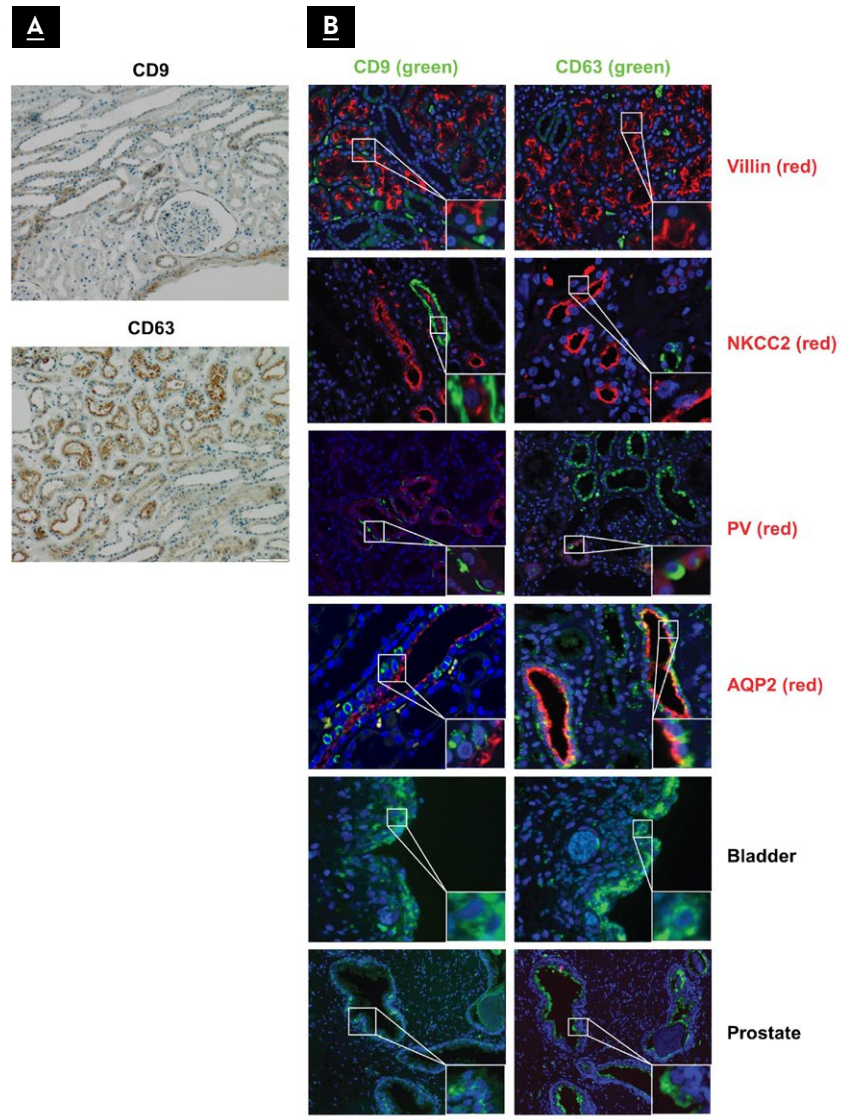

Comparison of particle quantification techniques

Representative raw image data of NTA, EVQuant, and CD9-TR-FIA are shown in Figure 4.S7. Urine particle concentrations as measured by NTA and EVQuant correlated strongly (R2 = 0.95, Figure 4.5A). However, EVQuant identified 2.8 ± 0.1 times more particles (P < 0.001). Bland-Altman analysis demonstrated a high agreement between the two methods, but a skewed curve towards lower particle concentrations (P < 0.001, Figure 4.5B). This is in line with the "pseudo-increase" in particle excretion rate after water loading with NTA (Figure 4.3A). This skewing was relevant for urine creatinine concentrations below 3 mmol/L, or urine osmolalities below 337 mOsm/kg (Figures 4.5C-D). Bland-Altman comparisons of particle quantification by CD9-TR-FIA demonstrated weaker correlations with NTA and EVQuant (Figures 4.5E-H). Again, there was skewing at lower particle concentrations with NTA (P < 0.05), but not with EVQuant (P = 0.10).

CD9 and CD63 in kidney and uEVs

Although CD9 and CD63 are considered general markers for exosomes, and as such used as capture proteins for the TR-FIA assays, it is not known from which tubular segments EVs are isolated. CD9 and CD63 co-localized selectively with the distal convoluted tubule marker parvalbumin and the collecting duct marker AQP2 (Figure 4.6). Both tetraspanins were also detectable in prostate and bladder tissue. To analyze this further, the distribution of CD9+ and CD63+ particles in human urine was assessed using EVQuant (Figure 4.7A). This showed that 32 ± 3% of particles were CD9+ and 8 ± 2% were CD63+, while 10% of CD9+ particles were also CD63+, and 33% of CD63+ particles were also CD9+. Pull-down by both tetraspanins resulted in an immunoblot signal for NCC (another distal convoluted tubule marker) and AQP2, but not for NHE3, NaPi-IIa, and NKCC2 (markers of the proximal tubule and thick ascending limb, Figures 4.7B-C, Figure 4.S8). Pull-down of AQP2 appeared more efficient with CD9 than with CD63. Co-localization was repeated with another CD9 and CD63 antibody and CD81, which only showed co-localizations of CD63 with parvalbumin and CD81 with the proximal tubule marker villin (Figure 4.S9).

FIGURE 4.7 **Characterization of CD9+ and CD63+ particles**

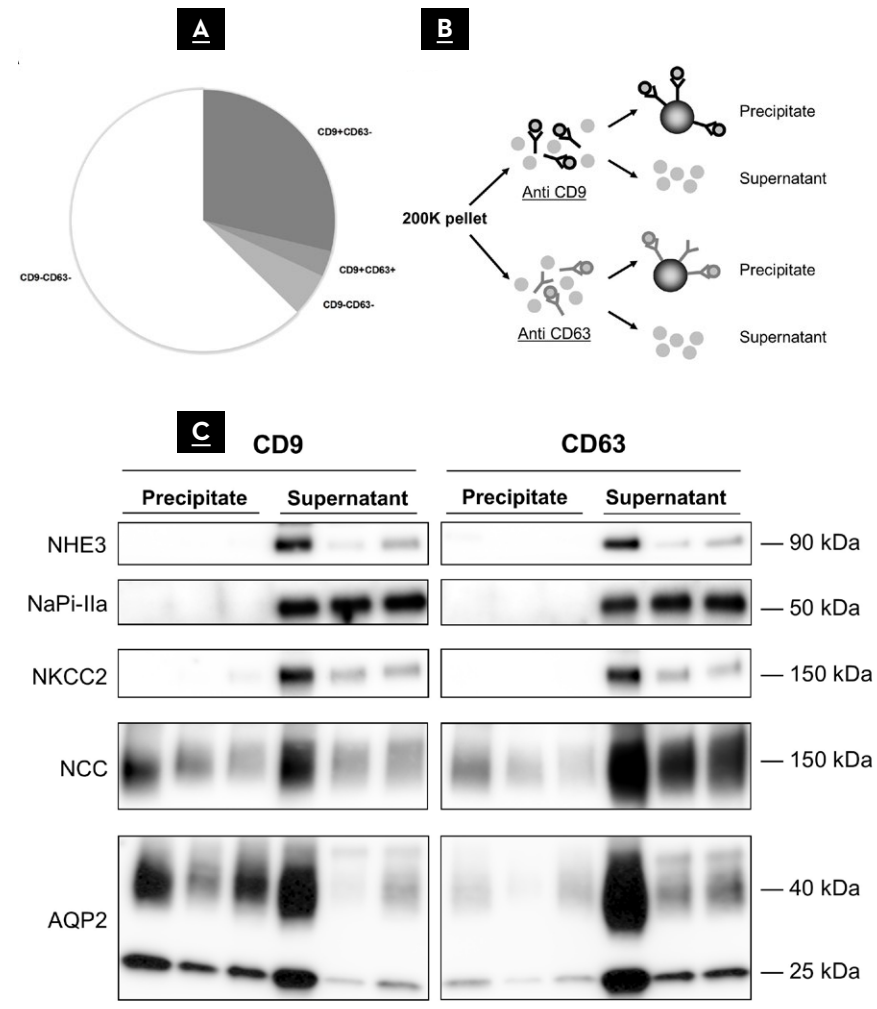

A Pie chart showing CD9+ and CD63+ distribution of particles as measured by EVQuant in second void morning spot urines (n = 6).

B The 200K pellet was divided and subjected to either anti-CD9 or anti-CD63 antibodies. The magnetic beads were added to separate antibody bound (precipitate) from non-bound particles (supernatant).

C Immunoblots of NHE3 and NaPi-IIa (proximal tubule marker), NKCC2 (thick ascending limb marker), NCC (distal convoluted tubule marker), and AQP2 (collecting duct marker) in particles precipitated from 200K pellets (n = 3 subjects) by either CD9- or CD63-antibody coated magnetic beads. See also Figure S8 for the 3 additional subjects.

FIGURE 4.8 **Use of detergent to enhance intracellular epitope recognition**

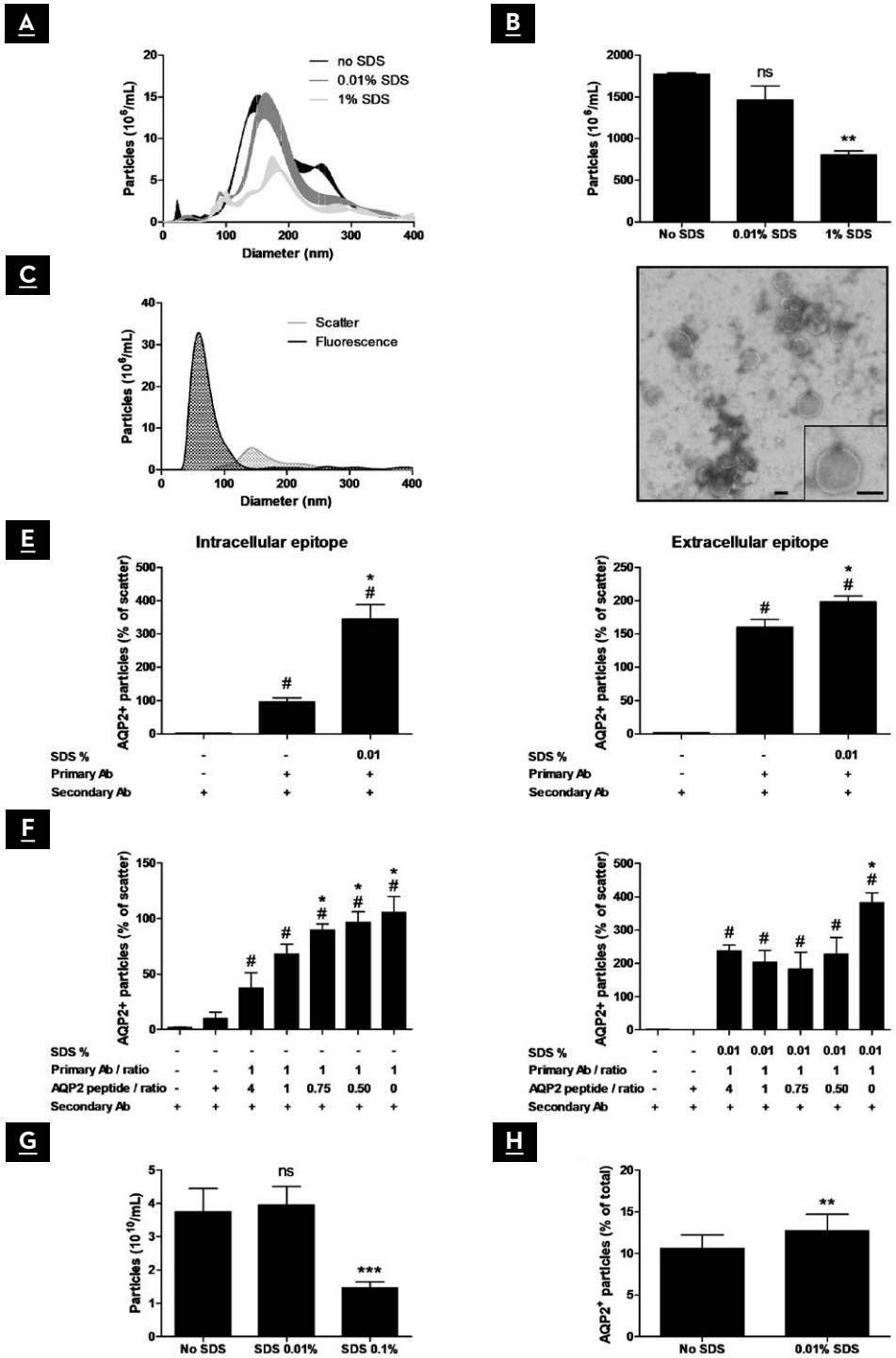

FIGURE 4.8 **Use of detergent to enhance intracellular epitope recognition**

A NTA size distribution graph of whole urine samples without SDS and treated by 0.01% v/v or 1% v/v SDS (*n* = 3/treatment).

B NTA particle counts without SDS, with 0.01% v/v or 1% v/v SDS (*n* = 3/treatment, ** *P* < 0.01 *vs.* no SDS).

C Representative TEM image of 0.01% v/v SDS-treated 200K pellets. The bar represents 100 nm.

D Fluorescence NTA-based representative size distribution of uEVs treated with 0.01% v/v SDS vs. controls using a NanoSight NS300 in fluorescent mode (AQP2-488) and in scatter mode.

E Use of intracellular-epitope and extracellular-epitope AQP2 antibodies to determine the percentage of AQP2+ particles (relative to particle count in scatter mode) without SDS and with 0.01% v/v SDS (*n* = 3-7/treatment). See Figure 4.S11 for characteristics of the extracellular-epitope AQP2 antibody. To determine the background noise, urine samples were also treated with only secondary antibody (*n* = 3-6). # *P* < 0.05 *vs.* secondary antibody only, * *P* < 0.05 *vs.* primary and secondary antibody without SDS.

F AQP2 antibody and anti-AQP2 peptide inhibition experiment (*n* = 3-4/treatment, * and # P < 0.05 vs. 1:4 ratio and anti-AQP2 peptide + secondary antibody, respectively), in the absence (left panel) or presence (right panel) of SDS

G Particle counts by EVQuant of urine samples without SDS, with 0.01% SDS or 0.1% SDS (*n* = 15/treatment, *** *P* < 0.001 *vs.* no SDS).

H Percentage of EVQuant-detected particles which co-localized with AQP2-alexa488nm in urine samples without SDS *vs.* 0.01% SDS (*n* = 15/treatment, ** P < 0.01).

Use of detergent for intracellular epitope recognition

Current uEV characterization methods only allow for antibody characterization of extracellular epitopes of uEVs, while often antibodies against intracellular epitopes are used.[108, 338] Alternatively, the detergent sodium dodecyl sulphate (SDS) can be used to provide antibodies access to intracellular epitopes of uEVs.[24] To this end, the effect of various SDS concentrations on whole urine particle size distribution and concentration was determined using fluorescence NTA. While 1% v/v SDS significantly lowered particle concentration, SDS 0.01% v/v only elicited a small right shift of the size distribution (Figure 4.8A) and did not significantly reduce particle count (Figure 4.8B). Few particles were detected when using buffer with SDS or ultrafiltered urine with SDS (Figure 4.S10A). TEM of 0.01% v/v SDS treated urine samples demonstrated

particles resembling those of non-treated samples (Figure 4.8C). Fluorescent AQP2+ particles had a smaller size distribution than total particles as measured in scatter mode (AQP2 63 ± 7 nm, scatter mode 150 ± 9 nm, Figure 4.8D). Few particles were detected when using buffer or secondary antibody only (Figure 4.S10B). An intracellular and extracellular epitope antibody against AQP2 were added to whole urine and secondarily labelled with fluorescent dye to study the influence of SDS 0.01% v/v on the number of fluorescent particles on NTA. SDS significantly increased the detection of AQP2+ particles with both type of antibodies, although the enhancement was more prominent with the intracellular-epitope antibody (~3.5-fold increase, Figure 4.8E). With decreasing anti-AQP2 peptide to antibody ratio, the AQP2+ signal significantly increased with and without 0.01% v/v SDS, showing the signal specificity (Figure 4.8F). Finally, we addressed whether detergent could also increase AQP2 signal with EVQuant. SDS 0.01% v/v did not change particle count, while SDS 0.1% v/v markedly reduced the number of particles (Figure 4.8G). 0.01% v/v SDS significantly increased the percentage of AQP2+ particles (Figure 4.8G).

4.5 Discussion

This study addresses two important questions for high-throughput analysis of uEVs, namely how to normalize uEV concentration and how to quantify uEVs in spot urines. Using an intervention that produced maximal differences in urine concentration, both urinary creatinine and uEV excretion rates remained constant and were highly correlated. In random spot urines from healthy volunteers and kidney patients, the correlation between particle and creatinine concentration was also high. This suggests that urine creatinine can be used as a normalization marker for uEV concentration in spot urines. Because differences in muscle mass and diet influence creatinine production, this should be taken into account in uEV studies using urine creatinine as normalization variable. This may also explain the lower correlation in men who have higher muscle mass; an alternative explanation could be the presence of prostate-derived EVs. A previous study concluded that urine creatinine and osmolality are equally suitable for normalization [274]. Our data suggest that urine osmolality is less suitable in the specific setting of large differences in urinary concentration. This may be explained by water deprivation limiting osmolar excretion and water loading relieving this.

This study also identified several novel technical aspects that are relevant for future uEV studies in whole urine (summarized in Table 4.1). This includes (1) the interference of THP with NTA in whole urine, (2) excretion of larger uEVs in dilute urine, (3) selective tubular staining of CD9 and CD63 (frequently used as capture antibodies in TR-FIA), and (4) the ability to use detergent with NTA and EVQuant to increase intracellular epitope recognition. These findings will be discussed in more detail below.

TABLE 4.1 Comparison of the three uEV techniques for quantification and protein characterization

	NTA	CD9/63-TR-FIA	EVQUANT
Quantification	++	+	+++
Comments	• Absolute number and uEV size • Affected by urinary dilution, Tamm-Horsfall protein, and proteinuria • Detection threshold for smaller uEVs	• Only relative number of CD9/CD63+ uEVs	• Absolute number • Detects most particles
uEV-protein detection	++	+	++
Comments	• Can be combined with SDS and intracellular-epitope antibodies	• Can be combined with SDS and intracellular-epitope antibodies • EV selection depends on isoform affinity of capture antibodies used	• Can be combined with SDS and intracellular-epitope antibodies

Our study clearly shows that THP should be taken into account when studying uEVs, as emphasized previously [25, 202]. More THP was detected in dilute urine, suggesting that urinary concentration reduces THP polymerization generating more THP oligomers. This is one possible explanation why only NTA detected more particles after water loading. Indeed, adding THP to urine increased particle count measured by NTA. Conversely, adding hypertonic solution to urine reduced particle count, likely because hypertonic saline enhanced THP polymerization, caused a "salting out" effect [339], or caused passive or active movement of water through aquaporins. A previous study showed that uEVs are remarkably resistant to osmotic stress [340], rendering osmotic damage to membrane integrity unlikely. Of interest, both the addition of hypotonic and hypertonic solution increased particle size. We propose that the hypertonic solution increased THP polymerization leading to larger THP aggregates that may have also captured EVs. Conversely, our electron microscopy data indicate that uEV size truly increases in dilute urine, confirming a previous study [341]. The increase in uEV-size causes more uEVs to reach NTA's size detection limit and provides a second explanation why NTA detected more particles after water loading. Because previous studies have shown that NTA also detects more particles in proteinuric samples [256, 257], it must be concluded that NTA has important caveats when applied to whole urine samples. A previous study showed that this interference persists when analyzing particles in the low centrifugation pellet [25]. This is relevant because NTA is cur-

rently recommended as the key method for uEV characterization [5]. The novel EVQuant method is therefore an attractive alternative for uEV quantification, because it allows fast analysis of multiple proteins at a single vesicle level, while labeling only lipid particles and not protein aggregates. When using NTA, an overestimation of uEV-number in urines with a creatinine concentration below 3 mmol/L or a urine osmolality below 337 mOsm/kg should be anticipated.
TR-FIA facilitates signal amplification making it suitable for low-abundant proteins. However, our study also revealed an important caveat when using this approach with the commonly used uEV markers CD9 and CD63. Depending on the antibody used, CD9 and CD63 co-localized only with distal convoluted tubule and collecting duct markers, whereas the predicted expression in rat kidney is more general [342]. Indeed, immunoprecipitation isolated uEVs only from these tubular segments. CD9 and CD63 are expressed in multiple isoforms and cell-specific expression patterns of these isoforms may cause selective antibody recognition. Therefore, the choice of the capture antibody in TR-FIA likely determines from which tubular segments EVs will be isolated.

In addition to quantification of uEVs, NTA, EVQuant and TR-FIA can also be used in combination with antibodies targeting extracellular epitopes on uEVs. Plasma membrane permeabilization is required when using antibodies targeting intracellular epitopes. Previously, we used the detergent SDS in a CD9-TR-FIA assay to permeabilize uEVs and gain access to intracellular epitopes [24]. In the current study, 0.01% v/v SDS was demonstrated to increase detection of intracellular epitopes with NTA and EVQuant, while leaving the number and integrity of uEVs largely intact. This is in line with previous data showing that SDS does not decrease the CD9 signal, but does increase NCC and AQP2 signal with CD9-TR-FIA [24]. Interestingly, without detergent, the fluorescent particle count was not at control levels. Oosthuyzen *et al.* [22] also reported that AQP2+ uEVs could be detected without detergent despite using an AQP2 antibody against an intracellular epitope. This suggests the presence of vesicles with reverse topology, such as endosomes or an inside-out switch of membrane proteins, as was previously found in EVs in cell culture [343]. Reverse topology was also supported by our findings using a new extracellular-epitope AQP2 antibody. SDS-enhancement was greater with the intracellular-epitope AQP2 antibody, but still significant with the extracellular-epitope antibody, suggesting that some of the extracellular domains are present within uEVs. Interestingly, fluorescent AQP2+ particles were smaller than total uEVs as determined by the scatter mode of NTA. The same was observed by Oosthuyzen *et al.*, and implies that uEVs containing AQP2 are smaller than average [22]. Fluorescent signals are stronger than general light scatter, which explains why smaller uEVs can be detected in fluorescent mode, but not in scatter mode.

In this study we have investigated approaches that can quantify and characterize uEVs in whole urine, replacing the need for ultracentrifugation. These approaches are attractive for higher throughput analyses towards clinical application of uEV analysis. Furthermore, ultracentrifugation has a number of limitations [134]. Although we showed that the uEV yield was similar in the water deprived and water loaded urine samples, differences in density and viscosity may influence the sedimentation rate. Some authors have therefore normalized urine composition using dilution [200] or dialysis [189].

Our study met all of the currently recommended quality controls for EV research [5]. However, several methodology and knowledge gaps remain in the evolving field of uEV research. We believe the current study addresses some of these technical challenges, but will require further validation and follow-up by future studies.

In conclusion, uEV concentration is highly correlated with urine creatinine, potentially replacing the need for uEV-quantification to normalize spot urines. Additional findings are relevant for future uEV studies in whole urine, including the interference of THP with NTA, excretion of larger uEVs in dilute urine, capture of nephron segment-specific EVs with CD9 and C63, and the ability to use detergent to increase intracellular epitope recognition in uEVs.

Supplemental Table of Contents

TABLE 4.S1 Characteristics of healthy subjects

	AGE (YEARS)	SEX (F/M)	WEIGHT (KG)	BMI (KG/M2)	CREATININE EXCRETION* (MMOL/DAY)
Healthy subjects subjected to water deprivation followed by water loading					
Subject 1#	46	M	80.8	25.8	N.A.
Subject 2#	27	M	92.6	27.7	N.A.
Subject 3#	40	M	91.8	27.4	N.A.
Subject 4	27	M	96.6	25.7	21.3
Subject 5	27	M	103.5	27.2	18.5
Subject 6	30	M	85.7	25.6	17.8
Subject 7	28	M	93.0	26.9	18.7
Subject 8	27	M	65.3	21.1	17.6
Subject 9	43	M	90.4	25.0	17.8
Subject 10	34	M	75.1	22.4	14.1
Subject 11	30	M	70.9	22.4	16.1
Average	33±7	M	86±12	25±2	18±2
Healthy subjects who provided random spot urine					
Subject 12	26	M	70	23.7	N.A.
Subject 13	29	M	89	26.6	N.A.
Subject 14	42	M	74	22.6	N.A.
Subject 15	28	M	76	23.5	N.A.
Subject 16	25	M	75	22.6	N.A.
Subject 17	31	M	63	19.7	N.A.
Subject 18	55	M	90	24.9	N.A.
Subject 19	29	M	70	24.2	N.A.
Subject 20	26	F	65	23.0	N.A.
Subject 21	27	F	69	23.9	N.A.
Subject 22	35	F	55	22.9	N.A.
Subject 23	30	F	75	25.6	N.A.
Subject 24	41	F	58	21.3	N.A.
Subject 25	26	F	74	23.1	N.A.
Subject 26	53	F	85	29.8	N.A.
Average	34±10	F: 47%	73±10	24±2	N.A.

N.A., not available.
* Extrapolated from excretion in 12 hours
# These subjects participated both in the water loading study and as time-controls on a separate day.

TABLE 4.S2

Characteristics of patients

	AGE (YEARS)	SEX (F/M)	WEIGHT (KG)	BMI (KG/M²)	CREATININE EXCRETION* (MMOL/DAY)	EGFR (ML/MIN /1.73M²)	ACR (SPOT URINE) (MG/MOL)
Patient 1	41	F	54.8	19.2	11.5	64	7.2
Patient 2	22	M	82.8	24.5	N.A.	103	0.6
Patient 3	58	F	77.0	25.4	12.5	20	0.9
Patient 4	58	M	90.0	29.7	11.6	18	176.3
Patient 5	49	F	72.0	25.5	11.0	86	5.8
Patient 6	55	F	94.0	32.5	9.4	37	0.5
Patient 7	43	M	86.5	23.0	17.4	73	9.7
Patient 8	23	F	74.0	25.6	11.7	107	6.6
Patient 9	54	F	90.0	31.5	10.6	20	7.6
Patient 10	39	M	107.0	30.3	15.6	103	4.5
Patient 11	54	M	98.3	26.7	14.6	82	0.0
Patient 12	43	F	67.1	24.6	12.2	75	1.5
Patient 13	53	M	91.5	26.4	20.0	60	2.0
Patient 14	36	F	65.0	22.0	13.3	107	7.1
Patient 15	58	M	105.0	27.3	26.9	66	0.6
Patient 16	64	M	78.0	24.6	19.7	34	2.0
Patient 17	57	F	68.0	25.6	8.1	66	0.6
Patient 18	54	F	78.6	26.0	11.3	62	0.8
Patient 19	34	F	79.6	30.7	13.0	87	1.9
Patient 20	24	F	86.7	28.0	11.3	120	0.4
Patient 21	43	F	60.9	23.8	9.8	101	0.7
Patient 22	36	F	71.2	26.8	10.3	86	3.3
Patient 23	54	M	74.0	24.2	12.6	58	13.9
Patient 24	51	M	90.7	24.6	19.9	73	14.2
Patient 25	45	F	64.0	21.6	9.2	90	1.1
Patient 26	60	M	90.0	26.6	15.8	16	9.2
Average	46±12	F: 58%	81±13	26±3	14±4	70±30	2 (0.7-7)

Abbreviations: **ACR**, albumin to creatinine ratio; **BMI**, body mass index; **eGFR**, estimated glomerular filtration rate according to CKD-EPI equation; N.A., not available.

TABLE 4.S3

Antibodies

USED WITH	ANTIBODY	TYPE	SPECIES	CONC.	SOURCE	CAT#/ CLONE	EPITOPE
NTA	AQP2 (intracell)	Primary	Rabbit	1:1000	Millipore	178612	254-271
	AQP2 (extracell)	Primary	Rabbit	1:1000	Fenton	Rb323	178-191
	Rabbit, alexa488	Sec.	Goat	1:300	Thermo SC	A-11008	N.A.
EVQuant	CD9 alexa-647	Primary	Mouse	1:25	Thermo SC	MA5-18154	EC2
	CD63 alexa-488	Primary	Mouse	1:80	Santa Cruz	SC5275	N.A.
	AQP2 ATTO-488	Primary	Rabbit	1:100	Stressmarq	Spc-503	253–262
CD9-TRFIA	CD9-biotin	Capture	Mouse	1:500	Thermo SC	SN4 C3-3A2	N.A.
	CD9-Europium	Primary	Mouse	25ng/mL	CellGS	CGS12A	N.A.
IP	CD9-biotin	Capture	Mouse	1:50	Thermo SC	SN4 C3-3A2	N.A.
	CD63-biotin	Capture	Mouse	1:50	Biolegend	H5C6	C-term
Immunoblot	CD9	Primary	Mouse	1:500	R&D Syst	MAB1880	1-228
	CD63	Primary	Mouse	1:500	BD Biosc	556019	N.A.
	CD81	Primary	Mouse	1:500	Novus Biol	MAB4615	N.A.
	ALIX	Primary	Mouse	1:200	Santa Cruz	SC53540	N.A.
	TSG101	Primary	Mouse	1:333	Abcam	ab83	167-374
	AQP2	Primary	Rabbit	1:1000	Stressmarq	9398	253–262
	NHE3	Primary	Rabbit	1:1000	Stressmarq	H7644	621–640
	NaPi-IIa	Primary	Rabbit	1:500	Abcam	ab151129	15-97
	NKCC2	Primary	Rabbit	1:1000	Stressmarq	Spc-401D	33-55
	NCC	Primary	Rabbit	1:2000	Millipore	AB3553	N-term
	Mouse HRP	Sec.	Goat	1:3000	Biorad	L005680	N.A.
	Rabbit HRP	Sec.	Goat	1:3000	Biorad	L005679	N.A.
IHC/IF	CD9 (1)	Primary	Mouse	1:800	R&D Syst	MAB1880	1-228
	CD63 (1)	Primary	Mouse	1:500	BD Biosc	556019	N.A.
	WT-1	Primary	Mouse	3.7mg/L	Cell Marq	348M-9	N.A.
	Villin	Primary	Rabbit	1:500	Abcam	ab133510	650-750
	NKCC2	Primary	Rabbit	1:400	Stressmarq	Spc401D	33-55
	Parvalbumin	Primary	Rabbit	1:800	Swant	PV27	N.A.
	AQP2	Primary	Rabbit	1:4000	Stressmarq	9398	253-262
	CD9 (2)	Primary	Mouse	1:250	Novusbio	5G6	N.A.
	CD63 (2)	Primary	Mouse	1:250	Novusbio	MEM-259	N.A.
	CD81	Primary	Rabbit	1:400	Genetex	Gtx101766	Center

Abbreviations: **Conc**., concentration; **IHC/IF**, immunohistochemistry/immunofluorescence; **IP**, immunoprecipitation; N.A., not available; **Sec**., secondary.

TABLE 4.S4

Differential ultracentrifugation steps

CENTRIFUGE CHARACTERISTICS	STEP 1	STEP 2	STEP 3	STEP 4
Force, x g	2,000	17,000	17,000	200,000
Time, min	10	20	20	120
Temperature, °C	4	4	4	4
Rotor	Standard Hettich Rotanta	45 Ti	70.1 Ti	45 Ti
Fixed angle vs swing	Swing	Fixed	Fixed	Fixed
K factor	25000	1839	965.4	156.3
Tube	Falcon 50mL	#355655	#355603	#355655
Deceleration time	90 sec	Max (6 min)	Max (6 min)	Max (6 min)

All tubings and rotors are from Beck Coulter.

TABLE 4.S5

Overview of statistical analyses

FIGURE	STATISTICAL METHODS	DATA DISTRIBUTION
Figure 1	Pearson correlation coefficient	Normal
Figure 2	Repeated measures ANOVA	Normal
Figure 3	Repeated measures ANOVA	Normal
Figure 4	Paired T-test (A) Repeated measures ANOVA (C-D) Mixed linear model (F-G)	Normal Normal Normal
Figure 5	Pearson correlation coefficient and Bland-Altman	Normal
Figure 8	ANOVA with post-hoc test (B, E, F) Repeated measures ANOVA (G) Paired T-test (H)	Normal Normal Normal

TABLE 4.S6

Additional characteristics and urine biochemistries of the water loading experiment

VARIABLE	T1	T2	W1	W2	W3	W4	ANOVA
Additional characteristics							
Void deviation from schedule (min)	2±4	0±1	-2±4	-1±4	0±1	0±2	0.09
Process time (min)	62±7	55±7	58±6	57±7	52±10	65±7*	0.001
Time in bladder (hours)	3.06	1.97	1.96	1.02	2.02	1.99	-
Urine volume (mL)	105±24	76±27	713±188***	354±214***	248±130*	110±35	<0.0001
Urinary flow rate (ml/min)	0.6±0.2	0.6±0.2	6±2***	6±4***	2±0.9	1.0±0.3	<0.0001
Weight before time point (kg)	85±13	85±13	87±14***	86±14***	86±13*	85±13	<0.0001
Urine biochemistries							
Na+ (mmol/min)	67±37	83±62	113±67	110±46	98±31	81±24	0.03
K+ (mmol/min)	60±21	85±28	103±41	123±73**	78±32	56±14	0.0005
Cl- (mmol/min)	88±34	113±41	113±38	115±36	96±23	82±19	0.01
H_2PO_4- (mmol/min)	11±5	10±3	15±4	13±6	21±8***	26±8***	<0.0001
Urea (mmol/min)	218±70	214±55	349±87***	335±88***	304±84**	247±56	<0.0001

* $P < 0.05$, ** $P < 0.01$, *** $P < 0.001$ *vs.* T2.a

FIGURE 4.S1 **Schematic overview of water loading test**

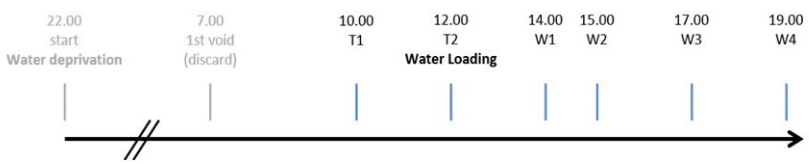

Schematic overview of the time points in the water loading test in healthy subjects. Water deprivation started at 10 p.m. the day before the test. The first urine void at 7.00 a.m. was discarded. T1-2 (urine voids at 10.00 a.m. and noon, respectively) are samples obtained during the water deprivation period, while W1-4 (urine voids at 2.00, 3.00, 5.00, and 7.00 p.m.) are samples obtained after water loading. Participants did not urinate between these time points. Water loading consisted of 20 mL/kg water within 30 minutes at noon, and was combined with a standardized meal.

FIGURE 4.S2 **Particle yield of differential ultracentrifugation**

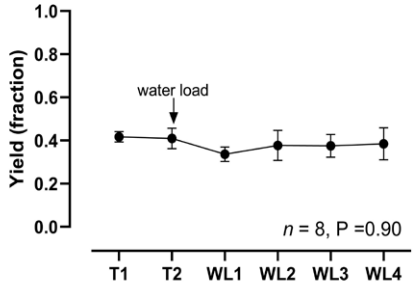

To establish the yield, the 200K pellet was re-dissolved in the original volume. EVQuant was used to count the number of particles prior to and after ultracentrifugation. The yield is expressed as the fraction of the particles present after ultracentrifugation compared to the number of particles present before ultracentrifugation.

FIGURE 4.S3 **Effect of centrifugation on particle size**

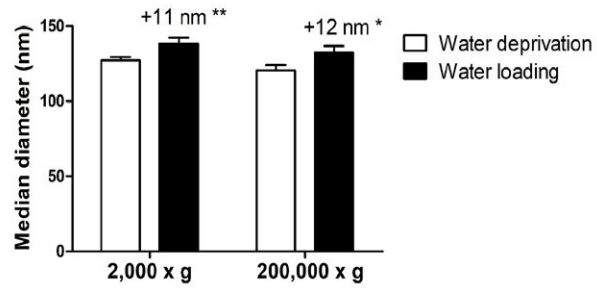

Particle size was measured using NTA in 6 water deprivation and 6 water loading samples in whole urine or in the 200,000 x g pellet. The difference in particle size between water loading and water deprivation was +11 nm after 2,000 x g centrifugation (** $P < 0.01$) and +12 nm after 200,000 x g centrifugation (* $P < 0.05$). After ultracentrifugation, particles were on average 6 nm smaller ($P = 0.04$).

FIGURE 4.S4 **Correlation CD9+ particles with urine creatinine**

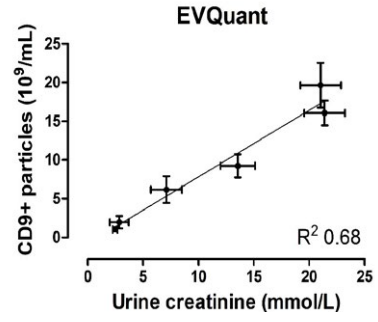

Analyzed in urine samples collected from 8 participants in the water loading study.

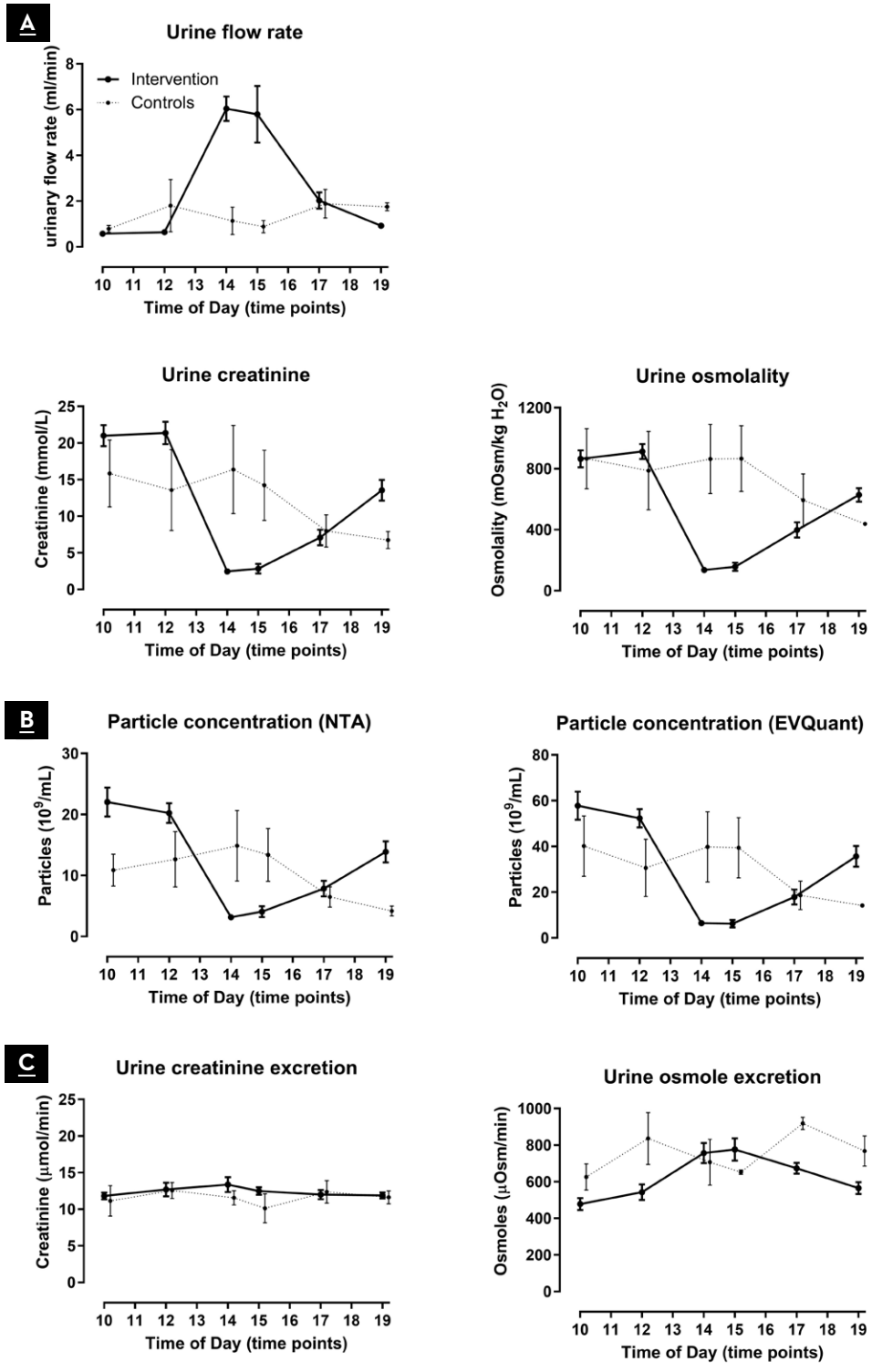

FIGURE 4.S5 **Urine characteristics and particle concentrations after water loading or time-control**

A Urine flow rate (ml/min), urine creatinine (mmol/L), and urine osmolality (mOsm/kg H2O) before and after water load at 12.

B Particle concentration as measured by NTA or EVQuant (109/mL) before and after water load.

C urine creatinine (umol/min) and osmole (uOsm/min) excretion before and after water load.

FIGURE 4.S6 **Particle size distribution per time point in the water loading study**

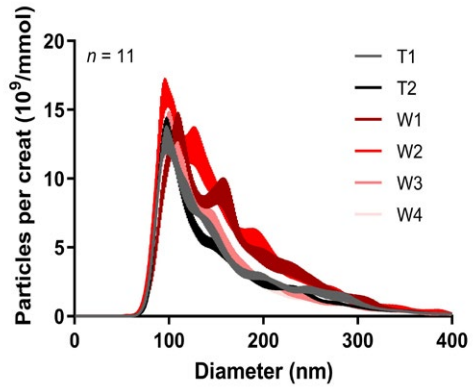

Particle size distribution by NTA of each of the time points of the water loading, of combined version is shown in Figure 4.3B.

FIGURE 4.S7 Representative raw image data of NTA **A**, EVQuant **B**, CD9-TR-FIA **C**

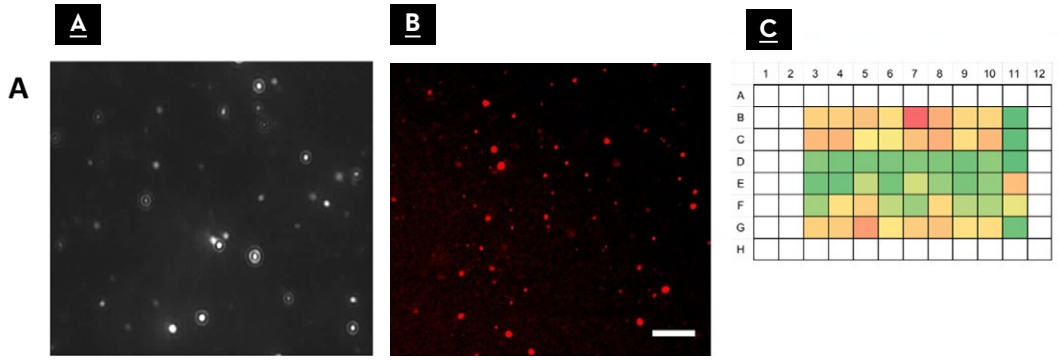

FIGURE 4.S8 **Additional immunoblots of CD9 and CD63 precipitations**

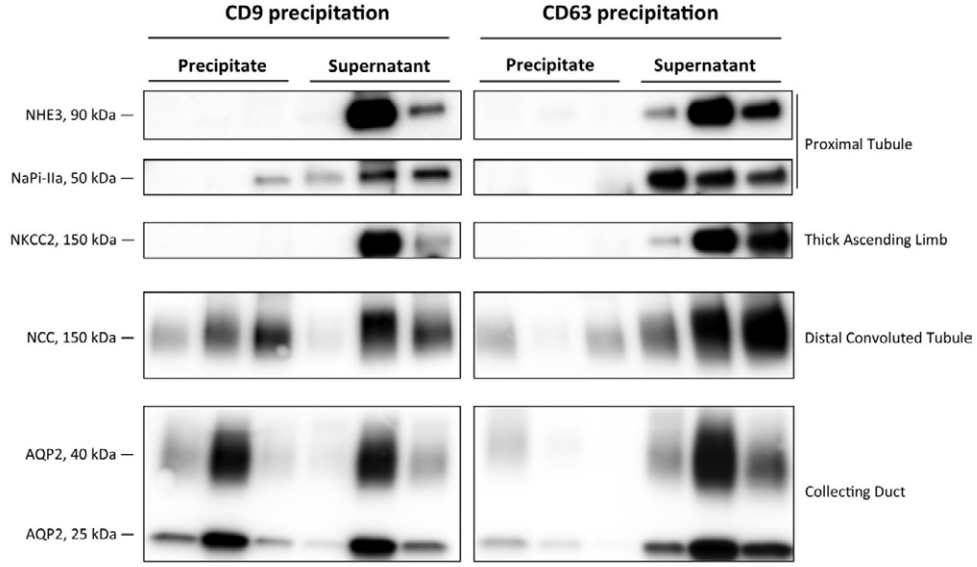

Characterization of CD9+ and CD63+ uEVs of Patients 4 – 6 (supplement to Figure 4.7 which shows Patients 1 – 3). Immunoblot comparison of uEVs precipitated from 200K urine pellets by CD9- or CD63-antibody coated magnetic beads, and respective supernatant, with the nephron-segment markers NHE3, NKCC2, NCC, and AQP2.

FIGURE 4.S9 **Co-localization studies for a second CD9 and CD63 antibody, and for CD81**

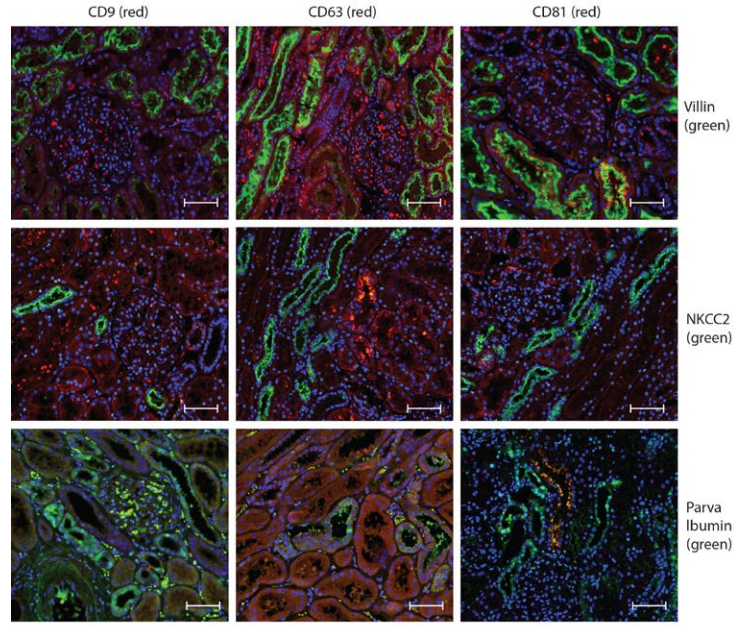

FIGURE 4.S10 **Additional controls to the data shown in Figure 4.8A and D**

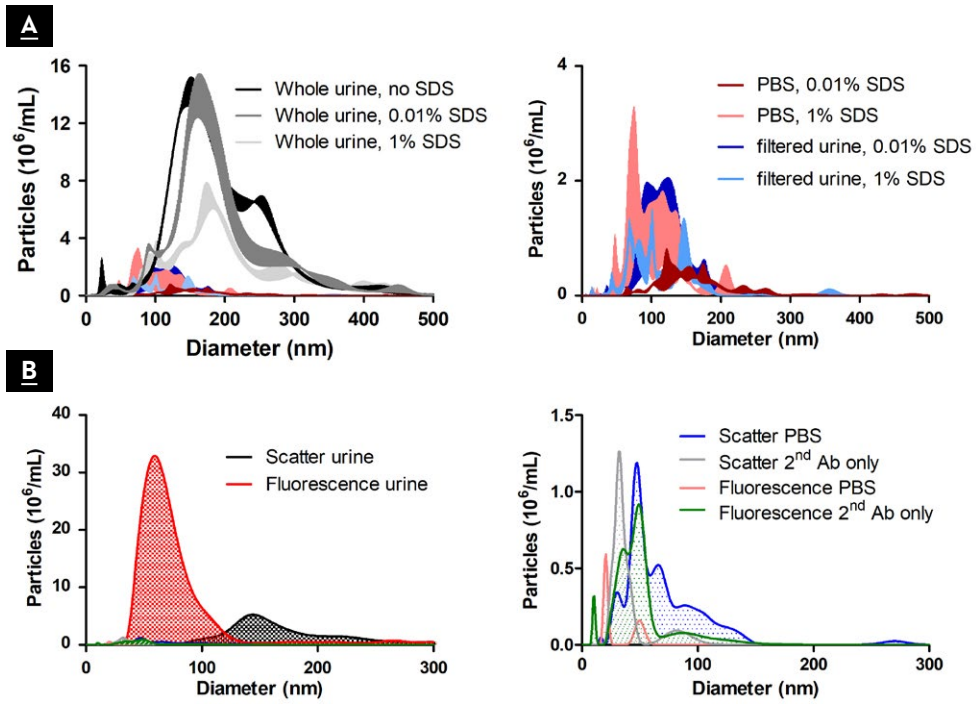

A Left: Figure 4.8A with the addition of PBS or filtered urine (no uEVs) with 0.01% or 1% SDS. Right: close-up of the additional controls only.

B Left: Figure 4.8D with the addition of PBS only and 2nd antibody only in either scatter or fluorescence mode. Right: close-up of the additional controls only.

FIGURE 4.S11 **Characteristics of the extracellular-epitope AQP2 antibody**

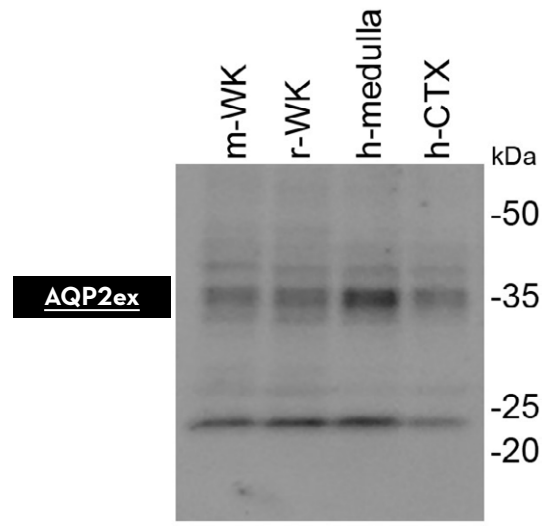

Immunoblotting of 10 μg protein homogenates from mouse whole kidney (m-WK), rat whole kidney (r-WK), human kidney medulla (h-medulla) or human cortex (h-CTX). Signals representing the glycosylated (~35 kDa) and non-glycosylated (~22 kDa) forms of AQP2 were observed in all samples.

Extracellular AQP2 antibody production: A 15-amino acid peptide, CYFTGCSMNPARSLAP (the NH2 terminal cysteine added for conjugation) corresponding to amino acids 177-191 of mouse AQP2 accession #AAB71414.1 (94% identity to human) was produced by standard solid phase techniques and conjugated to keyhole limpet hemocyanin (KLH) via covalent linkage to the NH2-terminal cysteine (Genscript USA). The antibody was affinity purified from terminal bleed serum using the immunizing peptide as described previously. The antibody titer was determined to be >1:512,000 using ELISA and AQP2 peptide conjugated plates. Antibody specificity was determined by: a) western blotting of human whole kidney, cortex or medulla tissue, showing a strong band of the characteristic molecular mass of AQP2 (Figure above); b) immunohistochemical labeling of mouse and human kidney showing characteristic labeling of tubules morphologically similar to collecting ducts (not shown).

CHAPTER 5

Nephron Mass Determines the Excretion Rate of Urinary Extracellular Vesicles

Charles J. Blijdorp, Thomas A. Hartjes, Kuang-Yu Wei, Martijn H. van Heugten, Dominique M. Bovée, Ricardo P.J. Budde, Jacqueline van de Wetering, Joost G.J. Hoenderop, Martin E. van Royen, Robert Zietse, David Severs, Ewout J. Hoorn

Journal of Extracellular Vesicles 2022

5.1 Abstract

Urinary extracellular vesicles (uEVs) are emerging as non-invasive biomarkers for various kidney diseases, but it is unknown how differences in nephron mass impact uEV excretion. To address this, uEV excretion was measured before and after human kidney donor nephrectomy and rat nephrectomy. In male and female donors, uEVs were quantified in cell-free spot and 24-hour urine samples using nanoparticle tracking analysis, EVQuant, and CD9-time-resolved fluorescence immunoassay. Female donors had significantly lower total kidney volume (TKV) and excreted 49% fewer uEVs than male donors. uEV excretion correlated positively with estimated glomerular filtration rate (eGFR), creatinine clearance, and TKV (R's between 0.6 and 0.7). uEV excretion rate could also be predicted from spot urines after multiplying spot uEV/creatinine by 24-hour urine creatinine. Donor nephrectomy reduced eGFR by 36 ± 10%, but the excretion of uEVs by only 19% (CD9+ uEVs -30%, CD9- uEVs no decrease). Donor nephrectomy increased the podocyte marker WT-1 and the proximal tubule markers NHE3, NaPi-IIa, and cubilin in uEVs 2- to 4-fold when correcting for the nephrectomy. In rats, the changes in GFR and kidney weight correlated with the changes in uEV excretion rate (R = 0.46 and 0.60, $P < 0.01$). Furthermore, the estimated degree of hypertrophy matched the change in uEV excretion rate (1.4- to 1.5-fold after uninephrectomy and 4-fold after 5/6th nephrectomy). Taken together, our data show that uEV excretion depends on nephron mass, and that nephrectomy reduces uEV excretion less than expected based on nephron loss due to compensatory hypertrophy. The major implication of our findings is that a measure for nephron mass or uEV excretion rate should be included when comparing uEV biomarkers between individuals.

5.2 Introduction

Urinary extracellular vesicles (uEVs) are nanosized membrane vesicles excreted by cells of the kidney and urinary tract. They are derived either from fusion of multivesicular bodies with the cell membrane ("exosomes") or from direct outward budding of the cell membrane (microvesicles and apoptotic bodies) [4]. Because the uEV proteome and transcriptome contain many disease-associated proteins and transcripts, uEVs are being explored for non-invasive biomarkers of kidney function, kidney disease and urological disease [9, 344]. uEV biomarker discovery has been pursued in patients with acute kidney injury [333, 334], polycystic kidney disease [46, 90], glomerular disease [336], and tubulopathies [12, 245]. In addition, uEVs have been analyzed to identify biomarkers for kidney transplant function and rejection [345, 346]. Despite the myriad of proteins detectable in uEVs, several methodological questions regarding uEV research must still be addressed prior to clinical application.

It would be preferable to analyze uEV biomarkers in spot urines because of clinical throughput and because it carries a lower risk of EV cargo degradation [131]. Therefore, we recently compared several approaches to normalize, quantify, and characterize uEVs directly in spot urines (i.e., without the need for uEV isolation) [347]. In this previous study, uEVs were quantified and characterized using nanoparticle tracking analysis (NTA), a CD9-based time-resolved fluorescence immunoassay (CD9-TR-FIA), and a recently developed method called EVQuant [348]. Using these methods, we identified positive intra-individual and inter-individual correlations between spot urinary creatinine and uEV concentration in various settings, including kidney disease [347]. Accordingly, we proposed that urinary creatinine can be used to normalize uEV proteins in spot urines. A still unresolved question, however, is whether uEV excretion depends on nephron mass and what the effect of nephron loss is on uEV excretion [349]. As a large fraction of uEVs are excreted by kidney epithelial cells, nephron loss would be expected to evenly reduce uEV excretion.

Therefore, in the current study, we hypothesize that kidney function, kidney volume or kidney weight (as proxies for nephron mass) determine uEV excretion and that nephrectomy reduces uEV excretion. To address this, we analyzed uEV excretion in 24-hour and spot urines from kidney donors before and after nephrectomy and in rats before and after nephrectomy. We show that kidney function, kidney volume, and kidney weight are related to uEV excretion rate, but that nephrectomy causes a lower than expected decrease in uEV excretion due to hypertrophy.

5.3 Methods

Donor nephrectomy study

The protocol for the prospective study in 19 kidney donors was approved by the medical ethics committee of the Erasmus Medical Center (MEC-2017-068), and all participants provided informed consent. The only exclusion criterion was inability to comply with the study procedure. Participants were requested to collect 24-hour urine and spot urine before the donor nephrectomy. These urine collections were repeated during a follow-up visit three months after the donor nephrectomy. The urine samples were processed immediately after collection. A protease inhibitor cocktail (Roche cOmplete protease inhibitor cocktail tablets, Switzerland) was added to spot urines, but not to the 24-hours urines because of the large number of tablets required for this volume. All urines were centrifuged at 2,000 x g, for 10 minutes at 4°C and then immediately aliquoted and stored at -80°C until further analysis. Routine laboratory parameters were measured by the Department of Clinical Chemistry of the Erasmus MC. Estimated glomerular filtration rate (eGFR) was calculated using the CKD-EPI equation and adjusted for body surface area.

Total kidney volume

Baseline CT scans were performed before donor nephrectomy as part of the standard clinical work-up. CT images were analyzed using commercially available post-processing software (Intellispace, Philips, the Netherlands). Using a standard multiplanar viewer, imaging planes, fixed at 90°-angles to each other, were aligned with the long and short axis of the kidney. Total kidney volume (TKV) was measured by segmenting the cortex and parenchyma using a smart segmentation tool in the "tumor tracking" application in the Intellispace software. Renal cysts, the pyelum and vascular structures were excluded from the segmentation. The total volume of the segmented kidney was automatically calculated by the software. Measurements were performed for both kidneys by a radiologist (R.B.).

Nephrostomy drain study

To compare uEVs derived from the kidney and the urological tract we also performed a study in patients with a unilateral nephrostomy drain (MEC-2016-069). Exclusion criteria were kidney replacement therapy, neobladder, and urogenital cancer. Timed urine samples were collected from the nephrostomy drain and from normal micturition ("bladder" samples). Urine samples were processed as described above and then prepared for quantification with EVQuant and uEV isolation with differential ultracentrifugation (see below). Finally, uEVs were analyzed pairwise by liquid chromatography and mass spectrometry (LC-MS/MS) using a Q Exactive mass spectrometer (Thermo Fisher Scientific, Rockford, IL), as described previously [90]. For quantitative analysis, individual peptide samples were TMT labeled (TMT10plex isobaric label reagent set, Thermo Fisher Scientific). The DAVID bioinformatics resource (version 6.7) was used to calculate Gene Ontology term enrichment.

Rat nephrectomy studies

Rat nephrectomy studies were performed to correlate kidney weight with uEV excretion. These studies were approved by the Animal Welfare Committee of the Erasmus Medical Center (16-790-02).[350] Briefly, male Sprague Dawley rats (6 weeks old, average weight 200 g) were randomly assigned to undergo sham surgery (n = 10), uninephrectomy (n = 8) or 5/6th nephrectomy (n = 8). 5/6th nephrectomy was performed in two steps, including right uninephrectomy followed by surgical excision of the upper and lower poles of the left kidney ten days later. Before and 8 weeks after nephrectomies GFR was measured by transcutaneous measurement of fluorescein isothiocyanate (FITC)-sinistrin clearance, as reported previously.[351] Both before and 8 weeks after surgery, 24-hour urine was collected using metabolic cages with protease inhibitor tablets in the urine collection reservoir. All urines were stored at -80°C after centrifugation (2,000 x g, 10 minutes at 4°C). During the entire study the rats were on regular chow and had free access to water.

Nanoparticle tracking analysis

Nanoparticle tracking analysis (NTA) was performed using a NanoSight NS300 (Sysmex, The Netherlands) with Nanoparticle Tracking Analysis 3.1 software (NanoSight, UK). Whole urine samples were vortexed and diluted in phosphate buffered saline (PBS, pH 7.4, 137 mM Na+, used throughout the studies) to obtain 40 – 100 particles per field, then inserted in an O-ring top plate NTA chamber with a syringe. Particle scattering of 405 nm light was recorded by a CCD camera (5 videos of 30 seconds each, camera level = 14, detection threshold = 3), and the Brownian motion was determined frame to frame. The lower limit of detection was approximately 70 nm.

EVQuant

EV quantification was performed using a newly developed assay (EVQuant).[348] Briefly, the whole urine sample was labeled with CD9-Alexa647 (Table 5.S1) in 0.03% w/v bovine serum albumin for two hours, then diluted threefold in PBS and non-specifically labeled by the generic fluorescent membrane dye Rhodamine R18 (0.33 ng/μl, 568 nm). Subsequently, without any isolation or purification procedures, the labelled samples were mixed with a non-denaturing polyacrylamide gel solution (final ratio of 16% w/w acrylamide/bisacryl). The mixtures were transferred to a 96-wells plate (SensoPlate glass bottom 96-well plate, Austria). Immobilized uEVs were imaged using a spinning disk confocal microscope system (Opera Phenix, Perkin Elmer, USA). uEV concentration was corrected by dye in control solution (PBS). In this analysis, each detected EV (Rhodamine-R18 +) was assessed for CD9 expression. The detection threshold (mean plus three times the standard deviation) was determined using a 100 nm liposome sample lacking protein markers.

CD9-TR-FIA

The CD9-TR-FIA was performed as previously described.[113] Briefly, a white neutravidin-coated plate (Life Technologies) was coated with biotinylated anti-human CD9 (1:500, EBioscience, USA) overnight at 4˚C (Table 5.S1). 100 µl of thawed urine was vortexed and added to incubate for 1 hour at room temperature. Next, Europium-conjugated anti-CD9 (0.25 ng/µl, CellGS, United Kingdom) was added and incubated for 1 hour at room temperature. Incubation steps were performed on a plate shaker and were followed by 6 washes with wash buffer (Kaivogen, Finland). Before signal measurement on a Victor 1420 multilabel counter, a Europium enhancer (Kaivogen, Finland) was added to the empty well and incubated for 15 minutes in the dark.

Differential ultracentrifugation and immunoblotting

A "200K pellet" was obtained with ultracentrifugation using 50 ml whole urine as starting volume. Briefly, after a 17,000 x g spin (to remove remaining whole cells, large membrane fragments, and other debris), the pellet was dissolved in 250 µl freshly made 200 mg/ml dithiothreitol (DTT) diluted in ddH2O, heated and added to isolation buffer (10 mM triethanolamine, 250 mM sucrose, pH 7.6) and again centrifuged at 17,000 x g. The two supernatants were combined and centrifuged at 200,000 x g for 2 hours. The 200K pellet was suspended in PBS, 6X Laemmli solution (440 mM Tris HCl pH 6.8, SDS 10% w/v, glycerol 25% v/v, bromphenolblue 0.1% w/v, β-mercaptoethanol 6% v/v) was added and the sample was heated for 10 minutes at 60˚C. SDS-PAGE was carried out on a gradient gel (4-12% Criterion precast gel, 26 well, 15 µl, Bio-Rad, USA) and transferred to PVDF membranes (0.2 µm PVDF, Bio-Rad, USA) using a Trans-Blot Turbo Transfer system (Bio-Rad, USA) at 25V, 1A during 30 minutes. The membranes were blocked (TBS with 0.1% v/v Tween-20 and 5% w/v BSA or milk) and probed overnight at 4°C with a primary antibody (Table 5.S1). Subsequently, membranes were washed and incubated with a secondary antibody. After washing of the membranes, they were exposed to enhanced chemiluminescence substrate (Clarity Western ECL substrate, Bio-Rad, USA) and analyzed by an Amersham system (GE Life Sciences, USA). uEV protein abundances were normalized by urine creatinine and analyzed with and without adjustment for total kidney volume.

Statistical analysis

The data were analyzed for normal distribution and the statistical tests were selected accordingly. The data are expressed as means with standard deviations or medians with interquartile range (IQR), as appropriate. Comparisons between males and females were performed using Student's T-test. Correlations were analyzed by Pearson or Spearman's rho (R). Comparisons before and after nephrectomy were performed using paired T-test or Wilcoxon signed rank test. Intra-individual comparisons were performed in spot urines using uEV/creatinine.[347] For inter-individual comparisons with spot urines a "calculated spot uEV excretion" was determined by multiplying the uEV-to-creatinine ratio in spot urine by 24-hour urinary creatinine: calculated spot urine uEV excretion (uEVs/min) = spot uEV concentration (uEVs/L) x creatinine excretion (mmol/min) / spot urine creatinine concentration (mmol/L). This approach has been used previously to estimate 24-hour sodium excretion from spot urine [352], and corrects for differences in creatinine excretion caused by variation in muscle mass. In addition, we validated this equation with data from a previous study [347] with which we calculated spot uEV excretions (n = 8) and compared these to measured 12-hour uEV excretions; this analysis showed high correlations (R2 0.79-0.99). The uEV protein comparisons were performed by Mann-Whitney test with correction for multiple testing using the Holm-Bonferroni method. A P-value ≤ 0.05 was considered statistically significant.

5.4 Results

Female donors excrete fewer uEVs

Nineteen subjects (12 females, 7 males, Table 5.1) were analyzed before (Figures 5.1-2) and after (Figure 5.3) donor nephrectomy . One 24-hour urine collection was discarded because it was incomplete (as indicated by the participant and confirmed by a discrepancy between creatinine clearance and eGFR). Compared to male donors, female donors had a lower urinary creatinine excretion (9.0 ± 2.6 vs 17.1 ± 1.3 mmol/day, P < 0.001), lower creatinine clearance (99 ± 33 vs. 128 ± 7 mL/min, P = 0.04), and lower total kidney volume (TKV, 300 ± 57 ml vs. 351 ± 37 mL, P = 0.05); eGFR was not significantly different (89 ± 25 vs 99 ± 18 mL/min, P = 0.4; Figure 5.1A-B, Table 5.S2). Female donors excreted 49% fewer uEVs per day than male donors (22 [IQR 16–31] vs. 43 [IQR 37–45] x 109 uEVs/min, P < 0.05, Figure 5.1C). In spot urines, creatinine concentrations strongly correlated with uEV concentrations measured with EVQuant or NTA (Figure 5.1D). Spot uEV/creatinine, however, did not correlate with 24-hour uEV excretion measured with EVQuant (Figure 5.1E). Calculated spot uEV excretion (multiplying spot uEV/creatinine by 24-hour urinary creatinine excretion) did correlate with measured 24-hour uEV excretion (Figure 5.1F). When calculated spot uEV excretions were compared between men and women (Figure 5.1G), the lower uEV excretion in women was similar to the analysis with 24-hour uEV excretion (Figure 5.1C). In a Bland-Altman analysis, calculated spot uEV excretion largely agreed with 24-hour uEV excretion (Figure 5.S1).

Kidney function and volume determine uEV excretion rate

eGFR (adjusted by body surface area) and creatinine clearance correlated positively with TKV (Figure 5.2A). eGFR also correlated positively with measured 24-hour uEV excretion (Figure 5.2B) and calculated spot uEV excretions (Figure 5.2C), although the correlation with uEVs quantified by NTA was not statistically significant. In addition, creatinine clearance correlated

positively with measured 24-hour uEV excretion (Figure 5.2D) and calculated spot uEV excretions (Figure 5.2E). TKV correlated positively with measured 24-h uEV excretion (Figure 5.2F) and calculated spot uEV excretions (Figure 5.2G), although the correlation with uEVs quantified by EVQuant was not statistically significant. Of note, the correlations between eGFR, creatinine clearance and uEV excretion were slightly stronger than for TKV and uEV excretion.

TABLE 5.1 **General characteristics of the kidney donors**

VARIABLE	PRE-NEPHRECTOMY (N = 19)	POST-NEPHRECTOMY (N = 19)	*P*-VALUE
General characteristics			
Age, years	58 ± 12	-	
Female sex, n (%)	12 (63)	-	
Body mass index, kg/m2	26 ± 5	27 ± 6	0.004
Plasma sodium, mmol/L	142 ± 2	141 ± 3	0.1
Plasma potassium, mmol/L	4.0 ± 0.4	4.3 ± 0.4	0.02
eGFR, mL/min*	91 ± 20	58 ± 14	< 0.001
Creatinine clearance, mL/min	110 ± 29	66 ± 17	< 0.001
24-hour urine			
Volume, mL	1981 ± 754	2393 ± 830	0.01
Osmolality, mOsm/kg	474 ± 252	432 ± 213	0.4
Creatinine, mmol/day	11.8 ± 4.7	11.5 ± 4.6	0.3
Sodium, mmol/day	132 ± 51	155 ± 75	0.2
Potassium, mmol/day	80 ± 34	76 ± 20	0.5
Protein, mg/day	82 ± 18	97 ± 32	0.07
Spot urine			
Osmolality, mOsm/kg	554 ± 263	442 ± 225	0.07
Creatinine, mmol/L	8.5 ± 5.7	7.0 ± 5.4	0.30
Protein to creatinine ratio, g/mmol	9.2 ± 4.8	10.2 ± 4.4	0.20

* Estimated glomerular filtration rate (eGFR) adjusted for body surface area.

FIGURE 5.1 **Total kidney volume and urinary extracellular vesicle excretion in males and females**

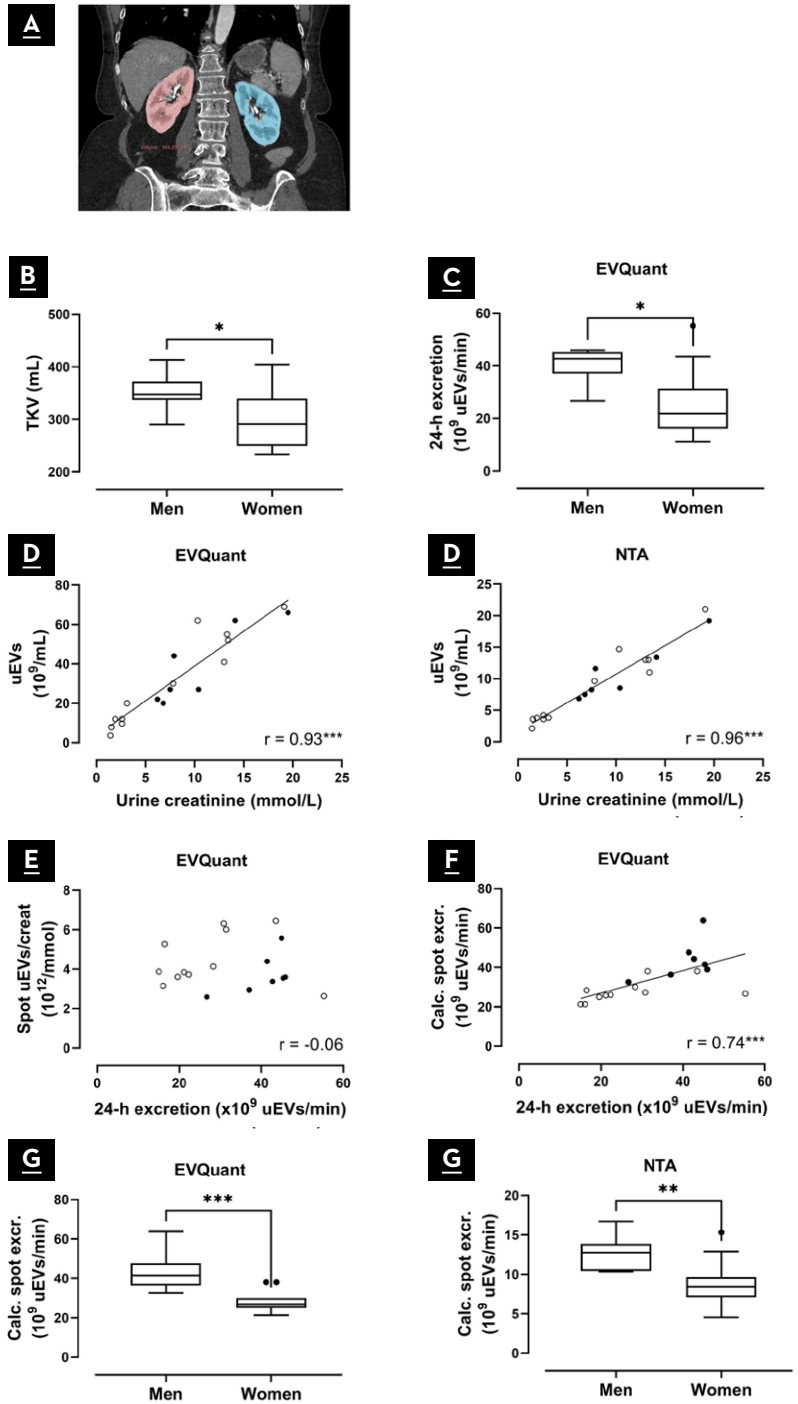

FIGURE 5.1 **Total kidney volume and urinary extracellular vesicle excretion in males and females**

(previous page)

A Example of total kidney volume determination by segmentation in a computed tomography (CT) image of the kidneys (right kidney red, left kidney blue).

B Comparison of total kidney volume (TKV) between men and women.

C Urinary extracellular vesicle (uEV) excretion in men *versus* women measured by EVQuant in 24-hour urine.

D Pearson correlations of urine creatinine versus uEV concentration in men (●) and women (○), measured by nanoparticle tracking analysis (NTA) and EVQuant.

E Spearman correlation of 24-hour uEV excretion *versus* spot uEV/creatinine measured by EVQuant.

F Spearman correlation of 24-hour uEV excretion *versus* calculated spot uEV excretion (spot uEV/creatinine * 24-hour urine creatinine) measured by EVQuant.

G Calculated spot uEV excretion in men versus women measured by NTA and EVQuant. Box plots are Tukey plots. Men are represented by ● and women by ○; *$P \leq 0.05$, ** $P < 0.01$, *** $P < 0.001$.

FIGURE 5.2 **Correlations between total kidney volume, kidney function, and urinary extracellular vesicle excretion**

A Pearson correlations of total kidney volume (TKV) with estimated glomerular filtration rate (eGFR, corrected for body surface area), and creatinine clearance (CrCl).

B Pearson correlation of 24-hour urinary extracellular vesicle (uEV) excretion and eGFR.

C Spearman correlations of calculated spot uEV excretions (measured by EVQuant **C** or NTA **D**) with eGFR.

E Spearman correlation of 24-hour uEV excretion and CrCl.

F Spearman correlations of calculated spot uEV excretions (measured by EVQuant **F** or NTA **G**) with CrCl.

H Spearman correlation of 24-hour uEV excretion and TKV.

I Spearman correlations of calculated spot uEV excretions (measured by EVQuant **I** or NTA **J**) with TKV. Men are represented by ● and women by ○; *$P \leq 0.05$, ** $P < 0.01$, *** $P < 0.001$.

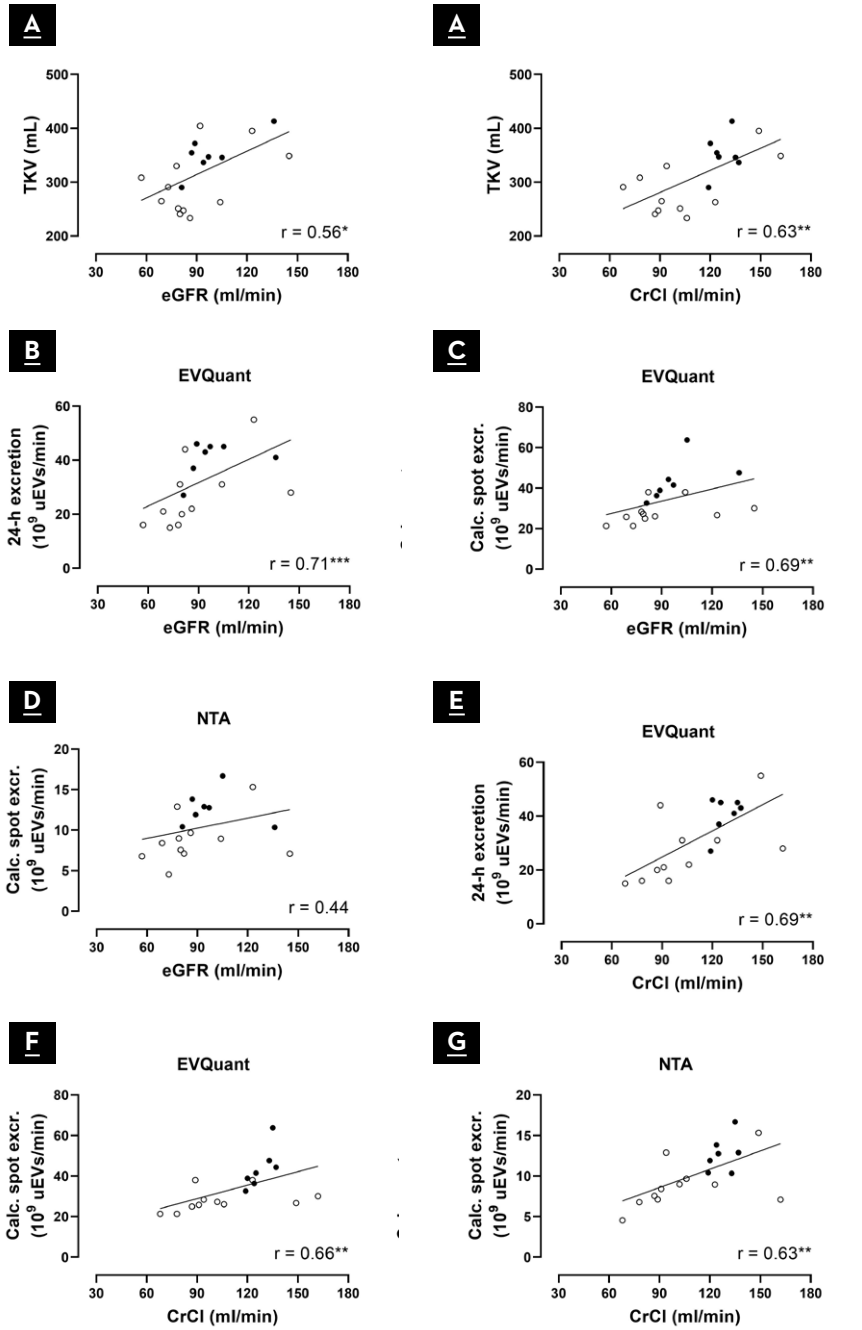

Figure 5.2 continues on the next page

FIGURE 5.2

(Continued)

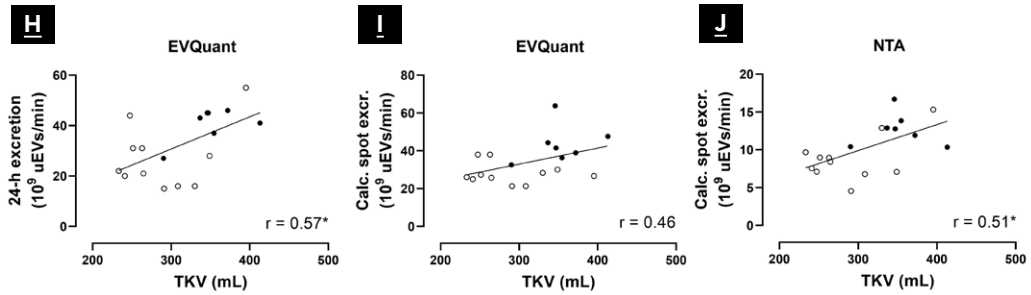

FIGURE 5.3 **Effect of donor nephrectomy on urinary extracellular vesicle excretion**

A Urinary extracellular vesicle (uEV) excretion before (Pre) versus after (Post) donor nephrectomy measured by EVQuant in 24-hour urine.

B Urinary excretion of CD9- uEVs (left panel) and CD9+ uEVs (right panel) before and after donor nephrectomy measured by EVQuant in 24-hour urine.

C Spot uEV/creatinine before and after donor nephrectomy measured by EVQuant.

D Spot uEV/creatinine ratios of CD9- (left panel) and CD9+ uEVs (right panel) before and after donor nephrectomy measured by EVQuant.

E Spot uEV/creatinine before versus after donor nephrectomy measured by nanoparticle tracking analysis (NTA).

F Size distribution of uEVs by NTA (left panel) and percentage change of size distribution (right panel, uEV/creatinine ratio ± SEM per 1 nm size bin.

G CD9-Europium signal to urine creatinine ratio (Lum./creat) before and after donor nephrectomy measured by CD9-TR-FIA (signal pre-donation normalized to 1).

H Representative immunoblots of CD9 and TSG101 in the 200K uEV pellet before and after donor nephrectomy, loaded relative to individual urine creatinine concentrations, with corresponding densitometry. *$P \leq 0.05$, ** $P < 0.01$, *** $P < 0.001$.

FIGURE 5.3 **Effect of donor nephrectomy on urinary extracellular vesicle excretion**

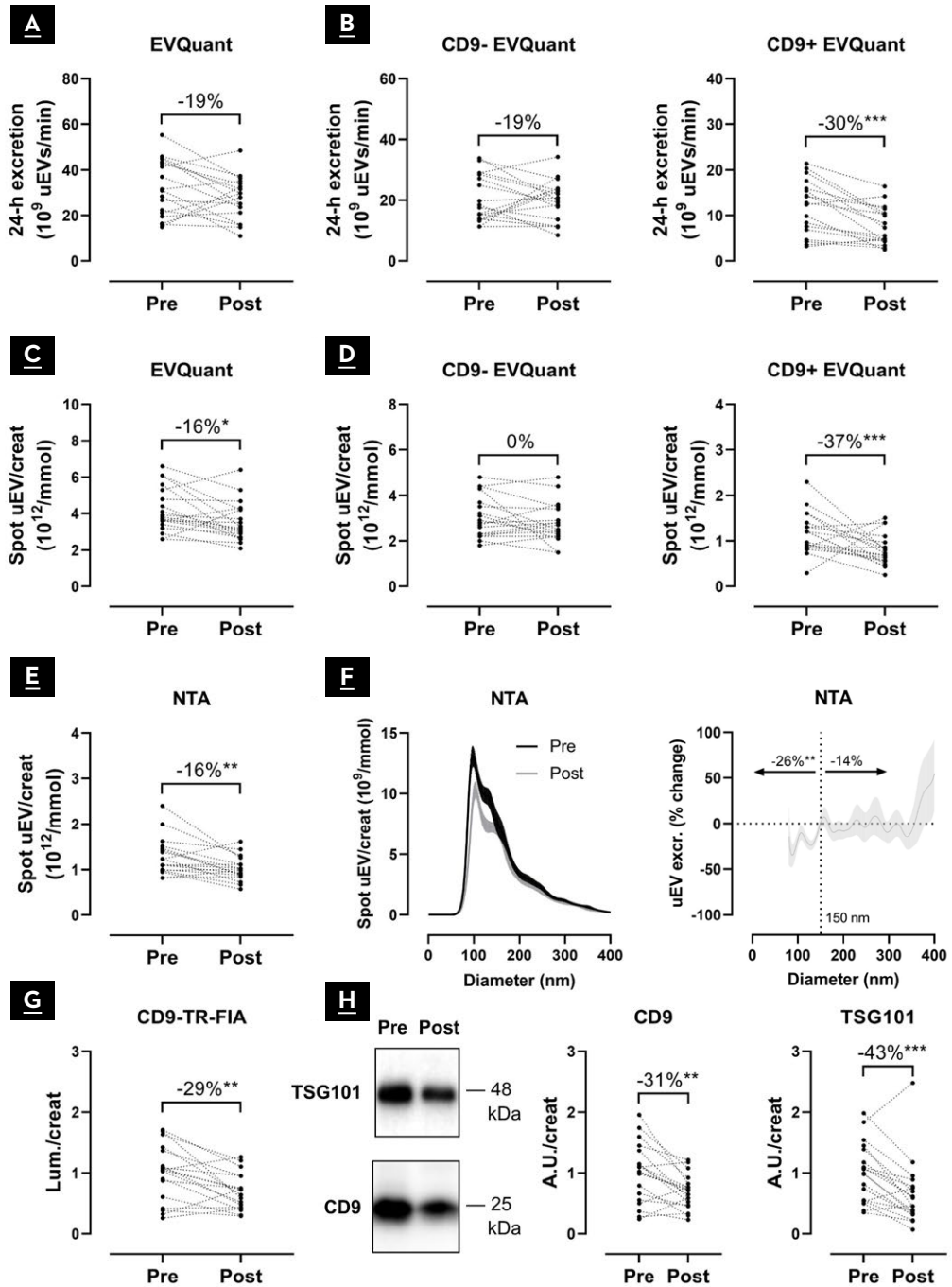

Effect of donor nephrectomy on uEV excretion

Donor nephrectomy reduced eGFR from 91 ± 20 to 58 ± 14 ml/min (-36 ± 10 %) and creatinine clearance from 110 ± 29 to 66 ± 17 ml/min (-38 ± 11 %, *P* < 0.001 for both, Table 5.1). Plasma potassium significantly increased from 4.0 ± 0.4 to 4.3 ± 0.4 mmol/L (*P* = 0.02). The degree of proteinuria or albuminuria increased non-significantly after donor nephrectomy. Body mass index did increased significantly but this was not caused by an increase in muscle mass (non-significant decrease in 24-hour creatinine excretion). The donor kidney was most often the left kidney (13 out of 19) and had a similar TKV as the remaining kidney (158 ± 30 vs. 159 ± 30 mL), implying that nephron number was reduced by 50 ± 3%. Donor nephrectomy reduced uEV excretion (measured by EVQuant) by 19% (IQR -11 to 34), although this was not statistically significant (*P* = 0.09, Figure 5.3A). Interestingly, when classified by surface marker CD9, CD9- uEVs did not decrease, whereas CD9+ uEVs decreased by 30% (IQR 20 to 48, *P* < 0.001, Figure 5.3B). This was also observed with spot uEV/creatinine which showed a significant decrease of 16% (IQR 4 to 26, *P* = 0.02) for all uEVs (Figure 5.3C) and 37% (IQR 17 to 58, *P* = 0.01) for CD9+ uEVs (Figure 5.3D). The same decrease was found when using NTA for uEV counts (16%, IQR 2 to 36, *P* = 0.003, Figure 5.3E), especially for smaller uEVs (< 150 nm, 26%, IQR 10 to 45, *P* = 0.002, Figure 5.3F). The effect on CD9 was confirmed when using CD9-TR-FIA for uEV quantification, which showed a decrease of 29% (IQR 13 to 49, *P* = 0.004, Figure 5.3G). Immunoblot analysis of the urinary exosome markers CD9 and TSG101 in uEVs showed a decrease of 31% (IQR 16 to 42, *P* = 0.004) and 43% (IQR 28 to 60, *P* = 0.003), respectively (Figure 5.3H, Figure 5.S2).

Donor nephrectomy causes nephron segment-specific changes

In addition to quantifying uEVs, we also analyzed nephron segment-specific proteins in uEVs isolated from spot urines (Figure 5.4A, Figure 5.S2), including Wilm's Tumor 1 (WT1, a podocyte marker), sodium-hydrogen exchanger 3 (NHE3), sodium/phosphate co-transporter IIa (NaPi-IIa), and cubilin (proximal tubule markers), sodium-potassium-chloride co-transporter 2 (NKCC2, loop of Henle marker), the sodium-chloride cotransporter (NCC, distal convoluted tubule marker), and aquaporin-2 (AQP2, collecting duct marker). Donor nephrectomy affected these nephron segment-specific proteins in uEVs differently with a significant increase in cubilin and decrease in NCC and AQP2 abundance in uEVs (Figure 5.4B). Corrected for initial kidney volume, however, WT1 and the proximal tubule markers NHE3, NaPi-IIa, and cubilin were significantly increased by a factor 2 to 4, while distal nephron markers did not change (Figure 5.4B). This implies that a 2-fold increase in an uEV-related protein (e.g., NHE3) would remain undetected when not correcting for the nephrectomy (Figure 5.4C).

FIGURE 5.4 **Changes in urinary extracellular vesicle nephron marker proteins after donor nephrectomy**

A

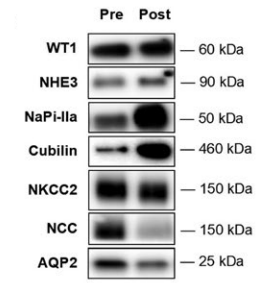

B

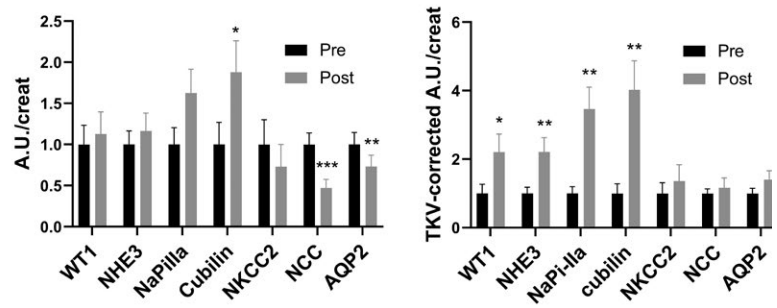

C

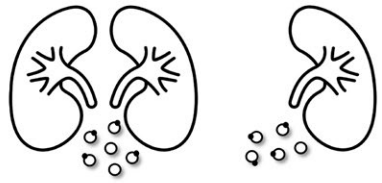

	Pre	Post
uEVs with protein of interest (unadjusted)	4	4
uEVs with protein of interest (nephron mass adjusted)	2	4

A Representative immunoblots before and after donor nephrectomy of nephron marker proteins in urinary extracellular vesicles (uEVs) isolated from spot urine, including the podocyte marker Wilm's tumor 1 (WT1), the proximal tubule markers sodium-hydrogen exchanger 3 (NHE3), sodium/phosphate co-transporter IIa (NaPi-IIa), and cubilin, the loop of Henle marker sodium-potassium-chloride co-transporter 2 (NKCC2), the distal convoluted tubule marker sodium-chloride cotransporter (NCC), and the collecting duct marker aquaporin-2 (AQP2). All proteins were loaded relative to urine creatinine

FIGURE 5.4

(Continued)

B Densitometry of absolute changes in uEV protein abundances before (Pre) and after (Post) donor nephrectomy (n = 19; A.U., arbitrary units). Densitometry of uEV protein abundances relative to total kidney volume (TKV-corrected A.U./creat) before (Pre) and after (Post) donor nephrectomy.

C Cartoon illustrating the changes in uEV and uEV biomarker excretion before (Pre) and after (Post) donor nephrectomy. Donor nephrectomy reduces the overall uEV excretion rate by ~19% (6 to 5 uEVs in the cartoon). In the example, 4 out of 6 uEVs contain an uEV biomarker of interest before donor nephrectomy and 4 out of 5 uEVs after donor nephrectomy. This illustrates the need to normalize by kidney volume otherwise the doubling in uEV biomarker would remain undetected. This example illustrates the observations for WT1 and NHE3 (no change when not adjusting for total kidney volume vs. 2-fold increase when adjusting for total kidney volume, Figure 5.4B). *P ≤ 0.05, ** P < 0.01, *** P < 0.001.

Comparison of uEVs derived from kidney vs. bladder urine

To compare the contribution of the kidney and the other parts of the urinary tract to overall uEV excretion, we performed a study in patients with a nephrostomy drain (see Tables S3 and S4 for patient and urine characteristics). This allowed a comparison between uEVs derived directly from the kidney (nephrostomy drain) with uEVs derived from the kidneys and urinary tract ("bladder"). The nephrostomy drain samples contained more uEVs than the bladder samples, although this was not statistically significant (7.4 ± 1.6 vs 3.3 ± 1.0 x 1010 uEVs/min, *P* = 0.08). Mass spectrometry identified 2814 proteins that were present in both the nephrostomy and bladder samples, while 3 and 12 proteins were only identified in the nephrostomy and bladder samples, respectively (Figure 5.5A). Of all proteins identified, 66% was associated with extracellular exosomes. uEV proteins in the nephrostomy samples were enriched for extracellular region, blood microparticles, and immune response; uEV proteins in the bladder samples were enriched for membrane, extracellular exosome, and endocytosis proteins (*P* for all < 0.001). The abundance of 2462 proteins could be determined by mass spectrometry (Table 5.S5). When the abundance of these uEV proteins in the nephrostomy and bladder samples was compared, the abundance of the majority of the uEV proteins was similar in both sources (nephrostomy / bladder uEV protein abundance ratio 1.0, IQR 0.9 – 1.2, Figure 5.5B-C).

Nephrectomy in rats reduces uEV excretion

uEV excretions were also analyzed by NTA in rats before and eight weeks after sham surgery, uninephrectomy (as comparison for donor nephrectomy) or 5/6th nephrectomy (a commonly used model for chronic kidney disease).[350] Baseline uEV excretion was similar between the three groups (8.3, IQR 6.3 to 9.0, 6.6, IQR 6.4 to 6.8 and . 7.7, IQR 7.3 to 9.1 x 1011 uEVs/day, *P* = 0.09). Eight weeks after sham surgery, an increase in body weight (183 ± 22 grams), FITC-GFR

FIGURE 5.5 **Comparison of the number and abundance of uEV proteins from nephrostomy or bladder urine**

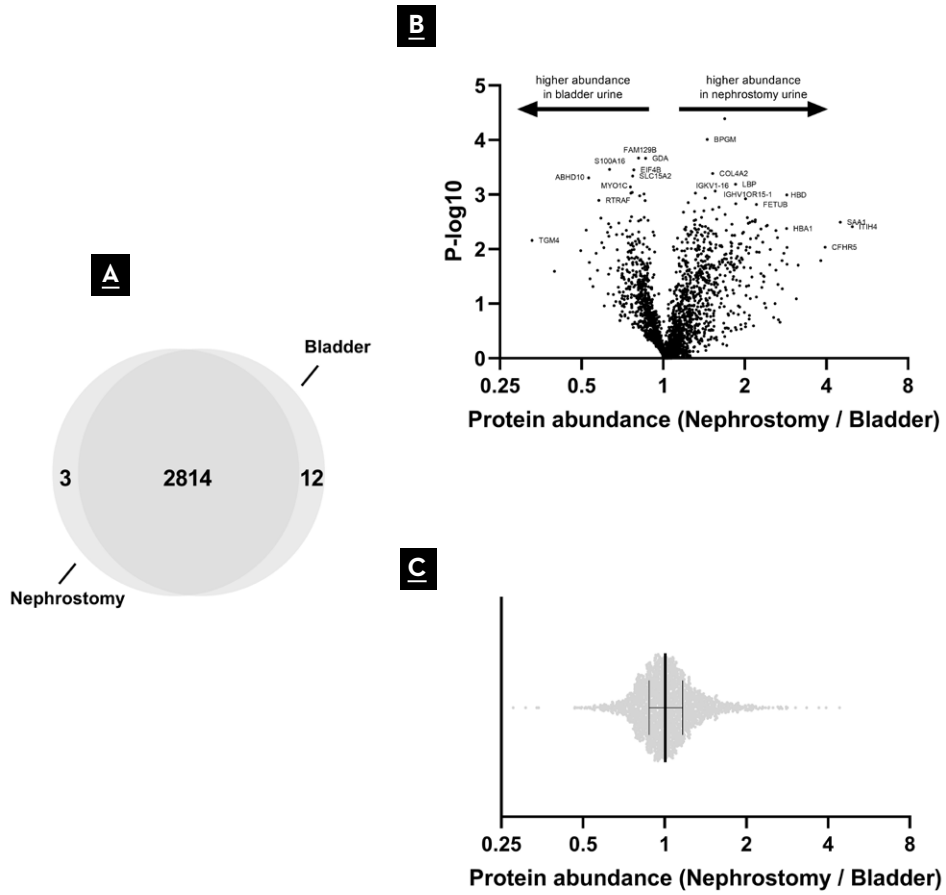

A In nine patients with a nephrostomy drain urine samples for uEV analysis were collected from both the nephrostomy drain and normal micturition ("bladder", see also Table 5.S3 and S4). Mass spectrometry identified 2829 proteins of which 2814 were identified in uEVs isolated from the nephrostomy drain and bladder urines and 3 and 12 proteins were only identified in the nephrostomy and bladder urine samples, respectively.

B A Vulcano plot is shown for the 2462 proteins for which the abundance could be determined indicating whether protein abundance was higher in the bladder or nephrostomy urine sample.

C The distribution of the nephrostomy/bladder uEV protein abundance ratios is shown illustrating that the abundance of the majority of the uEV proteins was similar in both sources (nephrostomy / bladder uEV protein abundance ratio 1.0, IQR 0.9 – 1.2).

(2.4 ± 0.5 to 3.7 ± 1.0 mL/min, 65 ± 63%), and uEV excretion (33%, IQR 28 to 36%) was observed; the sham operation did not affect uEV size distribution (Figure 5.6A).

Eight weeks after uninephrectomy body weight increased similarly as in sham rats (186 ± 21 grams), while the increase FITC-GFR was less (from 3.8 ± 0.7 to 4.4 ± 1.1 ml/min, 19 ± 33%), and uEV excretion decreased by 24 ± 6% (P = 0.04, Figure 5.6B). Eight weeks after 5/6th nephrectomy body weight increased by 145 ± 20 grams (less than sham, P = 0.002), whereas FITC-GFR decreased from 3.3 ± 0.6 to 1.3 ± 0.4 mL/min (-61 ± 13%, 76% lower than sham), and uEV excretion decreased by 34 ± 6% (Figure 5.6C). This decrease especially concerned uEVs with a diameter between 100 and 200 nm (Figure 5.6C). In a direct comparison, uEV excretion was significantly lower in rats after uninephrectomy and 5/6th nephrectomy compared with sham-operated rats (P < 0.001 for both), especially regarding uEVs between 100 and 200 nm (Figure 5.6D). The change in FITC-sinistrin GFR correlated with the change in uEV excretion (R = 0.46, P < 0.01, Figure 5.6E). Furthermore, the change in kidney weight correlated with the change in uEV excretion (R = 0.60, P < 0.01, Figure 5.6F). Finally, the estimated degree of hypertrophy matched the change in uEV excretion rate in the remaining kidney tissue (Table 5.2).

TABLE 5.2 **Estimated hypertrophy and change in uEV excretion after rat nephrectomy**

		UNINEPHRECTOMY	5/6TH NEPHRECTOMY
Kidney	Kidney weight at uninephrectomy, grams	1.2 ± 0.0	1.2 ± 0.1
	Terminal kidney weight, grams	1.7 ± 0.1	1.6 ± 0.2
	Projected weight remaining kidney without hypertrophy, grams	1.2	1/3 x 1.2 = 0.4
	Estimated degree of hypertrophy*	1.4-fold	4-fold
uEVs	uEV excretion at baseline, 1012 uEVs/day	0.66 ± 0.13	0.81 ± 0.14
	uEV excretion at sacrifice, 1012 uEVs/day	0.50 ± 0.15	0.56 ± 0.16
	Projected uEV excretion without hypertrophy**	1/2 x 0.66 = 0.33	1/6 x 0.81 = 0.14
	Estimated change in uEV excretion rate in remaining kidney tissue***	1.5-fold	4-fold

* Calculated by (terminal kidney weight) / (projected weight remaining kidney)
** Assuming both kidneys contribute equally and with limited extra-renal contribution to uEVs
*** Calculated by (uEV excretion at sacrifice) / (projected uEV excretion without hypertrophy)

FIGURE 5.6 **Effect of sham, uninephrectomy or 5/6th nephrectomy on urinary extracellular vesicle excretion in rats**

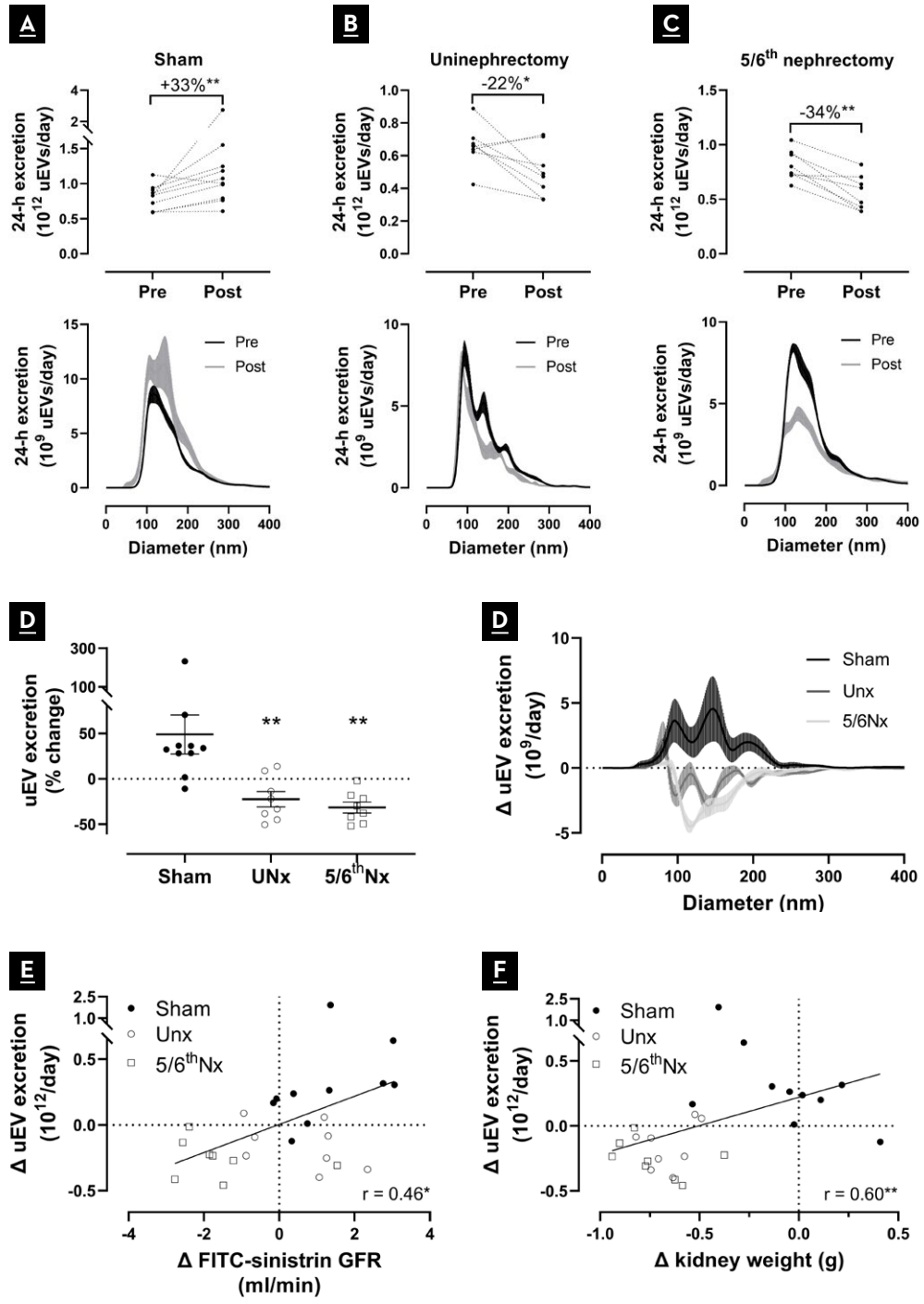

FIGURE 5.4

(previous page) **A** 24-hour urinary extracellular vesicle (uEV) excretion before (Pre) and 8 weeks after (Post) sham surgery (n = 10) and uEV size distribution (right panel, ± SEM per 1 nm bin size).

B 24-hour uEV excretion before and 8 weeks after uninephrectomy (n = 8) and uEV size distribution (lower panel, ± SEM per 1 nm bin size).

C 24-hour uEV excretion before and 8 weeks after 5/6th nephrectomy (n = 8) and uEV size distribution (lower panel, ± SEM per 1 nm bin size)

D Percentage change in uEV excretion before-after sham surgery, uninephrectomy or 5/6th nephrectomy, including uEV size distribution (right panel, ± SEM per 1 nm size bin).

E Spearman correlation between the change in uEV excretion and FITC-sinistrin glomerular filtration rate (GFR); ·, sham surgery; ○ uninephrectomy; □ 5/6th nephrectomy

F Spearman correlation between the change in 24-hour uEV excretion and kidney weight. *$P \leq 0.05$, ** $P < 0.01$, *** $P < 0.001$.

5.5 Discussion

Here, we show that uEV excretion is related to eGFR, creatinine clearance, total kidney volume, and kidney weight, and that nephrectomy reduces uEV excretion less than would be expected based on the loss of nephron mass. Our findings have two important implications for the evolving field of uEV biomarker research and its clinical applicability, namely that (1) nephron mass or uEV excretion should be included for inter-individual comparisons and (2) changes in uEV excretion rate are disproportional to nephron loss after nephrectomy due to compensatory hypertrophy.

We identified a sex difference in uEV excretion with women excreting 49% fewer uEVs. This is likely explained by higher nephron endowment in men. Although prostate-derived uEVs could also contribute to this difference, these are usually low abundant except after digital rectal examination [113, 276]. The identification of this sex difference in uEV excretion implies that when the excretion rate of a uEV biomarker is studied in males and females, the results should be corrected for uEV excretion to avoid under- or overestimation of biomarker levels.
The sex difference in urinary creatinine excretion likely explains why a previous study concluded that females excrete *more* EVs than males based on spot uEV/creatinine assessment alone [323]. We do show that uEV excretion can be estimated using spot urines when multiplying spot uEV/creatinine by 24-hour urinary creatinine, an approach that has been used previously for predicting urinary sodium excretion [352]. In addition to sex, genes involved in nephron endowment and age-related glomerulosclerosis cause considerable variation in nephron number between healthy individuals [31, 32], and therefore likely also in uEV excretion rate. The dependence on nephron mass has been shown previously for other urinary biomarkers such as uromodulin [353]. This implies that for inter-individual comparisons of uEV-biomarkers, an adjustment for nephron mass or uEV excretion is required. This may also explain why a previous study reported a lack of correlations between markers in kidney tissue and uEVs [262, 354], although other studies did identify such correlations [317, 355]. Of note, kidney-uEV correlations may also vary because proteins are processed differently into uEVs. The strong inter-individual correlation between urine creatinine and uEV concentration may be explained by the association between creatinine excretion (muscle mass) and measured GFR (nephron mass) [356].

After human kidney donor nephrectomy or rat nephrectomy, the reduction in uEV excretion was lower than expected based on the reduction in kidney mass. This implies that the compensatory hypertrophy that is known to occur after nephrectomy [357-359] contributes to the relative increase in uEV excretion [360]. Indeed, in our rat studies the estimated degree of hypertrophy matched the fold-change in uEV excretion rate suggesting that hypertrophied tissue is capable of secreting uEVs. These findings also have implications for uEV biomarker research. This was illustrated by our analysis of nephron-specific markers in uEVs before and after donor nephrectomy. Without correction for the loss of nephron mass after the donor nephrectomy, the nephron-specific marker profile in uEVs was completely different than with this correction. Of further interest was that donor nephrectomy especially affects the CD9+ population of uEVs. Previously we showed that the uEV abundance of CD9 was significantly reduced in patients with CKD stages G2-4 compared with healthy controls [90]. According to the Kidney Tubules Expression Atlas, CD9 is increasingly expressed in the distal nephron, but is virtually absent in the proximal tubule [342]. Indeed, we recently showed that CD9 does not immunoprecipitate with NHE3 and NaPi-IIa in uEVs [347]. Together, this suggests that the proximal tubule undergoes more hypertrophy than downstream nephron segments after uninephrectomy causing more CD9- uEV excretion (100% increase after correction for nephrectomy). This impression was confirmed by showing that several proximal tubule markers were upregulated when correcting for nephron loss. This is also in agreement with previous work showing that uninephrectomy increases NHE3 activity and abundance by compensatory cell growth in mice [361-363]. This is likely caused by chronic hyperfiltration [364], and is clinically relevant because it was previously linked to the development of salt-sensitive hypertension in sheep after fetal uninephrectomy [365, 366], and in rats after adult uninephrectomy [367]. While some epidemiological studies show that kidney donors remain normotensive after donation [368], others find an increase in blood pressure [369, 370], which could be a consequence of increased proximal tubular salt reabsorption [371, 372]. Increased proximal tubular salt reabsorption would be expected to reduce distal

sodium delivery, which could impair distal potassium secretion. This may explain the minor rise in plasma potassium after kidney donation, an observation that has been made previously [373].

We also performed a study in patients with a nephrostomy drain in order to compare uEVs from urine directly derived from the kidney to urine derived from the complete urinary tract. In this analysis it was striking to see that the vast majority of uEV proteins was identified in both types of urine. Three possible explanations for this observation are that (1)the kidney is the main source of uEVs , (2) the kidney and the other parts of the urinary tract secrete the same proteins in uEVs, (3) plasma-derived EVs contribute to uEVs. Although the protein identification analysis cannot differentiate between these options, our analysis of uEV protein abundances did show that the quantitative contribution of the post-kidney urinary tract is limited. Although systemically infused EVs can reach the urine[360], the quantitative contribution of plasma-derived EVs also appears to be limited as a recent analysis showed that only 2 of 5113 uEV proteins were not detected at the RNA level in the urinary tract [227].

This study is only the first step in establishing the determinants of uEV excretion, and therefore a number of limitations should be acknowledged. First, we did not measure GFR in the kidney donors as this is not routinely performed in our center. Ideally, uEV excretion would be compared to measured GFR and a true estimation of nephron number, for example by combining unenhanced computed tomography and biopsy-based stereology [374]. Similarly, linking a spot urine to the time of last void could facilitate the use of a timed uEV excretion for spot urines. Second, for this initial study, we chose a relatively "clean" model of nephron loss, i.e. surgical removal of nephrons either by donor nephrectomy or 5/6th nephrectomy. Future studies should address how uEV excretion changes over time during other forms of nephron loss, e.g. progression of CKD. Finally, we acknowledge that not all particles are uEVs [232], but this limitation mainly pertains to NTA and not EVQuant and CD9-TR-FIA [347].

Taken together, our data show that uEV excretion depends on nephron mass, and that nephrectomy reduces uEV excretion less than expected based on nephron loss due to compensatory hypertrophy. The major implication is that a measure for nephron mass or uEV excretion rate should be included when comparing uEV biomarkers between individuals.

Supplemental Table of Contents

TABLE 5.S1

Antibodies

TECHNIQUES	ANTIBODY	TYPE	SPECIES	CONCENTRATION	COMPANY	CAT#/CLONE
EVQuant	CD9 alexa-647	Primary	Mouse	1:25	Thermo SC	MA5-18154
CD9-TR-FIA	CD9-biotin	Capture	Mouse	1:500	Bioscience	SN4 C3-3A2
	CD9-Europium	Primary	Mouse	0.25ng/µL	CellGS	CGS12A
Immunoblot	WT1	Primary	Mouse	1:1000	Ventana	6F-H2
	CD9	Primary	Mouse	1:500	Bioscience	MAB1880
	TSG101	Primary	Mouse	1:333	Abcam	ab83
	Cubilin	Primary	Rabbit	1:12,000	Nielsen lab	-
	NHE3	Primary	Rabbit	1:1000	Stressmarq	7644
	NaPi-IIa	Primary	Rabbit	1:500	Abcam	Ab83
	NKCC2	Primary	Rabbit	1:1000	Stressmarq	Spc-401D
	NCC	Primary	Rabbit	1:2000	Millipore	3553
	AQP2	Primary	Rabbit	1:1000	Stressmarq	9398
	Mouse HRP	Secondary	Goat	1:3000	Biorad	L005680
	Rabbit HRP	Secondary	Goat	1:3000	Biorad	L005679

TABLE 5.S2

Kidney donors before donation: women versus men

VARIABLE	WOMEN (N = 12)	MEN (N = 7)	P-VALUE
Age, years	61 ± 11	52 ± 12	0.1
Body mass index, kg/m2	26 ± 7	25 ± 2	0.7
eGFR, ml/min*	89 ± 25	99 ± 18	0.4
Creatinine clearance, ml/min	99 ± 33	128 ± 7	0.04
Plasma sodium, mmol/L	143 ± 2	142 ± 2	0.4
Plasma potassium, mmol/L	4.0 ± 0.3	4.3 ± 0.3	0.05
24h urine			
Volume, mL	2096 ± 671	1581 ± 803	0.2
Osmolality, mOsm/kg	334 ± 130	734 ± 216	< 0.001
Creatinine, mmol/day	9.0 ± 2.6	17.1 ± 1.3	< 0.001
Sodium, mmol/day	109 ± 33	173 ± 44	0.002
Potassium, mmol/day	63 ± 23	101± 39	0.01
Protein, mg/day	80 ± 21	83 ± 18	0.8
Spot urine			
Protein to creatinine ratio, g/mmol	10.5 ± 5.5	7.1 ± 2.6	0.1

* Estimated glomerular filtration rate (eGFR) adjusted for body surface area.

TABLE 5.S3

Patient characteristics

#	SEX, M/F	AGE, YEARS	EGFR, ML/MIN/1.73M²	REASON FOR NEPHROSTOMY DRAIN	TIME DRAIN PLACED, DAYS	COLLECTION TIME, MIN.
1	M	54	67	Kidney stones	1	105
2	F	30	118	Abscess	78	105
3	M	62	58	Colorectal cancer	27	135
4	F	62	35	Endograft	14	90
5	F	80	83	Colorectal cancer	55	120
6	M	86	22	Colorectal cancer	47	180
7	F	60	47	Metastatic cancer	38	N/A
8	M	59	99	Colorectal cancer	33	105
9	F	36	53	Kidney stones	27	90

TABLE 5.S4

Characteristics urine samples from nephrostomy drain and bladder

VARIABLE	NEPHROSTOMY (N = 9)	BLADDER (N = 9)	P-VALUE
Collection time, min*	116 ± 30	116 ± 30	-
Creatinine clearance, ml/min*	31 ± 21	33 ± 18	0.60
Protein/creatinine, g/mmol	95 ± 56	68 ± 71	0.4
Albumin/creatinine, mg/mmol	69 ± 40	45 ± 52	0.4
Sodium excretion, µmol/min*	23 ± 10	23 ± 14	1.0
Potassium excretion, µmol/min*	11 ± 4	13 ± 7	0.4
Diuresis, ml/min*	0.3 ± 0.2	0.3 ± 0.1	0.5

* These data were available for 8 patients because collection time was not available in particpant #7.

FIGURE 5.S1 **Bland Altman analysis of calculated spot vs. 24-hour uEV excretion**

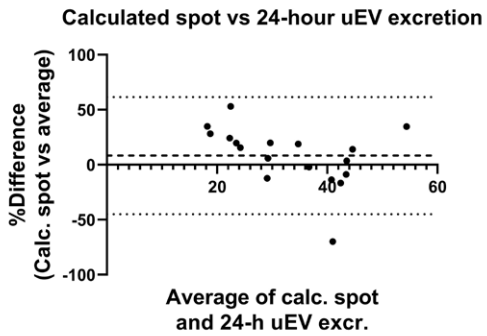

The X-axis depicts the average of the two uEV excretion methods; on the Y-axis the percent difference of calculated spot excretion vs. the average of the uEV excretion methods is shown. Shown are Bias (---) and 95% Limits of agreement (••••).

FIGURE 5.S2 **Complete immunoblots of kidney donors before and after nephrectomy (*n* = 19)**

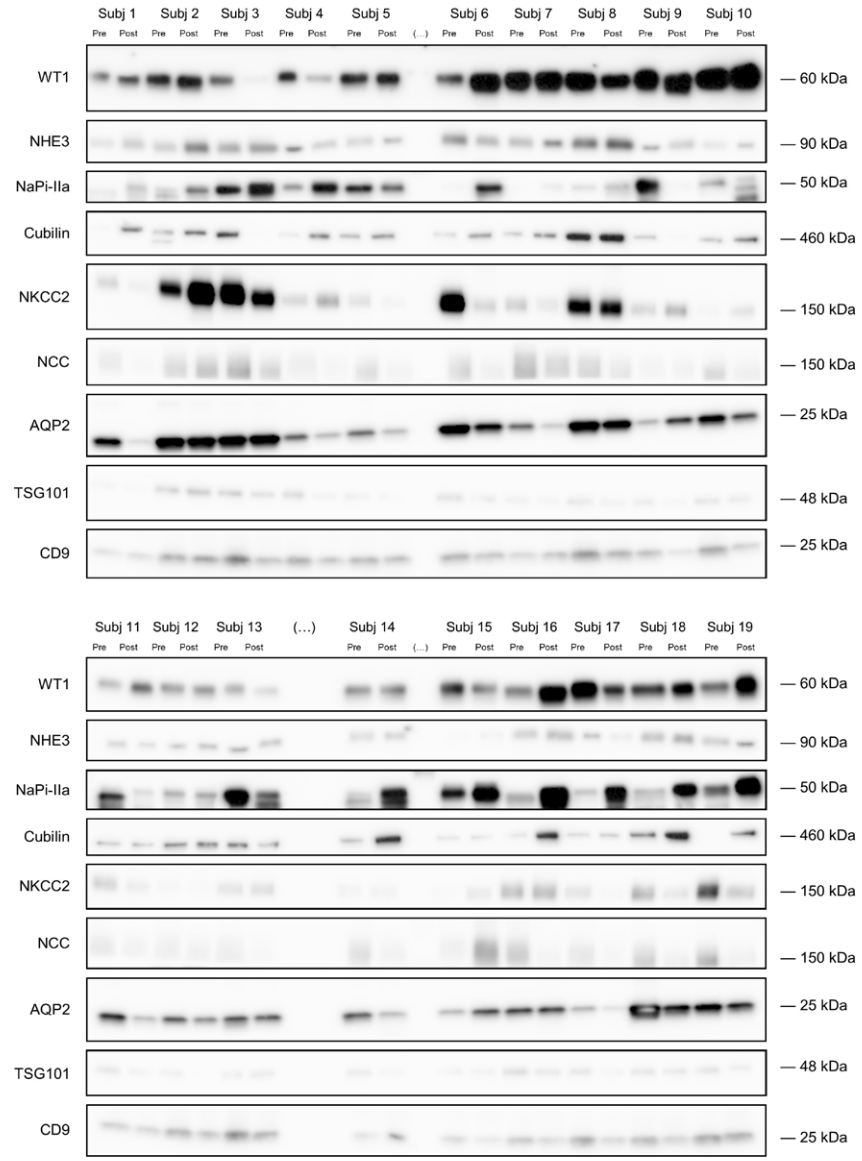

PART 2

URINARY EXTRACELLULAR VESICLES: AND OTHER MARKERS OF POLYCYSTIC KIDNEY DISEASE

“Prediction is very difficult, especially if it’s about the future”

- Niels Bohr

CHAPTER 6

Matrilysin (MMP-7) in Urinary Extracellular Vesicles Predicts Rapid Disease Progression in Polycystic Kidney Disease

Martijn H. van Heugten*, Charles J. Blijdorp*, Usha M. Musterd-Bagghoe, Karel Besztarosti, Jeroen A.A. Demmers, Hester van Willigenburg, Esther Meijer, Ron T. Gansevoort, Robert Zietse, Mahdi Salih*, Ewout J. Hoorn*, on behalf of the DIPAK consortium

* Authors contributed equally
Submitted

6.1 Abstract

Background: Disease progression in autosomal dominant polycystic kidney disease (ADPKD) is highly variable. Distinguishing patients with rapid disease progression (RDP) from patients with slow disease progression (SDP) is crucial to facilitate adequate counseling and selection of patients that may benefit most from therapy. In this study we aimed to identify markers of RDP in urinary extracellular vesicles (uEVs).

Methods: We used ultracentrifugation followed by Tandem Mass Tag labelled proteomics to compare the uEV proteome from two independent and 1:1 matched cohorts of patients with ADPKD with either RDP or SDP (both *n* = 10, estimated glomerular filtration rate [eGFR] decline of respectively ≥4 or ≤2 mL/min/1.73 m2/year). The identified candidate biomarkers were validated in a third independent and matched cohort (*n* = 24) using immunoblotting.

Results: No differences in established predictors were found between the groups in our selected cohorts. In the discovery and verification cohorts the abundance of 65 and 36 proteins was significantly different between RDP and SDP. In both cohorts, Matrilysin (MMP-7) was higher and Charged Multivesicular Body Protein 4a (CHMP4A) was lower in RDP than in SDP. In the validation cohort, MMP-7 but not CHMP4A differentiated between RDP and SDP.

Conclusion: uEV-associated MMP-7 discriminates RDP from SDP in patients with ADPKD independent of established markers of disease progression. MMP-7 is a biologically plausible biomarker as it increases with kidney injury.. This finding warrant further evaluation of this novel candidate biomarker in a larger cohort of patients.

6.2 Introduction

Autosomal dominant polycystic kidney disease (ADPKD) is the most common inherited form of kidney disease, caused by mutations in the *PKD1* or *PKD2* gene as well a number of infrequent mutations [375, 376]. The disease is characterized by the development of multiple bilateral kidney cysts frequently leading to kidney failure. The rate of disease progression in ADPKD is highly variable, even within families that carry the same genetic mutation [377]. Several prognostic classifications have been developed, of which the Mayo Clinic ADPKD classification tool and the PRO-PKD score are most commonly used [40, 41]. These methods rely on height-adjusted total kidney volume (htTKV) or *PKD* gene analysis, and are less reliable at early stages of the disease. Importantly, the actual disease progression varies considerably among those with predicted rapid disease progression, limiting the value of these methods at an individual patient level [43].

Therefore, there is an unmet need for novel biomarkers that can identify patients with rapid disease progression (RDP), the group that benefits most from treatment. Moreover, such a biomarker could avoid unnecessary treatment with potential side effects in patients with a favorable kidney prognosis. The approval of tolvaptan as a treatment option for ADPKD further highlights this need [38].

Urinary extracellular vesicles (uEVs) represent an attractive source of kidney biomarkers. uEVs are nanoparticles that bud off from cell membranes (microparticles or apoptotic bodies) or are released by multivesicular bodies (exosomes) and therefore contain proteins and RNA from their host cells. By studying their content, (patho)physiological processes of epithelial cells lining the nephron and urinary tract can be assessed. The isolation and characterization of uEVs has therefore become a powerful approach to identify biomarkers for kidney diseases, including ADPKD [349]. Several groups, including ours, have previously performed proteomic studies of uEVs to identify proteins unique to ADPKD and its progression [44, 90, 378-380]. These studies, however, did not address whether uEVs can be used to differentiate patients with ADPKD with RDP from those with slow disease progression (SDP). Here, we present the results of an explorative proteomics approach to identify uEV proteins that distinguish patients with ADPKD who subsequently have RDP or SDP.

6.3 Methods

Setting and subjects

Patients with RDP and SDP were selected from the DIPAK intervention trial, an open-label randomized clinical trial to examine the effect of Lanreotide on disease progression in patients with ADPKD with an eGFR of 30–60 mL/min/1.73 m2 (n = 309) [381]. The baseline and follow-up measurements, including blood pressure, body weight, MRI-based hTKV, and kidney function assessment were described here. RDP was defined as an eGFR decline of ≥4 mL/min/1.73 m2 per year and SDP with ≤2 mL/min/1.73m2 per year. Patients with RDP were 1:1 matched to patients with SDP, based on age, sex, baseline eGFR, and truncating *PKD1* mutation. Three cohorts were subsequently created: a discovery, a verification and a validation cohort (Figure 6.1). At 2.5 years of follow-up, urine was collected from patients within the discovery cohort, to determine which biological processes and uEV proteins change over time. After subject selection, potential risk factors of disease progression were scored to calculate the Mayo and PROPKD scores.

Sample collection and uEV isolation

Fifty milliliter random spot urine samples were stored at -80 °C after addition of a protease inhibitor (cOmplete Protease Inhibitor Cocktail, Roche Diagnostics, Germany). uEVs were isolated using a differential ultracentrifugation protocol [347] (Table 6.S1). Briefly, frozen samples were thawed, vortexed and centrifuged at 2,000 x g for 10 minutes, and then at 17,000 x g for 20 minutes, after which the resultant supernatant was temporarily stored on ice. Pellets were suspended in a 200 mg/ml dithiothreitol (DTT) solution, kept at 37 °C and intermittently vortexed for seven minutes to dissociate THP polymers. After DTT treatment, the suspended pellets were centrifuged at 17,000 x g for 20 minutes. The resultant supernatant was subsequently combined with the stored supernatant from the first 17,000 x g cycle and uEVs were initially pelleted by 120 minutes 200,000 x g (discovery), which was later adapted to 160 minutes 150,000 g (verification and validation), because of lowering of the maximum RPM of the ultracentrifuge. After discarding the final supernatant, the uEV pellet was suspended in 150 µl PBS and stored at -80 °C until analysis by mass spectrometry or immunoblot.

Mass spectrometry

uEV isolates were lysed by sonication for 10 minutes using a Bioruptor (Diagenode, United States), before processing 20 µg of protein for digestion using the SP3 protocol [382]. Proteins were digested and fractionated using 0.5 µg MS-grade trypsin and 0.5 µg Lys-C in 100 mM Tris/HCl at pH 8.3, before the tryptic digests were acidified using Trifluoroacetic acid (TFA) and desalted using StageTips. Individual peptide samples were Tandem Mass Tag (TMT) labeled using the TMT10plex isobaric reagent set (Thermo Scientific, United States, catalog number A34808), according to the supplier's instructions. Labeled samples were then combined and quantified by MS/MS using liquid chromatography coupled to the QExactive orbitrap tandem

FIGURE 6.1 **Study design including three independent cohorts**

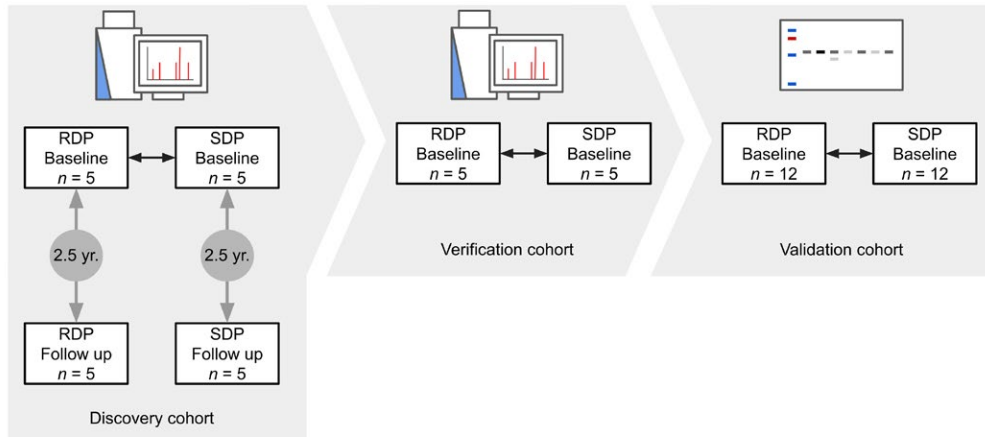

Left and middle panel show the discovery cohort (*n* = 10) and verification cohort (*n* = 10). Quantitative proteomics was performed using MS/MS with Tandem Mass Tag-labelled samples. A follow-up after 2.5 years was included in the discovery cohort. Protein candidates were analyzed in the validation cohort (*n* = 24, right panel) using immunoblotting.

mass spectrometer (Thermo Scientific, United States). Peptide spectra and protein abundances were computed using Proteome Discoverer (Thermo Scientific, United States), and abundance data equaled for all TMT channels normalized before statistical processing using R. The discovery baseline experiment, discovery follow-up experiment, and verification baseline experiment were all performed in their own pooled TMT analysis, maximizing sample comparability. Unique identified protein numbers were compared to the *Vesiclepedia* database [383].

Immunoblotting

Immunoblotting was performed using primary antibodies against MMP-7 (1:100, Santa Cruz, United States, sc-515703), CHMP4A (1:100, Santa Cruz, United States, sc-514869), and secondary goat anti-mouse IgG antibodies (1:3000, Biorad, United States, L005680). uEV isolates from the validation cohort were solubilized in Laemmli buffer for immunoblot analysis, and samples were equally loaded relative to urine creatinine. We used Criterion TGX precast polyacrylamide midi gels (Biorad, United States), transferred to membranes using a Trans-Blot Turbo (Biorad, United States). Membranes were blocked using 5% bovine serum albumin in TBS with 0.1% Tween 20 (Sigma-Aldrich, United States) for one hour and visualized using an Amersham AI600 Chemiluminescent imager (GE Healthcare, United States) and Clarity Western ECL substrate (Biorad, United States). Acquisition images were processed using Image Studio version 5.2 (LI-COR Biotechnology, United States) and background normalized values were exported to R for statistical processing.

TABLE 6.1

Baseline characteristics of discovery, verification and validation cohorts

	DISCOVERY COHORT			VERIFICATION COHORT			VALIDATION COHORT		
	RDP *n = 5*	**SDP** *n = 5*	**P-value**	**RDP** *n = 5*	**SDP** *n = 5*	**p-value**	**RDP** *n = 12*	**SDP** *n = 12*	**p-value**
Age (years) ± SD	51±8	50±7	-	42±2	44±7	-	49±10	48±8	-
Gender (% female)	60%	60%	-	40%	40%	-	58%	58%	-
PKD1 mutation (%)	100%	100%	-	100%	100%	-	80%	80%	-
Truncating (%)	60%	60%	-	80%	80%	-	30%	30%	-
eGFR (ml/min/1,73m2) ± SD	49±7	52±10	-	52±11	53±8	-	55±12	55±9	-
PROPKD score	4.4 (2.7)	5.2 (1.6)	0.59	6.2 (2.2)	6.2 (1.6)	1.00	3.9	3.8	0.87
Mayo classification score	3.0 (1.0)	3.0 (0.7)	1.00	4.2 (1.1)	3.6 (1.5)	0.49	3.3	3.1	0.44
htTKV baseline (mL/m) ± SD	817±366	898± 203	0.68	1487±749	1309±1069	0.77	1067±762	1071±598	0.99
SBP baseline (mmHg) ± SD	129±10	134±14	0.54	147±9	129±20	0.09	137±13	129±10	0.11
ACE-inhibitor or ARB use (%)	80%	60%	0.49	100%	80%	0.29	75%	75%	1.00
Diuretic use (%)	40%	20%	0.49	40%	0%	0.11	42%	58%	0.68
Cardiovascular disease score	0 (0)	0.6 (0.9)	0.17	0.8 (1.1)	0.8 (0.8)	1.00	0.6 (0.7)	0.9 (0.7)	0.24
Smoking (recent) (%)	20%	20%	1.00	80%	20%	0.06	58%	33%	0.41
BMI (kg/m2) ± SD	27±6	25±2	0.47	31±9	25±0.6	0.13	26±4	29±4	0.11
HbA1c (mmol/mol) ± SD	36±2	36±7	0.85	36±1	37±3	0.34	36±3	38±3	0.27
Protein excretion (mg/24h) ± SD	0.18±0.07	0.07±0.10	0.06	0.60±0.64	0.18± 0.14	0.19	0.26±0.20	0.15±0.14	0.12

All mutations were genetically confirmed, and either in PKD1 or PKD2. PROPKD is scored based on sex (female = 0 points, male = 1 point), hypertension before age 35 (2 points), first urologic event before age 35 (points), and mutation (PKD2 = 0 points, PKD1 nontruncating = 2 points, PKD1 truncating is 4 points. Mayo class is based on hTKV relative to age, 1A = 1, 1B = 2, etc. (Recent) smoking includes patients that currently smoke, or have done so in the past 10 years. There were no missing data.

Statistical analysis

Patient baseline characteristics other than matching variables were compared using students' t-test or chi-square tests, as appropriate. For each cohort the eGFR slope was fitted with univariate linear regression for visual comparison. MS/MS identified and TMT normalized proteins were only included in our analysis when they were quantified with certainty for all included cases. Protein abundances were subsequently normalized using the *Bioconductor VSN*-package for R, to address the observed dependence of variance on protein abundance means [384, 385].

The differential protein abundance was calculated using two-tailed independent samples student's t-tests, and protein fold changes were calculated dividing the mean change in abundance by the mean of the reference group, and Vsn/log transformed. Pathway analysis was performed using the *ReactomePA* package for R, using the Reactome pathway database, version 1.34.0 [386, 387]. For the follow-up data paired t-tests were used. The ratio by which protein abundance changed over time in RDP patients was compared to that of SDP patients by independent samples t-test. Immunoblots of MMP-7 and CHMP4A were loaded relative to creatinine and compared using an independent samples student's T test. In addition, a "calculated spot uEV excretion" was determined by multiplying the uEV-to-creatinine ratio in spot urine by 24-hour urinary creatinine: calculated spot urine uEV excretion (uEVs/min) = spot uEV concentration (uEVs/L) x creatinine excretion (mmol/min) / spot urine creatinine concentration (mmol/L) [388]. P-values < 0.05 were considered statistically significant.

6.4 Results

Clinical characteristics

The baseline characteristics for the discovery, verification, and validation cohorts are shown in Table 6.1. No significant differences in htTKV or established predictors (Mayo classification, PROPKD score) were found. The decline in eGFR in our selected cohorts is shown in Figure 6.2. During a follow-up of 2.5 years, the average eGFR decline was 5.9 ml/min/1.73m2/year in RDP vs. 1.2 ml/min/1.73m2/year in SDP in the discovery cohort. In the verification cohort, eGFR decline was 9.6 ml/min/1.73m2/year in RDP vs. 1.9 ml/min/1.73m2/year in SDP. Finally, in the validation cohort, eGFR decline was 8.8 ml/min/1.73m2/year in RDP vs. 0.5 ml/min/1.73m2/year in SDP.

FIGURE 6.2 **Kidney function over time within the three cohorts**

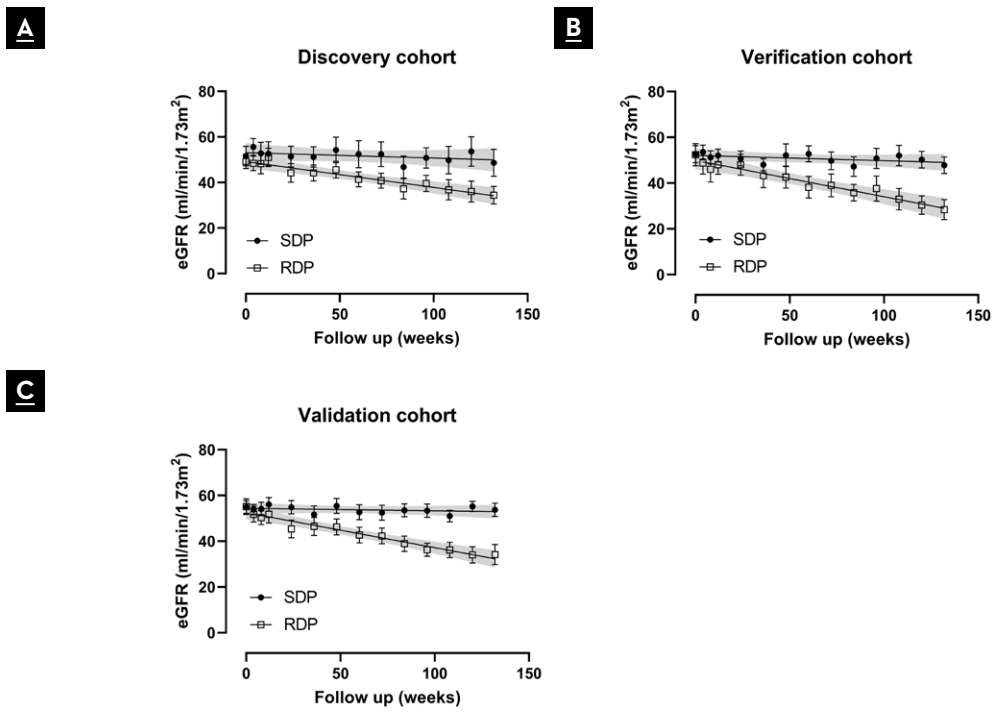

Comparison of eGFR course in patients with RDP and SDP for the discovery cohort **A**, the verification cohort **B**, and the validation cohort **C**, depicting mean ± SEM for eGFR, with fitted linear regression including 95% confidence interval in grey.

Protein identification and pathway analysis

Proteomic analysis of uEVs identified between 2055 and 2983 unique proteins in the discovery cohorts. In the verification cohort 1115 unique proteins were identified. A Venn diagram of the unique, reliably identified proteins for all cohorts compared to extracellular vesicles from any source is shown in Figure 6.3A. The identified unique and overlapping proteins from the four proteomics experiments are shown in Figure 6.3B. To determine altered biological processes that differ between RDP and SDP, and explore the possible biological role of individual differential proteins we performed pathway analysis. In the Reactome database we identified 176 enriched pathways (q-value < 0.05) in the discovery cohort, including nested pathways (Supplemental data S1). These include *protein folding*, *ERK/MAPK* functions, but also many signaling pathways including *insulin*, *glucagon*, *WNT*, *FGFR2* and *FGFR-4*, as well as *prostacyclin* and *thromboxane signaling.*

FIGURE 6.3 **Number of proteins identified in the MS/MS experiment**

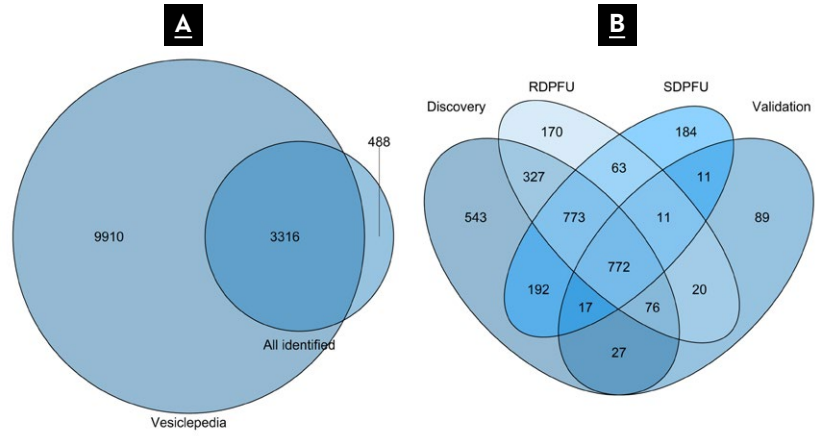

A Venn diagram comparing the proteins identified in isolated uEVs within the MS/MS experiments combined with the extracellular proteome reported on Vesiclepedia.

B Venn diagram comparing the proteins identified in isolated uEVs among the four MS/MS experiments: the discovery cohort at baseline (1); follow up vs baseline of patients with RDP (2) or SDP (3) of the discovery cohort; and the verification cohort (4).

MMP-7 and CHMP4A in rapid disease progression

Comparing uEV-derived protein abundances from RDP and SDP, we identified 65 proteins with significantly different abundances in the discovery cohort (Figure 6.4). Of these 65 differentially

FIGURE 6.4 **Volcano plots of the MS/MS cohorts**

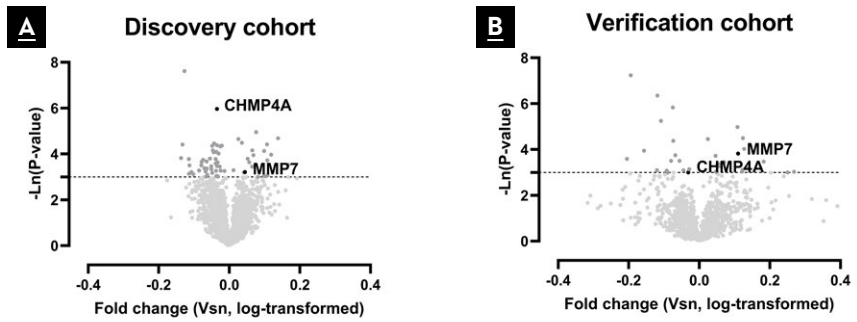

Comparison of protein abundance in isolated uEVs of patients with RDP vs SDP in the discovery cohort (**A**, *n* = 10) and the verification cohort (**B**, *n* = 10). X-axis depicts Vsn-normalized abundance ratio (RDP/SDP), which includes a log transformation. Y-axis depicts naturally log-transformed P-value of student's T-test, with cut-off at -Ln(0.05). All significantly different proteins (P < 0.05) are marked in darker grey, while the recurring significantly differentially abundant proteins (MMP-7 and CHMP4A) are marked black.

abundant proteins, the top proteins selected for greatest positive and negative change, are provided in Table 6.2. In the verification cohort 36 proteins were identified with significantly different abundances between RDP and SDP. The heatmaps of the significantly differentially abundant proteins are shown in Figure 6.5. Two of these proteins were consistently higher or lower in both the discovery and verification cohort, including Matrilysin (MMP-7) and Charged Multivesicular Body Protein 4a (CHMP4A) (Figure 6.6 and Table 6.2).

Confirmation of MMP-7 in the validation cohort, and in ADPKD vs. CKD and healthy uEV samples

Validation of the MS/MS results by immunoblotting confirmed a significantly higher abundance of MMP-7 in RDP compared to SDP (Figure 6.7A and B). In contrast to the mass spectrometry data, CHMP4A was higher in RDP than in SDP (Figure 6.7C). Extrapolated 24-hour MMP-7 excretion remained significantly higher in RDP than SDP (p-value 0.008, data not shown). Similarly, in RDP, 24-hour CHMP4A was significantly increased (p-value 0.046, data not shown). Additionally we re-analyzed our previous proteomics data, where we compared uEV protein abundances of patients with ADPKD with healthy subjects and those with non-ADPKD chronic kidney disease (CKD) (9). There, MMP-7 was undetectable in healthy subjects, whereas it was detected and 13-fold higher in ADPKD compared to non-ADPKD CKD (Figure 6.7D).

TABLE 6.2 **Top proteins selected for greatest positive and negative change in the discovery and verification cohorts.**

DISCOVERY COHORT

Increased in RDP				Decreased in RDP			
Rank	**p-value**	**Protein**	**Change**	**Rank**	**p-value**	**Protein**	**Change**
1	0.05	SERPINA1	3.6	1	0.01	SLC4A4	-0.86
2	0.01	ANTXR1	2.0	2	0.02	ALYREF	-0.84
3	0.03	EFEMP1	1.9	3	0.04	ADD3	-0.80
4	0.03	A1BG	1.4	4	0.03	CSNK2A1	-0.79
5	0.02	SVIL	1.3	5	0.04	NPY	-0.78
6	0.05	LYPLA2	1.3	6	<0.01	WFS1	-0.75
7	0.02	PLTP	1.2	7	0.04	RPS24	-0.73
8	0.01	FLG2	1.2	8	0.02	PUF60	-0.71
9	0.02	FTL	1.0	9	0.03	KYAT3	-0.71
14	**0.04**	**MMP-7**	**0.47**	**39**	**<0.01**	**CHMP4A**	**-0.44**

VERIFICATION COHORT

Increased in RDP				Decreased in RDP			
Rank	**p-value**	**Protein**	**Change**	**Rank**	**p-value**	**Protein**	**Change**
1	0.03	SWT1	1.9	1	0.05	PDZK1IP1	-0.49
2	0.04	IGHV6-1	1.0	2	<0.01	XPNPEP2	-0.38
3	0.05	IGHV3-74	1.0	3	<0.01	NIT2	-0.36
4	0.05	CALR	0.80	4	0.02	SLC36A2	-0.34
5	0.01	IGKV3D-11	0.71	5	0.01	PSMC3	-0.32
6	0.02	IGLV7-46	0.66	6	0.02	CMBL	-0.32
7	**0.02**	**MMP-7**	**0.64**	7	0.03	SBDS	-0.31
8	0.03	IGLC2	0.57	8	0.03	CA2	-0.29
9	0.03	IGHV3-49	0.56	9	0.01	ATP1B1	-0.27
10	0.05	KRT80	0.56	**15**	**0.05**	**CHMP4A**	**-0.01**

Only proteins with P-value < 0.05 are shown. Change is presented as Vsn-normalized fold change, which includes Log transformation. MMP7 and CHMP4A were highlighted because they are consistently differentially expressed in both cohorts.

FIGURE 6.5

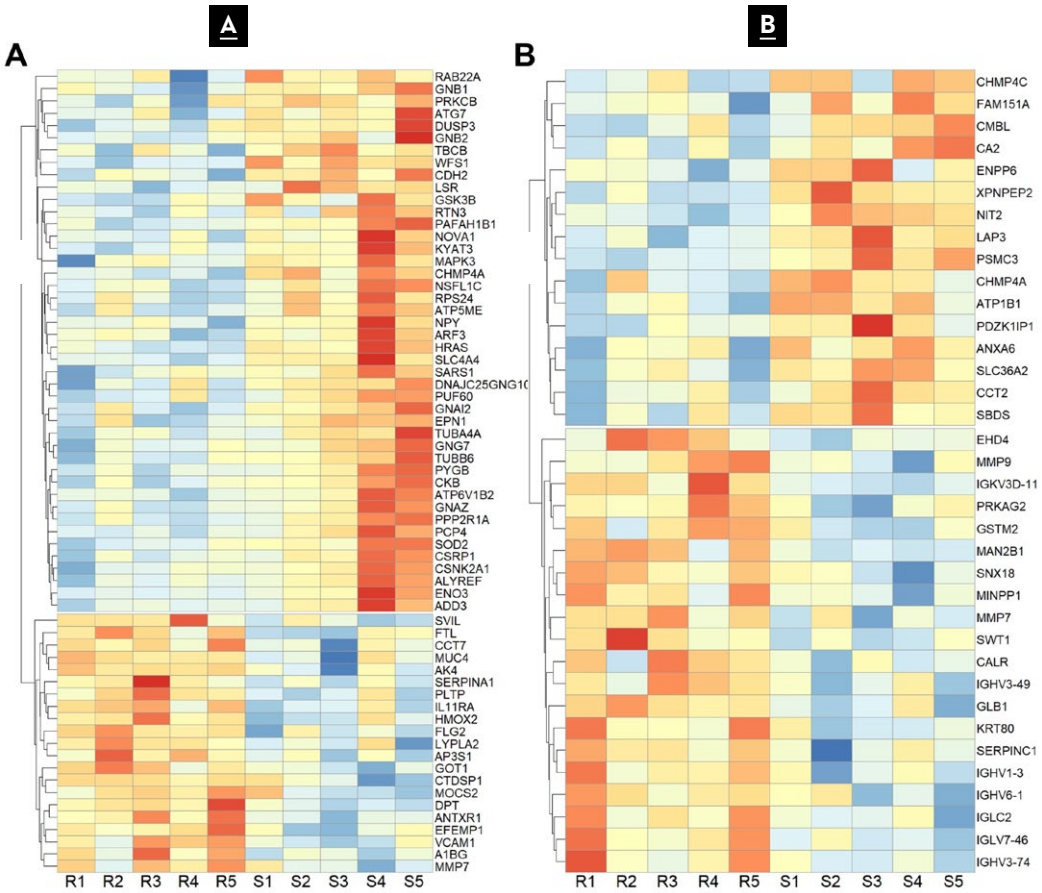

Heatmap images with agglomerative hierarchical clustering of significantly differentially abundant proteins from the baseline MS/MS experiments comparing RDP (R1, R2, etc.) and SDP cases (S1, S2, etc.), the discovery cohort **A** and verification cohort **B**, with all abundances scaled for equal visual contrast. Selected significance and fold change values for these proteins are provided in Table 2.

FIGURE 6.6 **Abundance of MMP-7 and CHMP4A in the MS/MS cohorts**

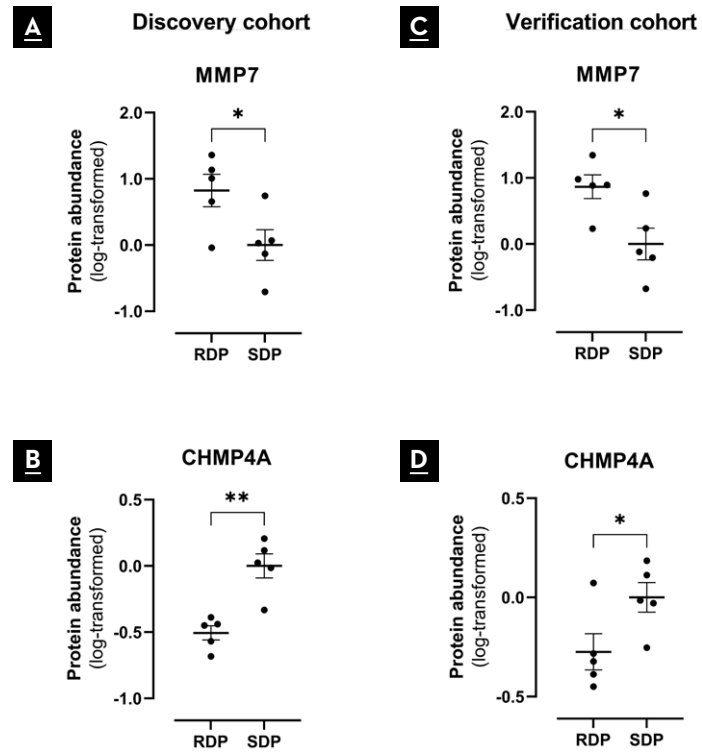

Protein abundance in isolated uEVs (including mean ± SEM) of MMP-7 **A** and CHMP4A **B** in the discovery cohort, and of MMP-7 **C** and CHMP4A **D** in the verification cohort, comparing patients with RDP and SDP. Abundances were Vsn-normalized, which includes log-transformation, and presented relative to the average of patients with SDP. Asterisks represent significance by student's T-test; *P < 0.05, ** P < 0.01.

Follow-up

We studied the changes in uEV protein abundance between paired baseline and follow-up samples of the patients in the discovery cohort (Figure 6.1). In the uEV proteome of RDP, we reliably identified 2261 proteins, of which 173 were significantly changed from baseline; in SDP we reliably identified 2055 proteins in uEVs, of which 431 significantly changed during follow-up (Figure 6.S1). There was an enrichment of complement activation and Wnt-signaling in both RDP and SDP over time, while SDP cases additionally showed an enrichment of cell cycle con-

trol pathways, including the *Stabilization of p53* and *Apoptosis* pathways (Supplemental data S3-S4). The change in protein abundance was compared between RDP and SDP cases, which revealed that 292 proteins showed a significantly different change in RDP compared to SDP. The mean MMP-7 abundance did not significantly change in either RDP or SDP after 2.5 years (P = 0.19 and P = 0.21 respectively, not shown).

FIGURE 6.7 **Abundance of MMP-7 and CHMP4A in the validation cohort**

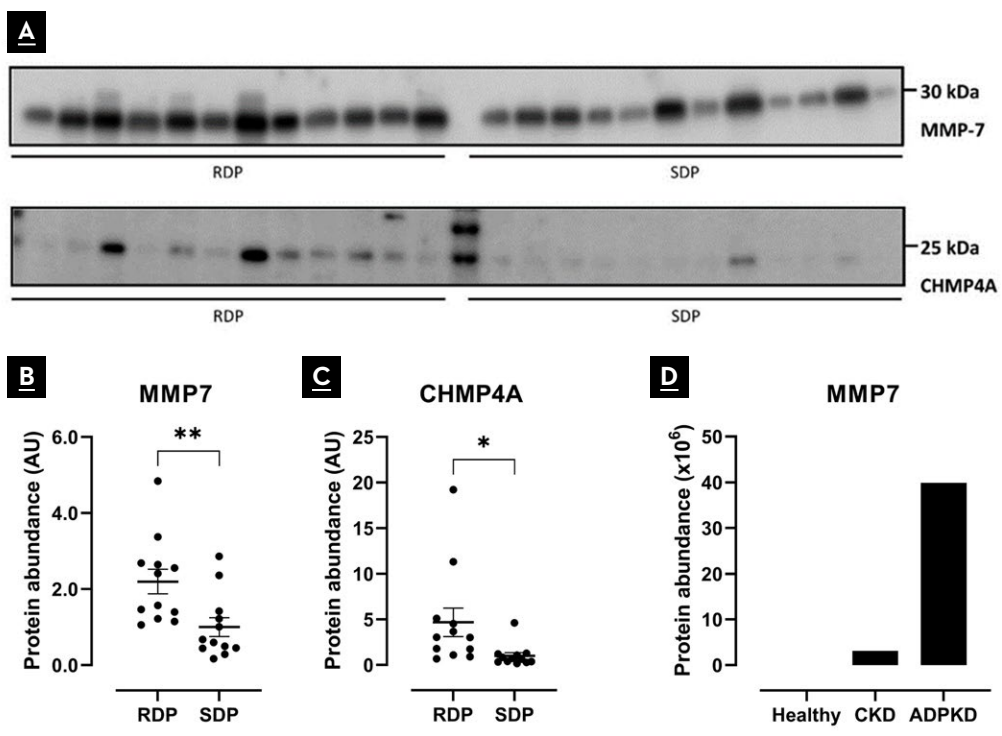

A Complete immunoblots of MMP-7 and CHMP4A in isolated uEVs, comparing patients with SDP vs patients with RDP (*n* = 24). Proteins were loaded relative to urine creatinine. **B-C** Densitometry (including mean ± SEM) of uEV protein abundances of MMP-7 **B** and CHMP4A **C** in patients with RDP and SDP, relative to the average of patients with SDP. Asterisks represent significance by student's T-test; *P < 0.05, ** P < 0.01. **D** MS/MS comparison of MMP7 in pooled healthy, non-ADPKD CKD, and ADPKD uEV samples (as described in Salih *et al.* J Am Soc Nephrol 2016). The values presented are relative to uEVs from healthy subjects.

6.5 Discussion

Here, we aimed to identify and validate novel uEV biomarkers that predict rapid disease progression (RDP) in ADPKD. Using a step-wise approach with three independent, well-characterized and matched patient cohorts, MMP-7 consistently and significantly differentiated patients with RDP from those with slow disease progression (SDP). Because we used an unbiased approach with several independent cohorts, and applied two platforms to study the proteins in uEVs, we believe MMP-7 is a promising biomarker for RDP in ADPKD.

MMP-7 is an endopeptidase matrix metalloproteinase with proteolytic activity against a wide range of extracellular proteins that regulate different biological processes, such as apoptosis, fibrosis and inflammation [389-392]. MMP-7 is detected at the tubular level (mainly in the S3 segment of the proximal tubule) in acute and chronic kidney diseases, including progressive IgA nephropathy, acute kidney transplant rejection, and ADPKD, while it is not detected in healthy kidney tissue [391-394]. MMP-7 knock-out mice show reduced collagen deposition, reduced interstitial fibrosis, and increased albuminuria [392, 395-399]. During kidney injury MMP7 is upregulated by beta-catenin, the principal mediator of canonical Wnt signaling, leading to apoptosis of interstitial fibroblasts, thereby reducing the development of kidney fibrosis [395]. Indeed, MMP-7 knockout mice are more susceptible to ischemia/reperfusion injury and cisplatin, which was reversible when MMP-7 was supplemented [396]. Polycystin 1 and 2 can both influence Wnt signaling through a number of different intermediates, although this interaction is best characterized for polycystin-2 [400-403]. Loss of *Pkd2* activates β-catenin, stimulating kidney epithelial cell proliferation and cystogenesis, and inhibition of Wnt and β-catenin suppressed cyst formation, directly implicating Wnt signaling in ADPKD disease progression [400]. Here, we demonstrate, to our best knowledge for the first time, that MMP7, a member of the Wnt signaling pathway, is significantly increased in uEVs of patients with ADPKD and RDP. In addition, we demonstrate that MMP7 was significantly increased in uEVs of patients with ADPKD compared to patients with non-ADPKD CKD, while it is undetectable in uEVs of healthy individuals. This suggests a central role for MMP-7 in ADPKD pathophysiology. Whether MMP-7 has kidney-protective or detrimental effects in patients with ADPKD warrants further evaluation.

CHMP4A is a part of the endosomal sorting complexes required for transport machinery (ESCRT), which is involved in the formation multivesicular bodies (MVBs) and in part responsible for exosome biogenesis, protein loading, and lysosomal repair and autophagy [404]. Autophagy is suppressed in PKD, which is associated with increased apoptosis and fibrosis. In addition, autophagy may suppress apoptosis and proliferation in PKD and may reduce cyst growth [405]. Decreased CHMP4A in uEVs of patients with ADPKD and RDP may therefore be an early marker of disturbed autophagy mechanisms, which may lead to apoptosis, fibrosis and progression of ADPKD. While CHMP4A was consistently downregulated in uEVs of patients with

ADPKD and RDP, this finding was not confirmed in the validation cohort. The discrepant results for CHMP4A when analyzed by mass spectrometry or immunoblotting may be related to the normalization methods that were used. Immunoblots were normalized to urine creatinine [347] or - because creatinine excretion differs between individuals - extrapolated to 24-hour excretion [388]. In contrast, MS/MS results were normalized to total protein [349]. Importantly, this discrepancy may be a sign that CHMP4A is not a sufficiently robust biomarker, whereas MMP7 is. Indeed, a clinically applicable biomarker should show the same results on various platforms. Therefore, ideally, we would have found a marker ratio of proteins regulated in opposite directions in patients with ADPKD and RDP [349].

Our study approach allowed us to identify markers that differentiate patients with RDP independently of currently used prognostic markers, including PKD mutation, htTKV, PROPKD score or Mayo classification. However, a number of limitations should also be mentioned. First, our study is limited by a low number of included patients (44 patients divided over three cohorts). We believe, however, that our findings are robust because: (1) we used a step-wise approach with three independent and well-matched cohorts of patients; (2) TMT labelling allowed us to perform statistical comparisons within the experiments, improving the accuracy of our findings; (3) we validated our findings using a different platform; (4) MMP7 was still upregulated after 2.5 years of follow up in the discovery cohort, suggesting it may be used at different stages of the disease. Second, because we selected patients from the DIPAK-1 study, all included patients had CKD stage G3. Whether or not our identified proteins have prognostic value at earlier stages of the disease is yet unknown and requires further evaluation.

In conclusion we identified uEV-associated MMP-7 as biomarker of ADPKD progression. This warrants further investigation in a larger cohort of patients with ADPKD, and possibly other causes of kidney disease.

Supplemental table and figures

TABLE 6.S1 **Differential ultracentrifugation steps**

CHARACTERISTICS	STEP 1	STEP 2	STEP 3	STEP 4	
Cohorts	**All**	**All**	**All**	**Discovery; validation**	**Verification**
Force, x g	2,000	17,000	17,000	200,000	150,000
Time, min	10	20	20	120	160
Temperature, °C	4	4	4	4	4
Rotor	Standard Hettich Rotanta	45 Ti	70.1 Ti	45 Ti	45 Ti
Fixed angle vs swing	Swing	Fixed	Fixed	Fixed	Fixed
K factor	25000	1839	965.4	156.3	208
Tube	Falcon 50mL	#355655	#355603	#355655	#355655
Deceleration time	90 sec	6 min	6 min	6 min	6 min

All tubings and rotors are from Beck Coulter, United states.

FIGURE 6.S1 **Volcano plot visualization of the follow up experiments' MS/MS results**

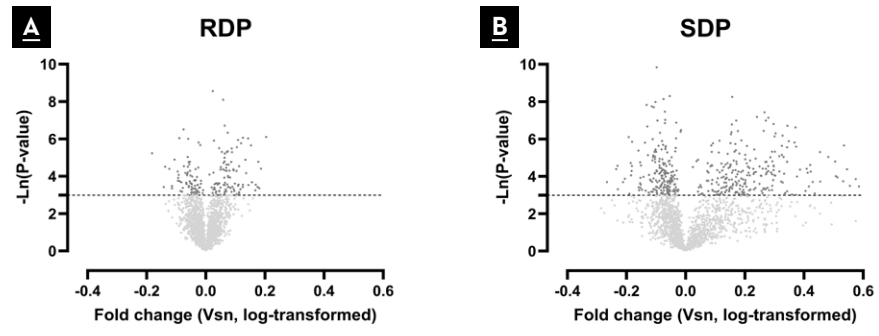

Comparison of protein abundance from isolated uEV from baseline and follow up samples from RDP cases (**A**, *n* = 5), and from SDP cases (**B**, *n* = 5). X-axis depicts Vsn-normalized abundance ratio (RDP/SDP), which includes a log transformation. Y-axis depicts naturally log-transformed P-value of student's T-test, with cut-off at -Ln(0.05). All significantly different proteins (P < 0.05) are marked in darker grey.

CHAPTER 7

Serum Bicarbonate is Associated with Kidney Outcomes in Autosomal Dominant Polycystic Kidney Disease

Charles J. Blijdorp, David Severs, Usha M. Musterd-Bhaggoe, Ronald T. Gansevoort, Robert Zietse, Ewout J. Hoorn, DIPAK consortium.

Nephrology Dialysis Transplantation 2021

7.1 Abstract

Background: Metabolic acidosis accelerates progression of chronic kidney disease, but whether this is also true for autosomal dominant polycystic kidney disease (ADPKD) is unknown.

Methods: Patients with ADPKD from the DIPAK trial were included (n = 296, eGFR 50 ± 11 ml/min/1.73 m2, 2.5 years follow-up). Outcomes were worsening kidney function (30% decrease in eGFR or kidney failure), annual eGFR change, and height-adjusted total kidney and liver volumes (htTKV, htTLV). Cox and linear regression were used adjusted for prognostic markers for ADPKD (Mayo image class and PROPKD scores) and acid-base parameters (urinary ammonium excretion).

Results: Patients in the lowest tertile of baseline serum bicarbonate (23.1 ± 1.6 mmol/L) had a significantly greater risk of worsening kidney function (hazard ratio 2.95, 95% confidence interval [CI], 1.21 – 7.19) compared to patients in the highest tertile (serum bicarbonate 29.0 ± 1.3 mmol/L). Each mmol/L decrease in serum bicarbonate increased the risk of worsening kidney function by 21% in the fully adjusted model (hazard ratio 1.21, 95% CI 1.06 to 1.37). Each mmol/L decrease of serum bicarbonate was also associated with further eGFR decline (-0.12 mL/min/1.73 m2 per year, 95% CI -0.20 to -0.03). Serum bicarbonate was not associated with changes in htTKV or htTLV growth.

Conclusions: In patients with ADPKD, a lower serum bicarbonate within the normal range predicts worse kidney outcomes independent of established prognostic factors for ADPKD and independent of urine ammonium excretion. Serum bicarbonate may add to prognostic models and should be explored as a treatment target in ADPKD.

7.2 Introduction

The combination of a typical Western diet and endogenous metabolism generates a nonvolatile acid load of 70 mEq/day, which is excreted by the kidney primarily as ammonium, but also as free hydrogen ions, and titratable acid [406]. As chronic kidney disease (CKD) progresses, per-nephron ammonium excretion eventually fails to excrete the daily acid load and metabolic acidosis ensues [407]. The prevalence of metabolic acidosis (defined as serum bicarbonate < 22 mmol/L) increases from 2% in patients with a GFR of 60-90 ml/min to 39% in patients with GFR < 20 ml/min [408]. In CKD patient cohorts, several studies identified an association between a lower serum bicarbonate and accelerated eGFR decline [409-414]. Potential mechanisms include increased synthesis of angiotensin II, aldosterone, and endothelin-1, that are produced to facilitate acid excretion, but also promote inflammation and fibrosis [415]. Of note, the association between serum bicarbonate and accelerated eGFR decline was not found in patients with diabetic kidney disease, suggesting differences between kidney disease etiologies [416]. Several clinical trials found that bicarbonate supplementation reduces or stabilizes eGFR decline [417, 418], although this has not been a universal finding [419].

Autosomal dominant polycystic kidney disease (ADPKD) is the most common inherited kidney disease and represents approximately 3% of the CKD etiology [420]. Torres *et al.* showed that patients with ADPKD and normal GFR excrete less ammonium than healthy controls after an acid load [51]. This reduction in urinary ammonium excretion was not explained by lower production of ammonia or impaired proton secretion. Instead, they attributed the lower urinary ammonium excretion to structural changes associated with ADPKD [51]. In a rat model of PKD, acid loading with ammonium chloride caused acidosis, ammoniagenesis, GFR loss, and increased kidney weight, cystic dilatation, and interstitial inflammation [52]. Another study showed that in these rats potassium citrate completely prevented the decline in GFR and reduced cyst size and interstitial damage [53]. Although these preclinical data suggest that acidosis also promotes disease progression in ADPKD, clinical data are lacking.

Therefore, here, our hypothesis was that serum bicarbonate is associated with kidney outcomes in patients with ADPKD. To address this hypothesis, we used data from the DIPAK intervention trial to analyze whether a lower serum bicarbonate at baseline predicts eGFR decline, and an increase in total kidney or liver volume [381]. We show that serum bicarbonate predicts kidney outcomes independent of established ADPKD prognostic factors and independent of urinary ammonium excretion.

7.3 Materials and Methods

Setting and subjects

We included subjects from the DIPAK intervention trial, an open-label randomized clinical trial to examine the effect of lanreotide on disease progression in later-stage ADPKD (*n* = 309) [381]. The study protocol and outcomes of the DIPAK intervention trial have been published previously [381, 421]. Briefly, patients with ADPKD between 18 and 60 years and with an eGFR 30-60 ml/min per 1.73 m2 were randomized to standard care or lanreotide in a 1:1 ratio. They were followed up every 12 weeks for 2.5 years. Main exclusion criteria were bradycardia, a history of gall stones or pancreatitis, and diseases or medication that could confound outcome assessment (such as diabetes mellitus, and use of non-steroidal anti-inflammatory drugs, lithium or tolvaptan). The DIPAK intervention trial was performed in adherence to the Declaration of Helsinki and all patients provided written informed consent.

Measurements

At each visit blood pressure and body weight were measured, and blood and 24-hour urine were stored for analysis. At baseline, end of treatment, and end of study (12 weeks after end of treatment), an MRI scan without contrast was performed to obtain total kidney volume (TKV) and total liver volume (TLV). TKV and TLV were measured on T2-weighted coronal images by manual tracing, and adjusted for height. GFR was estimated using the CKD-EPI equation [422]. eGFR slope was determined using 14 eGFR values per patient. Serum bicarbonate was measured at baseline as a pre-specified measurement of the DIPAK trial [421]. Serum bicarbonate was measured by the clinical laboratories of the separate treatment study sites by means of a phosphoenolpyruvate reaction. The serum bicarbonate levels were measured using Cobas 8000 (Roche) at the Erasmus Medical Center in Rotterdam and Leiden University Medical Center, ABL720 (Radiometer) at the University Medical Center Groningen, or RAPIDPoint 500 (Siemens) at the Radboudumc in Nijmegen. Baseline urinary ammonium excretion was measured using the phenol-hypochlorite reaction in 24-hour urine. Daily dietary protein intake (g per day) was calculated using the equation: 6.25 x (urine urea nitrogen in g/day + weight in kg) x 0.031 [423]. Net endogenous acid production was estimated by -10.2 + (54.5 x protein intake in g/day) / urine potassium in mEq/day [424].

Outcomes

The primary outcome of this study was worsening kidney function, which was pre-defined in the original DIPAK trial as 30% decrease in baseline eGFR or the development of kidney failure, defined as eGFR < 15 ml/min per 1.73 m^2 [421, 425-427]. Secondary outcomes were annualized eGFR slope (mL/min per 1.73 m^2 per year), change in height-adjusted TKV (htTKV), change in height-adjusted TLV (htTLV), and change in htTLV in patients with polycystic liver disease, defined previously for this patient study as liver size > 2,000 mL [421]. For our analysis we used the htTKV and htTLV values obtained at the end of study.

Statistical analysis

Serum bicarbonate was studied both in tertiles and as continuous variable. Multivariable linear regression was used to analyze which baseline variables were associated with serum bicarbonate. We used Cox regression to determine the effect of serum bicarbonate on the primary outcome. Censoring was applied at end of study (after 132 weeks) or in case of loss to follow-up. The unadjusted effect of serum bicarbonate was assessed, before correcting for fifteen covariates in three additive models. Model 1 was adjusted for age, sex, eGFR, htTKV, treatment group and study site, because these are the main factors associated with ADPKD progression [40]. Model 2 was additionally adjusted for onset of hypertension before age 35, onset of urological events before age 35, and *PKD* mutation (*PKD1* truncating, *PKD1* non-truncating, or *PKD2*), because those have previously also been defined as prognostic predictors of ADPKD [41]. In model 3 we included urinary excretion of ammonium, serum potassium, renin-angiotensin inhibitor use, diuretic use, estimated dietary protein intake, and body mass index, all variables we considered relevant for acid-base homeostasis [428, 429]. We also analyzed serum bicarbonate in regression models in which only Mayo image class, PROPKD score, CKD stage, or study site was added. Serum bicarbonate (tertiles) met the assumptions of the Cox proportional hazard model based on the partial residuals. We used linear regression to evaluate the association between serum bicarbonate and the secondary outcomes. Homoscedasticity of the multivariable analysis was checked by a fitted vs. residual plot, and normality using a Q-Q-plot. The statistical analyses were performed using SPSS (IBM, version 25.0.0.1). A *P* value < 0.05 was considered statistically significant.

7.4 Results

Baseline characteristics

Of the 309 DIPAK participants that were randomized, serum bicarbonate was available in 296 patients. The average serum bicarbonate was 26.1 ± 2.8 mmol/L (Table 7.1). Patients in the highest tertile of serum bicarbonate had lower body mass index, lower serum potassium, and lower urine ammonium excretion (Table 7.1). Most patients were of primarily European descent; 5 patients were of Asian descent and ethnicity was not reported in 5 patients. The distributions for Mayo image class, PROPKD scores, CKD stage, and study sites are shown in Table 7.S1. No patients used alkali supplementation at baseline, while four patients used it during follow-up (three in the lowest tertile, one in the highest tertile). Serum bicarbonate showed a positive association with diuretic use and eGFR, and a negative association with male sex, body mass index, study sites 2 and 3, serum potassium, and Mayo image class (Table 7.2).

TABLE 7.1

Baseline characteristics according to serum bicarbonate tertiles

VARIABLE	TOTAL (*n*)=296	TERTILE 1 (*n* = 99)	TERTILE 2 (*n* = 99)	TERTILE 3 (*n* =98)	P-VALUE
General characteristics					
Age, years	48 ± 7	48 ± 7	48 ± 7	49 ± 8	0.3
Men, n (%)	137 (46)	45 (45)	47 (47)	45 (46)	0.9
Body mass index, kg/m2	27 ± 5	28 ± 6	27 ± 4	26 ± 4	0.002
Systolic blood pressure, mm Hg	133 ± 13	132 ± 13	134 ± 14	134 ± 13	0.4
RAS blocking agents, n (%)	223 (75)	74 (75)	74 (75)	75 (77)	0.8
Diuretics, n (%)	103 (35)	29 (29)	35 (35)	39 (40)	0.1
Laboratory values					
eGFR, ml/min per 1.73 m2	50 ± 11	49 ± 11	49 ± 12	52 ± 11	0.07
Creatinine clearance, ml/min	73 ± 27	71 ± 25	71 ± 25	78 ± 30	0.2
Serum bicarbonate, mmol/L	26.1 ± 2.8	23.1 ± 1.6	26.2 ± 0.8	29.0 ± 1.3	-
Serum potassium, mmol/L	4.2 ± 0.4	4.4 ± 0.4	4.2 ± 0.4	4.1 ± 0.5	< 0.001
Urine sodium, mmol/day	161 ± 65	168 ± 65	160 ± 66	156 ± 65	0.4
Urine ammonium, mmol/kg/day	0.21 ± 0.09	0.20 ± 0.09	0.20 ± 0.08	0.22 ± 0.09	0.03
Dietary protein, g/d	87 ± 25	90 ± 26	86 ± 26	84 ± 23	0.1
ADPKD characteristics					
Height-adjusted total kidney volume, ml/m	1083 (728-1679)	1209 (864-1797)	1037 (677-1688)	987 (668-1554)	0.07
Height-adjusted total liver volume, ml/m	1188 (998-1526)	1210 (1007-1512)	1127 (970-1507)	1210 (1041-1660)	0.7
TLV > 2,000 mL, n (%)	170 (57)	56 (57)	54 (55)	60 (61)	0.5
Truncating *PKD1*, n (%)	133 (45)	48 (48)	44 (44)	41 (42)	0.3
Nontruncating *PKD1*, n (%)	69 (23)	18 (18)	25 (25)	26 (27)	0.2
Other mutation, n (%)	94 (32)	33 (33)	30 (30)	31 (32)	0.8
Hypertension < 35 yrs, n (%)	116 (39)	41 (41)	41 (41)	34 (35)	0.3
Urologic events < 35 yrs, n (%)	68 (23)	16 (16)	25 (25)	27 (28)	0.06

Abbreviations: **ADPKD**, autosomal dominant polycystic kidney disease; **eGFR**, estimated glomerular filtration rate; **RAS**, renin-angiotensin system; **TLV**, total liver volume; yrs, years.

TABLE 7.2

Variables independently associated with serum bicarbonate

VARIABLE*	B (95% CI)	ST. β	P VALUE
Male sex	-0.72 (-1.33;-0.09)	-0.13	0.02
Body mass index, kg/m2	-0.08 (-0.14;-0.02)	-0.13	0.02
Diuretic use	0.89 (0.24;1.54)	0.15	0.01
Study site 2	-2.34 (-3.09;-1.59)	-0.36	< 0.0001
Study site 3	-0.67 (-1.36;0.20)	-0.11	0.06
eGFR, ml/min per 1.73 m2	0.03 (0.02;0.06)	0.11	0.04
Serum potassium, mmol/L	-1.07 (-1.83;-0.31)	-0.17	0.01
Mayo image class	-0.55 (-0.91;-0.19)	-0.17	0.003

Footnote: * Covariates related to acid-base homeostasis or ADPKD progression were included in the model, including age, sex, body mass index, systolic blood pressure, renin-angiotensin inhibitor use, diuretic use, study site, eGFR, creatinine clearance, serum potassium, 24-hour urinary sodium excretion, 24-hour urinary ammonium excretion, NEAP, dietary protein intake, Mayo image class and PROPKD score.

Lower serum bicarbonate increases the risk of worsening kidney function

Patients with lower serum bicarbonate had a greater risk of worsening kidney function (Figure 7.1, log-rank *P* = 0.004). When compared to the third serum bicarbonate tertile, patients in the first tertile had a significantly greater risk of worsening kidney function in the fully adjusted model (hazard ratio 2.95, 95% confidence interval [CI], 1.21 – 7.19, Figure 7.2). The same trend was observed for patients in the second tertile, although this was not statistically significant. In the continuous analysis, each mmol/L decrease in serum bicarbonate increased the risk of worsening kidney function by 21% in the fully adjusted model (hazard ratio 1.21, 95% CI 1.06 to 1.37, Figure 7.2). The covariates Mayo image class, PROPKD, CKD stage, and study site, were also added individually in a model with serum bicarbonate (Table 7.S2). In these analyses serum bicarbonate was also independently associated with the primary outcome. We also analyzed if NEAP or dietary protein intake (as measures of dietary acid load), and urinary ammonium (as measure of kidney acidifying capacity) were associated with the primary or secondary outcomes, which was not the case (data now shown).

FIGURE 7.1 **Survival analysis for worsening kidney function by baseline serum bicarbonate tertiles**

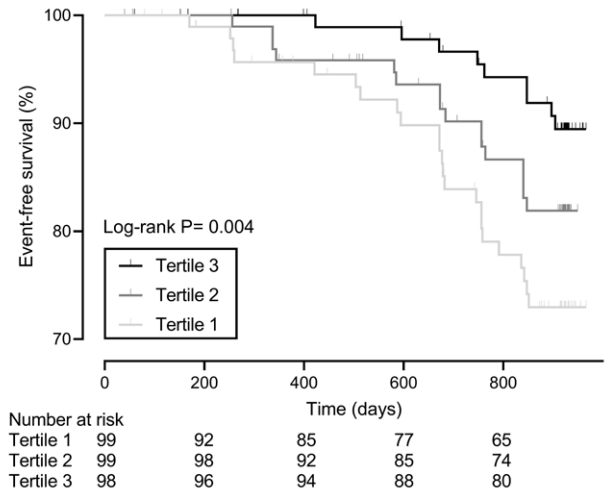

Worsening kidney function (primary outcome) was defined as >30% eGFR loss or kidney failure. Censoring was applied at end of study (after 132 weeks) or in case of loss to follow-up.

Serum bicarbonate independently predicts changes in eGFR but not TKV and TLV

A lower serum bicarbonate was associated with greater annual eGFR decline (*P* for trend < 0.001, Figure 7.3A). Each mmol/L decrease in serum bicarbonate increased the annual decline in eGFR by 0.12 mL/min per 1.73m2 per year (95% CI -0.20 to -0.03) in the fully adjusted model (Table 7.3). A lower serum bicarbonate was not associated with a change in htTKV (0.1 percentage point, 95% CI -0.2 to 0.4, Figure 7.3B, Table 7.3). Serum bicarbonate was also not associated with TLV growth in all participants (-0.02 percentage point, 95% CI -0.40 to 0.37) or in the subset of participants with polycystic liver disease (-0.06 percentage point, 95% CI -0.61 to 0.50).

FIGURE 7.2 **Graphical display of hazard ratios with 95% confidence intervals for serum bicarbonate tertiles and serum bicarbonate**

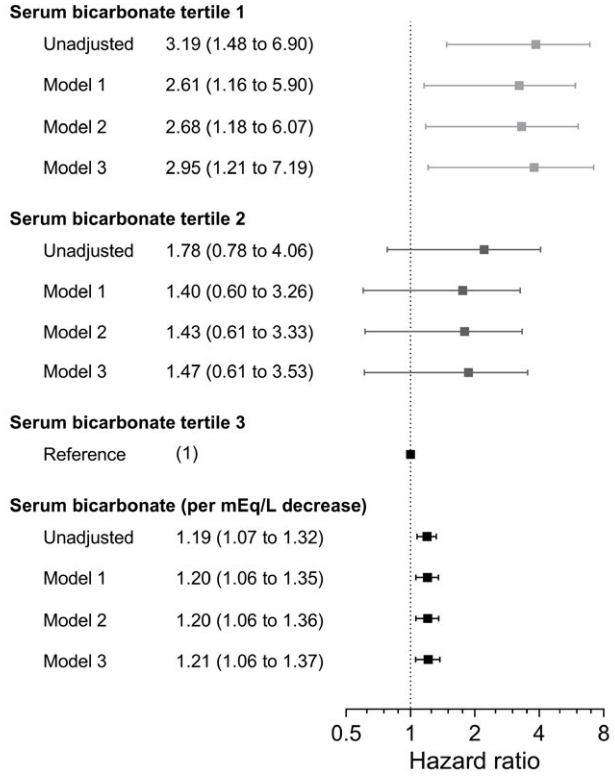

FIGURE 7.3 **eGFR slope A and change in total kidney volume (TKV, B) by serum bicarbonate tertile.**

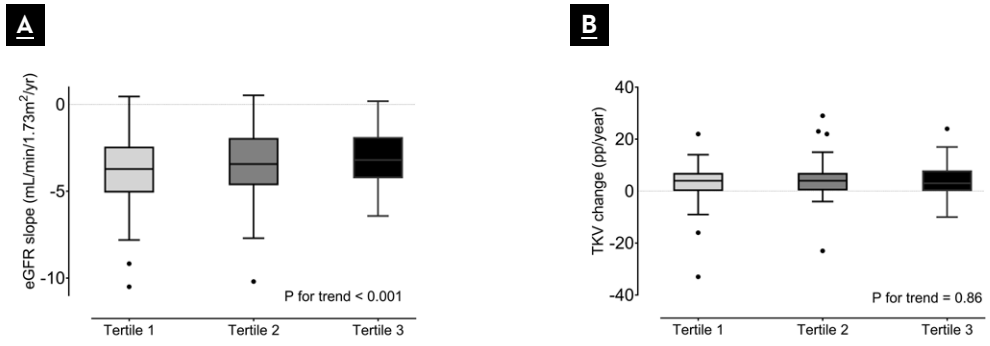

TABLE 7.3

Linear regression analysis for associations between serum bicarbonate and secondary outcomes

OUTCOMES	UNADJUSTED			MODEL 1*			MODEL 2			MODEL 3		
	β (95% CI)	P-value	R2	β (95% CI)	P-value	R2	β (95% CI)	P-value	R2	β (95% CI)	P-value	R2
eGFR, ml/min/ 1.73m2/year	-0.15 (-0.23;-0.07)	<0.001	0.05	-0.13 (-0.22;-0.05)	0.001	0.18	-0.13 (-0.21;-0.05)	0.003	0.20	-0.12 (-0.20;-0.03)	0.008	0.20
htTKV, pp/year	0.1 (-0.2; 0.4)	0.5	0.00	0.1 (-0.2; 0.4)	0.5	0.17	0.1 (-0.2; 0.4)	0.4	0.20	0.1 (-0.2; 0.4)	0.5	0.23
htTLV, pp/year	-0.1 (-0.4; 0.1)	0.3	0.00	-0.1 (-0.4; 0.2)	0.4	0.05	-0.1 (-0.4; 0.2)	0.5	0.06	-0.1 (-0.5; 0.2)	0.3	0.07
htTLV in PLD, pp/year	-0.2 (-0.4; 0.2)	0.4	0.01	-0.2 (-0.7; 0.3)	0.5	0.06	-0.2 (-0.7; 0.3)	0.5	0.08	-0.2 (-0.8; 0.3)	0.4	0.10

Footnote: * Model 1: Age, sex, baseline eGFR, baseline htTKV, treatment group (lanreotide or not), study site; Model 2: Model 1 and hypertension before age 35, urologic events before age 35, *PKD* mutation; Model 3: Model 2 and urinary ammonium excretion, baseline serum potassium, renin-angiotensin inhibitor use, diuretic use, dietary protein, body mass index.

Abbreviations: **eGFR**, estimated glomerular filtration rate; **htTKV**, height adjusted total kidney volume; **htTLV**, height adjusted total liver volume; **PLD**, polycystic liver disease; percentage point.

7.5 Discussion

In this study we show that in patients with ADPKD and eGFR 30-60 ml/min per 1.73 m2 serum bicarbonate is independently associated with kidney outcomes. A lower serum bicarbonate was associated with a greater risk of 30% eGFR decline or kidney failure (the composite primary outcome) and a more rapid annual eGFR-decline (secondary outcome). A lower serum bicarbonate was not associated with a greater increase in height-adjusted total kidney or liver volume. Of interest, the association between serum bicarbonate and kidney outcomes was independent of variables that are included in two established prognostic models for ADPKD, the Mayo image class and PROPKD score [40, 41]. Furthermore, the association was also independent of urinary ammonium excretion, a measure of urinary acidification capacity. Our data suggest that serum bicarbonate adds to the current prognostic models for ADPKD, and may be considered as a treatment target.

Several studies in patients with CKD have shown that serum bicarbonate is associated both with kidney outcomes and mortality [409-414]. Furthermore, there is low-to-moderate certainty evidence that alkali supplementation slows the rate of kidney function decline in patients with CKD.[49] Of interest, several of these cohorts or trials also included patients with ADPKD, although they likely represented a minority and were not analyzed separately. Compared to CKD, the effect size of the association between serum bicarbonate and kidney outcomes appears to be similar or even greater for ADPKD [409-414]. However, two differences in acid-base balance between ADPKD and CKD merit emphasis. First, dietary acid load or urinary ammonium did not predict kidney outcomes in our ADPKD cohort. This was unexpected because previous studies in CKD cohorts identified dietary acid load and urinary ammonium excretion as risk factor for kidney outcomes independent of serum bicarbonate [428-430]. This suggests that in CKD ammonium handling is affected differently than in ADPKD, as has been suggested previously [51]. Second, the average serum bicarbonate concentration was higher in our ADPKD cohort than in previous CKD cohorts with similar eGFR range [413, 429]. In fact, only 7.4% of the patients in our cohort had a serum bicarbonate < 22 mmol/L that would classify as metabolic acidosis [407]. Although serum bicarbonate was correlated with diuretic use, fewer participants used di-

uretics in our cohort than in the CKD cohorts (35 vs. >50%). This suggests that the target value for serum bicarbonate may depend on the underlying kidney disease. A possible explanation for higher serum bicarbonate in patients with ADPKD may be that the urinary concentrating defect causes slight volume depletion with angiotensin II-mediated bicarbonate reabsorption [431]. Of interest, a tubular form of metabolic alkalosis was recently reported in the so-called Oak Ridge polycystic kidney mouse, which exhibits increased sodium-hydrogen exchanger activity in the cortical collecting duct [432]. Therefore, an alternative explanation may be that the higher serum bicarbonate in ADPKD is caused by a change in tubular acid-base handling. It is not clear if a serum bicarbonate in the high-normal range can also cause complications. Some studies identified U- or J-shaped associations between serum bicarbonate and mortality[410, 412], although this finding is not consistent [411, 413, 414]. In the Chronic Renal Insufficiency Cohort a higher serum bicarbonate was associated with heart failure, but this study excluded patients with ADPKD [413].

Although our study cannot prove causality between a lower serum bicarbonate and faster kidney function decline, experimental models of both CKD and ADPKD do support a direct link between acid retention and kidney injury [52, 433]. Three of the explanations why metabolic acidosis can cause kidney damage in CKD may also be relevant for ADPKD. First, the renin-angiotensin system in the kidney has been implicated in acidosis-induced kidney injury and also in the progression of ADPKD [415, 434, 435]. Recently we showed that patients with ADPKD have a five- to six-fold higher urinary excretion of renin and angiotensinogen compared with matched CKD patients [436]. Second, increased ammoniagenesis by dietary acid loads may activate the complement system and promote kidney fibrosis [50]. The complement system has also been implicated in the progression of PKD [52, 437]. In a recent proteomic analysis, we detected more complement in urinary extracellular vesicles of patients with ADPKD than with CKD [335]. Third, metabolic acidosis causes hypocitraturia which may promote crystal deposition in the kidney, which in turn may promote the progression of ADPKD [438, 439]. Hypocitraturia is common in ADPKD, and calculi can be found in up to 25% of patients with ADPKD [440]. Challenging PKD rat models with calcium oxalate or phosphate deposition increased cystogenesis and disease progression through an mTOR-dependent pathway [438]. A higher serum bicarbonate could also reflect higher dietary intake of citrate, which will reduce crystal deposition, and was linked to slower disease progression [53, 438].

To our knowledge, this is the first study to specifically analyze the association between serum bicarbonate and kidney outcomes in patients with ADPKD. A strength of this study is that the data are based on a randomized clinical trial, with standardized procedures and prospectively defined outcomes. In the DIPAK trial lanreotide reduced the rate of growth in total kidney volume [381] and therefore treatment allocation was included in our models. Furthermore, we were able to correct for multiple confounders, including established risk factors for progression of ADPKD, urinary ammonium excretion (measured specifically for this study), and use of renin-angiotensin inhibitors and diuretics. However, a number of limitations should be mentioned. First, follow-up time was too short to analyze kidney failure or mortality, outcomes that have previously been associated with serum bicarbonate [409-414]. Second, different analyzers were used to measure serum bicarbonate, although interchangeability has previously been established [441]. The average serum bicarbonate was significantly lower in one study site despite the use of the same analyzer as in one of the other sites. However, stratification nor correction for study site changed the results.

In conclusion, in patients with ADPKD, a lower serum bicarbonate within the normal range predicts worse kidney outcomes independent of established prognostic factors for ADPKD and independent of urine ammonium excretion. Serum bicarbonate may add to prognostic models and should be explored as a treatment target in ADPKD.

Supplemental tables

TABLE 7.S1

Distribution of patients per study site, CKD stage, Mayo image class, and PROPKD score

VARIABLE	TOTAL (N=296)	TERTILE 1 (N = 99)	TERTILE 2 (N = 99)	TERTILE 3 (N = 98)	P-VALUE
Study site					
Site 1, n (%)	67 (23)	20 (20)	21 (21)	26 (27)	0.02
Site 2, n (%)	73 (25)	42 (42)	21 (21)	10 (10)	< 0.001
Site 3, n (%)	83 (28)	19 (19)	39 (39)	25 (26)	0.27
Site 4, n (%)	73 (25)	18 (18)	18 (18)	37 (38)	0.001
CKD stage					
G2, n (%)	57 (19)	16 (16)	20 (20)	21 (21)	0.3
G3A, n (%)	129 (44)	42 (42)	38 (38)	49 (50)	0.3
G3B, n (%)	104 (35)	39 (39)	38 (38)	27 (28)	0.08
G4, n (%)	6 (2)	2 (2)	3 (3)	1 (1)	0.6
Mayo image class					
Class 1B, n (%)	35 (12)	7 (7)	11 (11)	17 (17)	0.03
Class 1C, n (%)	119 (40)	37 (37)	42 (42)	40 (41)	0.7
Class 1D, n (%)	108 (36)	41 (41)	36 (36)	31 (32)	0.1
Class 1E, n (%)	34 (11)	14 (14)	10 (10)	10 (10)	0.4
PROPKD score					
Score 0-3 (low risk)	117 (40)	42 (42)	35 (35)	40 (41)	0.8
Score 4-6 (intermediate risk)	137 (46)	43 (43)	47 (47)	47 (48)	0.5
Score 7-9 (high risk)	42 (14)	14 (14)	17 (17)	11 (11)	0.6

TABLE 7.S2

Two-variable Cox regression analyses for the association between serum bicarbonate and the primary outcome

VARIABLE ADDED TO MODEL	β (95% CI)	P-VALUE
Mayo image class	1.16 (1.05 – 1.29)	0.004
PROPKD score	1.18 (1.07 – 1.31)	0.001
CKD stage	1.19 (1.06 – 1.33)	0.002
Study site	1.24 (1.11 – 1.39)	0.0002

CHAPTER 8

Summary, Discussion and Future Directions

Summary

The diagnosis of kidney disease is typically established by an increase in serum creatinine level, erythrocyturia, proteinuria and/or kidney abnormalities detected by imaging techniques. Kidney biopsy is currently the only procedure to analyze kidney disease at a histological and molecular level. However, this is an invasive procedure with potential risks, and therefore only performed when kidney tissue is required to make a definitive diagnosis that might affect treatment or provides information about disease progression or prognosis. Therefore, an important challenge is to identify methods to non-invasively analyze kidney disease. Analysis of urine is a logical approach because it is a product of the kidneys and can be analyzed without the need for invasive procedures. Urinary extracellular vesicles (uEVs) are of particular interest because they reflect processes in cells lining the kidney tubules and contain markers for many glomerular and tubular diseases. The studies presented in this thesis aimed to increase clinical applicability of uEVs by improving ways of normalization and reliable high-throughput characterization (part 1), and by exploring their use as biomarkers in a specific kidney disease, namely autosomal dominant polycystic kidney disease (ADPKD, part 2).

Part 1 Urinary Extracellular Vesicles: Steps Towards Clinical Application

uEVs derive from all cells of the urogenital tract while some may enter from the circulation. They contain protein, RNA, lipids, and metabolites, which can be used as biomarkers for kidney, urologic and other diseases. **chapter 2** reports the state-of-the-art of uEV analysis and identifies challenges and knowledge gaps in the field. Recommendations are provided to improve rigor, reproducibility, and interoperability in uEV research, in collection, processing of urine, isolation, characterization, and normalization. Reporting on urine collection, processing and storage should be thorough, because these are major sources of data variability that limit reproducibility. For example, urine could be collected midstream, full void, or (24-hour) timed, all of which have their own advantages and limitations. uEVs may be isolated by ultracentrifugation, precipitation, hydrostatic dialysis, ultrafiltration, size exclusion chromatography, sucrose density gradient, acoustic trapping and immunocapture. Isolation (or enrichment) of uEVs is essential for certain characterization methods such as proteomics and electron microscopy. However, the efficacy and yield of all these methods is limited and varies between techniques and operators. Important challenges include co-isolation of uromodulin and - in case of glomerular disease - albumin and other proteins from the circulation. Of note, direct quantification and characterization of uEVs (using NTA, FCM, TRPS, EVQuant, TR-FIA etc.) has the potential to circumvent the variability of isolation techniques and may be the step towards clinical application. Normalization is particularly important in uEV research because of urine concentration variation, unknown uEV contributions by different parts of the urinogenital tract, and variability induced by isolation. uEV excretion can be reported as a relative excretion rate – a ratio of a uEV biomarker to total uEV, uEV biomarker, total protein, or disease specific protein – or absolute excretion rate, which is determined by timed collection or can be approximated by urine creatinine.

chapter 3 is a comment on a paper by Sabaratnam *et al.* reporting to have found no correlation between the level of tubular transport proteins in the kidney – in all cases removed because of a kidney tumor - vs uEVs collected before the extirpation. We propose that the absence of correlation is caused by the time between uEV and kidney tissue collection, which may have changed protein expression. Therefore, the analysis of proteins in uEVs may be more fruitful during kidney disease because this will likely overrule normal regulation and cause a more generalized and prolonged change in protein or RNA abundance. In addition, we state that normalization is crucial for the correct interpretation of uEV content and is related not only to proper use of urine creatinine as normalization tool but may also involve kidney size.

In **chapter 4** we aimed to validate the use of urine creatinine for normalization of uEVs. To do so we quantified uEVs directly in whole urine – rather than as isolated uEVs – using NTA, EVQuant, and TR-FIA. To address the hypothesis that urine creatinine can be used for normalization, we quantified urine particles in dilute and concentrated urines during a water deprivation and water loading study in eleven healthy participants. We validated the results in random urine collections from fifteen healthy subjects and twenty-six patients with ADPKD. In these various settings, urine creatinine was highly correlated with uEV counts, suggesting that it can be used as a normalization variable. When comparing the techniques, uEV quantification by EVQuant and NTA resulted in highly comparable uEV counts, but NTA detected less particles and skewed the results in dilute urine samples. We propose that this is due to a lower size limit of detection at 70 nm of NTA, while most uEVs were smaller, as determined by EM. Furthermore, by using EM and NTA we show that uEV size increases in dilute urines, which further explains skewing in comparison to EVQuant. Importantly, we confirm findings from earlier studies that NTA results are confounded by uromodulin. CD9-TR-FIA was found to have more variation than NTA and EVQuant. Moreover, the capture proteins CD9 and CD63 used for TRFIA are not expressed in all parts of the urinary tract but are limited to the distal part of the nephron, the urothelium and prostate. This demonstrates that capture assays such as TR-FIA cannot be simply applied to all markers of all origins. Finally, we demonstrate that the use of the detergent SDS allows for the detection of intracellular epitopes, because it permeabilizes uEVs but leaves them intact (confirmed by EM and NTA). This finding extends the use of NTA and EVQuant to protein analysis with the use of intracellular epitope antibodies. Comparison of antibodies against the intracellular epitope versus antibodies against the extracellular epitope of AQP2 demonstrates that a minority of AQP2 protein has a reversed topology. This result is an *ex vivo* confirmation of the possibility of inside out morphology of EVs which was had so far only been demonstrated *in vitro*.

chapter 5 describes the relationship between nephron mass and uEV excretion in one human study and two animal studies. We collected spot and 24-hour urine from nineteen kidney donors before and after donor nephrectomy. We determined kidney size by CT-scans before nephrectomy, and kidney function using 24-hour creatinine clearance and eGFR before and after nephrectomy. First, we confirmed the results in **chapter 4** that urine creatinine and uEV concentration are highly correlated, and that comparison of uEV excretion between individuals is enhanced by correcting for urinary creatinine excretion (or muscle mass if no timed collection is available). We used this correction to demonstrate that men excrete more uEVs than women, which was confirmed in 24-hour urine collections. This contradicts a previous study which concluded that women excrete more uEVs. However, the authors of this publication reported women to have higher uEV to creatinine ratio but failed to correct for a lower muscle mass and therefore creatinine excretion in women. Second, we found that kidney size, kidney function and uEV excretion are highly correlated. Indeed, donor nephrectomy decreased uEV excretion, especially of CD9+ uEVs. Importantly, glomerular, and proximal tubule uEVs were more abundant than uEVs derived from the distal nephron, implying compensatory growth of the proximal tubule after donor nephrectomy. In addition, we studied the relative contribution of "post-kidney uEV secretion" (in other words uEVs secreted by ureter, bladder, and prostate) in 9 patients with a one-sided nephrostomy drain. To do so, we compared the urine of the nephrostomy drain with the bladder urine in each patient individually. The samples were analyzed using labelled mass spectrometry, which demonstrated that the post-kidney structures added only a handful unique proteins, and did not increase protein abundance, showing that the uEV secretion of post-kidney structures is limited compared to kidney secretion. The effect of nephron loss was further studied in a rodent model of uninephrectomy and 5/6th nephrectomy. In this set-up 8 rats underwent uninephrectomy, 8 rats underwent 5/6th nephrectomy, and 10 rats were sham operated. The control animals demonstrated an increase in uEV excretion measured by NTA, while uninephrectomy and 5/6th nephrectomy led to significant decrease of uEV excretion. This decrease was less than expected based on the number of nephrons removed but correlated to the (imputed) hypertrophy of the remaining kidney.

Part 2 – Urinary Extracellular Vesicles and Other Markers of Polycystic Kidney Disease

In **chapter 6** we used a quantitative proteomics approach to identify early markers for ADPKD progression. We used urine samples from control patients of the DIPAK intervention trial (**appendix**), selecting those patients with rapid disease progression (RDP) and slow disease progression (SDP). We matched these based on age, sex, eGFR and PKD mutation, and found that they had similar prognosis based on Mayo class and PROPKD scores. In the discovery cohort (n = 10) we found 65 proteins, and in the verification cohort we found 36 proteins that were significantly and differentially expressed between RDP and SDP patients. Two proteins were recovered in both cohorts: matrilysin (MMP7) abundance was higher in RDP and CHMP4A abundance was higher in SDP. We analyzed these proteins by Western Blotting in a validation cohort (n = 24), in which MMP7 demonstrated the same direction as in the discovery/verification cohorts with high sensitivity and specificity. Importantly, MMP7 remained higher throughout the follow-up period of the intervention trial. MMP7 was previously found to be upregulated in kidney tissue of ADPKD patients and other kidney pathologies, and is part of the canonic Wnt signaling pathway, which is related to ADPKD disease progression, where MMP7 may have a renoprotective effect. In addition, MMP7 is related to acute and chronic kidney injury, implying it may function as promising early progression marker not only in ADPKD but also in other kidney diseases.

In **chapter 7** we analyzed the association between serum bicarbonate and ADPKD progression. Deteriorating kidney function leads to impaired acid excretion and to metabolic acidosis. Treatment of metabolic acidosis improves kidney outcomes in patients with (non-ADPKD) chronic kidney disease. In ADPKD, acid excretion is already impaired in patients with preserved kidney function, while treatment with alkali halts disease progression in animal models. In our study we analyzed serum bicarbonate levels in 309 patients included the DIPAK1 cohort (**appendix**), and studied whether it was related to ADPKD outcomes, including worsening kidney function – a composite of incidence of 30% decrease in eGFR and kidney failure (primary outcome), TKV growth and eGFR decline (secondary outcomes). We demonstrate that a high-normal level of serum bicarbonate was associated with a lower risk of worsening kidney function, compared to low-normal serum bicarbonate. In addition, serum bicarbonate was inversely correlated to eGFR decline. This was independent of sex, age, and other variables that are known to be related to ADPKD progression. However, serum bicarbonate was not related to TKV or TLV growth. This study therefore suggests that bicarbonate supplementation may also be beneficial for patients with ADPKD, although intervention studies are required to confirm this. Of note, patients with ADPKD in our cohort had a relatively high serum bicarbonate, suggesting that the target value for serum bicarbonate may be higher in ADPKD than in other causes of chronic kidney disease.

The **appendix** describes an open label randomized clinical trial that included 309 patients with ADPKD to compare Lanreotide (n = 153) to standard care (n = 152). The primary outcome was the annual change in eGFR assessed as eGFR slope during the 2.5-year treatment phase. Secondary outcomes included change in eGFR before vs. after treatment, incidence of worsening kidney function (start of dialysis or 30% decrease in eGFR), change in total kidney volume and change in quality of life. Among patients with later-stage ADPKD, treatment with Lanreotide compared with standard care did not slow the decline in kidney function over 2.5 years of follow-up. The patients included in **chapters 6 and 7** were selected from this study.

Discussion and Future Directions

Urinary Extracellular Vesicles: Steps Towards Clinical Application

The analysis of uEVs has the potential to become a new and safe approach to the diagnosis of various kidney diseases. Important challenges in the process towards clinical application include isolation and characterization procedures, and the pressing question how to normalize uEVs in random spot urines (**chapter 2**). Until these challenges are addressed, it will be crucial to meticulously report the methods used for collection, processing, storage, isolation and characterization steps, and normalization (**chapter 2**).

uEV isolation

Many specific questions concerning uEV research have been addressed in this thesis and by others in recent years. These insights have resulted in a recent position paper outlining areas of consensus and knowledge gaps (**chapter 2**). Important aspects of uEV isolation are storage temperature, which is most optimal at -70 °C or lower, and methods to reduce the interference of THP using reducing agents. To date, however, the choice of the isolation method remains dependent on characteristics of the urine samples, available techniques, and the choice of downstream analysis (**chapter 2**). It is crucial to include the technical aspects of each technique in the choice of isolation method. For example, ultracentrifugation (UC) relies on particle density of uEVs. However, with this method most particles are either entrapped by THP polymers or remain in the supernatant (**chapter 2 and 4**), while non-EV particles with similar density are co-isolated [67, 197, 203, 210, 211]. It is recommended to report this contamination for example by quantifying non-EV related proteins [5]. Although methods exist to further purify uEVs, such as density gradient or size exclusion chromatography, these further alter and reduce recovery of uEVs [228] and increase processing time. Alternatives for UC include acoustic trapping, hydrostatic filtration dialysis or ultrafiltration, but these techniques may still lead to a loss of uEVs [134, 201]. Importantly, the subset of uEVs that are either recovered or lost differs between these techniques, because the uEV properties used to isolate them by each technique are variable [153, 228]. Because osmolality varies in kidney tubule segments, affecting vesicle size (**chapter 4**), it is likely that these technical differences affect kidney-derived EV populations. Nonetheless, these isolation methods remain essential for biomarker discovery studies such as described in **chapter 6**, emphasizing the need to further study the impact of the isolation method (**chapter 2**).

Key to increase the reliability of studies using isolation methods is to identify a set of proteins or RNAs that can be used to directly assess both yield and contamination. This is the most appropriate approach because these proteins or RNAs will undergo the same isolation and

analysis steps as the biomarkers of interest. Steps to accomplish this are currently made by the normalization work group of the urine task force of the International Society of Extracellular Vesicles (ISEV). With this group, we plan to combine efforts to create a uniform biobank containing uEV samples from patients that suffer from the most common kidney or urologic conditions, including kidney transplant recipients, patients with CKD or ADPKD, benign prostate hypertrophy, bladder cancer and prostate cancer. These uEVs will be stored and partly isolated using one well-defined approach. Next, the samples will be analyzed by mass spectrometry and RNA sequencing on several platforms with the aim to identify a set of uEV proteins and RNAs that are indifferently and robustly expressed between individuals and platforms.

Direct uEV quantification

Clinical application of uEVs ultimately requires platforms that entirely bypass the need for isolation. Although few systems are sensitive enough to directly characterize uEVs, several have been developed, including NTA, TRPS, FCM, TR-FIA, EVQuant and RTM (Chapter 2). In **chapter 4** we compared quantification by NTA, EVQuant, and TR-FIA. NTA was chosen because it was one of the first available methods to directly quantify EVs and has been thoroughly studied [22, 205, 256, 257, 442]. However, it also has the most reported disadvantages of all techniques, including the interference by THP (**chapter 4**) and albuminuria [256, 257], as well as other particles in the same size range. In this thesis, we identified two additional limitations of NTA: (1) half to two-thirds of uEVs are undetected because they are smaller than the lower limit of detection of NTA – at approximately 70 nm, and (2) uEV count in dilute urine samples is relatively overestimated by an increase in uEV size (more uEVs exceeding the lower limit of detection of NTA, **chapter 4**). EVQuant and TR-FIA are currently the only high throughput quantification methods without these disadvantages, allowing quantification of hundreds of samples per day (**chapter 2**). We show that EVQuant correlated highly to NTA and detects 2-3 times more uEVs than NTA (**chapter 4**). We argue that this is caused by a lower limit of detection of EVQuant, with established detection of liposomes smaller than 50 nm [27]. EVQuant makes use of a lipid staining, which does not detect protein aggregates, and may therefore be less susceptible to influences of THP and albumin than NTA [27]. However, this requires further validation. The outcome of TR-FIA quantification depends on the selection of the capture protein. We chose the most well-defined exosome marker CD9 [5] for capture and quantification in **chapter 4**. The results using this method are quite comparable to NTA and EVQuant, but they only provide a semi-quantitative output as it does not count single uEVs but CD9 signal. Importantly, we found that the use of CD9 and CD63 as capture antibodies may select uEVs from distal nephron segments, as well as urothelium and prostate, but not uEVs from proximal tubule segments. In our hands this distribution of CD9 was in part dependent on the antibody, but was later confirmed by mRNA expression along the kidney's tubules by Chen *et al.* [443]. The relevance of this finding was shown in **chapter 5**, where we demonstrated that uninephrectomy decreased CD9+ uEVs but not CD9- uEVs. Again, this change was related to shifts of protein abundances in the proximal vs. distal nephron segment. While EVQuant and NTA detect a larger subset of EVs, this includes also apoptotic bodies and potentially viruses or EVs derived from bacteria [7, 114, 115]. CD9-TR-FIA may therefore be a fast alternative to selectively study uEVs enriched for exomes [5], provided they are not from the proximal tubule.

The next step will be to simplify the direct quantification methods, as EVQuant and NTA use highly specific applications (the Opera system and Nanosight, respectively), which are only available in specialized laboratories. Some steps in this direction have been made for NTA-like systems with microfluidic application [246, 247, 250], demonstrating that it is feasible to simplify this technique within the coming years. It may be more challenging for EVQuant to be simplified as the Opera system is a highly advanced system, which makes use of confocal microscopy in combination with spinning disc technology. However, the resolution achieved by confocal microscopy in combination with the speed achieved by the spinning disc is also the strength of this technique.

Direct uEV protein characterization

Of the direct quantification methods that were mentioned previously, NTA, FCM, EVQuant and TRFIA allow for protein labeling. FCM comprises several techniques, including via anti-tetraspanin coated magnetic beads, imaging flow cytometry and nano-flow cytometry (**chapter 2**). None of these methods are high-throughput, but the latter two enable sorting and isolation of EVs, although to do so one needs an extreme dilution of the biomaterial to prevent clustering [232], extending the processing time. Particularly valuable is the possibility of labeling multiple proteins on a single vesicle level (with FCM and EVQuant) because it allows for selecting specific uEVs for analysis of the biomarker of interest. Possibilities include selection of uEVs of one tubule segment or a particular type of EV (e.g., immune- or exosome-related), while other uEVs may be excluded from analysis based on their protein content. This advantage is demonstrated in **chapter 5** where EVQuant was used to distinguish an effect on CD9+ and CD9- uEVs after donor nephrectomy. For clinical application, the first step is to validate known uEV markers on the new high throughput platforms: EVQuant, TRFIA and possibly the new microfluidics options. The high throughput property of EVQuant allows for analysis of large cohorts (1,000+ samples within several days), especially if the technique will be made available for 384-well plates.

Importantly, all the direct uEV protein characterization methods have been validated on intact (u)EVs. For most transport proteins, antibodies against intracellular but not extracellular epitopes are available. Labelling of intracellular epitopes after membrane permeabilization by 0.01% SDS was first demonstrated for TRFIA [245]. In **chapter 4** we show that this treatment leaves uEVs intact, while making the intracellular epitope accessible to antibodies for both NTA and EVQuant. Importantly, we demonstrate that a subset of uEVs has a reversed topology, first described *in vitro* by Cvjetkovic *et al.* [343]. Indeed, several groups have now detected EV proteins on intact EVs using antibodies against the intracellular epitope [22, 323]. Future re-

search should point out what type of uEVs have reversed topology: are these endosomes and possibly a sign of cell decay, or does something change in protein folding which is reflected in some EVs? One way to approach this is to select uEVs by either the AQP2 antibody against the extracellular epitope or the AQP2 antibody against the intracellular epitope. Next, with and without detergent one could study other common membrane proteins with known orientation by labelling them with antibodies. In endosomes, all proteins should have a reversed topology while a change in protein folding of AQP2 would only reverse the direction of AQP2. Overrepresentation of endosomes in the sample selected by the AQP2 antibody against the intracellular epitope could be confirmed by analyzing endosome specific markers such as CD4 or IGF2R. Another important challenge is to use these direct quantification techniques to study uEV proteins that are not membrane bound or RNAs, because using detergent to allow for the detection of these proteins or RNAs also results in loss/drainage of uEV content.

Normalization of uEVs

Current uEV isolation and characterization techniques are used to report uEV concentration. uEV concentration is, however, highly variable because of differences in urinary flow rate, the EV excretion rate of the organ of interest (including circadian rhythm [182]), and variation induced by the isolation or characterization method. Correction for urinary flow rate can be circumvented by using timed urine collection. In practice this has several shortcomings, including the required patient effort and collection errors [271] and possible loss of uEV content [22, 131]. Urinary creatinine is therefore the most practical and simple method to normalize urinary flow rate [275], and has been used frequently in the past years to normalize uEVs [33-35, 245]. In **chapter 4** we demonstrate for the first time that this method of uEV normalization is justified because, just as creatinine excretion rate, uEV excretion rate is constant in healthy individuals. Within individuals, uEV and creatinine concentration have higher correlation than between individuals. In **chapter 5** we propose two reasons for this: first, individuals have differences in muscle mass and therefore creatinine excretion [444-446], leading to underestimation of uEV excretion in men, and an overestimation in patients with low muscle mass [447-450]. Secondly, individuals have differences in uEV excretion rate, which we demonstrate is largely caused by variability in nephron mass. We therefore present a formula that can be applied if creatinine excretion (or muscle mass) is known. Because muscle mass and nephron mass are also correlated [356], this step could potentially be redundant, as is demonstrated by the good inter-individual correlation between creatinine and uEV concentration in **chapter 5**. But before this can be applied, this approach should be evaluated in larger cohorts, including various diseases of kidney and urogenital tract, which will be part of the objectives pursued by the normalization work group of the urine task force of ISEV.

In **chapter 5** we demonstrate that changes in nephron number significantly influence uEV excretion rate. Interestingly, reducing the number of nephrons by half only reduced uEV number by 20%. Initially, we proposed two possible explanations for this: (1) the majority of uEVs is secreted by "post kidney structures" – in other words ureter, bladder and prostate – or (2) there is compensatory growth of the remaining kidney tissue leading to increased uEV secretion per nephron. The first explanation was refuted by comparing the nephrostomy uEV proteome to the bladder uEV proteome in patients with a one-sided nephrostomy drain. This set-up demonstrated that "post-kidney structures" added no new unique proteins to the uEV proteome, nor was an increase of protein abundance observed in bladder compared to nephrostomy derived urine. In addition, the number of uEVs was not increased in the bladder derived samples. Another observation was that the reduction of uEV excretion was similar in men and women, suggesting that the prostate did not secrete relevant amounts of uEVs in this setting. These findings were expected, as the total surface area of nephrons is much higher than that of bladder and prostate. At the same time, we did find evidence of compensatory growth. Firstly, there was an increase per nephron of CD9- uEVs as well as proximal tubular markers on uEVs, while CD9+ uEVs and distal tubular markers did not significantly increase per nephron, suggesting hypertrophy of the proximal tubule segments specifically, which was demonstrated previously in animal models [361-363]. Secondly, we demonstrated hypertrophy of the remaining kidney tissue both after uninephrectomy and after 5/6th nephrectomy. Importantly this hypertrophy was in the same range as the per nephron increase of uEV excretion within these models, further demonstrating that compensatory growth may have led to increased per-nephron uEV secretion. As such, the influence of nephron mass is crucial in the normalization of uEV samples, as we also emphasized in **chapter 3**.

Besides involving muscle mass and nephron mass in the normalization of uEVs, future research should also focus on finding a general kidney-specific marker (**chapter 2**). Indeed, normalization of isolated uEVs should not only correct for the aforementioned variables, but also correct for isolation-induced variability. Therefore, it is more reasonable to use EV markers that are co-isolated in the same process (**chapter 2**). General EV markers such as CD9 and CD63 have been used for this purpose, but in **chapter 4** we demonstrated some important disadvantages of this method, including selective presence of these proteins in the distal nephron, urothelium and prostate, potentially complicating comparisons between men and women, or comparing men of different ages (even though the contribution of these structures to uEV secretion should be limited). Ideally, multiple organ-specific uEV markers are used to normalize uEVs after isolation, allowing for more balanced normalization, of which the benefits were extensively described in **chapter 2**. Taken together, an important focus for future research remains to study the contribution of urine flow, kidney size and variation of isolation techniques to the variation in uEV concentration, enabling a more considered choice of normalization method. This is one of the objectives of the normalization work group of the urine task force of ISEV, with the use of a biobank with urine samples of various origins.

Considering the limitations of each normalization technique, we recommend the use of a disease-specific marker ratio if available, which corrects for all these factors. A specific marker

ratio – preferably of markers both involved in the same biological process or pathways – would also allow for comparison among patients with different kidney functions. Moreover, a ratio is more reliably reproduced by other methods, including isolation techniques, omitting the use of normalization methods. However, this should be validated for each marker ratio. This conclusion again emphasizes the benefits of using direct characterization methods that allow for labeling of multiple proteins per single vesicle.

Urinary Extracellular Vesicles and Other Markers of Polycystic Kidney Disease

uEV markers of ADPKD progression

While ADPKD often leads to kidney failure, not all patients reach this stage [36, 37]. Hence, prediction of progression in patients with ADPKD is important to determine who is eligible for the only treatment option tolvaptan [38, 39], which is expensive and has important side-effects such as polyuria. Known characteristics that predict ADPKD progression are summarized in the Mayo classification (hTKV, with addition of eGFR, age and sex) [40] and PROPKD score (age, sex, PKD mutation, onset of hypertension and first macroscopic hematuria) [41]. Other known kidney injury markers have added little to their predictive value [42, 43]. The analysis of uEVs of ADPKD patients has revealed a whole new set of proteins related to molecular processes in ADPKD [44, 335]. In this regard, we were the first to demonstrate that the uEV protein matrilysin or MMP7 predicts ADPKD progression in three independent patient cohorts (**chapter 6**). Importantly, in these cohorts, we matched patients with rapid disease progression (RDP) with patients with slow disease progression (SDP) based on sex, age, eGFR and PKD mutation. Furthermore, these groups were also found to have similar hTKV, Mayo prediction and PROPKD score. Thus, MMP7 in uEVs is expected to predict disease progression independent of the currently established disease progression tools. Importantly, MMP7 is molecularly associated to ADPKD, primarily because it is upregulated in rodent models of ADPKD [398, 399], as well as in kidney tissue and uEVs of patients with ADPKD [335, 394], and secondly because it is part of the canonic Wnt signaling pathway [400] where it may be renoprotective [393]. Interestingly, MMP7 and other metalloproteases are also linked to generalized acute and chronic kidney injury [390]. As such, we propose that MMP7 should be studied as a predictive marker both in larger ADPKD cohorts – for example in the DIPAK observational cohort which has >600 patients included with a follow up period of 3-6 years – as well as in non-ADPKD CKD cohorts. Theoretically, the most optimal platform for these large numbers is EVQuant, but this should be validated in advance.

As mentioned before, we would ideally have reported a marker ratio of markers that demonstrate an opposite direction. CHMP4A is the only other protein found differentially expressed in both patient cohorts. While MMP7 had higher abundance in patients with RDP, CHMP4A had lower abundance in these patients. However, CHMP4A did not have predictive value in the validation cohort. In addition, MMP7 and CHMP4A reflect distinct biological processes. Therefore, we concluded that CHMP4A was not robust enough to be a marker of ADPKD progression. Alternatively, this may provide another indication that different platforms lead to different outcomes, which is a compelling argument to use a marker ratio. Therefore, we propose that future research into clinical application of MMP7 should include analysis of the MMP7/CHMP4A ratio, ideally at single vesicle level on the EVQuant platform. While we included CD9 as a control marker, normalization to creatinine revealed that also CD9 was significantly upregulated in the patients with RDP. Future research should point out why this is the case; is the contribution of distal tubule segments to the uEV population larger in patients with RDP? Or is CD9 upregulated in more active ADPKD by a yet unknown process? The first question could be studied by comparing proximal and distal tubule markers in ADPKD patients. To answer the second question the expression of CD9 should be studied in an animal model for ADPKD, for example in mice with kidney-specific, tamoxifen-inducible Pkd1 deletion, leading to variable severity of ADPKD, as was described in Salih *et al.* [335].

Acid-base balance in ADPKD

Our finding that serum bicarbonate is associated to kidney outcomes in ADPKD (**chapter 7**) fits with the increased focus on acid-base balance in non-ADPKD CKD. Not only is serum bicarbonate associated with kidney outcomes in CKD [409-414], supplementation of alkali also attenuates CKD progression, provided a high dose of alkali is supplemented [417, 418, 451]. There are two important signals that alkali supplementation in ADPKD may also improve kidney outcomes; firstly, we demonstrated that a lower serum bicarbonate concentration was associated with worse kidney outcomes. Secondly, multiple animal studies demonstrated a beneficial effect of alkali supplementation on cyst progression and kidney outcomes [52, 53]. Therefore, the next step is to study the effect of alkali supplementation in patients with polycystic kidney disease in a randomized controlled trial with kidney outcomes as primary outcome (primarily incidence of worsening kidney function, but also eGFR slope and cyst growth). In addition, the effects could be studied mechanistically in humans, by identifying processes on which alkali may have a positive effect, including activation of intrarenal RAS [434, 436], the complement system, kidney fibrosis [50, 437, 452], and formation of crystal deposition [440, 453].

References

1. Kouba, E., E.M. Wallen, and R.S. Pruthi, *Uroscopy by Hippocrates and Theophilus: prognosis versus diagnosis.* J Urol, 2007. **177**(1): p. 50-2.

2. Rosenhek, J., *Liquid Gold.* Doctor's Rev: Med Move, 2005.

3. Armstrong, J.A., *Urinalysis in Western culture: a brief history.* Kidney Int, 2007. **71**(5): p. 384-7.

4. Karpman, D., A.L. Stahl, and I. Arvidsson, *Extracellular vesicles in renal disease.* Nat Rev Nephrol, 2017. **13**(9): p. 545-562.

5. Thery, C., et al., *Minimal information for studies of extracellular vesicles 2018 (MISEV2018): a position statement of the International Society for Extracellular Vesicles and update of the MISEV2014 guidelines.* J Extracell Vesicles, 2018. **7**(1): p. 1535750.

6. Oosthuyzen, W., et al., *Vasopressin Regulates Extracellular Vesicle Uptake by Kidney Collecting Duct Cells.* J Am Soc Nephrol, 2016.

7. Hiemstra, T.F., et al., *Human urinary exosomes as innate immune effectors.* J Am Soc Nephrol, 2014. **25**(9): p. 2017-27.

8. Pisitkun, T., R.F. Shen, and M.A. Knepper, *Identification and proteomic profiling of exosomes in human urine.* Proc Natl Acad Sci U S A, 2004. **101**(36): p. 13368-73.

9. Salih, M., R. Zietse, and E.J. Hoorn, *Urinary extracellular vesicles and the kidney: biomarkers and beyond.* Am J Physiol Renal Physiol, 2014. **306**(11): p. F1251-9.

10. Dimuccio, V., et al., *Acute and chronic glomerular damage is associated with reduced CD133 expression in urinary extracellular vesicles.* Am J Physiol Renal Physiol, 2020. **318**(2): p. F486-f495.

11. Morikawa, Y., et al., *Elevated Levels of Urinary Extracellular Vesicle Fibroblast-Specific Protein 1 in Patients with Active Crescentic Glomerulonephritis.* Nephron, 2018: p. 1-11.

12. Dominguez, J.H., et al., *Renal Tubular Cell-Derived Extracellular Vesicles Accelerate the Recovery of Established Renal Ischemia Reperfusion Injury.* J Am Soc Nephrol, 2017. **28**(12): p. 3533-3544.

13. Higashijima, Y., et al., *Excretion of urinary exosomal AQP2 in rats is regulated by vasopressin and urinary pH.* Am J Physiol Renal Physiol, 2013. **305**(10): p. F1412-21.

14. Terker, A.S., et al., *Unique chloride-sensing properties of WNK4 permit the distal nephron to modulate potassium homeostasis.* Kidney Int, 2016. **89**(1): p. 127-34.

15. Lim, J.H., et al., *Novel urinary exosomal biomarkers of acute T cell-mediated rejection in kidney transplant recipients: A cross-sectional study.* PLoS One, 2018. **13**(9): p. e0204204.

16. Park, J., et al., *Integrated Kidney Exosome Analysis for the Detection of Kidney Transplant Rejection.* ACS Nano, 2017. **11**(11): p. 11041-11046.

17. Moon, P.G., et al., *Proteomic analysis of urinary exosomes from patients of early IgA nephropathy and thin basement membrane nephropathy.* Proteomics, 2011. **11**(12): p. 2459-75.

18. Feng, Y., et al., *Urinary Exosomes and Exosomal CCL2 mRNA as Biomarkers of Active Histologic Injury in IgA Nephropathy.* Am J Pathol, 2018. **188**(11): p. 2542-2552.

19. Tutakhel, O.A.Z., et al., *NaCl cotransporter abundance in urinary vesicles is increased by calcineurin inhibitors and predicts thiazide sensitivity.* PLoS One, 2017. **12**(4): p. e0176220.

20. Lytvyn, Y., et al., *Assessment of urinary microparticles in normotensive patients with type 1 diabetes.* Diabetologia, 2017. **60**(3): p. 581-584.

21. Musante, L., et al., *Recovery of urinary nanovesicles from ultracentrifugation supernatants.* Nephrology Dialysis Transplantation, 2013. **28**(6): p. 1425-1433.

22. Oosthuyzen, W., et al., *Quantification of human urinary exosomes by nanoparticle tracking analysis.* J Physiol, 2013. **591**(23): p. 5833-42.

23. Coumans, F.A., et al., *Reproducible extracellular vesicle size and concentration determination with tunable resistive pulse sensing.* J Extracell Vesicles, 2014. **3**: p. 25922.

24. Salih, M., et al., *An Immunoassay for Urinary Extracellular Vesicles.* Am J Physiol Renal Physiol, 2016: p. ajprenal 00463 2015.

25. Musante, L., et al., *Rigorous characterization of urinary extracellular vesicles (uEVs) in the low centrifugation pellet - a neglected source for uEVs.* Sci Rep, 2020. **10**(1): p. 3701.

26. Tian, Y., et al., *Quality and efficiency assessment of six extracellular vesicle isolation methods by nano-flow cytometry.* J Extracell Vesicles, 2020. **9**(1): p. 1697028.

27. Hartjes, T.A., et al., *EVQuant; high-throughput quantification and characterization of extracellular vesicle (sub)populations.* bioRxiv, 2020: p. 2020.10.21.348375.

28. Gunasekaran, P.M., J.M. Luther, and J.B. Byrd, *For what factors should we normalize urinary extracellular mRNA biomarkers?* Biomol Detect Quantif, 2019. **17**: p. 100090.

29. Erdbrugger, U., Blijdorp C.J., Llorente A., Martens-Uzunova E.S., Musante L., Burger D., *A survey of current trends in urinary extracellular vesicle research.* European Urology Open Science, 2021. **32**: p. S174.

30. Sands, J.M. and H.E. Layton, *Advances in understanding the urine-concentrating mechanism.* Annu Rev Physiol, 2014. **76**: p. 387-409.

31. Bertram, J.F., et al., *Human nephron number: implications for health and disease.* Pediatr Nephrol, 2011. **26**(9): p. 1529-33.

32. Puelles, V.G., et al., *Glomerular number and size variability and risk for kidney disease.* Curr Opin Nephrol Hypertens, 2011. **20**(1): p. 7-15.

33. Damkjaer, M., et al., *Selective renal vasoconstriction, exaggerated natriuresis and excretion rates of exosomic proteins in essential hypertension.* Acta Physiol (Oxf), 2014. **212**(1): p. 106-18.

34. Esteva-Font, C., et al., *Are sodium transporters in urinary exosomes reliable markers of tubular sodium reabsorption in hypertensive patients?* Nephron Physiol, 2010. **114**(3): p. p25-34.

35. Hinrichs, G.R., et al., *A novel mutation affecting the arginine-137 residue of AVPR2 in dizygous twins leads to nephrogenic diabetes insipidus and attenuated urine exosome aquaporin-2.* Physiol Rep, 2016. **4**(8).

36. Chebib, F.T., et al., *Effect of genotype on the severity and volume progression of polycystic liver disease in autosomal dominant polycystic kidney disease.* Nephrol Dial Transplant, 2016. **31**(6): p. 952-60.

37. Torres, V.E., P.C. Harris, and Y. Pirson, *Autosomal dominant polycystic kidney disease.* Lancet, 2007. **369**(9569): p. 1287-1301.

38. Torres, V.E., et al., *Tolvaptan in patients with autosomal dominant polycystic kidney disease.* N Engl J Med, 2012. **367**(25): p. 2407-18.

39. Torres, V.E., et al., *Tolvaptan in Later-Stage Autosomal Dominant Polycystic Kidney Disease.* N Engl J Med, 2017. **377**(20): p. 1930-1942.

40. Irazabal, M.V., et al., *Imaging classification of autosomal dominant polycystic kidney disease: a simple model for selecting patients for clinical trials.* J Am Soc Nephrol, 2015. **26**(1): p. 160-72.

41. Cornec-Le Gall, E., et al., *The PROPKD Score: A New Algorithm to Predict Renal Survival in Autosomal Dominant Polycystic Kidney Disease.* J Am Soc Nephrol, 2016. **27**(3): p. 942-51.

42. Messchendorp, A.L., et al., *Urinary Biomarkers to Identify Autosomal Dominant Polycystic Kidney Disease Patients With a High Likelihood of Disease Progression.* Kidney Int Rep, 2018. **3**(2): p. 291-301.

43. Messchendorp, A.L., et al., *Rapid Progression of Autosomal Dominant Polycystic Kidney Disease: Urinary Biomarkers as Predictors.* Am J Nephrol, 2019. **50**(5): p. 375-385.

44. Hogan, M.C., et al., *Identification of Biomarkers for PKD1 Using Urinary Exosomes.* J Am Soc Nephrol, 2015. **26**(7): p. 1661-70.

45. Kathem, S.H., A.M. Mohieldin, and S.M. Nauli, *The Roles of Primary cilia in Polycystic Kidney Disease.* AIMS Mol Sci, 2014. **1**(1): p. 27-46.

46. Hogan, M.C., et al., *Characterization of PKD protein-positive exosome-like vesicles.* J Am Soc Nephrol, 2009. **20**(2): p. 278-88.

47. Chacon-Heszele, M.F., et al., *The exocyst and regulatory GTPases in urinary exosomes.* Physiol Rep, 2014. **2**(8).

48. Wang, J. and M.M. Barr, *Ciliary Extracellular Vesicles: Txt Msg Organelles.* Cell Mol Neurobiol, 2016. **36**(3): p. 449-57.

49. Navaneethan, S.D., et al., *Effects of Treatment of Metabolic Acidosis in CKD: A Systematic Review and Meta-Analysis.* Clin J Am Soc Nephrol, 2019. **14**(7): p. 1011-1020.

50. Nath, K.A., M.K. Hostetter, and T.H. Hostetter, *Pathophysiology of chronic tubulo-interstitial disease in rats. Interactions of dietary acid load, ammonia, and complement component C3.* J Clin Invest, 1985. **76**(2): p. 667-75.

51. Torres, V.E., et al., *Renal ammonia in autosomal dominant polycystic kidney disease.* Kidney Int, 1994. **45**(6): p. 1745-53.

52. Torres, V.E., et al., *Renal cystic disease and ammoniagenesis in Han:SPRD rats.* J Am Soc Nephrol, 1994. **5**(5): p. 1193-200.

53. Tanner, G.A., *Potassium citrate/citric acid intake improves renal function in rats with polycystic kidney disease.* J Am Soc Nephrol, 1998. **9**(7): p. 1242-8.

54. Magiorkinis, E. and A. Diamantis, *The fascinating story of urine examination: From uroscopy to the era of microscopy and beyond.* Diagn Cytopathol, 2015. **43**(12): p. 1020-36.

55. Santiago-Rodriguez, T.M., et al., *The human urine virome in association with urinary tract infections.* Front Microbiol, 2015. **6**: p. 14.

56. Harpole, M., J. Davis, and V. Espina, *Current state of the art for enhancing urine biomarker discovery.* Expert Rev Proteomics, 2016. **13**(6): p. 609-26.

57. Decramer, S., et al., *Urine in clinical proteomics.* Mol Cell Proteomics, 2008. **7**(10): p. 1850-62.

58. Parolini, I., et al., *Microenvironmental pH is a key factor for exosome traffic in tumor cells.* J. Biol. Chem, 2009. **284**(49): p. 34211-34222.

59. Nagaraj, N. and M. Mann, *Quantitative analysis of the intra- and inter-individual variability of the normal urinary proteome.* J Proteome Res, 2011. **10**(2): p. 637-45.

60. Guo, Z., et al., *A Proteomic Analysis of Individual and Gender Variations in Normal Human Urine and Cerebrospinal Fluid Using iTRAQ Quantification.* PLoS One, 2015. **10**(7): p. e0133270.

61. Molina, L., et al., *Analysis of the variability of human normal urine by 2D-GE reveals a "public" and a "private" proteome.* J Proteomics, 2011. **75**(1): p. 70-80.

62. Wiggins, R.C., et al., *Procoagulant activity in normal human urine associated with subcellular particles.* Kidney Int, 1986. **29**(2): p. 591-7.

63. Scherberich, J.E., *Immunological and ultrastructural analysis of loss of tubular membrane-bound enzymes in patients with renal damage.* Clin Chim Acta, 1989. **185**(3): p. 271-82.

64. Pascual, M., et al., *Identification of membrane-bound CR1 (CD35) in human urine: evidence for its release by glomerular podocytes.* J Exp Med, 1994. **179**(3): p. 889-99.

65. Gonzales, P.A., et al., *Large-scale proteomics and phosphoproteomics of urinary exosomes.* J Am Soc Nephrol, 2009. **20**(2): p. 363-79.

66. Santucci, L., et al., *From hundreds to thousands: Widening the normal human Urinome (1).* J Proteomics, 2015. **112**: p. 53-62.

67. Merchant, M.L., et al., *Isolation and characterization of urinary extracellular vesicles: implications for biomarker discovery.* Nat Rev Nephrol, 2017. **13**(12): p. 731-749.

68. Erdbrugger, U. and T.H. Le, *Extracellular Vesicles in Renal Diseases: More than Novel Biomarkers?* J Am Soc Nephrol, 2016. **27**(1): p. 12-26.

69. Li, Y., et al., *Proteomic identification of exosomal LRG1: a potential urinary biomarker for detecting NSCLC.* Electrophoresis, 2011. **32**(15): p. 1976-83.

70. Fraser, K.B., et al., *Ser(P)-1292 LRRK2 in urinary exosomes is elevated in idiopathic Parkinson's disease.* Movement Disorders, 2016. **31**(10): p. 1543-1550.

71. Dhondt, B., et al., *Urinary extracellular vesicle biomarkers in urological cancers: From discovery towards clinical implementation.* Int J Biochem Cell Biol, 2018. **99**: p. 236-256.

72. Leiblich, A., *Recent Developments in the Search for Urinary Biomarkers in Bladder Cancer.* Curr Urol Rep, 2017. **18**(12): p. 100.

73. Fujita, K., et al., *Proteomic analysis of urinary extracellular vesicles from high Gleason score prostate cancer.* Sci. Rep. , 2017. **7**: p. 42961.

74. Øverbye, A., et al., *Identification of prostate cancer biomarkers in urinary exosomes.* Oncotarget, 2015. **6**(30): p. 30357-30376.

75. Sequeiros, T., et al., *Targeted proteomics in urinary extracellular vesicles identifies biomarkers for diagnosis and prognosis of prostate cancer.* Oncotarget, 2017. **8**(3): p. 4960-4976.

76. Bijnsdorp, I.V., et al., *Exosomal ITGA3 interferes with non-cancerous prostate cell functions and is increased in urine exosomes of metastatic prostate cancer patients.* J Extracell. Vesicles, 2013. **2**.

77. Skotland, T., et al., *Molecular lipid species in urinary exosomes as potential prostate cancer biomarkers*. Eur. J. Cancer, 2017. **70**: p. 122-132.

78. Rodriguez, M., et al., *Identification of non-invasive miRNAs biomarkers for prostate cancer by deep sequencing analysis of urinary exosomes*. Mol Cancer, 2017. **16**(1): p. 156.

79. Koppers-Lalic, D., et al., *Noninvasive prostate cancer detection by measuring miRNA variants (isomiRs) in urine extracellular vesicles*. Oncotarget, 2016. **7**(16): p. 22566-22578.

80. Nilsson, J., et al., *Prostate cancer-derived urine exosomes: a novel approach to biomarkers for prostate cancer*. Br. J. Cancer, 2009. **100**(10): p. 1603-1607.

81. Mitchell, P.J., et al., *Can urinary exosomes act as treatment response markers in prostate cancer?* J. Transl. Med, 2009. **7**: p. 4.

82. Clos-Garcia, M., et al., *Metabolic alterations in urine extracellular vesicles are associated to prostate cancer pathogenesis and progression*. J Extracell Vesicles, 2018. **7**(1): p. 1470442.

83. Chen, C.L., et al., *Comparative and targeted proteomic analyses of urinary microparticles from bladder cancer and hernia patients*. J Proteome Res, 2012. **11**(12): p. 5611-29.

84. Lee, J., et al., *Altered Proteome of Extracellular Vesicles Derived from Bladder Cancer Patients Urine*. Mol Cells, 2018. **41**(3): p. 179-187.

85. Del Boccio, P., et al., *A hyphenated microLC-Q-TOF-MS platform for exosomal lipidomics investigations: application to RCC urinary exosomes*. Electrophoresis, 2012. **33**(4): p. 689-696.

86. Zhan, Y., et al., *Expression signatures of exosomal long non-coding RNAs in urine serve as novel non-invasive biomarkers for diagnosis and recurrence prediction of bladder cancer*. Molecular Cancer, 2018. **17**.

87. Raimondo, F., et al., *Differential protein profiling of renal cell carcinoma urinary exosomes*. Mol Biosyst, 2013. **9**(6): p. 1220-33.

88. McKiernan, J., et al., *A Novel Urine Exosome Gene Expression Assay to Predict High-grade Prostate Cancer at Initial Biopsy*. JAMA Oncol, 2016. **2**(7): p. 882-889.

89. McKiernan, J., et al., *A Prospective Adaptive Utility Trial to Validate Performance of a Novel Urine Exosome Gene Expression Assay to Predict High-grade Prostate Cancer in Patients with Prostate-specific Antigen 2-10ng/ml at Initial Biopsy*. Eur Urol, 2018.

90. Salih, M., et al., *Proteomics of Urinary Vesicles Links Plakins and Complement to Polycystic Kidney Disease*. J Am Soc Nephrol, 2016. **27**(10): p. 3079-3092.

91. Raimondo, F., et al., *Urinary proteomics for the study of genetic kidney diseases*. Expert Rev Proteomics, 2016. **13**(3): p. 309-24.

92. Bourderioux, M., et al., *A new workflow for proteomic analysis of urinary exosomes and assessment in cystinuria patients*. J Proteome Res, 2015. **14**(1): p. 567-77.

93. Zubiri, I., et al., *Diabetic nephropathy induces changes in the proteome of human urinary exosomes as revealed by label-free comparative analysis*. J Proteomics, 2014. **96**: p. 92-102.

94. Abe, H., et al., *Urinary Exosomal mRNA of WT1 as Diagnostic and Prognostic Biomarker for Diabetic Nephropathy*. Journal of Medical Investigation, 2018. **65**(3-4): p. 208-215.

95. Sonoda, H., et al., *Decreased abundance of urinary exosomal aquaporin-1 in renal ischemia-reperfusion injury*. Am J Physiol Renal Physiol, 2009. **297**(4): p. F1006-16.

96. Chun-Yan, L., et al., *Liquid biopsy biomarkers of renal interstitial fibrosis based on urinary exosome*. Exp Mol Pathol, 2018. **105**(2): p. 223-228.

97. Tangtanatakul, P., et al., *Down-regulation of let-7a and miR-21 in urine exosomes from lupus nephritis patients during disease flare*. Asian Pac J Allergy Immunol, 2018.

98. Stokman, M.F., et al., *Changes in the urinary extracellular vesicle proteome are associated with nephronophthisis-related ciliopathies*. J Proteomics, 2019. **192**: p. 27-36.

99. Raimondo, F., et al., *Urinary Extracellular Vesicles and Salt-Losing Tubulopathies: A Proteomic Approach*. Proteomes, 2020. **8**(2).

100. Williams, T.L., et al., *Making urinary extracellular vesicles a clinically tractable source of biomarkers for inherited tubulopathies using a small volume precipitation method: proof of concept*. J Nephrol, 2020. **33**(2): p. 383-386.

101. Corbetta, S., et al., *Urinary exosomes in the diagnosis of Gitelman and Bartter syndromes*. Nephrol Dial Transplant, 2015. **30**(4): p. 621-30.

102. La Salvia, S., et al., *Extracellular Vesicles in Essential Hypertension: Hidden Messengers*. Curr Hypertens Rep, 2020. **22**(10): p. 76.

103. Salih, M., et al., *Increased Urinary Extracellular Vesicle Sodium Transporters in Cushing Syndrome With Hypertension*. J Clin Endocrinol Metab, 2018. **103**(7): p. 2583-2591.

104. Gonzalez-Calero, L., et al., *Urinary exosomes reveal protein signatures in hypertensive patients with albuminuria*. Oncotarget, 2017. **8**(27): p. 44217-44231.

105. Wolley, M.J., et al., *In Primary Aldosteronism, Mineralocorticoids Influence Exosomal Sodium-Chloride Cotransporter Abundance*. J Am Soc Nephrol, 2017. **28**(1): p. 56-63.

106. Kwon, S.H., et al., *Elevated urinary podocyte-derived extracellular microvesicles in renovascular hypertensive patients*. Nephrol Dial Transplant, 2017. **32**(5): p. 800-807.

107. Qi, Y., et al., *Activation of the Endogenous Renin-Angiotensin-Aldosterone System or Aldosterone Administration Increases Urinary Exosomal Sodium Channel Excretion*. J Am Soc Nephrol, 2016. **27**(2): p. 646-56.

108. van der Lubbe, N., et al., *The phosphorylated sodium chloride cotransporter in urinary exosomes is superior to prostasin as a marker for aldosteronism*. Hypertension, 2012. **60**(3): p. 741-8.

109. Zaichick, V., *The prostatic urethra as a Venturi effect urine-jet pump to drain prostatic fluid*. Med Hypotheses, 2014. **83**(1): p. 65-8.

110. van Niel, G., G. D'Angelo, and G. Raposo, *Shedding light on the cell biology of extracellular vesicles*. Nat Rev Mol Cell Biol, 2018. **19**(4): p. 213-228.

111. Kalluri, R. and V.S. LeBleu, *The biology, function, and biomedical applications of exosomes*. Science, 2020. **367**(6478).

112. Hendriks, R.J., et al., *Comparative analysis of prostate cancer specific biomarkers PCA3 and ERG in whole urine, urinary sediments and exosomes*. Clin Chem Lab Med, 2016. **54**(3): p. 483-92.

113. Duijvesz, D., et al., *Immuno-based detection of extracellular vesicles in urine as diagnostic marker for prostate cancer*. Int J Cancer, 2015. **137**(12): p. 2869-78.

114. Nolte-'t Hoen, E., et al., *Extracellular vesicles and viruses: Are they close relatives?* Proc Natl Acad Sci U S A, 2016. **113**(33): p. 9155-61.

115. van Dongen, H.M., et al., *Extracellular Vesicles Exploit Viral Entry Routes for Cargo Delivery.* Microbiol Mol Biol Rev, 2016. **80**(2): p. 369-86.

116. Erozenci, L.A., et al., *Urinary exosomal proteins as (pan-)cancer biomarkers: insights from the proteome.* FEBS Lett, 2019.

117. Cheng, Y., et al., *A translational study of urine miRNAs in acute myocardial infarction.* J Mol Cell Cardiol, 2012. **53**(5): p. 668-76.

118. Longmire, M., P.L. Choyke, and H. Kobayashi, *Clearance properties of nano-sized particles and molecules as imaging agents: considerations and caveats.* Nanomedicine (Lond), 2008. **3**(5): p. 703-17.

119. Patrakka, J., et al., *The number of podocyte slit diaphragms is decreased in minimal change nephrotic syndrome.* Pediatr Res, 2002. **52**(3): p. 349-55.

120. Ndisang, J.F., *Glomerular Endothelium and its Impact on Glomerular Filtration Barrier in Diabetes: Are the Gaps Still Illusive?* Curr Med Chem, 2018. **25**(13): p. 1525-1529.

121. Londono, I. and M. Bendayan, *Glomerular handling of native albumin in the presence of circulating modified albumins by the normal rat kidney.* Am J Physiol Renal Physiol, 2005. **289**(6): p. F1201-9.

122. Kerjaschki, D., et al., *Transcellular transport and membrane insertion of the C5b-9 membrane attack complex of complement by glomerular epithelial cells in experimental membranous nephropathy.* J Immunol, 1989. **143**(2): p. 546-52.

123. Yaghobee, S., et al., *What are nanobacteria?* Journal Biotechnology & biotechnological Equipment, 2015(26): p. 826-833

.

124. Ciftcioglu, N., et al., *Nanobacteria: an infectious cause for kidney stone formation.* Kidney Int, 1999. **56**(5): p. 1893-8.

125. Hjelle, J.T., et al., *Endotoxin and nanobacteria in polycystic kidney disease.* Kidney Int, 2000. **57**(6): p. 2360-74.

126. Shoskes, D.A., K.D. Thomas, and E. Gomez, *Anti-nanobacterial therapy for men with chronic prostatitis/chronic pelvic pain syndrome and prostatic stones: preliminary experience.* J Urol, 2005. **173**(2): p. 474-7.

127. Lee, Y., et al., *Rapid Assessment of Microbiota Changes in Individuals with Autism Spectrum Disorder Using Bacteria-derived Membrane Vesicles in Urine.* Exp Neurobiol, 2017. **26**(5): p. 307-317.

128. Yoo, J.Y., et al., *16S rRNA gene-based metagenomic analysis reveals differences in bacteria-derived extracellular vesicles in the urine of pregnant and non-pregnant women.* Exp Mol Med, 2016. **48**: p. e208.

129. Kang, C.S., et al., *Extracellular vesicles derived from gut microbiota, especially Akkermansia muciniphila, protect the progression of dextran sulfate sodium-induced colitis.* PLoS One, 2013. **8**(10): p. e76520.

130. Kalra, H., et al., *Vesiclepedia: A Compendium for Extracellular Vesicles with Continuous Community Annotation.* PLOS Biology, 2012. **10**(12): p. e1001450.

131. Zhou, H., et al., *Collection, storage, preservation, and normalization of human urinary exosomes for biomarker discovery.* Kidney Int, 2006. **69**(8): p. 1471-6.

132. Bryzgunova, O.E., et al., *Comparative Study of Extracellular Vesicles from the Urine of Healthy Individuals and Prostate Cancer Patients.* PLoS One, 2016. **11**(6): p. e0157566.

133. Bijnsdorp, I.V., et al., *Feasibility of urinary extracellular vesicle proteome profiling using a robust and simple, clinically applicable isolation method.* J Extracell Vesicles, 2017. **6**(1): p. 1313091.

134. Dhondt, B., et al., *Unravelling the proteomic landscape of extracellular vesicles in prostate cancer by density-based fractionation of urine.* J Extracell Vesicles, 2020. **9**(1): p. 1736935.

135. Street, J.M., et al., *Urine Exosomes: An Emerging Trove of Biomarkers.* Adv Clin Chem, 2017. **78**: p. 103-122.

136. Gamez-Valero, A., et al., *Urinary extracellular vesicles as source of biomarkers in kidney diseases.* Front Immunol, 2015. **6**: p. 6.

137. Dimuccio, V., et al., *Urinary CD133+ extracellular vesicles are decreased in kidney transplanted patients with slow graft function and vascular damage.* PLoS One, 2014. **9**(8): p. e104490.

138. Skotland, T., et al., *Exosomal lipid composition and the role of ether lipids and phosphoinositides in exosome biology.* J Lipid Res, 2019. **60**(1): p. 9-18.

139. Puhka, M., et al., *Metabolomic Profiling of Extracellular Vesicles and Alternative Normalization Methods Reveal Enriched Metabolites and Strategies to Study Prostate Cancer-Related Changes.* Theranostics, 2017. **7**(16): p. 3824-3841.

140. Williams, C., et al., *Assessing the role of surface glycans of extracellular vesicles on cellular uptake.* Sci Rep, 2019. **9**(1): p. 11920.

141. Saraswat, M., et al., *N-linked (N-) glycoproteomics of urinary exosomes. [Corrected].* Mol Cell Proteomics, 2015. **14**(2): p. 263-76.

142. Williams, C., et al., *Glycosylation of extracellular vesicles: current knowledge, tools and clinical perspectives.* J Extracell Vesicles, 2018. **7**(1): p. 1442985.

143. Ratajczak, J., et al., *Embryonic stem cell-derived microvesicles reprogram hematopoietic progenitors: evidence for horizontal transfer of mRNA and protein delivery.* Leukemia, 2006. **20**(5): p. 847-56.

144. Baj-Krzyworzeka, M., et al., *Tumour-derived microvesicles carry several surface determinants and mRNA of tumour cells and transfer some of these determinants to monocytes.* Cancer Immunol Immunother, 2006. **55**(7): p. 808-18.

145. Valadi, H., et al., *Exosome-mediated transfer of mRNAs and microRNAs is a novel mechanism of genetic exchange between cells.* Nat. Cell Biol, 2007. **9**(6): p. 654-659.

146. Palanisamy, V., et al., *Nanostructural and transcriptomic analyses of human saliva derived exosomes.* PLoS One, 2010. **5**(1): p. e8577.

147. Miranda, K.C., et al., *Nucleic acids within urinary exosomes/microvesicles are potential biomarkers for renal disease.* Kidney Int, 2010. **78**(2): p. 191-199.

148. Bryant, R.J., et al., *Changes in circulating microRNA levels associated with prostate cancer.* Br. J Cancer, 2012. **106**(4): p. 768-774.

149. Barutta, F., et al., *Urinary exosomal microRNAs in incipient diabetic nephropathy.* PLoS One, 2013. **8**(11): p. e73798.

150. Delic, D., et al., *Urinary Exosomal miRNA Signature in Type II Diabetic Nephropathy Patients.* PLoS One, 2016. **11**(3): p. e0150154.

151. Ghai, V., et al., *Genome-wide Profiling of Urinary Extracellular Vesicle microRNAs Associated With Diabetic Nephropathy in Type 1 Diabetes.* Kidney Int Rep, 2018. **3**(3): p. 555-572.

152. Cheng, L., et al., *Characterization and deep sequencing analysis of exosomal and non-exosomal miRNA in human urine.* Kidney Int, 2014. **86**(2): p. 433-444.

153. Srinivasan, S., et al., *Small RNA Sequencing across Diverse Biofluids Identifies Optimal Methods for exRNA Isolation.* Cell, 2019. **177**(2): p. 446-462 e16.

154. Lozano-Ramos, S.I., et al., *Molecular profile of urine extracellular vesicles from normo-functional kidneys reveal minimal differences between living and deceased donors.* BMC Nephrol, 2018. **19**(1): p. 189.

155. Miranda, K.C., et al., *Massively parallel sequencing of human urinary exosome/microvesicle RNA reveals a predominance of non-coding RNA.* PLoS One, 2014. **9**(5): p. e96094.

156. Everaert, C., et al., *Performance assessment of total RNA sequencing of human biofluids and extracellular vesicles.* Sci Rep, 2019. **9**(1): p. 17574.

157. Barreiro, K., et al., *Comparison of urinary extracellular vesicle isolation methods for transcriptomic biomarker research in diabetic kidney disease.* J Extracell Vesicles, 2020. **10**(2): p. e12038.

158. Mateescu, B., et al., *Obstacles and opportunities in the functional analysis of extracellular vesicle RNA - an ISEV position paper.* J Extracell Vesicles, 2017. **6**(1): p. 1286095.

159. Veziroglu, E.M. and G.I. Mias, *Characterizing Extracellular Vesicles and Their Diverse RNA Contents.* Front Genet, 2020. **11**: p. 700.

160. Gildea, J.J., et al., *Exosomal transfer from human renal proximal tubule cells to distal tubule and collecting duct cells.* Clin Biochem, 2014. **47**(15): p. 89-94.

161. Street, J.M., et al., *Exosomal transmission of functional aquaporin 2 in kidney cortical collecting duct cells.* J Physiol, 2011. **589**(Pt 24): p. 6119-27.

162. Munkonda, M.N., et al., *Podocyte-derived microparticles promote proximal tubule fibrotic signaling via p38 MAPK and CD36.* J Extracell Vesicles, 2018. **7**(1): p. 1432206.

163. Clayton, A., et al., *Considerations towards a roadmap for collection, handling and storage of blood extracellular vesicles.* J Extracell Vesicles, 2019. **8**(1): p. 1647027.

164. Moore, H.M., et al., *Biospecimen Reporting for Improved Study Quality.* Biopreserv Biobank, 2011. **9**(1): p. 57-70.

165. Rabinovitch, A., MD, PhD, et al., *Urinalysis; Approved Guideline*, in *GP16-A3*. 2009, *SLCI* Clinical and Laboratory Standards Institute: 950 West Valley Road, Suite 2500, Wayne, PA 19087 USA.

166. Consortium, E.-T., et al., *EV-TRACK: transparent reporting and centralizing knowledge in extracellular vesicle research.* Nat Methods, 2017. **14**(3): p. 228-232.

167. Witwer, K.W., et al., *Standardization of sample collection, isolation and analysis methods in extracellular vesicle research.* J Extracell Vesicles, 2013. **2**.

168. Lotvall, J., et al., *Minimal experimental requirements for definition of extracellular vesicles and their functions: a position statement from the International Society for Extracellular Vesicles.* J Extracell Vesicles, 2014. **3**: p. 26913.

169. Betsou, F., et al., *Standard preanalytical coding for biospecimens: defining the sample PREanalytical code.* Cancer Epidemiol Biomarkers Prev, 2010. **19**(4): p. 1004-11.

170. Lehmann, S., et al., *Standard preanalytical coding for biospecimens: review and implementation of the Sample PREanalytical Code (SPREC).* Biopreserv Biobank, 2012. **10**(4): p. 366-74.

171. Nanni, U., et al., *SPRECware: software tools for Standard PREanalytical Code (SPREC) labeling - effective exchange and search of stored biospecimens.* Int J Biol Markers, 2012. **27**(3): p. e272-9.

172. Ransohoff, D.F. and M.L. Gourlay, *Sources of bias in specimens for research about molecular markers for cancer.* J Clin Oncol, 2010. **28**(4): p. 698-704.

173. Simeone, P., et al., *Extracellular Vesicles as Signaling Mediators and Disease Biomarkers across Biological Barriers.* Int J Mol Sci, 2020. **21**(7).

174. Wang, S., et al., *Proteomic analysis of urinary extracellular vesicles reveal biomarkers for neurologic disease.* EBioMedicine, 2019. **45**: p. 351-361.

175. Zhao, Y., et al., *Effect of pH on the isolation of urinary exosome.* Int Urol Nephrol, 2017. **49**(1): p. 165-169.

176. Trilok, G. and H.H. Draper, *Sources of protein-induced endogenous acid production and excretion by human adults.* Calcif Tissue Int, 1989. **44**(5): p. 335-8.

177. Trilok, G. and H.H. Draper, *Effect of a high protein intake on acid-base balance in adult rats.* Calcif Tissue Int, 1989. **44**(5): p. 339-42.

178. Cheah, S., et al., *An online tool for improving biospecimen data element reporting.* Biopreserv Biobank, 2012. **10**(6): p. 501-10.

179. Fisher, L.A., et al., *Collection of a clean voided urine specimen: a comparison among spoken, written, and computer-based instructions.* Am J Public Health, 1977. **67**(7): p. 640-4.

180. Thomas, C.E., et al., *Urine collection and processing for protein biomarker discovery and quantification.* Cancer Epidemiol Biomarkers Prev, 2010. **19**(4): p. 953-9.

181. Firsov, D. and O. Bonny, *Circadian rhythms and the kidney.* Nat Rev Nephrol, 2018. **14**(10): p. 626-635.

182. Koritzinsky, E.H., et al., *Circadian variation in the release of small extracellular vesicles can be normalized by vesicle number or TSG101.* Am J Physiol Renal Physiol, 2019. **317**(5): p. F1098-F1110.

183. Fujita, K. and N. Nonomura, *Urinary biomarkers of prostate cancer.* Int J Urol, 2018. **25**(9): p. 770-779.

184. Manoni, F., et al., *Mid-stream vs. first-voided urine collection by using automated analyzers for particle examination in healthy subjects: an Italian multicenter study.* Clin Chem Lab Med, 2011. **50**(4): p. 679-84.

185. Tataruch-Weinert, D., et al., *Urinary extracellular vesicles for RNA extraction: optimization of a protocol devoid of prokaryote contamination.* J Extracell Vesicles, 2016. **5**: p. 30281.

186. Barreiro, K. and H. Holthofer, *Urinary extracellular vesicles. A promising shortcut to novel biomarker discoveries.* Cell Tissue Res, 2017. **369**(1): p. 217-227.

187. Oeyen, E., et al., *Determination of variability due to biological and technical variation in urinary extracellular vesicles as a crucial step in biomarker discovery studies.* J Extracell Vesicles, 2019. **8**(1): p. 1676035.

188. Murakami, T., et al., *Development of glomerulus-, tubule-, and collecting duct-specific mRNA assay in human urinary exosomes and microvesicles.* PLoS One, 2014. **9**(9): p. e109074.

189. Barreiro, K., T.B. Huber, and H. Holthofer, *Isolating Urinary Extracellular Vesicles as Biomarkers for Diabetic Disease*. Methods Mol Biol, 2020. **2067**: p. 175-188.

190. Moatamed, N.A., *Biobanking of Urine Samples*. Methods Mol Biol, 2019. **1897**: p. 115-124.

191. Saetun, P., T. Semangoen, and V. Thongboonkerd, *Characterizations of urinary sediments precipitated after freezing and their effects on urinary protein and chemical analyses*. Am J Physiol Renal Physiol, 2009. **296**(6): p. F1346-54.

192. Armstrong, D.A., et al., *Pre-Analytical Handling Conditions and Small RNA Recovery from Urine for miRNA Profiling*. J Mol Diagn, 2018. **20**(5): p. 565-571.

193. Wachalska, M., et al., *Protein Complexes in Urine Interfere with Extracellular Vesicle Biomarker Studies*. J Circ Biomark, 2016. **5**: p. 4.

194. Havanapan, P.O. and V. Thongboonkerd, *Are protease inhibitors required for gel-based proteomics of kidney and urine?* J Proteome Res, 2009. **8**(6): p. 3109-17.

195. Thongboonkerd, V. and P. Saetun, *Bacterial overgrowth affects urinary proteome analysis: recommendation for centrifugation, temperature, duration, and the use of preservatives during sample collection*. J Proteome Res, 2007. **6**(11): p. 4173-81.

196. Welton, J.L., et al., *Proteomic analysis of bladder cancer exosomes*. Mol. Cell Proteomics, 2010. **9**(6): p. 1324-1338.

197. Royo, F., et al., *Different EV enrichment methods suitable for clinical settings yield different subpopulations of urinary extracellular vesicles from human samples*. J Extracell Vesicles, 2016. **5**: p. 29497.

198. Bunjevac, A., et al., *Preanalytics of urine sediment examination: effect of relative centrifugal force, tube type, volume of sample and supernatant removal*. Biochem Med (Zagreb), 2018. **28**(1): p. 010707.

199. Micanovic, R., et al., *Tamm-Horsfall Protein Regulates Mononuclear Phagocytes in the Kidney*. J Am Soc Nephrol, 2018. **29**(3): p. 841-856.

200. Puhka, M., et al., *KeepEX, a simple dilution protocol for improving extracellular vesicle yields from urine*. Eur J Pharm Sci, 2017. **98**: p. 30-39.

201. Musante, L., et al., *A Simplified Method to Recover Urinary Vesicles for Clinical Applications, and Sample Banking*. Scientific Reports, 2014. **4**.

202. Fernandez-Llama, P., et al., *Tamm-Horsfall protein and urinary exosome isolation*. Kidney Int, 2010. **77**(8): p. 736-42.

203. Mussack, V., G. Wittmann, and M.W. Pfaffl, *Comparing small urinary extracellular vesicle purification methods with a view to RNA sequencing-Enabling robust and non-invasive biomarker research*. Biomol Detect Quantif, 2019. **17**: p. 100089.

204. Ammerlaan, W., et al., *Method validation for preparing urine samples for downstream proteomic and metabolomic applications*. Biopreserv Biobank, 2014. **12**(5): p. 351-7.

205. Yuana, Y., et al., *Handling and storage of human body fluids for analysis of extracellular vesicles*. J Extracell Vesicles, 2015. **4**: p. 29260.

206. Cheng, Y., et al., *Effect of pH, temperature and freezing-thawing on quantity changes and cellular uptake of exosomes*. Protein Cell, 2019. **10**(4): p. 295-299.

207. Musante, L., et al., *Proteases and protease inhibitors of urinary extracellular vesicles in diabetic nephropathy*. J Diabetes Res, 2015. **2015**: p. 289734.

208. Coumans, F.A.W., et al., *Methodological Guidelines to Study Extracellular Vesicles*. Circ Res, 2017. **120**(10): p. 1632-1648.

209. Konoshenko, M.Y., et al., *Isolation of Extracellular Vesicles: General Methodologies and Latest Trends*. Biomed Res Int, 2018. **2018**: p. 8545347.

210. Royo, F., et al., *Comparative miRNA Analysis of Urine Extracellular Vesicles Isolated through Five Different Methods*. Cancers, 2016. **8**(12): p. E112.

211. Alvarez, M.L., et al., *Comparison of protein, microRNA, and mRNA yields using different methods of urinary exosome isolation for the discovery of kidney disease biomarkers*. Kidney International, 2012. **82**(9): p. 1024-1032.

212. Gonzales, P.A., et al., *Isolation and purification of exosomes in urine*. Methods Mol. Biol, 2010. **641**: p. 89-99.

213. Musante, L., et al., *Biochemical and Physical Characterisation of Urinary Nanovesicles following CHAPS Treatment*. Plos One, 2012. **7**(7).

214. Musante, L., et al., *Residual urinary extracellular vesicles in ultracentrifugation supernatants after hydrostatic filtration dialysis enrichment*. J Extracell Vesicles, 2017. **6**(1): p. 1267896.

215. Santucci, L., et al., *Biological surface properties in extracellular vesicles and their effect on cargo proteins*. Scientific Reports, 2019. **9**(1): p. 13048.

216. Rood, I.M., et al., *Comparison of three methods for isolation of urinary microvesicles to identify biomarkers of nephrotic syndrome*. Kidney Int, 2010. **78**(8): p. 810-6.

217. Inman, B.A., et al., *The impact of temperature and urinary constituents on urine viscosity and its relevance to bladder hyperthermia treatment*. International Journal of Hyperthermia, 2013. **29**(3): p. 206-210.

218. Momen-Heravi, F., et al., *Impact of Biofluid Viscosity on Size and Sedimentation Efficiency of the Isolated Microvesicles*. Frontiers in Physiology, 2012. **3**(162).

219. Raimondo, F., et al., *Effects of Hematuria on the Proteomic Profile of Urinary Extracellular Vesicles: Technical Challenges*. J Proteome Res, 2018. **17**(8): p. 2572-2580.

220. Huebner, A.R., et al., *Exosomes in urine biomarker discovery*. Adv. Exp. Med. Biol, 2015. **845**: p. 43-58.

221. Oeyen, E., et al., *Ultrafiltration and size exclusion chromatography combined with asymmetrical-flow field-flow fractionation for the isolation and characterisation of extracellular vesicles from urine*. J Extracell Vesicles, 2018. **7**(1): p. 1490143.

222. Wang, D. and W. Sun, *Urinary extracellular microvesicles: isolation methods and prospects for urinary proteome*. Proteomics, 2014. **14**(16): p. 1922-32.

223. Cheruvanky, A., et al., *Rapid isolation of urinary exosomal biomarkers using a nanomembrane ultrafiltration concentrator*. American Journal of Physiology-Renal Physiology, 2007. **292**(5): p. F1657-F1661.

224. Ku, A., et al., *Acoustic Enrichment of Extracellular Vesicles from Biological Fluids*. Anal Chem, 2018. **90**(13): p. 8011-8019.

225. Lozano-Ramos, I., et al., *Size-exclusion chromatography-based enrichment of extracellular vesicles from urine samples.* J Extracell Vesicles, 2015. **4**: p. 27369.

226. Dhondt, B., et al., *Preparation of Multi-omics Grade Extracellular Vesicles by Density-Based Fractionation of Urine.* STAR Protocols, 2020. **1**(2): p. 100073.

227. Svenningsen, P., R. Sabaratnam, and B.L. Jensen, *Urinary extracellular vesicles: Origin, role as intercellular messengers and biomarkers; efficient sorting and potential treatment options.* Acta Physiol (Oxf), 2020. **228**(1): p. e13346.

228. Freitas, D., et al., *Different isolation approaches lead to diverse glycosylated extracellular vesicle populations.* J Extracell Vesicles, 2019. **8**(1): p. 1621131.

229. Hiemstra, T.F., et al., *Uromodulin exclusion list improves urinary exosomal protein identification.* J Biomol Tech, 2011. **22**(4): p. 136-45.

230. Saliba, D.G., et al., *Composition and structure of synaptic ectosomes exporting antigen receptor linked to functional CD40 ligand from helper T cells.* Elife, 2019. **8**.

231. Rindler, M.J., et al., *Uromodulin (Tamm-Horsfall glycoprotein/uromucoid) is a phosphatidylinositol-linked membrane protein.* J Biol Chem, 1990. **265**(34): p. 20784-9.

232. Welsh, J.A., et al., *MIFlowCyt-EV: a framework for standardized reporting of extracellular vesicle flow cytometry experiments.* J Extracell Vesicles, 2020. **9**(1): p. 1713526.

233. Suarez, H., et al., *A bead-assisted flow cytometry method for the semi-quantitative analysis of Extracellular Vesicles.* Sci Rep, 2017. **7**(1): p. 11271.

234. Monguio-Tortajada, M., et al., *Extracellular-Vesicle Isolation from Different Biological Fluids by Size-Exclusion Chromatography.* Curr Protoc Stem Cell Biol, 2019. **49**(1): p. e82.

235. Wiklander, O.P.B., et al., *Systematic Methodological Evaluation of a Multiplex Bead-Based Flow Cytometry Assay for Detection of Extracellular Vesicle Surface Signatures.* Front Immunol, 2018. **9**: p. 1326.

236. Park, S., et al., *The profiles of microRNAs from urinary extracellular vesicles (EVs) prepared by various isolation methods and their correlation with serum EV microRNAs.* Diabetes Res Clin Pract, 2020. **160**: p. 108010.

237. Thomas, S., et al., *Biomarker discovery in mass spectrometry-based urinary proteomics.* Proteomics Clin Appl, 2016. **10**(4): p. 358-70.

238. Carreras-Planella, L., et al., *Urinary vitronectin identifies patients with high levels of fibrosis in kidney grafts.* J Nephrol, 2020.

239. Carreras-Planella, L., et al., *Proteomic Characterization of Urinary Extracellular Vesicles from Kidney-Transplanted Patients Treated with Calcineurin Inhibitors.* Int J Mol Sci, 2020. **21**(20).

240. Williams, C., et al., *Metabolomics Applied to the Study of Extracellular Vesicles.* Metabolites, 2019. **9**(11).

241. Ku, A., et al., *A urinary extracellular vesicle microRNA biomarker discovery pipeline; from automated extracellular vesicle enrichment by acoustic trapping to microRNA sequencing.* PLoS One, 2019. **14**(5): p. e0217507.

242. Karina, B., et al., *Comparison of urinary extracellular vesicle isolation methods for transcriptomic biomarker research in diabetic kidney disease.* J Extracell Vesicles, 2020. **in press**.

243. Knol, J.C., et al., *Peptide-mediated 'miniprep' isolation of extracellular vesicles is suitable for high-throughput proteomics.* EuPA Open Proteom, 2016. **11**: p. 11-15.

244. Ghosh, A., et al., *Rapid isolation of extracellular vesicles from cell culture and biological fluids using a synthetic peptide with specific affinity for heat shock proteins.* PLoS One, 2014. **9**(10): p. e110443.

245. Salih, M., et al., *An immunoassay for urinary extracellular vesicles.* Am J Physiol Renal Physiol, 2016. **310**(8): p. F796-F801.

246. Smith, J.T., et al., *Integrated nanoscale deterministic lateral displacement arrays for separation of extracellular vesicles from clinically-relevant volumes of biological samples.* Lab Chip, 2018. **18**(24): p. 3913-3925.

247. Liang, L.G., et al., *An integrated double-filtration microfluidic device for isolation, enrichment and quantification of urinary extracellular vesicles for detection of bladder cancer.* Sci Rep, 2017. **7**: p. 46224.

248. Yasui, T., et al., *Unveiling massive numbers of cancer-related urinary-microRNA candidates via nanowires.* Sci Adv, 2017. **3**(12): p. e1701133.

249. Woo, H.K., et al., *Exodisc for Rapid, Size-Selective, and Efficient Isolation and Analysis of Nanoscale Extracellular Vesicles from Biological Samples.* ACS Nano, 2017. **11**(2): p. 1360-1370.

250. Islam, M.K., et al., *A Nanoparticle-Based Approach for the Detection of Extracellular Vesicles.* Sci Rep, 2019. **9**(1): p. 10038.

251. Burbidge, K., et al., *Cargo and cell-specific differences in extracellular vesicle populations identified by multiplexed immunofluorescent analysis.* J Extracell Vesicles, 2020. **9**(1): p. 1789326.

252. Daaboul, G.G., et al., *Digital Detection of Exosomes by Interferometric Imaging.* Sci Rep, 2016. **6**: p. 37246.

253. Chiriaco, M.S., et al., *Lab-on-Chip for Exosomes and Microvesicles Detection and Characterization.* Sensors (Basel), 2018. **18**(10).

254. Iliescu, F.S., et al., *Microfluidic Technology for Clinical Applications of Exosomes.* Micromachines (Basel), 2019. **10**(6).

255. Hartjes, T.A., et al., *Extracellular Vesicle Quantification and Characterization: Common Methods and Emerging Approaches.* Bioengineering (Basel), 2019. **6**(1).

256. McNicholas, K., et al., *Albuminuria is not associated with elevated urinary vesicle concentration but can confound nanoparticle tracking analysis.* Nephrology (Carlton), 2017. **22**(11): p. 854-863.

257. Gleadle, J., et al., *Nanoparticle Tracking Analysis of Urine to Detect Exosomes Can Be Confounded by Albuminuria.* J Am Soc Nephrol, 2018. **29**(6): p. 1784.

258. Campos-Silva, C., et al., *High sensitivity detection of extracellular vesicles immune-captured from urine by conventional flow cytometry.* Sci Rep, 2019. **9**(1): p. 2042.

259. Blijdorp, C.J., et al., *Comparing Approaches to Normalize, Quantify, and Characterize Urinary Extracellular Vesicles.* J Am Soc Nephrol, 2021.

260. Kruglik, S.G., et al., *Raman tweezers microspectroscopy of circa 100 nm extracellular vesicles.* Nanoscale, 2019. **11**(4): p. 1661-1679.

261. Yuana, Y., R.M. Bertina, and S. Osanto, *Pre-analytical and analytical issues in the analysis of blood microparticles.* Thromb Haemost, 2011. **105**(3): p. 396-408.

262. Blijdorp, C.J. and E.J. Hoorn, *Urinary extracellular vesicles: the mothership connection.* Am J Physiol Renal Physiol, 2019. **317**(3): p. F648-f649.

263. Dijkstra, S., et al., *Prostate cancer biomarker profiles in urinary sediments and exosomes.* J Urol, 2014. **191**(4): p. 1132-8.

264. Samsonov, R., et al., *Lectin-induced agglutination method of urinary exosomes isolation followed by mi-RNA analysis: Application for prostate cancer diagnostic.* Prostate, 2016. **76**(1): p. 68-79.

265. Silvers, C.R., et al., *Identification of extracellular vesicle-borne periostin as a feature of muscle-invasive bladder cancer.* Oncotarget, 2016. **7**(17): p. 23335-45.

266. Adedeji, A.O., et al., *Investigating the Value of Urine Volume, Creatinine, and Cystatin C for Urinary Biomarkers Normalization for Drug Development Studies.* Int J Toxicol, 2019. **38**(1): p. 12-22.

267. Nisell, H., M. Trygg, and R. Bäck, *Urine albumin/creatinine ratio for the assessment of albuminuria in pregnancy hypertension.* Acta Obstet Gynecol Scand, 2006. **85**(11): p. 1327-30.

268. Xu, X., et al., *Management of Tamm-Horsfall Protein for Reliable Urinary Analytics.* Proteomics Clin Appl, 2019. **13**(6): p. e1900018.

269. Colombo, M., et al., *Analysis of ESCRT functions in exosome biogenesis, composition and secretion highlights the heterogeneity of extracellular vesicles.* J Cell Sci, 2013. **126**(Pt 24): p. 5553-65.

270. Koopman, M.G., et al., *Circadian rhythm of proteinuria: consequences of the use of urinary protein:creatinine ratios.* Nephrol Dial Transplant, 1989. **4**(1): p. 9-14.

271. Boyd, C., et al., *Accuracy in 24-hour Urine Collection at a Tertiary Center.* Rev Urol, 2018. **20**(3): p. 119-124.

272. Waikar, S.S., V.S. Sabbisetti, and J.V. Bonventre, *Normalization of urinary biomarkers to creatinine during changes in glomerular filtration rate.* Kidney Int, 2010. **78**(5): p. 486-94.

273. Forni Ogna, V., et al., *New anthropometry-based age- and sex-specific reference values for urinary 24-hour creatinine excretion based on the adult Swiss population.* BMC Med, 2015. **13**: p. 40.

274. Khamis, M.M., et al., *Comparative analysis of creatinine and osmolality as urine normalization strategies in targeted metabolomics for the differential diagnosis of asthma and COPD.* Metabolomics, 2018. **14**(9): p. 115.

275. Ginsberg, J.M., et al., *Use of single voided urine samples to estimate quantitative proteinuria.* N Engl J Med, 1983. **309**(25): p. 1543-6.

276. Ploussard, G. and A. de la Taille, *Urine biomarkers in prostate cancer.* Nat Rev Urol, 2010. **7**(2): p. 101-9.

277. Minciacchi, V.R., et al., *Extracellular vesicles for liquid biopsy in prostate cancer: where are we and where are we headed?* Prostate Cancer Prostatic Dis, 2017. **20**(3): p. 251-258.

278. Keller, S., et al., *CD24 is a marker of exosomes secreted into urine and amniotic fluid.* Kidney Int, 2007. **72**(9): p. 1095-102.

279. Paisrisarn, P., T. Yasui, and Y. Baba, *A Method to Analyze Urinary Extracellular Vesicles.* Anal Sci, 2020. **36**(7): p. 791-798.

280. Skotland, T., et al., *An emerging focus on lipids in extracellular vesicles.* Adv Drug Deliv Rev, 2020.

281. Nazarenko, I., *Extracellular Vesicles: Recent Developments in Technology and Perspectives for Cancer Liquid Biopsy.* Recent Results Cancer Res, 2020. **215**: p. 319-344.

282. Soekmadji, C., et al., *The future of Extracellular Vesicles as Theranostics - an ISEV meeting report.* J Extracell Vesicles, 2020. **9**(1): p. 1809766.

283. Vergauwen, G., et al., *Confounding factors of ultrafiltration and protein analysis in extracellular vesicle research.* Sci Rep, 2017. **7**(1): p. 2704.

284. Coughlan, C., et al., *Exosome Isolation by Ultracentrifugation and Precipitation and Techniques for Downstream Analyses.* Curr Protoc Cell Biol, 2020. **88**(1): p. e110.

285. Rikkert, L.G., et al., *Detection of extracellular vesicles in plasma and urine of prostate cancer patients by flow cytometry and surface plasmon resonance imaging.* PLoS One, 2020. **15**(6): p. e0233443.

286. Kowal, J., et al., *Proteomic comparison defines novel markers to characterize heterogeneous populations of extracellular vesicle subtypes.* Proc Natl Acad Sci U S A, 2016. **113**(8): p. E968-77.

287. Headland, S.E., et al., *Cutting-edge analysis of extracellular microparticles using ImageStream(X) imaging flow cytometry.* Sci Rep, 2014. **4**: p. 5237.

288. Koliha, N., et al., *A novel multiplex bead-based platform highlights the diversity of extracellular vesicles.* J Extracell Vesicles, 2016. **5**: p. 29975.

289. Wang, Y.T., et al., *Proteomic Analysis of Exosomes for Discovery of Protein Biomarkers for Prostate and Bladder Cancer.* Cancers (Basel), 2020. **12**(9).

290. Rigau, M., et al., *The present and future of prostate cancer urine biomarkers.* Int J Mol Sci, 2013. **14**(6): p. 12620-49.

291. Sole, C., et al., *An Exosomal Urinary miRNA Signature for Early Diagnosis of Renal Fibrosis in Lupus Nephritis.* Cells, 2019. **8**(8).

292. Yamamoto, C.M., et al., *Uromodulin mRNA from Urinary Extracellular Vesicles Correlate to Kidney Function Decline in Type 2 Diabetes Mellitus.* Am J Nephrol, 2018. **47**(5): p. 283-291.

293. Sun, A.L., et al., *Dipeptidyl peptidase-IV is a potential molecular biomarker in diabetic kidney disease.* Diab Vasc Dis Res, 2012. **9**(4): p. 301-8.

294. Zhu, C., et al., *Recent advances of aptasensors for exosomes detection.* Biosens Bioelectron, 2020. **160**: p. 112213.

295. Welton, J.L., et al., *Proteomics analysis of vesicles isolated from plasma and urine of prostate cancer patients using a multiplex, aptamer-based protein array.* J Extracell Vesicles, 2016. **5**: p. 31209.

296. Larssen, P., et al., *Tracing Cellular Origin of Human Exosomes Using Multiplex Proximity Extension Assays.* Mol Cell Proteomics, 2017. **16**(3): p. 502-511.

297. Mata Forsberg, M., et al., *Extracellular Membrane Vesicles from Lactobacilli Dampen IFN-gamma Responses in a Monocyte-Dependent Manner.* Sci Rep, 2019. **9**(1): p. 17109.

298. Cha, J.M., et al., *Efficient scalable production of therapeutic microvesicles derived from human mesenchymal stem cells.* Sci Rep, 2018. **8**(1): p. 1171.

299. Gori, A., et al., *Membrane-binding peptides for extracellular vesicles on-chip analysis.* J Extracell Vesicles, 2020. **9**(1): p. 1751428.

300. Peinado, H., et al., *Melanoma exosomes educate bone marrow progenitor cells toward a pro-metastatic phenotype through MET.* Nat Med, 2012. **18**(6): p. 883-91.

301. Royo, F., et al., *Transcriptomic profiling of urine extracellular vesicles reveals alterations of CDH3 in prostate cancer.* Oncotarget, 2016. **7**(6): p. 6835-46.

302. Avela, H.F. and H. Siren, *Advances in lipidomics*. Clin Chim Acta, 2020. **510**: p. 123-141.

303. Wu, Z., et al., *"Lipidomics": Mass spectrometric and chemometric analyses of lipids*. Adv Drug Deliv Rev, 2020.

304. Zullig, T. and H.C. Kofeler, *High Resolution Mass Spectrometry in Lipidomics*. Mass Spectrom Rev, 2020.

305. Glover, S.C., et al., *Lipidomic analysis of urinary exosomes from hereditary alpha-tryptasemia patients and healthy volunteers*. FASEB Bioadv, 2019. **1**(10): p. 624-638.

306. Tipthara, P. and V. Thongboonkerd, *Differential human urinary lipid profiles using various lipid-extraction protocols: MALDI-TOF and LIFT-TOF/TOF analyses*. Sci Rep, 2016. **6**: p. 33756.

307. Royo, F., et al., *Differences in the metabolite composition and mechanical properties of extracellular vesicles secreted by hepatic cellular models*. J Extracell Vesicles, 2019. **8**(1): p. 1575678.

308. Palomo, L., et al., *Considerations for applying metabolomics to the analysis of extracellular vesicles*. Front Immunol, 2014. **5**: p. 651.

309. Palviainen, M., et al., *Extracellular vesicles from human plasma and serum are carriers of extravesicular cargo-Implications for biomarker discovery*. PLoS One, 2020. **15**(8): p. e0236439.

310. Olinger, E., et al., *Hepsin-mediated Processing of Uromodulin is Crucial for Salt-sensitivity and Thick Ascending Limb Homeostasis*. Scientific Reports, 2019. **9**(1): p. 12287.

311. Hogan, M.C., et al., *Strategy and rationale for urine collection protocols employed in the NEPTUNE study*. BMC Nephrology, 2015. **16**(1): p. 190.

312. Rayyan, M., A. Zheutlin, and J.B. Byrd, *Clinical research using extracellular vesicles: insights from the International Society for Extracellular Vesicles 2018 Annual Meeting*. J Extracell Vesicles, 2018. **7**(1): p. 1535744.

313. Thomas, M.E., et al., *The definition of acute kidney injury and its use in practice*. Kidney Int, 2015. **87**(1): p. 62-73.

314. Fan, W., et al., *Current understanding and future directions in the application of TIMP-2 and IGFBP7 in AKI clinical practice*. Clin Chem Lab Med, 2018.

315. Kashani, K., et al., *Discovery and validation of cell cycle arrest biomarkers in human acute kidney injury*. Crit Care, 2013. **17**(1): p. R25.

316. Gaffney, A., RAC, *Flip a Coin: FDA Approves Kidney Diagnostic With 50% False Positive Results*, in *Regulatory Focus*. 2014, RAPS, Regulatory Affairs Professionals Society: Rockville, Maryland

317. Bazzell, B.G., et al., *Human Urinary mRNA as a Biomarker of Cardiovascular Disease*. Circ Genom Precis Med, 2018. **11**(9): p. e002213.

318. Donovan, M.J., et al., *A molecular signature of PCA3 and ERG exosomal RNA from non-DRE urine is predictive of initial prostate biopsy result*. Prostate Cancer Prostatic Dis, 2015. **18**(4): p. 370-5.

319. Hogan, M.C., et al., *Subfractionation, characterization, and in-depth proteomic analysis of glomerular membrane vesicles in human urine*. Kidney Int, 2014. **85**(5): p. 1225-37.

320. Kalani, A., et al., *Wilm's tumor-1 protein levels in urinary exosomes from diabetic patients with or without proteinuria*. PLoS One, 2013. **8**(3): p. e60177.

321. Prunotto, M., et al., *Proteomic analysis of podocyte exosome-enriched fraction from normal human urine*. J Proteomics, 2013. **82**: p. 193-229.

322. Grange, C., et al., *Urinary Extracellular Vesicles Carrying Klotho Improve the Recovery of Renal Function in an Acute Tubular Injury Model*. Mol Ther, 2020. **28**(2): p. 490-502.

323. Turco, A.E., et al., *Specific renal parenchymal-derived urinary extracellular vesicles identify age-associated structural changes in living donor kidneys*. J Extracell Vesicles, 2016. **5**: p. 29642.

324. Boulestreau, J., et al., *Mesenchymal Stem Cell Derived Extracellular Vesicles in Aging*. Front Cell Dev Biol, 2020. **8**: p. 107.

325. Welton, J.L., et al., *Proteomics analysis of bladder cancer exosomes*. Mol Cell Proteomics, 2010. **9**(6): p. 1324-38.

326. Conde-Vancells, J., et al., *Candidate biomarkers in exosome-like vesicles purified from rat and mouse urine samples*. Proteomics Clin Appl, 2010. **4**(4): p. 416-25.

327. Rao, M.S., et al., *Comparison of RNA-Seq and Microarray Gene Expression Platforms for the Toxicogenomic Evaluation of Liver From Short-Term Rat Toxicity Studies*. Front Genet, 2018. **9**: p. 636.

328. Langevin, S.M., et al., *Comparability of the small RNA secretome across human biofluids concomitantly collected from healthy adults*. PLoS One, 2020. **15**(4): p. e0229976.

329. Khurana, R., et al., *Identification of urinary exosomal noncoding RNAs as novel biomarkers in chronic kidney disease*. RNA, 2017. **23**(2): p. 142-152.

330. Sabaratnam, R., et al., *In human nephrectomy specimens, the kidney level of tubular transport proteins does not correlate with their abundance in urinary extracellular vesicles*. Am J Physiol Renal Physiol, 2019.

331. Terker, A.S., et al., *Potassium modulates electrolyte balance and blood pressure through effects on distal cell voltage and chloride*. Cell Metab, 2015. **21**(1): p. 39-50.

332. Sorensen, M.V., et al., *Rapid dephosphorylation of the renal sodium chloride cotransporter in response to oral potassium intake in mice*. Kidney Int, 2013. **83**(5): p. 811-24.

333. Zhou, H., et al., *Exosomal Fetuin-A identified by proteomics: a novel urinary biomarker for detecting acute kidney injury*. Kidney Int, 2006. **70**(10): p. 1847-57.

334. Panich, T., et al., *Urinary exosomal activating transcriptional factor 3 as the early diagnostic biomarker for sepsis-induced acute kidney injury*. BMC Nephrol, 2017. **18**(1): p. 10.

335. Salih, M., et al., *Proteomics of Urinary Vesicles Links Plakins and Complement to Polycystic Kidney Disease*. J Am Soc Nephrol, 2016.

336. Morikawa, Y., et al., *Elevated Levels of Urinary Extracellular Vesicle Fibroblast-Specific Protein 1 in Patients with Active Crescentic Glomerulonephritis*. Nephron, 2019. **141**(3): p. 177-187.

337. Olden, M., et al., *Common variants in UMOD associate with urinary uromodulin levels: a meta-analysis*. J Am Soc Nephrol, 2014. **25**(8): p. 1869-82.

338. Tutakhel, O.A., et al., *Alternative splice variant of the thiazide-sensitive NaCl cotransporter: a novel player in renal salt handling*. Am J Physiol Renal Physiol, 2016. **310**(3): p. F204-16.

339. Maurer, S.E. and G. Nguyen, *Prebiotic Vesicle Formation and the Necessity of Salts*. Orig Life Evol Biosph, 2016. **46**(2-3): p. 215-22.

340. Mitchell, P.J., et al., *Can urinary exosomes act as treatment response markers in prostate cancer?* J Transl Med, 2009. **7**: p. 4.

341. Miyazawa, Y., et al., *AQP2 in human urine is predominantly localized to exosomes with preserved water channel activities*. Clin Exp Nephrol, 2018. **22**(4): p. 782-788.

342. Limbutara, K., C.L. Chou, and M.A. Knepper, *Quantitative Proteomics of All 14 Renal Tubule Segments in Rat.* J Am Soc Nephrol, 2020. **31**(6): p. 1255-1266.

343. Cvjetkovic, A., et al., *Detailed Analysis of Protein Topology of Extracellular Vesicles-Evidence of Unconventional Membrane Protein Orientation.* Sci Rep, 2016. **6**: p. 36338.

344. McKiernan, J., et al., *A Prospective Adaptive Utility Trial to Validate Performance of a Novel Urine Exosome Gene Expression Assay to Predict High-grade Prostate Cancer in Patients with Prostate-specific Antigen 2-10ng/ml at Initial Biopsy.* Eur Urol, 2018. **74**(6): p. 731-738.

345. Braun, F., et al., *The proteomic landscape of small urinary extracellular vesicles during kidney transplantation.* J Extracell Vesicles, 2020. **10**(1): p. e12026.

346. El Fekih, R., et al., *Discovery and Validation of a Urinary Exosome mRNA Signature for the Diagnosis of Human Kidney Transplant Rejection.* J Am Soc Nephrol, 2021.

347. Blijdorp, C.J., et al., *Comparing Approaches to Normalize, Quantify, and Characterize Urinary Extracellular Vesicles.* J Am Soc Nephrol, 2021. **32**(5): p. 1210-1226.

348. Hartjes, T.A., et al., *EVQuant; high-throughput quantification and characterization of extracellular vesicle (sub)populations.* bioRxiv, 2020.

349. Erdbrugger, U., et al., *Urinary extracellular vesicles: A position paper by the Urine Task Force of the International Society for Extracellular Vesicles.* J Extracell Vesicles, 2021. **10**(7): p. e12093.

350. Bovee, D.M., et al., *Dietary salt modifies the blood pressure response to renin-angiotensin inhibition in experimental chronic kidney disease.* Am J Physiol Renal Physiol, 2021. **320**(4): p. F654-F668.

351. Schock-Kusch, D., et al., *Transcutaneous measurement of glomerular filtration rate using FITC-sinistrin in rats.* Nephrol Dial Transplant, 2009. **24**(10): p. 2997-3001.

352. Dong, J., et al., *Accuracy Validation of 8 Equations to Estimate 24-Hour Sodium by Spot Urine in Young Adolescents.* Am J Hypertens, 2019. **32**(3): p. 257-264.

353. Pivin, E., et al., *Uromodulin and Nephron Mass.* Clin J Am Soc Nephrol, 2018. **13**(10): p. 1556-1557.

354. Sabaratnam, R., et al., *In human nephrectomy specimens, the kidney level of tubular transport proteins does not correlate with their abundance in urinary extracellular vesicles.* Am J Physiol Renal Physiol, 2019. **317**(3): p. F560-F571.

355. Wu, Q., et al., *Large-Scale Proteomic Assessment of Urinary Extracellular Vesicles Highlights Their Reliability in Reflecting Protein Changes in the Kidney.* J Am Soc Nephrol, 2021. **32**(9): p. 2195-2209.

356. Tynkevich, E., et al., *Urinary creatinine excretion, measured glomerular filtration rate and CKD outcomes.* Nephrol Dial Transplant, 2015. **30**(8): p. 1386-94.

357. Brenner, B.M., et al., *Dynamics of glomerular ultrafiltration in the rat. II. Plasma-flow dependence of GFR.* Am J Physiol, 1972. **223**(5): p. 1184-90.

358. Hayslett, J.P., M. Kashgarian, and F.H. Epstein, *Functional correlates of compensatory renal hypertrophy.* J Clin Invest, 1968. **47**(4): p. 774-99.

359. Wessely, O., et al., *The bigger the better: determining nephron size in kidney.* Pediatr Nephrol, 2014. **29**(4): p. 525-30.

360. Oosthuyzen, W., et al., *Vasopressin Regulates Extracellular Vesicle Uptake by Kidney Collecting Duct Cells.* J Am Soc Nephrol, 2016. **27**(11): p. 3345-3355.

361. Nord, E.P., et al., *pH gradient-dependent increased Na+-H+ antiport capacity of the rabbit remnant kidney.* Am J Physiol, 1985. **249**(1 Pt 2): p. F90-8.

362. Girardi, A.C., et al., *Upregulation of NHE3 is associated with compensatory cell growth response in young uninephrectomized rats.* Am J Physiol Renal Physiol, 2002. **283**(6): p. F1296-303.

363. Pollock, C.A., et al., *Tubular sodium handling and tubuloglomerular feedback in compensatory renal hypertrophy.* Pflugers Arch, 1992. **420**(2): p. 159-66.

364. Preisig, P.A. and R.J. Alpern, *Increased Na/H antiporter and Na/3HCO3 symporter activities in chronic hyperfiltration. A model of cell hypertrophy.* J Gen Physiol, 1991. **97**(2): p. 195-217.

365. Lankadeva, Y.R., et al., *Blunted sodium excretion in response to a saline load in 5 year old female sheep following fetal uninephrectomy.* PLoS One, 2012. **7**(10): p. e47528.

366. Singh, R.R., et al., *Reduced nephron endowment due to fetal uninephrectomy impairs renal sodium handling in male sheep.* Clin Sci (Lond), 2010. **118**(11): p. 669-80.

367. Jung, J.Y., et al., *Effects of potassium on expression of renal sodium transporters in salt-sensitive hypertensive rats induced by uninephrectomy.* Am J Physiol Renal Physiol, 2011. **300**(6): p. F1422-30.

368. Kasiske, B.L., et al., *Long-term effects of reduced renal mass in humans.* Kidney Int, 1995. **48**(3): p. 814-9.

369. Boudville, N., et al., *Meta-analysis: risk for hypertension in living kidney donors.* Ann Intern Med, 2006. **145**(3): p. 185-96.

370. Lenihan, C.R., et al., *Longitudinal study of living kidney donor glomerular dynamics after nephrectomy.* J Clin Invest, 2015. **125**(3): p. 1311-8.

371. Veiras, L.C., et al., *Sexual Dimorphic Pattern of Renal Transporters and Electrolyte Homeostasis.* J Am Soc Nephrol, 2017. **28**(12): p. 3504-3517.

372. Gurley, S.B., et al., *AT1A angiotensin receptors in the renal proximal tubule regulate blood pressure.* Cell Metab, 2011. **13**(4): p. 469-75.

373. Kasiske, B.L., et al., *A prospective controlled study of living kidney donors: three-year follow-up.* Am J Kidney Dis, 2015. **66**(1): p. 114-24.

374. Sasaki, T., et al., *Estimation of nephron number in living humans by combining unenhanced computed tomography with biopsy-based stereology.* Sci Rep, 2019. **9**(1): p. 14400.

375. Bergmann, C., et al., *Polycystic kidney disease.* Nat Rev Dis Primers, 2018. **4**(1): p. 50.

376. Cornec-Le Gall, E., V.E. Torres, and P.C. Harris, *Genetic Complexity of Autosomal Dominant Polycystic Kidney and Liver Diseases.* J Am Soc Nephrol, 2018. **29**(1): p. 13-23.

377. Lanktree, M.B., et al., *Intrafamilial Variability of ADPKD.* Kidney Int Rep, 2019. **4**(7): p. 995-1003.

378. Bruschi, M., et al., *Proteomic Analysis of Urinary Microvesicles and Exosomes in Medullary Sponge Kidney Disease and Autosomal Dominant Polycystic Kidney Disease.* Clin J Am Soc Nephrol, 2019. **14**(6): p. 834-843.

379. Wang, J., et al., *Release and targeting of polycystin-2-carrying ciliary extracellular vesicles.* Curr Biol, 2020. **30**(13): p. R755-R756.

380. Raby, K.L., *Urinary exosome proteomic profiling defines stage-specific rapid progression of Autosomal Dominant Polycystic Kidney Disease and Tolvaptan efficacy.* BBA Advances pre-proof, 2021.

381. Meijer, E., et al., *Effect of Lanreotide on Kidney Function in Patients With Autosomal Dominant Polycystic Kidney Disease: The DIPAK 1 Randomized Clinical Trial.* JAMA, 2018. **320**(19): p. 2010-2019.

382. Hughes, C.S., et al., *Single-pot, solid-phase-enhanced sample preparation for proteomics experiments.* Nat Protoc, 2019. **14**(1): p. 68-85.

383. Kalra, H., et al., *Vesiclepedia: a compendium for extracellular vesicles with continuous community annotation.* PLoS Biol, 2012. **10**(12): p. e1001450.

384. Huber, W., et al., *Variance stabilization applied to microarray data calibration and to the quantification of differential expression.* Bioinformatics, 2002. **18 Suppl 1**: p. S96-104.

385. Valikangas, T., T. Suomi, and L.L. Elo, *A systematic evaluation of normalization methods in quantitative label-free proteomics.* Brief Bioinform, 2018. **19**(1): p. 1-11.

386. Jassal, B., et al., *The reactome pathway knowledgebase.* Nucleic Acids Res, 2020. **48**(D1): p. D498-D503.

387. Fabregat, A., et al., *Reactome pathway analysis: a high-performance in-memory approach.* BMC Bioinformatics, 2017. **18**(1): p. 142.

388. Charles J. Blijdorp, T.A.H., Kuang-Yu Wei, Martijn H. van Heugten, Dominique M. Bovée, Ricardo P.J. Budde, Jacqueline van de Wetering, Joost G.J. Hoenderop, Martin E. van Royen, Robert Zietse, David Severs, Ewout J. Hoorn, *Nephron Mass Determines the Excretion Rate of Urinary Extracellular Vesicles* Journal of Extracellular Vesicles, 2021. ***Accepted 8 dec 2021.***

389. Liu, Z., R.J. Tan, and Y. Liu, *The Many Faces of Matrix Metalloproteinase-7 in Kidney Diseases.* Biomolecules, 2020. **10**(6).

390. Wozniak, J., et al., *Key metalloproteinase-mediated pathways in the kidney.* Nat Rev Nephrol, 2021. **17**(8): p. 513-527.

391. Zhang, J., et al., *Serum Matrix Metalloproteinase-7 Level is Associated with Fibrosis and Renal Survival in Patients with IgA Nephropathy.* Kidney Blood Press Res, 2017. **42**(3): p. 541-552.

392. Zhou, D., et al., *Matrix Metalloproteinase-7 Is a Urinary Biomarker and Pathogenic Mediator of Kidney Fibrosis.* J Am Soc Nephrol, 2017. **28**(2): p. 598-611.

393. Jovanovic, V., et al., *Implication of matrix metalloproteinase 7 and the noncanonical wingless-type signaling pathway in a model of kidney allograft tolerance induced by the administration of anti-donor class II antibodies.* J Immunol, 2008. **180**(3): p. 1317-25.

394. Surendran, K., et al., *Matrilysin (MMP-7) expression in renal tubular damage: association with Wnt4.* Kidney Int, 2004. **65**(6): p. 2212-22.

395. Zhou, D., et al., *Kidney tubular beta-catenin signaling controls interstitial fibroblast fate via epithelial-mesenchymal communication.* Sci Rep, 2013. **3**: p. 1878.

396. Fu, H., et al., *Matrix metalloproteinase-7 protects against acute kidney injury by priming renal tubules for survival and regeneration.* Kidney Int, 2019. **95**(5): p. 1167-1180.

397. Tan, R.J., et al., *Tubular injury triggers podocyte dysfunction by beta-catenin-driven release of MMP-7.* JCI Insight, 2019. **4**(24).

398. Riera, M., S. Burtey, and M. Fontes, *Transcriptome analysis of a rat PKD model: Importance of genes involved in extracellular matrix metabolism.* Kidney Int, 2006. **69**(9): p. 1558-63.

399. Obermuller, N., et al., *A possible role for metalloproteinases in renal cyst development.* Am J Physiol Renal Physiol, 2001. **280**(3): p. F540-50.

400. Li, A., et al., *Canonical Wnt inhibitors ameliorate cystogenesis in a mouse ortholog of human ADPKD.* JCI Insight, 2018. **3**(5).

401. Kim, E., et al., *The polycystic kidney disease 1 gene product modulates Wnt signaling.* J Biol Chem, 1999. **274**(8): p. 4947-53.

402. Le, N.H., et al., *Aberrant polycystin-1 expression results in modification of activator protein-1 activity, whereas Wnt signaling remains unaffected.* J Biol Chem, 2004. **279**(26): p. 27472-81.

403. Qin, S., et al., *c-Met and NF-kappaB-dependent overexpression of Wnt7a and -7b and Pax2 promotes cystogenesis in polycystic kidney disease.* J Am Soc Nephrol, 2012. **23**(8): p. 1309-18.

404. Jia, J., et al., *MERIT, a cellular system coordinating lysosomal repair, removal and replacement.* Autophagy, 2020. **16**(8): p. 1539-1541.

405. Nowak, K.L. and C.L. Edelstein, *Apoptosis and autophagy in polycystic kidney disease (PKD).* Cell Signal, 2020. **68**: p. 109518.

406. Hamm, L.L., N. Nakhoul, and K.S. Hering-Smith, *Acid-Base Homeostasis.* Clin J Am Soc Nephrol, 2015. **10**(12): p. 2232-42.

407. Raphael, K.L., *Metabolic Acidosis in CKD: Core Curriculum 2019.* Am J Kidney Dis, 2019. **74**(2): p. 263-275.

408. Moranne, O., et al., *Timing of onset of CKD-related metabolic complications.* J Am Soc Nephrol, 2009. **20**(1): p. 164-71.

409. Shah, S.N., et al., *Serum bicarbonate levels and the progression of kidney disease: a cohort study.* Am J Kidney Dis, 2009. **54**(2): p. 270-7.

410. Kovesdy, C.P., J.E. Anderson, and K. Kalantar-Zadeh, *Association of serum bicarbonate levels with mortality in patients with non-dialysis-dependent CKD.* Nephrol Dial Transplant, 2009. **24**(4): p. 1232-7.

411. Menon, V., et al., *Serum bicarbonate and long-term outcomes in CKD.* Am J Kidney Dis, 2010. **56**(5): p. 907-14.

412. Navaneethan, S.D., et al., *Serum bicarbonate and mortality in stage 3 and stage 4 chronic kidney disease.* Clin J Am Soc Nephrol, 2011. **6**(10): p. 2395-402.

413. Dobre, M., et al., *Association of serum bicarbonate with risk of renal and cardiovascular outcomes in CKD: a report from the Chronic Renal Insufficiency Cohort (CRIC) study.* Am J Kidney Dis, 2013. **62**(4): p. 670-8.

414. Raphael, K.L., et al., *Higher serum bicarbonate levels within the normal range are associated with better survival and renal outcomes in African Americans.* Kidney Int, 2011. **79**(3): p. 356-62.

415. Wesson, D.E., J.M. Buysse, and D.A. Bushinsky, *Mechanisms of Metabolic Acidosis-Induced Kidney Injury in Chronic Kidney Disease.* J Am Soc Nephrol, 2020. **31**(3): p. 469-482.

416. Schutte, E., et al., *Serum Bicarbonate and Kidney Disease Progression and Cardiovascular Outcome in Patients With Diabetic Nephropathy: A Post Hoc Analysis of the RENAAL (Reduction of End Points in Non-Insulin-Dependent Diabetes With the Angiotensin II Antagonist Losartan) Study and IDNT (Irbesartan Diabetic Nephropathy Trial).* Am J Kidney Dis, 2015. **66**(3): p. 450-8.

417. de Brito-Ashurst, I., et al., *Bicarbonate supplementation slows progression of CKD and improves nutritional status.* J Am Soc Nephrol, 2009. **20**(9): p. 2075-84.

418. Mahajan, A., et al., *Daily oral sodium bicarbonate preserves glomerular filtration rate by slowing its decline in early hypertensive nephropathy.* Kidney Int, 2010. **78**(3): p. 303-9.

419. Bi, C.s.g., *Clinical and cost-effectiveness of oral sodium bicarbonate therapy for older patients with chronic kidney disease and low-grade acidosis (BiCARB): a pragmatic randomised, double-blind, placebo-controlled trial.* BMC Med, 2020. **18**(1): p. 91.

420. Groopman, E.E., et al., *Diagnostic Utility of Exome Sequencing for Kidney Disease.* N Engl J Med, 2019. **380**(2): p. 142-151.

421. Meijer, E., et al., *Rationale and design of the DIPAK 1 study: a randomized controlled clinical trial assessing the efficacy of lanreotide to Halt disease progression in autosomal dominant polycystic kidney disease.* Am J Kidney Dis, 2014. **63**(3): p. 446-55.

422. Levey, A.S., et al., *A new equation to estimate glomerular filtration rate.* Ann Intern Med, 2009. **150**(9): p. 604-12.

423. Maroni, B.J., T.I. Steinman, and W.E. Mitch, *A method for estimating nitrogen intake of patients with chronic renal failure.* Kidney Int, 1985. **27**(1): p. 58-65.

424. Frassetto, L.A., et al., *Estimation of net endogenous noncarbonic acid production in humans from diet potassium and protein contents.* Am J Clin Nutr, 1998. **68**(3): p. 576-83.

425. Levey, A.S., et al., *GFR decline as an end point for clinical trials in CKD: a scientific workshop sponsored by the National Kidney Foundation and the US Food and Drug Administration.* Am J Kidney Dis, 2014. **64**(6): p. 821-35.

426. Chang, W.X., et al., *Predictors and the Subsequent Risk of End-Stage Renal Disease - Usefulness of 30% Decline in Estimated GFR over 2 Years.* PLoS One, 2015. **10**(7): p. e0132927.

427. Coresh, J., et al., *Decline in estimated glomerular filtration rate and subsequent risk of end-stage renal disease and mortality.* JAMA, 2014. **311**(24): p. 2518-2531.

428. Vallet, M., et al., *Urinary ammonia and long-term outcomes in chronic kidney disease.* Kidney Int, 2015. **88**(1): p. 137-45.

429. Raphael, K.L., et al., *Urine Ammonium Predicts Clinical Outcomes in Hypertensive Kidney Disease.* J Am Soc Nephrol, 2017. **28**(8): p. 2483-2490.

430. Banerjee, T., et al., *High Dietary Acid Load Predicts ESRD among Adults with CKD.* J Am Soc Nephrol, 2015. **26**(7): p. 1693-700.

431. Zittema, D., et al., *Vasopressin, copeptin, and renal concentrating capacity in patients with autosomal dominant polycystic kidney disease without renal impairment.* Clin J Am Soc Nephrol, 2012. **7**(6): p. 906-13.

432. Olteanu, D., et al., *Increased Na+/H+ exchanger activity on the apical surface of a cilium-deficient cortical collecting duct principal cell model of polycystic kidney disease.* Am J Physiol Cell Physiol, 2012. **302**(10): p. C1436-51.

433. Wesson, D.E. and J. Simoni, *Acid retention during kidney failure induces endothelin and aldosterone production which lead to progressive GFR decline, a situation ameliorated by alkali diet.* Kidney Int, 2010. **78**(11): p. 1128-35.

434. Loghman-Adham, M., et al., *The intrarenal renin-angiotensin system in autosomal dominant polycystic kidney disease.* Am J Physiol Renal Physiol, 2004. **287**(4): p. F775-88.

435. Saigusa, T., et al., *Suppressing angiotensinogen synthesis attenuates kidney cyst formation in a Pkd1 mouse model.* FASEB J, 2016. **30**(1): p. 370-9.

436. Salih, M., et al., *Urinary renin-angiotensin markers in polycystic kidney disease.* Am J Physiol Renal Physiol, 2017. **313**(4): p. F874-F881.

437. Su, Z., et al., *Excessive activation of the alternative complement pathway in autosomal dominant polycystic kidney disease.* J Intern Med, 2014. **276**(5): p. 470-85.

438. Torres, J.A., et al., *Crystal deposition triggers tubule dilation that accelerates cystogenesis in polycystic kidney disease.* J Clin Invest, 2019. **130**: p. 4506-4522.

439. Brenner, R.J., et al., *Incidence of radiographically evident bone disease, nephrocalcinosis, and nephrolithiasis in various types of renal tubular acidosis.* N Engl J Med, 1982. **307**(4): p. 217-21.

440. Nishiura, J.L., et al., *Evaluation of nephrolithiasis in autosomal dominant polycystic kidney disease patients.* Clin J Am Soc Nephrol, 2009. **4**(4): p. 838-44.

441. Allardet-Servent, J., et al., *Point-of-Care Versus Central Laboratory Measurements of Hemoglobin, Hematocrit, Glucose, Bicarbonate and Electrolytes: A Prospective Observational Study in Critically Ill Patients.* PLoS One, 2017. **12**(1): p. e0169593.

442. Hole, P., et al., *Interlaboratory comparison of size measurements on nanoparticles using nanoparticle tracking analysis (NTA).* J Nanopart Res, 2013. **15**: p. 2101.

443. Chen, L., C.L. Chou, and M.A. Knepper, *A Comprehensive Map of mRNAs and Their Isoforms across All 14 Renal Tubule Segments of Mouse.* J Am Soc Nephrol, 2021.

444. Wyss, M. and R. Kaddurah-Daouk, *Creatine and creatinine metabolism.* Physiol Rev, 2000. **80**(3): p. 1107-213.

445. Keshaviah, P.R., et al., *Lean body mass estimation by creatinine kinetics.* J Am Soc Nephrol, 1994. **4**(7): p. 1475-85.

446. Welle, S., et al., *Utility of creatinine excretion in body-composition studies of healthy men and women older than 60 y.* Am J Clin Nutr, 1996. **63**(2): p. 151-6.

447. Sinkeler, S.J., et al., *Creatinine excretion rate and mortality in type 2 diabetes and nephropathy.* Diabetes Care, 2013. **36**(6): p. 1489-94.

448. ter Maaten, J.M., et al., *Creatinine excretion rate, a marker of muscle mass, is related to clinical outcome in patients with chronic systolic heart failure.* Clin Res Cardiol, 2014. **103**(12): p. 976-83.

449. Ix, J.H., et al., *Urinary creatinine excretion rate and mortality in persons with coronary artery disease: the Heart and Soul Study.* Circulation, 2010. **121**(11): p. 1295-303.

450. Oterdoom, L.H., et al., *Urinary creatinine excretion reflecting muscle mass is a predictor of mortality and graft loss in renal transplant recipients.* Transplantation, 2008. **86**(3): p. 391-8.

451. Hultin, S., D.W. Johnson, and S.V. Badve, *Recent evidence on the effect of treatment of metabolic acid on the progression of kidney disease.* Curr Opin Nephrol Hypertens, 2021. **30**(5): p. 467-473.

452. Raphael, K.L., et al., *Sodium Bicarbonate Supplementation and Urinary TGF-beta1 in Nonacidotic Diabetic Kidney Disease: A Randomized, Controlled Trial.* Clin J Am Soc Nephrol, 2020. **15**(2): p. 200-208.

453. Torres, J.A., et al., *Crystal deposition triggers tubule dilation that accelerates cystogenesis in polycystic kidney disease.* J Clin Invest, 2019. **129**(10): p. 4506-4522.

CHAPTER 9

Nederlandse samenvatting

Nederlandse samenvatting

De aanwezigheid van nierziekte kan worden vastgesteld door een toename van serum creatinine, de aanwezigheid van erytrocyturie, proteïnurie en/of nierafwijkingen bij beeldvorming. Het verkrijgen van een nierbiopt is momenteel de enige methode om nierziekte op histologisch en moleculair niveau te bestuderen. Dit is echter een invasieve procedure met potentiële risico's en wordt daarom alleen uitgevoerd wanneer nierweefsel daadwerkelijk nodig is om een definitieve diagnose te stellen die de behandeling kan beïnvloeden, dan wel informatie kan verschaffen over ziekteprogressie of prognose. Een belangrijke uitdaging is daarom het identificeren van methoden om nierziekte te analyseren op minder invasieve wijze. Urine is hierbij een logische denkrichting omdat het een product is van de nieren en kan worden geanalyseerd zonder gebruik van invasieve procedures. Urine extracellulaire vesikels (uEVs) zijn van bijzonder groot belang omdat ze processen weerspiegelen van cellen in de nierbuisjes, en markers bevatten voor een groot aantal glomerulaire en tubulaire nierziekten. De studies in dit proefschrift zijn gericht op het versnellen van klinische toepassing van uEVs door het verbeteren van normalisatiemethodes en betrouwbare 'high-throughput' karakteriseren van uEVs (deel 1), en door het bestuderen van uEVs als biomarkers in een specifieke nierziekte, namelijk autosomaal dominante polycysteuze nierziekte (ADPKD, deel 2).

Deel 1 urine extracellulaire vesikels: de weg naar de kliniek

UEVs zijn afkomstig van alle cellen van het urogenitale stelsel, met de kanttekening dat er ook aanwijzingen zijn dat een beperkt aantal uEVs uit de bloedsomloop komen. Ze bevatten eiwitten, RNA, lipiden en metabolieten, die kunnen worden gebruikt als biomarkers voor nier-, urologische en andere ziekten. **Hoofdstuk 2** beschrijft de huidige stand van zaken in het veld met betrekking tot uEV analyse en beschrijft uitdagingen en kennishiaten in het veld. Er worden aanbevelingen gedaan om de nauwkeurigheid, reproduceerbaarheid en interoperabiliteit in uEV-onderzoek te verbeteren bij het verzamelen en verwerken van urine, en bij isolatie, karakterisering en normalisatie. De beschrijving van de verzameling, verwerking en opslag van uEVs dient grondig te zijn, omdat dit belangrijke bronnen zijn van variatie, en beperkend werken op reproduceerbaarheid van data. Een verzameling van urine kan bijvoorbeeld worden gedaan door alle urine op te vangen, dan wel eerst wat uit te plassen en dan pas te verzamelen, dan wel door alle urine te verzamelen binnen een bepaalde tijd (meestal 24 uur). Al deze manieren hebben hun eigen voordelen en beperkingen. UEVs kunnen worden geïsoleerd door ultracentrifuge, filtratie, precipitatie, hydrostatische dialyse, ultrafiltratie, chromatografie met uitsluiting op grootte, sucrosegradiënt, akoestisch gevangen en selectie op immunologische eigenschappen. Isolatie (of verrijking) van uEVs is essentieel voor bepaalde methodes om uEVs te karakteriseren zoals massa spectrometrie en elektronenmicroscopie. De werkzaamheid en opbrengst van al deze methoden is echter beperkt en variabel tussen technieken en operators. Belangrijke uitdagingen zijn onder meer co-isolatie van uromoduline en - in het geval van glomerulaire aandoeningen - albumine en andere eiwitten uit de bloedsomloop. Directe kwantificering en karakterisering van uEVs (met behulp van NTA, FCM, TRPS, EVQuant, TR-FIA enz.) heeft de potentie om de variabiliteit van isolatietechnieken te omzeilen en kan een belangrijke stap zijn naar klinische toepassing. Vooral normalisatie is belangrijk in uEV-onderzoek vanwege de variatie in de urineconcentratie, onbekende uEV-uitscheiding door verschillende organen en de variabiliteit die veroorzaakt wordt door isolatie. UEV-excretie kan worden gerapporteerd als een relatieve excretie - een verhouding van een uEV-biomarker tot totale uEV, uEV-biomarker, totaal eiwit of ziekte-specifiek eiwit - of absolute excretie, die kan worden gemeten door een 24-uurs urineverzameling of kan worden benaderd door urine creatinine.

Hoofdstuk 3 is een commentaar op een publicatie van Sabaratnam *et al.*, waarin gerapporteerd werd dat er geen correlatie was gevonden tussen de hoeveelheid tubulaire transporteiwitten in de nier – chirurgisch uitgenomen in het kader van een niertumor - ten opzichte van uEVs verzameld vóór de uitname. In dit hoofdstuk stellen we dat correlatie niet gevonden wordt doordat er tijd zit tussen het inzamelen van urine en het opslaan van het nierweefsel, waardoor de eiwitexpressie waarschijnlijk al veranderd is. De analyse van deze eiwitten in uEVs is daarom waarschijnlijk meer bijdragend tijdens nierziekte, omdat de normale regulatie overstemd wordt door ziekte, hetgeen een algemene en langdurige verandering veroorzaakt in de hoeveelheid eiwit of RNA. Daarnaast stellen we dat normalisatie cruciaal is voor de juiste interpretatie van de aantallen uEVs en niet alleen afhankelijk is van het juiste gebruik van urine creatinine als instrument om te normaliseren, maar ook van de niergrootte.

In **hoofdstuk 4** beoogden we de normalisatie van uEVs door middel van urine creatinine te valideren. Hiertoe hebben we uEVs rechtstreeks gekwantificeerd in urine – in plaats van na isolatie – met behulp van NTA, EVQuant en TRFIA. Om de hypothese te bestuderen dat urine creatinine kan worden gebruikt voor normalisatie van uEVs, hebben we uEVs gekwantificeerd in verdunde en geconcentreerde urine verkregen door gezonde deelnemers respectievelijk te laten drinken en dorsten. We hebben de resultaten gevalideerd in willekeurige urines van vijftien gezonde proefpersonen en zesentwintig patiënten met ADPKD. In deze verschillende situaties was urine creatinine sterk gecorreleerd met het aantal uEVs, wat suggereert dat creatinine goed kan worden gebruikt als normalisatievariabele. UEV kwantificatie met EVQuant was sterk vergelijkbaar met kwantificatie middels NTA, hoewel NTA minder uEVs detecteerde en leidde tot vertekende resultaten in verdunde urinemonsters. We hebben laten zien dat dit verklaard kan worden door een lagere detectielimiet van NTA. Deze ligt namelijk rond 70 nm, terwijl bij elektronenmicroscopie (EM) de meeste uEVs kleiner zijn. Verder tonen we door het gebruik van EM en NTA dat uEVs groter zijn in verdunde urines, wat de vertekende resultaten

in vergelijking tot EVQuant verder verklaart. Een belangrijke bevinding is dat de resultaten van NTA beïnvloed worden door het eiwit uromoduline, hetgeen eerdere resultaten bevestigt. CD9-TR-FIA bleek variabelere uEV-tellingen op te leveren dan NTA en EVQuant. Bovendien komen de voor TRFIA gebruikte selectie-eiwitten CD9 en CD63 niet in alle delen van de urinewegen tot expressie, maar zijn ze vooral aanwezig in het distale deel van het nefron, het urotheel en de prostaat. Dit toont aan dat selectiemethodes zoals TR-FIA niet zomaar kunnen worden gebruikt voor markers van alle oorsprongen. Tenslotte tonen we aan dat intracellulaire eiwitepitopen kunnen worden gelokaliseerd door gebruik te maken van natriumdodecylsulfaat (een zeepsoort), omdat dit de membranen van uEVs permeabiliseert, maar de uEVs zelf intact laat (hetgeen is bevestigd met behulp van EM en NTA). Door deze bevinding kunnen NTA en EVQuant ook gebruikt worden voor eiwitanalyse waarbij alleen antilichamen beschikbaar zijn tegen intracellulaire epitopen. Door antilichamen tegen het intracellulaire epitoop te vergelijken met antilichamen tegen het extracellulaire epitoop van AQP2 hebben we kunnen aantonen dat een deel van het AQP2-eiwit een omgekeerde topologie heeft. Hiermee bevestigen we een oudere *in vivo* bevinding, namelijk dat een deel van de uEVs binnenste buiten gekeerd is.

Hoofdstuk 5 beschrijft de relatie tussen nefronmassa en uEV-excretie in een patiëntenstudie en twee dierstudies. Hiertoe verzamelden we een portie en 24-uurs urine van negentien nierdonoren voor en na donornefrectomie. We bepaalden de niergrootte door middel van CT-scans vóór nefrectomie, en nierfunctie met behulp van 24-uurs kreatinineklaring en eGFR zowel voor als na nefrectomie. Ten eerste bevestigden we hiermee de resultaten in **hoofdstuk 4** dat urine-creatinine en uEV-concentratie sterk gecorreleerd zijn, maar vonden bovendien dat vergelijking van uEV-excretie tussen individuen wordt verbeterd door te corrigeren voor uitscheiding van creatinine via de urine (of spiermassa als er geen getimede verzameling beschikbaar is). Met behulp van deze correctie konden we aantonen dat mannen meer uEVs uitscheiden dan vrouwen, hetgeen we bevestigden in 24-uurs verzamelingen. Dit is in tegenspraak met een eerdere studie waarin werd geconcludeerd dat vrouwen juist meer uEVs uitscheiden. De auteurs van deze publicatie rapporteerden dat vrouwen een hogere uEV tot creatinine-ratio hadden, maar corrigeerden niet voor een lagere spiermassa en dus voor creatinine-uitscheiding. Ten tweede ontdekten we dat niergrootte, nierfunctie en uEV-excretie sterk gecorreleerd zijn. Donornefrectomie verminderde de uEV-excretie van CD9+ uEVs. Hierbij waren uEVs uit de glomerulus en proximale tubulus meer vertegenwoordigd dan uEVs uit het distale nefron, hetgeen impliceert dat er compensatoire groei is van de proximale tubulus na donornefrectomie. Daarnaast bestudeerden we de relatieve bijdrage van "post-nier uEV uitscheiding" (ofwel uEV uitscheiding door ureter, blaas, prostaat) bij negen patiënten met een eenzijdige nefrostomiedrain. Hiertoe vergeleken we de urine van de nefrostomiedrain met de urine uit de blaas in iedere patiënt afzonderlijk. De monsters werden geanalyseerd met behulp van gelabelde massaspectrometrie, waarbij we aantoonden dat de urinewegen na de nieren slechts een handvol unieke eiwitten toevoegden en de hoeveelheid van alle eiwitten niet verhoogden. Hiermee toonden we aan dat de uEV-uitscheiding van de urinewegen na de nieren beperkt is in vergelijking met uitscheiding door de nier. Het effect van nefronverlies werd verder bestudeerd in ratten die een schijnoperatie, uninefrectomie of 5/6e nefrectomie ondergingen. De controledieren vertoonden een toename in uEV-excretie gemeten door NTA, terwijl uninefrectomie en 5/6e nefrectomie leidden tot een significante afname van uEV-excretie. Deze afname was minder dan verwacht op basis van het aantal verwijderde nefronen, maar dit correleerde met de (geschatte) hypertrofie van het resterende nierweefsel.

Deel 2 – urine extracellulaire vesikels en andere markers van polycysteuze nierziekte

In **hoofdstuk 6** hebben we gebruik gemaakt van massa spectrometrie om vroege markers van ADPKD-progressie te identificeren. Hierbij namen we urinemonsters van controlepatiënten uit de DIPAK-interventiestudie (**appendix**), waarin we onderscheid maakten tussen patiënten met snelle ziekteprogressie (SZP) en patiënten met langzame ziekteprogressie (LZP). Deze werden gekoppeld op basis van leeftijd, geslacht, eGFR- en PKD-mutatie en bleken tevens een vergelijkbare prognose te hebben op basis van Mayo-klasse en PROPKD-scores. In het ontdekkingscohort (n = 10) vonden we 65 eiwitten en in het verificatiecohort 36 eiwitten die significant verschillend tot expressie kwamen tussen SZP- en LZP-patiënten. Twee eiwitten kwamen terug in beide cohorten; matrilysin (MMP7) kwam meer tot expressie in patiënten met SZP terwijl CHMP4A meer tot expressie kwam in patiënten met LZP. Met behulp van Western Blotting werden deze eiwitten bestudeerd in een onafhankelijk validatiecohort (n = 24), waarin MMP7 in dezelfde richting veranderde als in de ontdekkings-/verificatiecohorten met een hoge sensitiviteit en specificiteit. Belangrijk is dat MMP7 hoger bleef gedurende het vervolg van de interventiestudie. Aangezien MMP7 ook meer tot expressie komt in nierweefsel van ADPKD-patiënten en andere nierziektes, en gerelateerd is aan acute en chronische nierschade, kan MMP7 een interessante vroege progressiemarker zijn, niet alleen bij ADPKD maar ook bij andere nierziekten.

In **hoofdstuk 7** bestudeerden we de associatie tussen serumbicarbonaat en ADPKD-progressie. Een afname van nierfunctie leidt tot een verminderde zuuruitscheiding en tot metabole acidose. Behandeling van metabole acidose verbetert de prognose bij patiënten met (niet-ADPKD) chronische nierinsufficiëntie. Bij ADPKD is de zuuruitscheiding zelfs al verminderd bij patiënten met een behouden nierfunctie, en in diermodellen blijkt behandeling met alkali de ziekteprogressie te stoppen. In onze studie onderzochten we serumbicarbonaat bij 309 patiënten uit de DIPAK1 interventiestudie (**appendix**), en onderzochten we of dit verband hield met ADPKD-uitkomsten, waaronder verslechtering van de nierfunctie – gedefinieerd als 30% afname van eGFR dan wel eindstadium nierfalen (primaire uitkomst), TKV-groei en eGFR-afname (se-

cundaire uitkomsten). We toonden aan dat een hoog-normaal serumbicarbonaat geassocieerd was met een lager risico op verslechtering van de nierfunctie, vergeleken met een laag-normaal serumbicarbonaat. Bovendien was de hoogte van serumbicarbonaat gecorreleerd met de mate van eGFR-afname. Dit was onafhankelijk van geslacht, leeftijd en andere variabelen waarvan bekend is dat ze verband houden met ADPKD-progressie. Serumbicarbonaat was echter niet gerelateerd aan TKV- of TLV-groei. Deze studie suggereert daarom dat suppletie met bicarbonaat ook gunstig kan zijn voor patiënten met ADPKD, hoewel interventiestudies nodig zijn om dit te bevestigen. Opvallend was dat patiënten met ADPKD in ons cohort een hoog serumbicarbonaat hadden, wat suggereert dat de streefwaarde voor serumbicarbonaat hoger kan zijn bij ADPKD dan bij andere oorzaken van chronische nierinsufficiëntie.

In de **appendix** wordt een open-label klinische studie beschreven waarin 309 patiënten met ADPKD werden gerandomiseerd tussen Lanreotide (n = 153) en standaardzorg (n = 152). De primaire uitkomstmaat was de jaarlijkse verandering in eGFR, hetgeen werd beoordeeld door het beloop van de eGFR te meten tijdens de behandelfase van 2,5 jaar. Secundaire uitkomsten waren verandering in eGFR voor en na behandeling, incidentie van verslechtering van de nierfunctie (start van dialyse of 30% afname van eGFR), verandering in TKV en verandering in kwaliteit van leven. Bij patiënten met ADPKD in een later stadium vertraagde behandeling met Lanreotide in vergelijking met standaardzorg de achteruitgang van de nierfunctie niet gedurende 2,5 jaar follow-up. De patiënten uit **hoofdstuk 6** en 7 namen deel aan deze studie.

CHAPTER 10

About the author

CURRICULUM VITAE

Charles Blijdorp was born on June 11th, 1990, in Leiderdorp. In 2007 he was admitted to the Young Honours program of the Technical University in Delft, where he studied implementation of the Hydrogen Car (2007) and Fear Simulations for patients with anxiety disorders (2008). He started his medical training at the Erasmus Medical Center in Rotterdam in 2008, from which he graduated in 2015 after elective internships at the Intensive Care (Delft), Internal Medicine (Dordrecht) and Emergency Medicine (Paramaribo, Suriname). During his study he was co-founder of Vocal Group Utrecht and took place in the board as chairman and treasurer, organizing over fifty performances among which at *Sensation White* (Amsterdam, 2015), and developing several music productions, among which *Lost in Space* (Utrecht, Rotterdam, Tianjin, Xuzhou, Nanjing en Shaoxing, 2012).

He was admitted to the Research Master Molecular Medicine in 2009, from which he graduated in 2016 on the topic of *Salt and Hypertension* at the Division of Nephrology and Transplantation of the Erasmus Medical Center. Here, he started his PhD under supervision of dr. M. Salih, prof. dr. E.J. Hoorn and prof. dr. R. Zietse, which led to this thesis. During this time, he also was coordinating research physician of the DIPAK intervention trial and observational cohort in Rotterdam (both supported by the Dutch Kidney Foundation), organized a patient symposium on polycystic kidney disease, and was part of the steering committee of the Urine Task Force of the International Society of Extracellular Vesicles, which resulted in the position paper that was published in 2021 in the *Journal of Extracellular Vesicles*. As part of this steering committee he organized the Inaugural Virtual Symposium on Urinary Extracellular Vesicles in 2022 (uEV2022).

In 2019 he started working as senior house officer at the Franciscus Gasthuis & Vliet land hospital in Rotterdam (supervisor: dr. Y.C. Schrama). In 2022 he started his residency in Internal Medicine at the Reinier de Graaf hospital in Delft (supervisor: dr. Boom). He currently lives in Moordrecht with his wife Brigitte, and three children, Anna, Oscar and Berend.

List of publications

Martijn H van Heugten*, **Charles J Blijdorp***, Usha M. Musterd-Bagghoe, Karel Besztarosti, Jeroen A A Demmers, Hester van Willigenburg, Esther Meijer, Ron T Gansevoort, Robert Zietse, Mahdi Salih*, Ewout J Hoorn*, on behalf of the DIPAK consortium.
Matrilysin (MMP-7) in Urinary Extracellular Vesicles Predicts Rapid Disease Progression in Polycystic Kidney Disease. *Submitted.*

Charles J Blijdorp, Dylan Burger, Alicia Llorente, Elena . Martens-Uzunova, Uta Erdbrügger.
Extracellular Vesicles as Novel Players in Kidney Disease. *J Am Soc Nephrol.* 2022. ASN.2021091232.

Charles J Blijdorp, Thomas A Hartjes, Kuang-Yu Wei, Martijn H van Heugten, Dominique M Bovée, Ricardo Budde, Jacqueline van de Wetering, Joost G J Hoenderop, Martin E van Royen, Robert Zietse, David Severs, Ewout J Hoorn.
Nephron mass determines the excretion rate of urinary extracellular vesicles. *J Extracell Vesicles.* 2022. 11: e12181.

Elena S Martens-Uzunova, **Charles J Blijdorp**, Dylan Burger, Uta Erdbrügger, Alicia Llorente.
Urinary Extracellular Vesicles in Urology: Current Successes and Challenges Ahead. *Eur Urol.* 2022. 81:127-128.

Uta Erdbrügger U*, **Charles J Blijdorp***, Irene V Bijnsdorp, Francesc E Borràs, Dylan Burger, Benedetta Bussolati, James Brian Byrd, Aled Clayton, James W Dear, Juan M Falcón-Pérez, Cristina Grange, Andrew F Hill, Harry Holthöfer, Ewout J Hoorn, Guido Jenster, Connie R Jimenez, Kerstin Junker, John Klein, Mark A Knepper, Erik H Koritzinsky, James M Luther, Metka Lenassi, Janne Leivo, Inge Mertens, Luca Musante, Eline Oeyen, Maija Puhka, Martin E van Royen, Catherine Sánchez, Carolina Soekmadji, Visith Thongboonkerd, Volkert van Steijn, Gerald Verhaegh, Jason P Webber, Kenneth Witwer, Peter S T Yuen, Lei Zheng, Alicia Llorente*, and Elena S Martens-Uzunova*.
Urinary Extracellular Vesicles: A Position Paper by the Urine Task Force of the International Society for Extracellular Vesicles. *J Extracell Vesicles.* 2021. 10: e12093.

Charles J Blijdorp*, Omar A T Tutakhel*, Thomas A Hartjes, Thierry P P van den Bosch, Martijn H van Heugten, Juan Pablo Rigalli, Rob Willemsen, Usha M Musterd-Bhaggoe, Eric R Barros, Roger Carles-Fontana, Cristian A Carvajal, Onno J Arntz, Fons A J van de Loo, Guido Jenster, Marian C Clahsen-van Groningen, Cathy A Cuevas, David Severs, Robert A Fenton, Martin E van Royen, Joost G J Hoenderop, René J M Bindels and Ewout J Hoorn.

Comparing Approaches to Quantify, Characterize, and Normalize Urinary Extracellular Vesicles. *J Am Soc Nephrol*. 2021. 32: 1210-1226.

Sophie E Aapkes, Robbert J de Haas, Lucas H P Bernts, **Charles J Blijdorp**, Sosha E I Dekker, Maatje D A van Gastel, Esther Meijer, Abigail Veldman, Joost P H Drenth, Ron T Gansevoort.
Incident Gallstones During Somatostatin Analog Treatment are Associated with Acute Biliary Complications Especially After Discontinuation. *Drugs R D*. 2021. 21:179-188.

Charles J Blijdorp, David Severs, Usha M Musterd-Bhaggoe, Ron T Gansevoort, Robert Zietse, Ewout J Hoorn.
Serum bicarbonate is associated with kidney outcomes in autosomal dominant polycystic kidney disease. *Nephrol Dial Transplant*. 2021. 36: 2248-2255.

Charles J Blijdorp, Ewout J Hoorn.
Urinary extracellular vesicles: mothership connection. *Am J Physiol Renal Physiol*. 2019. 317: F648-F649.

Rene M M van Aerts, Wietske Kievit, Hedwig M A D'Agnolo, **Charles J Blijdorp**, Niek F Casteleijn, Shosha E I Dekker, Johan W de Fijter, Maatje van Gastel, Tom J Gevers, Liyanne F M van de Laarschot, Marten A Lantinga, Monique Losekoot, Esther Meijer, A Lianne Messchendorp, Myrte K Neijenhuis, Michelle J Pena, Dorien J M Peters, Mahdi Salih, Darius Soonawala, Edwin M Spithoven, Folkert W Visser, Jack F Wetzels, Robert Zietse, Ron T Gansevoort, Joost P H Drenth.
Lanreotide Reduces Liver Growth in Patients with Autosomal Dominant Polycystic Liver and Kidney Disease. *Gastroenterology*. 2019. 157:481-491.

Lennart Tonneijk*, Marcel H A Muskiet*, **Charles J Blijdorp**, Mark M Smits, Jos W Twisk, Mark H H Kramer, A H J Danser, Michaela Diamant, Jaap A Joles, Ewout J Hoorn, Daniël H van Raalte.
Renal tubular effects of prolonged therapy with the GLP-1 receptor agonist lixisenatide in patients with type 2 diabetes mellitus. *Am J Physiol Renal Physiol*. 2019. 316:F231-F240.

Esther Meijer*, Folkert W Visser*, Rene M M Van Aerts, **Charles J Blijdorp**, Niek F Casteleijn, Hedwig M A D'Agnolo, Shosha E I Dekker, Joost P H Drenth, Johan W de Fijter, Maatje D A van Gastel, Tom J Gevers, Marten A Lantinga, Monique Losekoot, A Lianne Messchendorp, Myrte K Neijenhuis, Michelle J Pena, Dorien J M Peters, Mahdi Salih, Darius Soonawala, Edwin M Spithoven, Jack F Wetzels, Robert Zietse, Ron T Gansevoort.
Effect of Lanreotide on Kidney Function in Patients with Autosomal Dominant Polycystic Kidney Disease: The DIPAK 1 Randomized Clinical Trial. *JAMA*. 2018. 320: p. 2010-2019.

* Equal contributions

PhD Portfolio

PhD candidate:	Charles Johannes Blijdorp
PhD period:	June 2016 – September 2019
Erasmus MC department:	Internal Medicine, Division of Nephrology & Transplantation
Research school:	Molecular Medicine
Promotoren:	Prof. dr. E.J. Hoorn
	Prof. dr. R. Zietse
Copromotor:	Dr. M. Salih

Clinical research courses	**Year**	**ECTS**
Patient-Oriented research (CPO)	2016	0.2
Basic course on rules and organization of clinical trials (BROK)	2017	1
Rotterdam Course in Electrolyte and Acid-Base Disorders	2017	0.3
Dutch Kidney Foundation (DKF) Winter School	2017	1.2
Autosomal Dominant Polycystic Kidney Disease, Amersfoort	2017	0.3
Scientific Integrity	2018	0.3
Regional refresher course nephrology, Rotterdam**	2018	0.3
DIPAK symposium for patients, Rotterdam**/***	2018	1.6
Scientific courses		
Optical Imaging Course (OIC)	2015	1.8
Seminar NaCl (D Muller)	2016	0.1
Extracellular Vesicles Education Day (ISEV), Rotterdam	2016	0.4
Microvesicles symposium (Erasmus MC)	2016	0.1
Massive Open Online Course (MOOC) Extracellular Vesicles (1)	2016	0.7
Famelab / Shakespeare, Rotterdam	2016	0.1
Biomedical Statistics (NIHES)	2017	5.7
Teaching activities		
Supervising master's thesis of medical student	2017	0.6

National and international conferences	Year	ECTS
ISEV meeting, Rotterdam	2016	1.3
Hypertension symposium, Rotterdam	2016	0.2
Kidney Week (ASN), Chicago	2016	1.4
Nederlandse Nefrologiedagen, Veldhoven	2017	0.4
Kidney Week (ASN), New Orleans*	2017	1.6
NL-SEV meeting, Amsterdam*	2017	0.5
Regenerative Medicine, Rotterdam	2018	0.2
ISEV meeting, Barcelona*/**	2018	1.7
Kidney Physiology, San Diego**	2018	0.5
Kidney Week (ASN), San Diego*	2018	1.6
NL-SEV meeting, Amsterdam*	2018	0.5
Kidney Week (ASN), Washington DC* (3x)	2019	1.9
Urine task force symposium (ISEV/ASN), Washington DC**/***	2019	0.4
Other attendances		
New Kids on the block (NFN) - annually	2016-19	0.9
Najaarssymposium (NFN)* - annually	2016-17	0.7
PLAN (Platform researchers in Nephrology) - annually	2016-19	0.9
Molecular Medicine Day - annually	2016-17	0.6
Erasmus MC Internal Medicine Science Days ** - annually	2018-19	1
Internal Medicine trimester meetings ** - quarterly	2017-19	1.1
Laboratory meetings (Pharmacology) ** (7x) - weekly	2016-19	4.2
Research Group meetings (Nephrology) ** (12x) - weekly	2016-19	4.9
Nephrology & Transplantation meetings ** - weekly	2016-19	1.6
Nephrology Journal Club - weekly	2016-19	0.7
Academic Center of Excellence Kidney & Hypertension - monthly	2018-19	0.7
Quarterly DIPAK research meetings ** (5x) - quarterly	2016-19	1.8
Innovation Grant Meetings ** (4x) – semi-annually	2016-19	1
Erasmus MC EV meeting ** (5x) - quarterly	2017-19	1.6
Total		**48.6**

* Poster presentation, ** oral presentation, *** self-organized

Dankwoord

Waar dit alles toe leidt? Ik geloof niet dat ik dat weet, en ik vraag me af of het iets uitmaakt. Het schrijven van dit proefschrift, en al het werk daaraan voorafgegaan, is met name een waardevolle, leerzame en mooie weg geweest door de mensen die betrokken zijn geweest.

Mijn promotor, prof. dr. E. J. Hoorn, beste Ewout, ik kwam je tegen als oudste coassistent bij een moeilijk geval van hypokaliëmie waarbij we vanuit het Albert Schweitzer contact zochten met jou om licht op de zaak te werpen. Je inspireerde me toen met de manier waarop je nadacht en nieuwe mogelijkheden zag. Ik voel me bevoorrecht dat ik met jou mocht samenwerken, want je gaf me alle ruimte om dingen te ontdekken, fouten te maken, en eigen (soms doodlopende) paadjes te bewandelen. Ik hoop nog veel van je te leren in de toekomst.

Tevens mijn promotor, prof. dr. R. Zietse, beste Bob, ik heb je altijd gezien als een wandelende bron van creativiteit. Vanaf het eerste moment bij de Wokkels merkte ik dat iedereen rechtop ging zitten als jij je handen voor je borst vouwde, peinzend voor je uitstaarde, alvorens een korte doch diepzinnige opmerking te plaatsen die het gehele onderzoek in een nieuw daglicht zette. Het heeft me dan ook niets verbaasd dat je, in een tijd dat je deed alsof je op vakantie was om je administratie te kunnen bijwerken, ook de contrabas leerde bespelen.

Mahdi Salih, als mijn copromotor, maar zeker ook als een der reuzen op wiens schouders ik mocht staan. Mede dankzij jouw (voor)werk, kennis en contacten is dit proefschrift geworden wat het geworden is. Ik kan erg waarderen hoe jij rustig iets in je opneemt en dan precies weet welke stappen je zou willen zetten. Ik hoop wat van die rust en wijsheid mee te nemen.

Leden van de promotiecommissie, prof. dr. Jan Danser, prof. dr. Carla Baan en prof. dr. Dorien Peters, bedankt voor het doornemen en positief beoordelen van mijn proefschrift. Beste Jan, dank voor de gastvrijheid op Ee14, en dat ik af en toe even mocht aankloppen. Je had vaak een verfrissende en kritische blik op mijn onderzoek, waardoor het beter is geworden. Carla, het was zeer leerzaam om te sparren bij de EV-meetings en tijdens etentjes van het Erasmus MC. Dorien, dank voor de samenwerking binnen de DIPAK. De vergaderingen waren dragelijk en zelfs enigszins grappig doordat jij ze voorzat en ik heb groot respect gekregen voor jou als wetenschapper en als ADPKD expert.

Ook dank aan prof. dr. Joost Hoenderop, dr. Esther Meijer en dr. Uta Erdbrügger voor het plaatsnemen in de promotiecommissie. Beste Joost, ik keek altijd uit naar de vergaderingen, het brainstormen over urine vesicles en uiteraard ook de etentjes die daarbij hoorden in Nijmegen of Rotterdam. Beste Esther, dank je voor de samenwerking bij de DIPAK-studie, je was

altijd heel benaderbaar en enorm behulpzaam. Dear Uta, I am honored to be part of the steering committee of the urine task force with you. Without you I feel there would not have been a position paper, nor the first ever uEV meeting.

Mijn paranimfen, David Severs en Anne Leskens. David, door jou heb ik het onderzoek echt leren kennen, toen je mijn supervisor was tijdens mijn onderzoeksmaster. Ik heb van jou geleerd om iets grondig aan te pakken en door te blijven zoeken. Dat ik hierdoor soms om tot diep in de avond mijn 192ste PCR sample aan het isoleren was, neem ik op de koop toe. Anne, dank voor de avonturen en de discussies over het leven. Door met jou (en Arjen) de hort op te gaan kon ik het hele onderzoek af en toe even van me af laten glijden, en lekker dansen of naar muziek luisteren. Of met twee volslagen onbekende Engelsen een vierstemmig Amazing Grace inzetten in een leegstaande kerk in Corsica (maken we die route nog eens af?).

De wokkelaars, bedankt voor jullie hulp en gezelligheid tijdens de Wokkels en tijdens de congressen. Madhi, David, Estrellita, Annegien, het was een feestje om met jullie Chicago te verkennen, van een champagne in de Roof Top Bar tot een cabaretvoorstelling in Down Town. Dominique, dank voor de mooie tijden tussen de alligators en tijdens Halloween in New Orleans. Martin, dank voor de scherpe gesprekken in San Diego. Frank, ik heb goede herinneringen aan meerdere (uit de hand gelopen) wandelingen in Washington. Martijn, wij hebben weliswaar nooit een congres samen beleefd (dat komt vast nog wel) maar je stond altijd voor me klaar toen ik weg was en de tijdschriften vroegen om meer experimenten bij mijn onderzoek. Mede dankzij jouw inzet is het werk beter geworden dan ik van tevoren had durven bedenken. Usha, bedankt voor al je inzet, zonder jou was ik nu nog steeds samples aan het isoleren.

De DIPAK-studie was een hele ervaring op zich, die mooi was om mee te maken samen met de arts-onderzoekers die in hetzelfde schuitje zaten (René, Shosha, Lianne, Niek, Bart, en de anderen) en natuurlijk de leiders van de studie, naast Esther en Dorien ook Folkert (bedankt voor het mede coördineren van de trial), prof. dr. Jack Wetzels, prof. dr. Joost Drenth, prof. dr. Johan De Fijter en prof. dr. Ron Gansevoort. Dank ook aan de collega's in het Erasmus MC die hebben meegeholpen aan de DIPAK-studie, de poli-assistenten, de radiologie, het triallab, en in het bijzonder de onderzoeksverpleegkundigen, Marieken, Monique, Nelly en Brigitte.
Brigitte (Nome), je was een ster, bedankt voor je geduld in het begin en je hulp gedurende de weg. Je had altijd mooie verhalen over je gezin, waar je ontzettend veel van houdt. Ik denk nog vaak aan jullie.

Dit proefschrift was niet tot stand gekomen zonder de vele samenwerkingen met mensen die een passie hebben voor urine vesicles. Onze collega's in Nijmegen, in het bijzonder naast prof. dr. Hoenderop ook prof. dr. René Bindels en Omar Tutakhel. Onze collega's van de urologie in het Erasmus, waaronder Martin van Royen, Thomas Hartjes en Guido Jenster. Thomas, bedankt voor al je hulp met de EVQuant, de OPERA en de bijbehorende berekeningen, het proefschrift is erdoor op een hoger level gekomen.

Dear (Uta,) Elena, Alicia and Dylan, it is a pleasure to be part of the steering committee of the urine task force with you. I was thrilled to see the interest that has been evoked in the field, with over 300 registrants for our uEV meeting. I am looking forward to our future efforts in the uEV field. All the members of the urine task force, in particular those in the normalization work group, thanks for the interesting meetings, the brainstorm sessions and exciting plans that we are making.

Ik wil de patiënten bedanken die hebben meegewerkt aan de studies beschreven in dit proefschrift. Jullie hebben veel van jullie tijd geïnvesteerd in het onderzoek, en bijgedragen aan meer kennis over cystenieren en andere nierziekten.

De collega's van de farmacologie, ik heb genoten van jullie gastvrijheid, de lunches en de borrels samen, en de uitstekende kerstdiners. Collega's in het Franciscus en het Reinier de Graaff, dank voor jullie steun en voor de leerzame periode.

Lieve vrienden, het was altijd lekker om het even over heel andere dingen te hebben tijdens mijn promotie. Ik kijk met heel veel liefde en plezier terug op deze tijd, al waren het de weekendjes in Friesland, de mooie en diepgaande momenten in de kring (en weekendjes en vakanties), samen zingen (liefst zonder de dansjes en dan met de ogen dicht proberen te mengen tot je het van binnen voelt). Nummers jammen, klaverjas avondjes bij een goed glas wijn, of met de bassen samen borrelen of naar een festival: het waren mooie tijden mede dankzij jullie.

Lieve familie, jullie zijn er altijd. Mama, je denkt altijd mee, zeer inhoudelijk, waardoor je me bij mijn onderzoek soms op andere sporen hebt gezet. Daarnaast sta je altijd voor me klaar, of het nu is om te sparren, of omdat Brigitte en ik er even samen uit moesten en je de kinderen weer moest opvangen. Mede door jou en papa konden we van de mooie dingen in het leven genieten, en meer doen dan alleen werken en de kinderen opvoeden. En je laat heel goed merken dat je van ons en de kinderen houdt. Papa, je bent mijn grote voorbeeld, door hoe je luistert en loslaat. Dat is soms precies wat ik nodig heb, en de reden voor heel veel goede dingen in mijn leven. Ik hoop deze rol ook voor mijn kinderen te kunnen vervullen. Tante Lida, bedankt voor de goede zorgen en dat u de kinderen wat gedegen literatuur bij brengt. Martine, je bent ontzettend zorgzaam en positief. Hoewel niet bewust heb jij waarschijnlijk mijn interesse opgewekt in de nefrologie (en bedankt dat je Bram hebt uitgeleend voor het vormgeven van dit proefschrift; hij heeft zichzelf weer overtroffen). Karin, je bent mega relaxed en daarin een voorbeeld van hoe ik internist zou willen zijn. Lidy, heel soms doet alles er niet meer toe, want dan speel je iets op de cello en dan gaat het alleen nog maar om dat verhaal. Het is een wereld die je creëert, waarbij alle problemen vervagen en alles wat belangrijk lijkt, onbelangrijk blijkt. Ik waardeer onze dagjes Amsterdam heel erg, dit gaan we nog vaak doen. Ik hou van jullie allemaal.

Lieve Anna, je bent geweldig zoals je bent, je bent lief, je zorgt goed voor je broertjes, je bent slim en mooi, en ik houd van je, ook als je fouten maakt. Lieve Oscar, je bent geweldig zoals je bent, je bent grappig, onderzoekend, rustig en relaxed, en ik houd van je, wat er ook gebeurt. Lieve Berend, je bent altijd vrolijk, ik geniet enorm van je kletspraatjes, ook al versta ik er niets van, en ik houd van je.

Brigitte, allerliefste ever ooit op de aardbodem. Sterkste vrouw die ik ken. We schijnen moeilijke tijden te hebben meegemaakt, maar als ik terug kijk zie ik alleen maar liefde en vriendschap, en heel veel plezier en mooie avonturen. Je gaf me op momenten alle ruimte die ik nodig had, maar zorgde er ook soms juist voor dat ik mijn werk even liet voor wat het was en belangrijke tijd kon doorbrengen met jou en de kinderen. Je haalde soms het bloed onder mijn nagels vandaan met je koppigheid, maar ik zou het niet anders hebben gewild en je hebt me daarmee ook ontzettend veel geleerd. Ik denk dat ik door jou een betere arts en beter mens ben geworden. We worden samen oud, lelijk en grijs, want ik houd van je.

APPENDIX

Effect of Lanreotide on Kidney Function in Patients with Autosomal Dominant Polycystic Kidney Disease: The DIPAK 1 Randomized Clinical Trial.

Esther Meijer*, Folkert W. Visser*, Rene M.M. Van Aerts, **Charles J. Blijdorp**, Niek F. Casteleijn, Hedwig M. A. D'Agnolo, Shosha E. I. Dekker, Joost P. H. Drenth, Johan W. de Fijter, Maatje D. A. van Gastel, Tom J. Gevers, Marten A. Lantinga, Monique Losekoot, A. Lianne Messchendorp, Myrte K. Neijenhuis, Michelle J. Pena, Dorien J. M. Peters, Mahdi Salih, Darius Soonawala, Edwin M. Spithoven, Jack F. Wetzels, Robert Zietse, Ron T. Gansevoort.

JAMA 2018

Key Points

Question: Can the somatostatin analogue lanreotide slow the rate of decline in kidney function in patients with autosomal dominant polycystic kidney disease (ADPKD)?

Findings: In this randomized clinical trial that included 305 patients with later-stage ADPKD, treatment with lanreotide, 120 mg subcutaneously once every 4 weeks, compared with standard care resulted in a decline of estimated glomerular filtration rate of 3.53 vs 3.46 mL/min/1.73 m2 per year over 2.5 years, a difference that was not statistically significant.

Meaning: Lanreotide was not effective in slowing the decline in kidney function in patients with later-stage ADPKD.

Abstract

Importance: Autosomal dominant polycystic kidney disease (ADPKD) is characterized by progressive cyst formation in both kidneys and loss of renal function, eventually leading to a need for kidney replacement therapy. There are limited therapeutic management options.

Objective: To examine the effect of the somatostatin analogue lanreotide on the rate of kidney function loss in patients with later-stage ADPKD.

Design, Setting, and Participants: An open-label randomized clinical trial with blinded end point assessment that included 309 patients with ADPKD from July 2012 to March 2015 at 4 nephrology outpatient clinics in the Netherlands. Eligible patients were 18 to 60 years of age and had an estimated glomerular filtration rate (eGFR) of 30 to 60 mL/min/1.73 m2. Follow-up of the 2.5-year trial ended in August 2017.

Interventions: Patients were randomized to receive either lanreotide (120 mg subcutaneously once every 4 weeks) in addition to standard care (n = 153) or standard care only (target blood pressure <140/90 mm Hg; n = 152).

Main Outcomes and Measures: Primary outcome was annual change in eGFR assessed as slope through eGFR values during the 2.5-year treatment phase. Secondary outcomes included change in eGFR before vs after treatment, incidence of worsening kidney function (start of dialysis or 30% decrease in eGFR), change in total kidney volume and change in quality of life (range: 1 [not bothered] to 5 [extremely bothered]).

Results: Among the 309 patients who were randomized (mean [SD] age, 48.4 [7.3] years; 53.4% women), 261 (85.6%) completed the trial. Annual rate of eGFR decline for the lanreotide vs the control group was −3.53 vs −3.46 mL/min/1.73 m2 per year (difference, −0.08 [95% CI, −0.71 to 0.56]; P = .81). There were no significant differences for incidence of worsening kidney function (hazard ratio, 0.87 [95% CI, 0.49 to 1.52]; P = .87), change in eGFR (−3.58 vs −3.45; difference, −0.13 mL/min/1.73 m2 per year [95% CI, −1.76 to 1.50]; P = .88), and change in quality of life (0.05 vs 0.07; difference, −0.03 units per year [95% CI, −0.13 to 0.08]; P = .67). The rate of growth in total kidney volume was lower in the lanreotide group than the control group (4.15% vs 5.56%; difference, −1.33% per year [95% CI, −2.41% to −0.24%]; P = .02). Adverse events in the lanreotide vs control group included injection site discomfort (32% vs 0.7%), injection site papule (5.9% vs 0%), loose stools (91% vs 6.6%), abdominal discomfort (79% vs 20%), and hepatic cyst infections (5.2% vs 0%).

Conclusions and Relevance: Among patients with later-stage autosomal dominant polycystic kidney disease, treatment with lanreotide compared with standard care did not slow the decline in kidney function over 2.5 years of follow-up. These findings do not support the use of lanreotide for treatment of later-stage autosomal dominant polycystic kidney disease.

Trial Registration: ClinicalTrials.gov Identifier: NCT01616927

Introduction

Autosomal dominant polycystic kidney disease (ADPKD) is characterized by progressive cyst formation in both kidneys and loss of renal function [1]. A 2017 review of epidemiology literature indicated a disease prevalence of approximately 3 to 4 per 10 000 [2]. End-stage kidney disease, for which dialysis or kidney transplantation is needed, occurs between the fourth and seventh decade of life in the majority of affected patients [1]. Registry data collected between 1991 and 2010 showed that approximately 10% of patients receiving kidney replacement therapy had ADPKD [3].

For patients with ADPKD, few treatments are available that can delay the rate of disease progression. Increasing knowledge of the pathophysiology of the disease allowed for the identification of several ADPKD-specific therapeutic targets. It appears that in renal tubular cells affected by polycystic kidney disease, cyclic adenosine monophosphate is increased [4]. This second messenger promotes growth of these affected cells and stimulates transepithelial fluid secretion, which are 2 important processes involved with cyst formation and growth [5].

Somatostatin is a peptide that is secreted by cells in the pancreas, nervous system, gastrointestinal tract, thyroid gland, and other organs [6]. When bound to the somatostatin receptor, it inhibits adenylyl cyclase, the enzyme that produces cyclic adenosine monophosphate in renal tubular cells [7]. In models for polycystic kidney disease, somatostatin analogues were shown to be renoprotective [8-11]. Furthermore, clinical trials in patients with ADPKD suggested that somatostatin analogues ameliorated the rate of growth in total kidney volume (TKV) [12-15]. These trials, however, included only a limited number of patients, were of short duration, and were partly uncontrolled, making it difficult to draw definitive conclusions on the merits of these agents. For these reasons, the DIPAK-1 study was designed to investigate the renoprotective efficacy and adverse events of the somatostatin analogue lanreotide in patients with later-stage ADPKD.

Methods

Trial Design and Participants

The design and methods of the DIPAK-1 study have been published [16] and the full trial protocol is available in Supplement 1. Briefly, an investigator-driven, randomized, open-label clinical trial with blinded end point analysis was performed to test the efficacy of and adverse events associated with lanreotide in patients with later-stage ADPKD. Because lanreotide is a gel, administration of this drug results in temporary injection infiltrates. Manufacturing a placebo that has a similar effect has not been possible from a technical point of view, which precluded execution of this trial as a double-blinded randomized trial. An academic steering committee designed the trial and oversaw its conduct with the assistance of an independent data and safety monitoring committee. The institutional review board at each site approved the protocol. All participants provided written informed consent.

The study included patients aged 18 to 60 years who had later stage ADPKD (diagnosis made in accordance to the modified Ravine criteria [17], defined as an estimated glomerular filtration rate (eGFR) of 30 to 60 mL/min/1.73 m2. Main exclusion criteria at the start of the study were bradycardia, a history of gallstones or pancreatitis, and diseases or medication use that could confound end point assessment (eg, diabetes mellitus, use of nonsteroidal anti-inflammatory drugs, use of lithium or tolvaptan).

Randomization

Patients were referred by physicians at 66 hospitals in the Netherlands to 1 of the 4 study centers (Groningen, Leiden, Nijmegen, and Rotterdam). At a screening visit, eligibility was checked, and, when confirmed, a baseline visit took place. At the baseline visit, patients were randomly assigned (1:1) to the lanreotide group, which received lanreotide and standard care, or to the control group, which received standard care alone. Randomization with a block size of 6 was performed centrally with the use of an interactive voice response system, with stratification according to sex, age (≤45 years or >45 years), and eGFR (≤45 mL/min/1.73 m2 or >45 mL/min/1.73 m2).

Interventions

Patients in the lanreotide group received 120 mg of lanreotide subcutaneously once every 4 weeks, which was down-titrated to 90 mg if eGFR decreased to less than 30 mL/min/1.73 m2 during the trial. Also, if patients did not tolerate 120 mg, lanreotide was down-titrated to 90 mg, 60 mg, or stopped. Lanreotide was injected by trained nurses via a home care service. Standard care was defined as a blood pressure less than 140/90 mm Hg, to be reached with a sodium-restricted diet and, as a first-choice blood pressure–lowering agent, an angiotensin-converting enzyme inhibitor or angiotensin receptor blocker. The choice of additional antihypertensive medication and dietary advice was left to the discretion of the treating physician.

Procedures

After the baseline visit at 1 of the 4 study centers, patients were seen at weeks 4, 8, 12, 48, 96, and 120. At the week-120 visit, lanreotide treatment was stopped and patients were seen again 12 weeks later at a posttreatment visit (week 132). In patients who stopped the trial prematurely, early end-of-treatment and posttreatment visits were performed. Every 12 weeks, blood was drawn for local assessment of safety laboratory data and for collection of a blood sample that was shipped to the central laboratory. These blood samples were stored at −80°C until measurement of serum creatinine, with the use of the IDMS-traceable Roche enzymatic method, and cystatin C, using reference material from the International Federation of Clinical Chemistry. All samples of a patient were assessed in 1 run to minimize bias induced by interassay variation. eGFR was calculated using the Chronic Kidney Disease Epidemiology Collaboration formulas for serum creatinine and cystatin C. [18] Measurement of creatinine and cystatin C was performed blinded for treatment allocation.

At the baseline (week 0), end of treatment (week 120), and posttreatment (week 132) visits, standardized magnetic resonance (MR) images were obtained without the use of a contrast agent. A quality check was performed within 24 hours, and, in cases of insufficient quality, MR imaging was repeated within 1 week. A detailed description of the methodology, accuracy, and precision of the TKV measurement has been published [19]. TKV was assessed with manual tracing planimetry by trained reviewers blinded to patient identity, treatment allocation, and order of study visit and was adjusted for height (htTKV). During these visits, health-related quality of life was also measured using the validated 18-question ADPKD Impact Scale [20]. The minimum score of 1 indicates "not bothered at all" and the maximum score of 5 indicates "extremely bothered." Information on race was determined by the researchers, according to fixed categories, to allow comparison with other studies and assessment of external validity.

Deviations From the Original Protocol

An interim safety analysis revealed 8 instances of hepatic cyst infection in 7 patients using lanreotide. Details of these patients have been published [21]. A history of hepatic cyst infection seemed to be a risk factor. This experience led to a protocol amendment that dictated to withdraw all patients from the study who had a history of hepatic cyst infection (3 in the lanreotide group and 0 in the control group) or who experienced a hepatic cyst infection during the study. Thereafter, only 1 additional hepatic cyst infection occurred, also in a patient treated with lanreotide.

Outcomes

The primary outcome was change in kidney function, assessed by the patient's slope via serial eGFR measurements over time (calculated using the creatinine values measured in 1 run per patient) during the treatment phase. The eGFR measurements from week 12 until the end of the treatment phase were used for analysis of the primary efficacy end point. The baseline and posttreatment eGFR measurements (ie, just before the start of and after stopping lanreotide) were not used because somatostatin analogues can induce acute, reversible renal hemodynamic effects that may compromise an accurate assessment of eGFR slope [22].

The key secondary outcomes were (1) change in eGFR between the pretreatment (the mean eGFR from the screening and baseline visits) and posttreatment visits; (2) incidence of worsening kidney function, defined as a sustained (2 consecutive measurements) 30% decrease from pretreatment eGFR or the need for kidney replacement therapy, whichever came first; (3) change in htTKV between the baseline and posttreatment visits; and (4) change in health-related quality of life between the baseline and end-of-treatment visits.

Other secondary outcomes included the patients' adverse event profile and tolerability of lanreotide. As defined in the statistical analysis plan in Supplement 2, change in total liver volume will be analyzed only in the subgroup of patients with a polycystic liver phenotype (ie, total liver volume >2000 mL). Results on total liver volume will therefore be reported separately.

Statistical Analysis

Enrollment of at least 150 patients per group (300 in total) was needed to show a 30% reduction in slope of eGFR loss on treatment (deemed clinically relevant because it would translate as 3 years of treatment leading to approximately 1 year delayed start of renal replacement therapy, and what exact percentage was also used in other studies [23-25]), assuming a mean (SD) slope in eGFR of −5.1 (4.2) mL/min/1.73 m2 per year in the control group, 80% power to detect this reduction, and a 2-sided μof .05, as well as taking into account 20% protocol violators and/or dropouts.

Continuous data are presented as mean (SD) or as median and interquartile range (IQR), in cases of nonnormal distribution. Categorical data are presented as percentages. For all analyses, we used an intention-to-treat approach, including all randomized patients who had primary efficacy postbaseline data available.

A mixed-model repeated-measures analysis was used to evaluate the primary outcome (ie, slope of eGFR loss during the treatment phase). If kidney replacement therapy was started or death occurred, only eGFR measurements before these events were used for analysis. Within-patient correlations were modeled using an unstructured covariance structure. In order to check model fit, additional models using Toeplitz, autoregressive-1, and compound symmetry

structures were performed. The unstructured covariance structure resulted in the best model fit. The following categorical covariates were used in the models as fixed effects: lanreotide treatment (yes/no), time, and lanreotide treatment × time interaction. Because there were no differences in baseline characteristics between the groups for the randomization stratification factors or a center effect, the final models were not adjusted for these covariates.

An exploratory mixed-model repeated-measures analysis of the secondary efficacy end points (change in eGFR, htTKV, and health-related quality of life) was also performed to account for possible differences in follow-up time between the groups. Change in htTKV was compared between the groups using log10-transformed htTKV data, the antilog of the treatment effect, and 95% CIs derived from the mixed-model analysis to provide annual percentage of change of htTKV. Incidence of worsening kidney function was investigated with a time-to-event analysis using a Cox proportional hazards model. The proportionality assumption was tested by calculating Schoenfeld residuals, running a model with the treatment group as a time-dependent covariate, and performing a proportionality test. For the secondary outcomes, missing data were few and therefore not imputed.

Subgroup analyses were a priori defined and performed for the primary and secondary outcomes, with treatment group (yes/no) and subgroup variable as independent variables and their interaction term (treatment group × subgroup variable). If this interaction term was significant, the subgroup variable was considered as a moderator for treatment effect.
The safety analysis population included all randomized patients. After early discontinuation of treatment in a patient, efforts were made to collect adverse event data during the rest of the planned study period. No adverse event data were collected after a patient started kidney replacement therapy (a study end point).

Mixed models were checked for presence of outliers; results were validated by testing measures of kidney function other than creatinine-based eGFR; and comparisons were made for change in htTKV, not only between baseline and posttreatment visits, but also as post hoc analysis between baseline and end-of-treatment visits.
All analyses were performed with the statistical software SAS version 9.4 (SAS Institute Inc). A 2-sided *P* value less than .05 indicated statistical significance. No adjustment of significance threshold for multiple comparisons was made for the analyses of secondary endpoints, which should therefore be interpreted as exploratory.

Results

A flowchart describing patient selection and follow-up is presented in **Figure A.1**. Of the 377 patients assessed for eligibility, 309 were enrolled in the study from July 2012 to February 2014. Follow-up was completed in August 2017. Of these 309 patients, 154 were randomized to the lanreotide group and 155 to the control group. Four patients withdrew immediately after randomization without having efficacy or adverse event data collected (1 in the lanreotide and 3 in the control group). Therefore, the primary efficacy as well as the safety analysis includes 153 patients in the lanreotide group and 152 in the control group.

Demographic and clinical characteristics at baseline were balanced between both study groups (**Table 10.1**). Thirty-five patients withdrew from the lanreotide group and 9 from the control group. No differences in baseline characteristics were noted per randomization group between patients who completed and patients who withdrew during the study (eTable 1 in Supplement 3). Mean duration of the treatment phase was 104 weeks (95% CI, 98-109) for the lanreotide group and 117 weeks (95% CI, 114-119) for the control group. Lanreotide was down-titrated in 26 patients (to 90 mg, subcutaneously, once every 4 weeks in 21 patients and to 60 mg, subcutaneously, once every 4 weeks in 5 patients). In 14 patients, this titration was done per protocol because they reached an eGFR less than 30 mL/min/1.73 m2. Thirty-five patients (23%) stopped lanreotide early, of whom 20 (13%) did so because of adverse events. In the patients who continued receiving lanreotide, the mean dose that was given at the end of the treatment phase was 112 mg.

Primary outcome

During the first 12 weeks of treatment, a slight, statistically significant eGFR decline of −1.6 mL/min/1.73 m2 (95% CI, −2.40 to −0.78) was observed in the lanreotide group compared with −0.6 mL/min/1.73 m2 (95% CI, −1.20 to 0.10) in the control group. During the 2.5-year treatment period, the slope of eGFR decline was −3.53 mL/min/1.73 m2 per year (95% CI, −4.00 to −3.07) in the lanreotide group vs −3.46 mL/min/1.73 m2 per year (95% CI, −3.89 to −3.02) in the control group (**Figure A.2**). The mean difference in slope of eGFR decline between both groups was −0.08 mL/min/1.73 m2 per year and was not significant (95% CI, −0.71 to 0.56; P = .81). A prespecified subgroup analysis did not provide evidence that lanreotide improved the primary outcome in any of the subgroups studied, including patients with more rapidly progressive disease, such as patients with class 1C, 1D, or 1E Mayo-classified ADPKD (**Figure A.3**).

TABLE 10.1 **Baseline Demographic and Clinical Characteristics**

CHARACTERISTIC	LANREOTIDE (N = 153)	CONTROL (N = 152)
Men, No. (%)	71 (46.4)	71 (46.7)
Women, No. (%)	82 (53.6)	81 (53.3)
Age, mean (SD), y	48.2 (7.4)	48.5 (7.2)
Race, No. (%)[a]		
White	147 (96.1)	148 (97.4)
Asian	2 (1.3)	3 (2.0)
Missing	4 (2.6)	1 (0.7)
PKD genotype[b], No. (%)		
PKD1 truncating	68 (44.4)	70 (46.1)
PKD1 nontruncating	37 (24.2)	41 (27.0)
PKD2	37 (24.2)	27 (17.8)
No mutation detected	6 (3.9)	9 (5.9)
Missing	5 (3.3)	5 (3.3)
Height, mean (SD), m	1.77 (0.1)	1.76 (0.1)
Weight, mean (SD), kg	84.5 (16.5)	83.6 (17.3)
BMI, mean (SD)	26.9 (4.5)	27.1 (4.8)
Blood pressure, mean (SD), mm Hg		
Systolic	132.3 (12.6)	133.4 (14.0)
Diastolic	82.3 (9.0)	82.1 (10.0)
Antihypertensive medication, No. (%)	134 (87.6)	136 (89.5)
RAAS blocker, No. (%)	124 (81.1)	126 (82.9)
Serum creatinine, mean (SD), mg/dL	1.46 (0.3)	1.45 (0.3)
eGFRc, mean (SD), mL/min/1.73 m2	51.0 (11.5)	51.4 (11.2)
CKD stages[d], No. (%)		
2 (mild CKD)	41 (26.8)	41 (27.0)
3a (mild to moderate CKD)	55 (35.9)	62 (40.8)
3b (moderate to severe CKD)	57 (37.3)	47 (30.9)
4 (severe CKD)	0	2 (1.3)
TKV, mL	2046 (1383-2964)	1874 (1245-2868)
htTKV, median (IQR), mL/m	1138 (790-1670)	1029 (723-1668)
ADPKD class, No. (%)[e]		
1A/1B (low-risk disease)	24 (15.7)	25 (16.4)
1C/1D/1E (high-risk disease)	119 (77.8)	120 (78.9)
2 (atypical disease)	6 (3.9)	5 (3.3)

TABLE 10.1 **Baseline Demographic and Clinical Characteristics** (previous page)

Abbreviations: **BMI**, body mass index calculated as weight in kilograms divided by height in meters squared; **CKD**, chronic kidney disease; **eGFR**, estimated glomerular filtration rate; **htTKV**, height-adjusted total kidney volume; **PKD**, polycystic kidney disease; **RAAS**, renin angiotensin aldosterone system; **TKV**, total kidney volume.

[a] As determined by the researcher.

[b] Mutation analysis was done by Sanger sequencing and multiplex ligation-dependent probe amplification. No *GANAB, HNF1-β*, or *PKHD1* mutations were detected.

[c] eGFR inclusion criterion for the trial was calculated with creatinine at the screening visit and the modification of diet in renal disease equation, whereas by protocol amendment eGFR results for the trial are calculated for all time points with the CKD-EPI equation.18

[d] Higher CKD stage indicates more impaired kidney function.

[e] Mayo ADPKD classification predicts prognosis, and is based on total kidney volume indexed for height and age. Classes 1C, 1D, and 1E indicate a worse prognosis than classes 1A and 1B. Class 2 is atypical disease, where no prognosis can be assessed.

FIGURE A.1 **Patient Enrollment and Flow Through the Study of Lanreotide for Polycystic Kidney Disease**

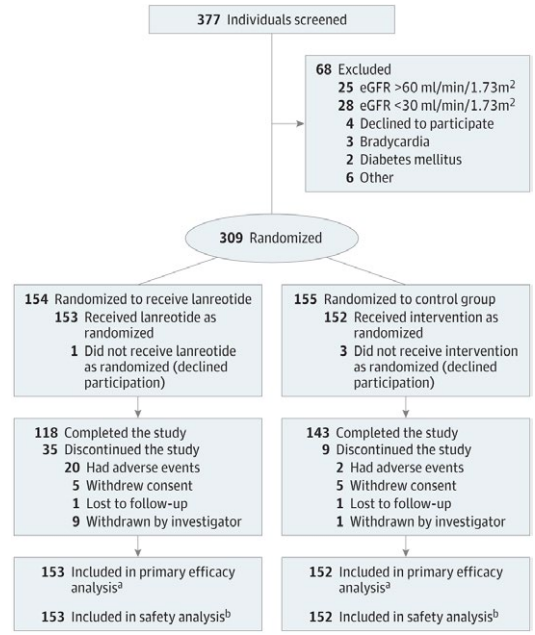

Enrollment occurred from July 2012 to February 2014, and follow-up of the 2.5-year trial was completed in August 2017. Supplement 3 contains additional information regarding specific reasons for exclusion and withdrawal.

a If patients did not complete the study, eGFR data for the primary efficacy analysis (slope of eGFR decline on treatment) was based on all available data points as long as medication was given.

b For the safety analysis, all information was used until patients withdrew consent or were lost to follow-up.

FIGURE A.2 **Effect of Lanreotide and Standard Care Compared With Standard Care Only on Change in Kidney Function in Patients With Autosomal Dominant Polycystic Kidney Disease**

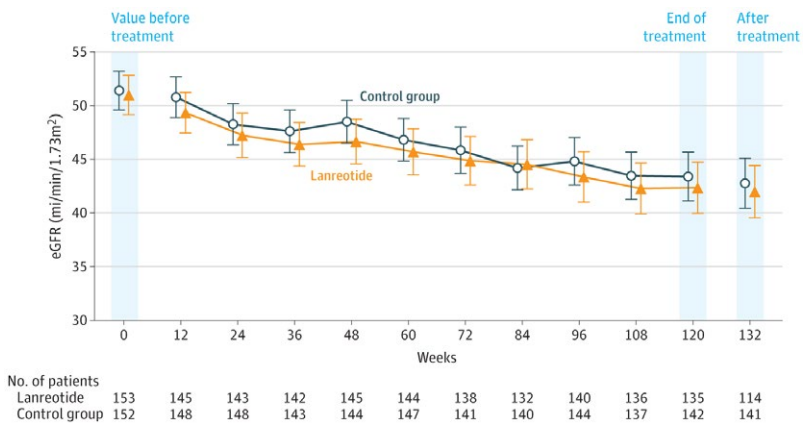

Enrollment occurred from July 2012 to February 2014, and follow-up of the 2.5-year trial was comKidney function over time, depicting mean and 95% CIs for estimated glomerular filtration rate (eGFR).

Secondary outcomes

Four secondary outcomes were analyzed. The change in eGFR between pretreatment and posttreatment visits was −3.58 mL/min/1.73 m2 per year in the lanreotide group vs −3.45 mL/min/1.73 m2 in the control group. The mean difference between the groups was not significant (−0.13 mL/min/1.73 m2 per year [95% CI, −1.76 to 1.50]; P = .88) (Figure 4A). The incidence of worsening kidney function was also not significantly different between groups, with 21 patients in the lanreotide group and 29 in the control group reaching this outcome (including 3 patients in the lanreotide group and 2 in the control group who started kidney replacement therapy), resulting in a hazard ratio of 0.87 (95% CI, 0.49-1.52; P = .87) with lanreotide (**Figure A.5**). The rate of change in htTKV between the pretreatment and posttreatment visits was significantly lower in the lanreotide group, with 4.15% per year in the lanreotide group and 5.56% per year in the control group (Figure 4B) (difference, −1.33% per year [95% CI, −2.41 to −0.24]; P = .02), corresponding with a 24% reduction in htTKV growth rate. Beneficial effects of lanreotide on increase in htTKV were observed in all subgroups tested (eFigure 3 in Supplement 3).

A post hoc model assessment indicated that 1 patient in the lanreotide group was an extreme outlier (high leverage) and influential to the model fit. This patient had a very steep increase in htTKV of 61% per year due to the rare event of a pathogenic truncating mutation in the PKD1 gene as well as a pathogenic truncating mutation in the PKD2 gene (Supplement 3). When this patient was removed from the analyses, the difference in htTKV growth rate between the lanreotide and control groups increased (3.84% and 5.56% per year, respectively; difference, −1.62% per year [95% CI, −2.59 to −0.64]; P = .001).

Detailed information on the change in htTKV can be found in eTables 2A and 2B in Supplement 3. These tables also show that, after stopping lanreotide, there was a modest rebound effect resulting in an increase in htTKV that was not observed in the control group. Quality of life was not affected in the lanreotide or control group, as measured by composite score (Figure 4C) (0.05 vs 0.07, respectively; difference, −0.03 units per year [95% CI, −0.13 to 0.08]; P = .67) or any of the 3 quality of life domains (ie, physical, emotional, fatigue). Prespecified subgroup analyses for the secondary outcomes did not show a consistent pattern suggesting benefit from lanreotide in any of the subgroups studied (eFigures 1-4 in Supplement 3).

FIGURE A.3 **Effect of Lanreotide and Standard Care Compared With Standard Care Only on Estimated Glomerular Filtration Rate (eGFR) in Patients With Autosomal Dominant Polycystic Kidney Disease**

	No. of Patients		Annual eGFR Slope mL/min/1.73 m² per Year		Treatment Effect, mL/min/1.73 m² per Year	*P* Value
	Lanreotide	Control	Lanreotide	Control		
Sex						
Male	71	71	−3.53	−3.64	0.12 (−0.79 to 1.03)	.50
Female	82	81	−3.55	−3.30	−0.24 (−1.14 to 0.65)	
Age, y						
≤45	52	53	−3.87	−4.52	0.74 (−0.40 to 1.88)	.87
>45	101	99	−3.39	−2.94	−0.45 (−1.19 to 0.29)	
eGFR (mL/min/1.73 m²)						
≤45	57	49	−3.77	−4.03	0.26 (−0.69 to 1.22)	.81
>45	96	103	−3.40	−3.19	−0.21 (−1.03 to 0.61)	
htTKV (mL/m)						
≥1000	88	79	−3.53	−3.60	0.07 (−0.73 to 0.86)	.53
<1000	61	71	−3.54	−3.32	−0.23 (−1.26 to 0.80)	
Mayo classification						
High risk (1C-1E)	119	120	−3.79	−3.70	−0.09 (−0.80 to 0.62)	.67
Low risk (1A, 1B, or 2)	30	30	−2.67	−2.53	−0.01 (−1.34 to 1.32)	
DNA class						
PKD1 truncating	68	70	−4.02	−4.01	−0.02 (−0.88 to 0.84)	.68
PKD1 nontruncating or *PKD2*	74	68	−3.10	−3.03	−0.07 (−1.04 to 0.91)	
Urine volume (mL/d)						
≥2500	53	67	−3.40	−3.74	0.33 (−0.76 to 1.42)	.61
<2500	98	82	−3.60	−3.24	−0.36 (−1.14 to 0.43)	
Overall	153	152	−3.53	−3.64	−0.08 (−0.71 to 0.56)	.81

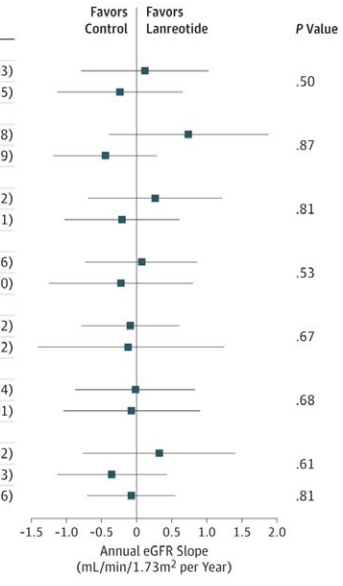

The effect of lanreotide on slope of eGFR decline during the treatment phase according to prespecified baseline subgroups. htTKV indicates height-adjusted total kidney volume.

FIGURE A.4 **Effect of Lanreotide and Standard Care Compared With Standard Care Only on Secondary Outcomes**

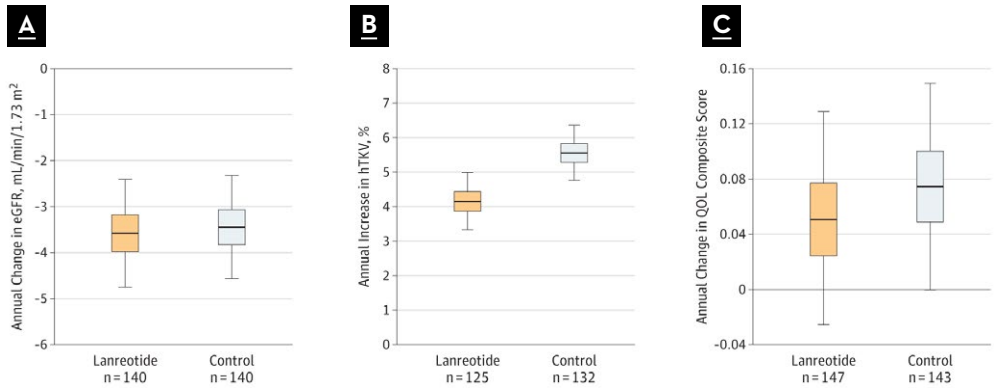

A Change in kidney function, calculated as change in estimated glomerular filtration rate (eGFR) measured 12 weeks after the end of treatment visit (ie, at the posttreatment visit) compared with the pretreatment value (difference, −0.13 mL/min/1.73 m2 per year [95% CI, −1.76 to 1.50]; P = .88).

B Change in height-adjusted total kidney volume (htTKV; difference, −1.33% per year [95% CI, −2.41 to −0.24]; P = .02).

C Change in health-related quality of life (QOL; difference −0.03 units per year [95% CI, −0.13 to 0.08]; P = .67). QOL is measured on a scale ranging from 1 (not bothered) to 5 (extremely bothered). For all panels, boxplots show predicted mean and 25th and 75th percentile, and lower and upper ends of the error bars show predicted 2.5th and 97.5th percentile, respectively, as derived from the mixed model analyses.

Post Hoc Analyses

Additional post hoc analyses were performed. First, creatinine was measured in a central laboratory after completion of the trial. To verify that taking measurements after completion of the study had not affected the results, the primary outcome of the study was also calculated using creatinine values that were measured during the trial in the laboratories of the 4 participating centers. Similar results were obtained, with a slope of eGFR decline in the lanreotide group of −3.45 and in the control group of −3.50 mL/min/1.73 m2 per year (difference, −0.05 mL/min/1.73 m2 per year [95% CI, −1.85 to 1.95]; P = .96). Second, some of the endpoints are based on GFR estimated with creatinine instead of GFR measured with exogenous tracers. We checked, therefore, whether this procedure may have influenced the results. No differences in 24-hour urinary creatinine excretion, 24-hour urinary urea excretion, serum urea, or plasma cystatin C were observed between the groups at any time during the study (eTable 3 in Supplement 3). No

significant difference between the lanreotide and control groups was found when the primary outcome was assessed as a slope using 24-hour creatinine clearance (−4.66 vs −5.50, respectively; difference, 0.87 mL/min/1.73 m2 per year [95% CI, −1.44 to 3.18]; P = .46) or eGFR cystatin C (−3.67 vs −3.34, respectively; difference, −0.34 mL/min/1.73 m2 per year [95% CI, −1.98 to 1.30]; P = .69) as measures for kidney function. Therefore, the primary data seem robust. Third, change in htTKV was also assessed using data from the MR images obtained at week 120 at the end-of-treatment visit instead of the MR images obtained at week 132 at the posttreatment visit (eTable 2 in Supplement 3). The difference between the lanreotide and control groups in the htTKV growth rate at week 120 was stronger (3.55 vs 5.81, respectively; difference, −2.14% per year [95% CI, −3.14% to −1.12%]; P < .001). Fourth, changes in eGFR from baseline to the end-of-treatment visit vs changes in htTKV from baseline to the end-of-treatment visit were correlated in the control group, but not in the lanreotide group (r = −0.26, P = .002, and r = 0.07, P = .45, respectively). In addition, blood pressure was not different between the groups throughout the trial, with difference in systolic blood pressure ranging from −1.1 to 1.9 mm Hg (eTable 6 in Supplement 3).

FIGURE A.5 **Effect of Lanreotide and Standard Care Compared With Standard Care Only on the Secondary Outcome of Worsening Kidney Function.**

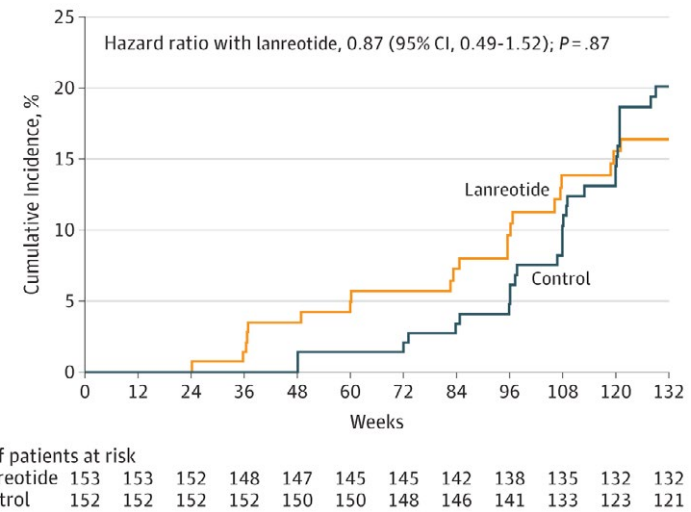

The cumulative incidence of worsening kidney function (30% decrease in estimated glomerular filtration rate or start of dialysis). Mean duration of the treatment phase was 104 and 117 weeks for the lanreotide and control group, respectively.

Adverse Events

Adverse events in the lanreotide group were predominantly related to the injection site (eg, pain, nodule, papule) or gastrointestinal (eg, feces abnormalities, abdominal discomfort, nausea) (**Table 10.2** and eTable 4 in Supplement 3). A total of 62 patients had 84 serious adverse events, of which 55 occurred in the lanreotide group and 29 in the control group (**Table 10.2** and eTable 5 in Supplement 3). Hepatic cyst infections occurred more frequently in the lanreotide group (9 instances in 8 patients). These hepatic cyst infections were managed with antibiotics and resolved without sequelae. Other serious adverse events potentially related to lanreotide treatment occurred as often in the control group, or were rare in the lanreotide group (**Table 10.2**). The physical examination and additional laboratory tests did not provide additional safety signal besides slight, significant increases in serum γ glutamyltransferase, glucose, and glycosylated hemoglobin (eTables 6 and 7 in Supplement 3). One patient died during the study. In this patient, lanreotide treatment was stopped after 24 weeks when a squamous cell lung carcinoma was discovered, which was the cause of death 6 months later.

TABLE 10.2 **Common Adverse Events and Serious Adverse Events [a], [b]** (next page)

	PATIENTS WHO HAD ADVERSE EVENT, NO. (%)	
	Lanreotide Group (n = 153)	Control Group (n = 152)
Adverse events		
Any adverse event	153 (100)	151 (99)
Adverse event leading to withdrawal	16 (10)	0
Specific adverse events		
Abnormal feces	139 (91)	10 (6.6)
Abdominal discomfort	121 (79)	30 (20)
Fatigue	64 (42)	32 (21)
Injection site discomfort	49 (32)	1 (0.7)
Nausea	45 (29)	7 (4.6)
Dizziness	31 (20)	12 (7.9)
Flatulence	27 (18)	0
Bradycardia	23 (15)	9 (5.9)
Alopecia	16 (10)	0
Chest pain	12 (7.8)	2 (1.3)
Decreased appetite	11 (7.2)	1 (0.7)
Injection papule	9 (5.9)	0
Glycated hemoglobin increased	8 (5.2)	1 (0.7)
Influenza-like illness	31 (20)	46 (30)
Nasopharyngitis	19 (12)	37 (24)
Serious adverse events		
Any serious adverse event	43 (28)	19 (12.5)
Serious adverse event leading to withdrawal	4 (2.6)	2 (1.3)
Specific serious adverse events		
Hepatic cyst infection[c]	8 (5.2)	0
Renal cyst infection	3 (2)	3 (2)
Pyelonephritis	2 (1.3)	1 (0.7)
Epigastric pain	2 (1.3)	0
Fever	2 (1.3)	0
Urinary tract infection	1 (0.7)	2 (1.3)
Pancreatitis	1 (0.7)	0
Cholelithiasis	1 (0.7)	0

[a] Listed are all adverse events with an incidence >5% that occurred significantly more often in the lanreotide or control group, and serious adverse events with an incidence >2% or that were at least possibly related to lanreotide treatment.

[b] Adverse events were collected by spontaneous report. A full list of adverse events as well as of serious adverse events is provided as eTables 4 and 5 in Supplement 3. Adverse events were categorized according to the preferred terms of the *Medical Dictionary for Regulatory Activities*.

[c] There were 8 patients with 9 instances of hepatic cyst infections. In 2 of these patients, this event led to treatment withdrawal. In the other 6 patients, treatment was withdrawn later by the investigator because of a protocol amendment.

Discussion

Among patients with later-stage ADPKD, treatment with lanreotide compared with standard care did not slow the decline in kidney function over 2.5 years of follow-up.

When this trial was started in 2011, limited clinical data were available on the efficacy of somatostatin analogues to preserve kidney function in patients with ADPKD (eTable 8 in Supplement 3). These studies suggested a beneficial effect, especially on the rate of TKV growth, in patients with ADPKD [12-15]. During the trial the results of the ALADIN study became available. This study investigated the effects of 3 years of treatment with the somatostatin analogue octreotide in 75 patients with ADPKD with an eGFR greater than 40 mL/min/1.73 m2 [26]. For the prespecified efficacy outcomes, no statistically significant effect was observed. However, a positive effect of octreotide was seen in post hoc analyses for slope in GFR decline on treatment and for change in TKV. Differences in baseline characteristics, which favored the octreotide group, did not allow firm conclusions [26]. In the present larger trial, the characteristics of both study groups were balanced. No effect was found on the prespecified primary outcome slope of eGFR decline on treatment or on any other eGFR-related outcome. The exploratory secondary outcome data do, however, suggest an association between lanreotide and rate of htTKV growth, as in the ALADIN study.

It has been hypothesized that in patients with ADPKD, drug effects on htTKV can be used as surrogate for possible effects on kidney function [27]. The present data suggest that the effects of lanreotide on eGFR and TKV are divergent and therefore may seem unrelated. However, it could also be that lanreotide has an intrinsic nephrotoxic effect that offsets any potential benefit that could be obtained from its effect on htTKV. Such a nephrotoxic effect is, however, not known from literature in patients without ADPKD. Other potential explanations could be that the association with TKV growth was not large enough to translate into a functional benefit during the duration of the clinical trial, that lanreotide was given in too low of a dose to have an effect on eGFR decline, or that the absence of a correlation may be because patients were included with later stage ADPKD, in whom growth in TKV may have a less dominant role in causing eGFR decline than in patients with earlier-stage ADPKD [27].

It remains uncertain whether the present results are specific for lanreotide or are class related. There are differences between somatostatin analogues with respect to their affinity for the various somatostatin receptor subtypes that can be found along the renal tubule [6, 28-31], as well as differences in efficacy and adverse event profile [9, 11, 32, 33]. In addition, it has been suggested that renoprotective drugs may be less efficacious in later-stage ADPKD [27]. Subgroup analysis, however, did not reveal an interaction between treatment efficacy and disease stage.

Lanreotide-related adverse events were, in general, to be expected from the known adverse event profile of this drug, and were predominantly injection-site–related or gastrointestinal. Most of the gastrointestinal symptoms occurred in the first months of treatment, were mild to moderate in intensity, and resolved spontaneously. With respect to serious adverse events, several hepatic cyst infections were observed with lanreotide treatment, especially in patients with a history of liver cyst infections. This may be a disease-specific adverse event of lanreotide, but, with other somatostatin analogues, hepatic cyst infections have also been observed in patients with ADPKD [34, 35].

The percentage of patients who stopped lanreotide, including those who did so because of adverse events, is similar to the percentage of patients with ADPKD who stopped treatment with the vasopressin V2 receptor antagonist tolvaptan in the TEMPO 3:4 study (23% and 15%, respectively) [36]. This latter study showed that tolvaptan treatment decreased the rate of growth in TKV during treatment, similarly as the present study with lanreotide. In contrast to lanreotide, tolvaptan also improved the rate of decline in kidney function [36, 37]. Both drugs are supposed to lower intracellular cyclic AMP by inhibiting adenylyl cyclase at the basolateral membrane of renal tubular cells [5], tolvaptan by blocking the vasopressin V2 receptor and lanreotide via stimulation of the somatostatin type 2 receptor [5]. Additional research is needed to explain the difference in renoprotective efficacy between these drugs. Somatostatin analogues and tolvaptan have been suggested to inhibit different isoforms of adenylyl cyclase [38] via different mechanisms [6], and that the 2 G protein-coupled receptors may interact with different downstream proteins [39].

The dropout rate was higher in the lanreotide group than in the control group (23% vs 6%). This rate is not expected to have had a major effect on the results because the primary outcome, slope through serial eGFR values on treatment only, is not affected by early stopping of treatment. In addition, the secondary endpoint, change in eGFR before treatment vs after treatment, does incorporate information on patients that stopped treatment early. Both analyses, although different in design, lead to the same conclusion that lanreotide did not improve the rate of eGFR decline.

Limitations

This study has several limitations. First, it had an open-label design. To minimize bias, the primary and most secondary endpoints were chosen to be based on objectively measured variables, which were assessed centrally by personnel blinded for treatment allocation. Second, the study population consisted predominantly of white patients. Whether the results hold true for other races requires additional study. Third, the rate of eGFR decline in the control group was less than expected in the power analysis (-3.46 vs -5.1 mL/min/1.73 m2 per year), but similar to recent literature (-3.5, -3.70, and -3.61 mL/min/1.73 m2 per year in the Everolimus, TEMPO 3:4, and REPRISE trials, respectively) [36, 37, 40]. The slower rate of eGFR decline in the control group

did, moreover, not affect the power because the SD of the rate of eGFR decline in the control group also was lower than expected (2.72 instead of 4.2).

Conclusions

Among patients with later-stage ADPKD, treatment with lanreotide compared with standard care did not slow the decline in kidney function over 2.5 years of follow-up. These findings do not support the use of lanreotide to preserve kidney function in later-stage ADPKD.

1. Ong AC, Devuyst O, Knebelmann B, Walz G, ERA-EDTA Working Group for Inherited Kidney Diseases . Autosomal dominant polycystic kidney disease: the changing face of clinical management. *Lancet*. 2015;385(9981):1993-2002.

2. Willey CJ, Blais JD, Hall AK, Krasa HB, Makin AJ, Czerwiec FS. Prevalence of autosomal dominant polycystic kidney disease in the European Union. *Nephrol Dial Transplant*. 2017;32(8):1356-1363.

3. Spithoven EM, Kramer A, Meijer E, et al. . Renal replacement therapy for ADPKD in Europe: prevalence and survival—an analysis of data from the ERA-EDTA Registry. *Nephrol Dial Transplant*. 2014;29(suppl 4):iv15-iv25.

4. Smith LA, Bukanov NO, Husson H, et al. . Development of polycystic kidney disease in juvenile cystic kidney mice: insights into pathogenesis, ciliary abnormalities, and common features with human disease. *J Am Soc Nephrol*. 2006;17(10):2821-2831.

5. Torres VE, Harris PC. Strategies targeting cAMP signaling in the treatment of polycystic kidney disease. *J Am Soc Nephrol*. 2014;25(1):18-32.

6. Patel YC. Somatostatin and its receptor family. *Front Neuroendocrinol*. 1999;20(3):157-198.

7. Friedlander G, Amiel C. Somatostatin and alpha 2-adrenergic agonists selectively inhibit vasopressin-induced cyclic AMP accumulation in MDCK cells. *FEBS Lett*. 1986;198(1):38-42.

8. Masyuk TV, Masyuk AI, Torres VE, Harris PC, Larusso NF. Octreotide inhibits hepatic cystogenesis in a rodent model of polycystic liver disease by reducing cholangiocyte adenosine 3μ5μcyclic monophosphate. *Gastroenterology*. 2007;132(3):1104-1116.

9. Masyuk TV, Radtke BN, Stroope AJ, et al. . Pasireotide is more effective than octreotide in reducing hepatorenal cystogenesis in rodents with polycystic kidney and liver diseases. *Hepatology*. 2013;58(1):409-421.

10. Hopp K, Hommerding CJ, Wang X, Ye H, Harris PC, Torres VE. Tolvaptan plus pasireotide shows enhanced efficacy in a PKD1 model. *J Am Soc Nephrol*. 2015;26(1):39-47.

11. Kugita M, Nishii K, Yamaguchi T, et al. . Beneficial effect of combined treatment with octreotide and pasireotide in PCK rats, an orthologous model of human autosomal recessive polycystic kidney disease. *PLoS One*. 2017;12(5):e0177934.

12. Ruggenenti P, Remuzzi A, Ondei P, et al. . Safety and efficacy of long-acting somatostatin treatment in autosomal-dominant polycystic kidney disease. *Kidney Int*. 2005;68(1):206-216.

13. van Keimpema L, Nevens F, Vanslembrouck R, van Oijen MG, Hoffmann AL, Dekker HM, de Man RA, Drenth JP. Lanreotide reduces the volume of polycystic liver: a randomized, double-blind, placebo-controlled trial. *Gastroenterology*. 2009;137(5):1661-1668.

14. Hogan MC, Masyuk TV, Page LJ, et al. . Randomized clinical trial of long-acting somatostatin for autosomal dominant polycystic kidney and liver disease. *J Am Soc Nephrol*. 2010;21(6):1052-1061.

15. Gevers TJ, Hol JC, Monshouwer R, Dekker HM, Wetzels JF, Drenth JP. Effect of lanreotide on polycystic liver and kidneys in autosomal dominant polycystic kidney disease: an observational trial. *Liver Int*. 2015;35(5):1607-1614.

16. Meijer E, Drenth JP, D'Agnolo H, et al. . Rationale and design of the DIPAK 1 study: a randomized controlled clinical trial assessing the efficacy of lanreotide to Halt disease progression in autosomal dominant polycystic kidney disease. *Am J Kidney Dis*. 2014;63(3):446-455.

17. Pei Y, Obaji J, Dupuis A, et al. . Unified criteria for ultrasonographic diagnosis of ADPKD. *J Am Soc Nephrol*. 2009;20(1):205-212.

18. Levey AS, Stevens LA, Schmid CH, et al. . A new equation to estimate glomerular filtration rate. *Ann Intern Med*. 2009;150(9):604-612.

19. Spithoven EM, van Gastel MD, Messchendorp AL, et al. . Estimation of total kidney volume in autosomal dominant polycystic kidney disease. *Am J Kidney Dis*. 2015;66(5):792-801.

20. Oberdhan D, Cole JC, Krasa HB, et al. . Development of the autosomal dominant polycystic kidney disease impact scale: a new health-related quality-of-life instrument. *Am J Kidney Dis*. 2018;71(2):225-235.

21. Lantinga MA, D'Agnolo HM, Casteleijn NF, et al. . Hepatic cyst infection during use of the somatostatin analog lanreotide in autosomal dominant polycystic kidney disease: an interim analysis of the randomized open-label multicenter DIPAK-1 study. *Drug Saf*. 2017;40(2):153-167.

22. Schmidt A, Pleiner J, Schaller G, et al. . Renal hemodynamic effects of somatostatin are not related to inhibition of endogenous insulin release. *Kidney Int*. 2002;61(5):1788-1793.

23. Ihle BU, Becker GJ, Whitworth JA, Charlwood RA, Kincaid-Smith PS. The effect of protein restriction on the progression of renal insufficiency. *N Engl J Med*. 1989;321(26):1773-1777.

24. Beck GJ, Berg RL, Coggins CH, et al. . Design and statistical issues of the modification of diet in renal disease trial. *Control Clin Trials*. 1991;12(5):566-586.

25. Wright JT Jr, Bakris G, Greene T, et al. . Effect of blood pressure lowering and antihypertensive drug class on progression of hypertensive kidney disease: results from the AASK trial. *JAMA*. 2002;288(19):2421-2431.

26. Caroli A, Perico N, Perna A, et al. . Effect of longacting somatostatin analogue on kidney and cyst growth in autosomal dominant polycystic kidney disease (ALADIN): a randomised, placebo-controlled, multicentre trial. *Lancet*. 2013;382(9903):1485-1495.

27. Grantham JJ, Torres VE. The importance of total kidney volume in evaluating progression of polycystic kidney disease. *Nat Rev Nephrol*. 2016;12(11):667-677.

28. Hofland LJ, Lamberts SWJ. The pathophysiological consequences of somatostatin receptor internalization and resistance. *Endocr Rev*. 2003;24(1):28-47.

29. Bhandari S, Watson N, Long E, et al. . Expression of somatostatin and somatostatin receptor subtypes 1-5 in human normal and diseased kidney. *J Histochem Cytochem*. 2008;56(8):733-743.

30. Bates CM, Kegg H, Grady S. Expression of somatostatin receptors 1 and 2 in the adult mouse kidney. *Regul Pept*. 2004;119(1-2):11-20.

31. Bates CM, Kegg H, Petrevski C, Grady S. Expression of somatostatin receptors 3, 4, and 5 in mouse kidney proximal tubules. *Kidney Int*. 2003;63(1):53-63.

32. Gadelha MR, Bronstein MD, Brue T, et al. . Pasireotide versus continued treatment with octreotide or lanreotide in patients with inadequately controlled acromegaly (PAOLA): a randomised, phase 3 trial. *Lancet Diabetes Endocrinol*. 2014;2(11):875-884.

33. McKeage K. Pasireotide in acromegaly: a review. *Drugs*. 2015;75(9):1039-1048.

34. Chrispijn M, Gevers TJ, Hol JC, Monshouwer R, Dekker HM, Drenth JP. Everolimus does not further reduce polycystic liver volume when added to long acting octreotide: results from a randomized controlled trial. *J Hepatol*. 2013;59(1):153-159.

35. Hogan MC, Masyuk TV, Page L, et al. . Somatostatin analog therapy for severe polycystic liver disease: results after 2 years. *Nephrol Dial Transplant*. 2012;27(9):3532-3539.

36. Torres VE, Chapman AB, Devuyst O, et al. . Tolvaptan in patients with autosomal dominant polycystic kidney disease. *N Engl J Med*. 2012;367(25):2407-2418.

37. Torres VE, Chapman AB, Devuyst O, et al. . Tolvaptan in later-stage autosomal dominant polycystic kidney disease. *N Engl J Med*. 2017;377(20):1930-1942.

38. Rieg T, Kohan DE. Regulation of nephron water and electrolyte transport by adenylyl cyclases. *Am J Physiol Renal Physiol*. 2014;306(7):F701-F709.

39. Moeller HB, Fenton RA. Cell biology of vasopressin-regulated aquaporin-2 trafficking. *Pflugers Arch*. 2012;464(2):133-144.

40. Walz G, Budde K, Mannaa M, et al. . Everolimus in patients with autosomal dominant polycystic kidney disease. *N Engl J Med*. 2010;363(9):830-840.